Universitat Autònoma de Barcelona

Nanoparticle-based sensors for pathogen nucleic acid detection with interest for agriculture

Mohga Wagdy Yehia Mohamed Khater

Nanoparticle-based sensors for pathogen nucleic acid detection with interest for agriculture

Mohga Wagdy Yehia Mohamed Khater

Thesis dissertation to apply for the PhD in Biotechnology

Department of Chemical, Biological and Environmental Engineering

Autonomous University of Barcelona

PhD Director

Prof. Arben Merkoci

ICREA& Nanobioelectronics and Biosensors Group

Institut Catala de Nanociencia i Nanotecnologia (ICN2)

2019

This work entitled “Nanoparticle-based sensors for pathogen nucleic acid detection with interest for agriculture”, presented by Mohga Wagdy Yehia Mohamed Khater to obtain the degree of doctor by Universitat Autònoma de Barcelona, was performed at the laboratories of the Nanobioelectronics and Biosensors Group at the Catalan Institute of Nanoscience and Nanotechnology (ICN2), under the supervision of Prof. Arben Merkoci, ICREA professor and Group Leader.

Bellaterra, April 2019

Director

_____

Prof. Arben Merkoci

ICREA professor

Nanobioelectronics & Biosensors Group

Institut Catalaà de Nanociencia i Nanotecnologia

Tutor

_____

Dr. Jordi Joan Cairo Badillo

Autonomous University of Barcelona

Mohga Khater

_____

Nanobioelectronics & Biosensors Group

Institut Catala de Nanociencia i Nanotecnologia

Acknowledgment

First and foremost I want to thank my supervisor Prof. Arben Merkoci. It has been an honor to be one of his Ph.D students. I appreciate all his contributions of time, ideas, and funding to make my Ph.D experience productive and stimulating. I am also thankful for the excellent example he has provided as a person and as a successful famous professor in the field of nanoscience, and I highly appreciate his kindness and confidence that he had in me during all that time that made me grow faster and stronger ready to face new challenges .

I would like to express my appreciation to Dr. Alfredo de la Escosura-Muñiz for his helpful and precious advice, suggestions and guidance for the achievement of my work, and special thanks for the time that he dedicated for me.

I wish to express my great thank to Dr. Laura Altet for her helpful collaboration.

Further, I wish to express my great thanks to all Prof. Arben's group members for being a source of friendship as well as good advice and collaboration especially Daniel Quesada-Gonzalez, Alejandro Chamorro Garcia and Amadeo Sena.

Finally, I would like to express my thanks love and craving to my family, particularly to my parents and my brother Ahmed and my little nephew YOUNIS <3 for their loving care, patience and support.

Mohga Khater

Table of Contents

Preface

Plant disease is considered the major threat to the global plant production and food security in the years to come and recent studies have estimated global economic losses exceeding billions of dollars annually.[1] While early detection of pathogens in pre-symptomatic plants is important as a first step to manage a plant disease especially in greenhouses, field conditions and at the country boundaries where laboratory is not accessible, there is a strong interest for developing new biosensing systems as point-of-care for early detection of plant diseases with high sensitivity and specificity.

In this context, major advances in nanotechnology have allowed plant pathologists to integrate innovative strategies with molecular biology techniques to overcome the conventional plant disease diagnostic limitations. In recent years, several reviews on developing biosensing systems for plant disease detection were reported, demonstrating the elevate potential of nanotechnology in this field.[2-5] Most of the reported applications rely generally on the use of different nanomaterials, taking advantage of their unique desirable characteristics in the development of advantageous biosensing systems for plant pathogen detection based on both antibody and DNA receptors.

This work emphasizes this point by employing nanomaterial-based biosensors with the aim of developing new, highly sensitive diagnostic tools for crop disease diagnosis. In this sense, the approaches presented herein can be relevant to plant, animal and human diagnostics which are involved in the need to overcome the practical barriers of the traditional molecular biology methodologies, as well as describing three proof of concept diagnostic applications related to *Citrus tristeza virus* (CTV), as model virus.

Tristeza is one of the destructive diseases of citrus causing by *citrus tristeza virus* (CTV). Historically, CTV has been associated with serious outbreaks of quick decline of citrus; therefore CTV monitoring is an important aspect for avoiding such re-emerging epidemics, which would threat citrus production through the world. According to European and Mediterranean Plant Protection Organization (EPPO), CTV is a quarantine pathogen. Most reported serological assays to identify the coat protein of CTV are mainly ELISA, direct tissue print immunoassays [6, 7] and very recently lateral flow immunoassay and label-free electrochemical immunosensor were developed for CTV detection.[8, 9] Since reverse transcription polymerase chain reaction (RT-PCR) and dot- blot hybridization based methods are the most commonly used in molecular diagnostics of CTV, a combination of reverse transcription with loop-mediated isothermal amplification technology (RT-LAMP) has been recently developed.[10-12] However, highly integrated approaches for in-field detection in pre-symptomatic plants, like the ones we are proposing in this work, are still missing.

References

(1) Agrios, G. N. Environmental effects on the development of infectious plant disease. Plant pathol. 5th edn, Elsevier Academic Press, 2005.

(2) Fang, Y. and Ramasamy, R.P. *Biosens*. **2015**, *5*, 537-561.

(3) Khater, M., de la Escosura-Muñiz, A., Merkoçi, A. *Biosens. Bioelectron.* **2017**, *93*, 72-86.

(4) Martinelli, F., Scalenghe, R., Davino, S., Panno, S., Scuderi, G., Ruisi, P., Villa, P., Stroppiana, D., Boschetti, M., Goulart, L.R., Davis, C.E. *Agron. Sustaine. Dev.* **2015**, *35*, 1-25.

(5) Nezhad, A.S. *Lab Chip* **2014**, *14*, 2887-2904.

(6) Bar-Joseph, M., Garnsey, S. M., Gonsalves, D., Moscovitz, M., Purcifull, D. E., Clark, M. F., Loebenstein, G. *Phytopathol*. **1979**, *69*, 190-194.

(7) Huang, Z., Rundell, P. A., Guan, X., & Powell, C. A. *Plant Dis*. **2004**, *88*, 625-629.

(8) Haji-Hashemi, H., Norouzi, P., Safarnejad, M. R., & Ganjali, M. R. *Sens. Actuator. B Chem.* **2017**, *244*, 211-216.

(9) Maheshwari, Y., Selvaraj, V., Hajeri, S., Ramadugu, C., Keremane, M. L., Yokomi, R. K. *Phytoparasit.* **2017**, *45*, 333-340.

(10) Korkmaz, S., Cevik, B., Onder, S., Koc, K., Bozan, O. *New Zeal. J. Crop Hort. Sci.* **2008**, *36*, 239-246.

(11) Yokomi, R. K., Saponari, M., Sieburth, P. J. *Phytopathology* **2010**, *100*, 319-327.

(12) Warghane, A., Misra, P., Bhose, S., Biswas, K. K., Sharma, A. K., Reddy, M. K., Ghosh, D. K. *J. Virol Methods* **2017**, *250*, 6-10.

Chapter I

Introduction

Plant pathogens are one of the causes for low agricultural productivity worldwide. Main reasons are new, old and emerging plant infectious diseases. Their rates of spread, incidence and severity have become a significant threat to the sustainability of world food supply. [1-4] Despite the lack of sufficient information for the economic losses, it was reported from plant disease loss estimates in U.S state of Georgia that total losses caused by plant diseases and their control costs reached roughly 647.2 million dollars in 2006 and then continued up to 821.85 million dollars in 2013. [5,6] Top ten list of economically and scientifically important plant pathogens includes fungi, bacteria and viruses (**Table 1**). [7-10]

Table 1. Top ten important plant pathogenic bacteria, fungi and viruses published by Molecular Plant pathology [7-10]

plant pathogen	Fungi	Bacteria	Virus
1	Magnaporthe oryzae	Pseudomonas syringae	Tobacco mosaic virus
2	Botrytis cinerea	Ralstonia solanacearum	Tomato spotted wilt
3	Puccinia spp.	Agrobacterium tumefaciens	Tomato yellow leaf curl
4	Fusarium graminearum	Xanthomonas oryzae	Cucumber mosaic
5	Fusarium oxysporum	Xanthomonas campestris	Potato virus Y
6	Blumeria graminis	Xanthomonas axonopodis	Cauliflower mosaic
7	Mycosphaerella	Erwinia amylovora	African cassava mosaic
8	Colletotrichum spp	Xylella fastidiosa	Plum pox
9	Ustilago maydis	Dickeya (dadantii and solani)	Brome mosaic
10	Melampsora lini	Pectobacterium carotovorum	Potato virus X

have been used to detect the pathogen antigens. [37-43] Immunoassay technology using monoclonal antibodies offers a high specificity for plant virus detection, being ideal for testing large scale plant samples and for the on-site detection of plant pathogens, as done with tissue print ELISA and LF devices. In contrast, nucleic acid based methods are more accurate and specific enough to detect single target pathogen within a mixture containing more than one analyte and highly effective for detection of multiple targets.

In spite of these advantages, molecular detection methods have some limitations in detecting pathogens at low titres in materials such as seeds and insect vectors or at early infection stages. Furthermore, false negative results can be produced from cross contamination with PCR reagents which completely block amplification of target DNA, while false positive results can be generated by cross-amplification of PCR-generated fragments of non-target DNA. . Another limitation is related to the disability to apply PCR for plant pathogen detection in the field. [44,45,11,22] To overcome such limitations, innovative and portable biosensors have emerged in the last years, being widely used as diagnostic tools in clinical, environmental and food analysis.

Pathogen biosensing strategies are based on biological recognition using different receptors such as antibodies, DNA probe, phage and others (**Fig.3**). [46-48]

.

Antibody-based biosensors can allow sensitive and rapid qualitative and quantitative analysis of pathogens offering also label-free possibilities. It is important to note that this general approach is limited by the quality of the antibody employed and its storage condition that could affect antibody stability. Also pathogen size can interfere in some measurements such as the ones based on surface plasmon resonance (SPR). DNA based biosensors show advantages over antibody based ones mostly related to their better sensitivity thanks to the use of nucleic acid amplification techniques, which allows to detect plant pathogen before appearance of disease symptoms. However, they have some limitations related to the selection and synthesis of specific DNA probes as well as to the fact that detecting short DNA sequence of long double stranded DNA is a common problem in applying biosensing systems for DNA detection. [49, 50, 21] Recently, phage-based DNA biosensor for sensing and targeting bacterial plant pathogens has been reported. [21] Bioluminescent-phage based technology was developed for determination the presence of *Pseudomonas cannabina* pv *alisalensis* that infects cruciferous vegetables. [52] The major advantage of this technology is that detecting nucleic acid of only viable bacterial cells, and as a result, no false positive was obtained. Nevertheless, the reporter phage expression can be inhibited by presence of some chemical compounds in the tested leaves such as thioethers glucosinolate and isothiocyanate.

Along the following sections, the most representative examples of antibody-based and DNA-based plant pathogen detection methods using optical and electrochemical techniques are summarized (see **Table 2**), also discussing advantages and limitations. An overview about the commercially available devices will also be shown together with concluding remarks.

Table 2. Summary of various biosensing techniques used for plant pathogen detection

Biosensors	Detection	Assay format	Sensing plant pathogen	Detection limit
Antibody-based	Electrochemical/Enzyme label Electrochemical/AuNPs tag	• Voltammetric Enzyme-based detection	• *Cucumber mosaic virus* • *Pantoea stewartii sbusp. stewartii*	• 0.5 ng/ml • 7.8×10^3 cfu/ml
	Electrochemical/label-free	• Electrochemical impedance spectroscopy (EIS)-based detection	• *Plum pox virus* • *Prunus necrotic ringspot virus*	• 10 pg/ml • Not reported
	Optical/AuNPs tag	• Quartz crystal microbalance-based approaches • Lateral Flow immunoassays	• *Maize chlorotic mottle virus* • *Potato virus x* • *Pantoea stewartii sbusp. Stewartii*	• 250 ng/ml. • 2 ng/ml • 10^5cfu/ml
	Optical/ fluorescent tag	• Fluorescent approaches	• *Pantoea stewartii sbusp. Stewartii* • *Acidovorax avenae subsp. citrulli* • *Chilli vein-banding mottle virus* • *Watermelon silver mottle virus* • *Melon yellow spot virus*	• 10^3 cfu/ml • 6×10^5 cfu/ml • 1.0 ng/ml • 20.5 ng/ml • 35.3 ng/ml
	Optical/ label free	• Surface plasmon resonance (SPR) systems	• *Cymbidium mosaic virus* • *Odontoglossum ringspot virus*	• 48 pg/ml • 42 pg/ml
DNA-based	Electrochemical/label-free	• DNA hybridization voltammetric detection	• *Plum pox virus* • sugarcane white leaf disease • *Trichoderma harzianum*	• 12.8 pg/ml • 4.7 ng/µl • 10^{-19} mol/L
	Optical/AuNPs tags	• Lateral Flow immunoassays • AuNPs aggregation-based DNA analysis	• *Acidovorax avenae subsp. Citrulli* • *Banana bunchy top virus* • *Pseudomonas syringae*	• 0.48nM • 0.13 nM • 15 ng/ml
	Optical/magnetic tag	• bridging flocculation	• *Pseudomonas syringae*	• 0.5 ng/µl
	Optical/fluorescent tag	• Fluorescent approach in DNA microarrays	• *Botrytis cinerea*	• 1 fM
	Optical/ luminescent tag	• Electrochemiluminscence-based DNA detection	• *Banana streak virus* • *Banana bunchy top virus*	• 50 fM • 50 fM

Antibody-based Biosensors

Electrochemical Immunosensors

Most of the reported electrochemical immunosensors for plant pathogen detection are based on label-free technologies (impedimetric and quartz crystal microbalance-based ones) and enzymatic label-based voltammetric approaches on mercury, gold and carbon electrodes as detailed in the following sections.

Voltammetric detection based on the use of enzymes

In the last three decades, enzyme-linked immunosorbent assay (ELISA) has become the most widely used serological technique in diagnostics since the first publication on using ELISA to quantify rabbit IgG levels.[53] Enzyme immunoassay has been coupled with electrochemical detection methods to diagnose both clinical and plant pathogens with higher sensitivity and selectivity.[54-56] This electrochemical enzyme-linked immunoassay (ECEIA) has incorporated enzyme catalysis (enzyme label- substrate complex in presence of H_2O_2) followed by electrochemical reducing reaction through amperometric and voltammetric techniques.[57-60] Stable voltammetric peaks are achieved by controlling the pH of both enzymatic reaction and electrolyte solutions. Highly preferred is the use of Horseradish peroxidase (HRP) and alkaline phosphatase (AP) as enzyme labels since they have a variety of suitable substrates to reach the required sensitivity.[61, 62] Despite of high sensitivity of these sensing systems, the low availability of enzyme-conjugated antibodies represents an important limitation. Furthermore, enzymatic products can be highly affected by the pH of the electrolyte solution being another drawback in case of enzymatic reactions occurring in the same medium of the final electrochemical measurement.

Jiao and co-workers applied a voltammetric indirect ELISA based on horseradish peroxidase (HRP) detection system to detect the plant virus called *Cucumber mosaic virus* (CMV) using two different HRP substrates: *o*-aminophenol (OAP) and *o*-phenylenediamine (OPD). [63] Such indirect ELISA has three main steps: i) immobilization of virus antigen which is either a purified CMV or leaf extract prepared by grinding infected nicotiana leaves with PBS buffer; ii) incubation with specific antibody for CMV detection; iii) immunoreaction with secondary antibody labeled with HRP. The current derived from the reduction of the enzymatic product is measured by linear sweep voltammetry using a hanging mercury electrode. The sensitivity found for the ECEIA detection of CMV is almost four to ten times higher than that of the standard spectrophotometric ELISA, reaching detection limits as low as 0.5 ng/ml using OAD as substrate, also exhibiting high selectivity against four different pathogens: *Tobacco mosaic virus* (TMV), *Potato virus Y* (PVY), *Southern bean mosaic virus* (SBMV), *Tomato aspermy virus* (ToAV) and *Turnip mosaic virus* (TuMV).

Recently gold nanoparticles have been used as tags to amplify the analytical signal and significantly enhance the immunological assay"s sensitivity. As an example, Zhao and co-workers presented for the first time an ECEIA using gold nanoparticle tags loaded by antibodies labeled with HRP to detect *Pantoea stewartii sbusp. stewartii* (PSS) plant bacterial pathogen (**Fig.4A**).[64]

Linear voltammetric measurements were done in PBS solution containing hydroquinone (HQ) as enzyme substrate and H_2O_2 as oxidant agent for monitoring the reduction of benzoquinone (BQ). In comparison to conventional ELISA assay, the ECEIA for PSS detection was 20 times more sensitive, reaching a detection limit of 7.8×10^3 cfu/ml. Besides sensitivity, this approach enabled sensitive and specific detection of the PSS antigen against other plant bacterial diseases such as panicle blight, leaf streak and *Cercospora* leaf spot on rice together with black spot of crucifer.

Label-free electrochemical impedance spectroscopy (EIS)-based detection

Over two decades ago, impedimetric based immunosensors were introduced by Newman and Martelet using techniques that involve electrochemical impedance spectroscopy (EIS) which studies the electrode-solution interface changes and detects that impedance changes produced by biomolecular interactions including DNA hybridization and protein immunocomplex formation.[66-71] Although impedance biosensing systems are sensitive and can effectively trace reactions occurring upon, their selectivity in real complex sample is a key problem limiting commercial applications. Most impedimetric biosensors are in label-free format and use self-assembled monolayers (SAMs) as immobilization method to obtain well-ordered monolayers on the surface of the electrode and achieve better antibody-antigen interaction efficiency. [72]

Thiol SAMs formation on gold electrodes is the most reported substrate that has been used for impedimetric detection of plant pathogens. [73, 74] One of these approaches has been reported by Jarocka and co-workers for *Plum pox virus* (PPV) detection on gold electrodes, taking also advantage of AuNPs for stable antibody immobilization while retaining higher biological activity.[75] Anti-PPV antibodies immobilized onto a 1, 6-hexanedithiol/AuNPs modified gold electrode were used for the recognition of purified PPV. Leaf extract from infected leaves of nicotiana was also prepared and used as plant virus antigen sources for

analysis. The resulting impedimetric PVV immunosensor was more sensitive than conventional detection methods assayed, such as AgriStrip rapid immunochromatographic assay, being able to detect the presence of 0.01% of infected plant material in the diluted healthy samples with a detection limit of 10 pg/ml.

The same group later reported a similar approach for the detection of *Prunus necrotic ringspot virus* (PNRSV) using in this case glassy carbon electrodes as platforms and transducers.[65] In this case, they took advantage of protein A, covalently connected to the electrode, for anti-PNRSV antibodies immobilization (**Fig. 4B**). The as-prepared immunosensor was incubated for 30 minutes with leaf extracts from healthy and PNRSV infected cucumber leaves. The stepwise preparation of the immunosensor was verified with electrochemical impedance spectroscopy (EIS) and cyclic voltammetry (CV) observing the expected increase in the electron-transfer resistance (R_{ct}), which was directly measured with EIS. The immunosensor displayed a very good sensitivity and selectivity against *Plum pox virus* (PPV) and was able to detect PNRSV in plant materials diluted up to ten thousand-fold

Label-free quartz crystal microbalance-based approaches

Quartz crystal microbalance (QCM) biosensors are based on recording changes in oscillation frequency on the surface of the crystal that produce electrical field [76]. QCM-based immunosensors are highly sensitive and allow label-free detection. . Many applications have been reported for detecting foodborne pathogens as well as on environmental and clinical analysis.[77-81] Since their use in identifying orchid viruses as a first application for plant disease detection [82], a number of piezoelectric label-free immunosensors based on the use of QCM for plant disease determination has been rightly reviewed by Skottrup et al. *(*2008), and continued in the last years presenting multiplexed detection of three significant plant pathogenic bacteria.[83] We highlight here the recent approach reported by Huang and co-workers developing QCM

immunosensor based on self-assembled monolayers (SAMs) for identification of *Maize chlorotic mottle virus* (MCMV).[84] SAMs were formed on the gold surface of QCM crystal layer by layer using mercaptopropanoic and mercaptoundecanoic acids and antibodies specific to MCMV. Quantification measurements were obtained by observing the changes in the QCM crystal frequency. This biosensor showed a similar sensitivity as ELISA, recording limit of detection of 250 ng/ml. Moreover the developed immunosensor showed high selectivity against similar viruses, such as *Maize Dwarf Mosaic Virus* (MDMV) and *Wheat streak mosaic virus* (WSMV).

In spite of their high sensitivity, QCM-based measurements are highly affected by the environmental conditions, representing an important limitation that should be solved for point-of-care applications.

Optical immunosensors

Main optical immunosensors for plant pathogen detection are based on lateral flow devices (paper-based sensors), fluorescence approaches and surface plasmon resonance (SPR) systems as explained in the following sections.

Lateral flow immunoassays (LFIAs)

Paper-based sensors are well known advantageous devices for diagnostics applications.[85] Lateral flow (LF) is a paper analytical device, also known as immunochromotographic strip, composed of four different pads: sample pad, made of cellulose, where the sample is dropped; conjugate pad made of glass fiber, impregnated with the bioconjugates solution (label particle and a receptor for the analyte), detection pad, made of nitrocellulose where test line (TL) and control line (CL) are printed and adsorption pad, also made of cellulose.[86] Sandwich and competitive lateral flow immunoassays (LFIAs) are the main LF formats. In a typical sandwich assay, when the sample is added on the sample pad the liquid starts flowing to the conjugate pad where the analyte (if present) is linked to the label particles, previously conjugated with a specific bioreceptor. The conjugate flows by capillarity along the detection pad to the absorbent

pad, passing through the TL, where it is captured only if the sample has the analyte (positive response), and to the CL, being here always captured, evidencing that the assay works.

In addition to antibodies, aptamers and DNA probes are employed as biological recognition elements which can be labeled with AuNPs, magnetic nanoparticles, fluorescent nanoparticles and enzymes among others so as to generate the color evolution at the test line. The advantages of LFIAs in terms of rapidity, stability and direct on-site analysis make them one of the most popular diagnostic tools in medical diagnostics, food safety, environmental analysis and plant disease detection. Workings with LFIAs have demonstrated very interesting opportunities for signal enhancements via use of nanomaterials (nanoparticles, graphene etc.) in addition to simple changes in platform architecture including vertical flow format.[87-92] The first LFIA for plant pathogen detection was designed to detect *Tobacco mosaic virus* (TMV).[93] Since this first design, LFIAs have been proposed for the detection of several plant pathogens.[94] Particularly, LFIAs in sandwich format using AuNPs tags have been utilized to plant viruses such as *Citrus tristeza virus* (CTV) and *Potato virus X* (PVX) and also plant pathogenic bacteria like *Erwinia amylovor*a, *Banana xanthomonas* and *Pantoea stewartii* as will be commented in the following paragraphs.

Salomone and co-workers developed a LFIA using standard antibody-based sandwich format and AuNPs as label to detect *Citrus tristeza virus* (CTV) from citrus leaves and fruits.[95] Qualitative results showed sensitivity as high as ELISA test with good correlation. The specificity of the assay was also acceptable, obtaining a level of 5% of false positive results.

A similar approach was later developed for the identification of *Potato virus x*.[96] The reported sensitivity was found to reach 2 ng/ml while selectivity was tested against major potato seed viruses such as *Potato virus Y* (PVY), *Potato virus M* (PVM) and *Potato virus A* (PVA). Very recently, Feng and co-workers performed a rapid detection of *Pantoea stewartii sbusp. stewartii* (PSS) extracted from corn seed samples using a LFIA (**Fig.5A**).[97] The LFIA was

performed in the presence of three other plant pathogenic bacteria (*Burkholderia glumae*, *Xanthomonas oryzae* and *Pseudomonas syringae*) and none were detected, evidencing an excellent selectivity. The assay displayed a detection limit of 10^5cfu/ml of PSS.

In addition to the use of AuNPs for colorimetric detection, fluorescent tags have also been proposed in LFIAs for plant pathogen detection. This is the case of lanthanide chelate-loaded silica nanoparticles that were used for the determination of *Pantoea stewartii sbusp. stewartii* (PSS), the bacterial pathogen of Stewart‟s wilt in sweet corn.[98] Samples from healthy and infected corn seeds were analyzed following the standard sandwich assay format. The fluorescence strips allowed to detect a low concentration of PSS (10^3 cfu/ml) in less than 30 minutes with limit of detection hundredfold lower than ELISA and AuNPs labeled strips.

In spite of their great advantages, LFIAs suffer important limitations related to their low sensitivity and only qualitative/semiquantitative results. Although the sensitivity is highly improved using fluorescent tags as alternative to traditional colorimetric ones, the need of fluorescence reader (no visual detection possibilities) is an important limitation for rapid and in-field qualitative analysis. For this reason, colorimetric LFIAs, mainly based on AuNPs, are still the most commonly used for point-of-care analysis.

Fluorescent approaches

Microsphere sandwich immunoassay technology based on fluorescence-loaded magnetic microsphere and fluorophore- antibodies has been applied for detecting multiple analytes such as biomarkers, food and plant pathogens.[100- 102] A recent study has taken a direct application in the use of microsphere immunoassay technology for multiplex plant pathogens simultaneously.[99] Specific antibodies to plant bacterial pathogen *Acidovorax avenae subsp. citrulli* (AAC) and three other plant viruses such as *Chilli vein-banding mottle virus* (CVbMV), *Watermelon silver mottle virus* (WSMoV) and *Melon yellow spot virus* (MYSV) were loaded onto a set of fluorescence-coded MagPlex microsphere (**Fig.5B).** This technology based on measuring the

In spite of great advantages, mainly related to sensitivity and ability to detect multiple pathogens in a single assay, the main limitations of these systems are related to the complexity of the assay together with the need of fluorescent readers.

Surface plasmon resonance (SPR) systems

Surface Plasmon resonance (SPR) technology is based on monitoring changes of refractive index on the sensor surface after ligand-biomolecule interaction. SPR biosensors have been used in detecting pathogenic microorganism causing microbial contamination, food spoilage and plant infection.[103-107] The most important advantages of this technique rely on the label-free possibilities together with their ability to effectively measure/follow the bioaffinity reactions. Since more than two decades ago, the first SPR biosensor for *Tobacco mosaic virus* (TMV) was described. [108]

SPR based biosensors have been object of a review so we detail here some representative examples. [49] For instance, label free biosensors based on SPR were developed to detect plant pathogens including *Cowpea mosaic virus, Tobacco mosaic virus* and *Lettuce mosaic virus* as plant viruses and *Fusarium culmorum, Phythothora infestans and Puccinia striiformis* as fungal plant pathogens.[109-113] A number of different SPR biosenosrs using DNA probe, antibody and aptamer are reported in the literature for monitoring plant pathogens.[114-116] In very recent years, Lin and co-workers developed a label free SPR immunosensor using gold nanorods (AuNRs) for investigation of two viruses of orchid *Cymbidium mosaic virus* (CymMV) or *Odontoglossum ringspot virus* (ORSV).[117] Antibodies specific to orchid viruses were modified with AuNRs as sensing layers that offer a wide spectral region help in decreasing the color interference problem caused by sample matrix. This technology was exploited for achieving 48 and 42 pg/ml as detection limits for CymMV and ORSV, respectively. The stability of the established SPR

biosensing system was not reported while the specificity was investigated using mixture of target and non-target viral antigen; performances were compared by observing signal changes due to viral antigen- antibody binding on the surface of AuNRs.

In spite of the above mentioned advantages, a serious drawback in the use of this technology are the non-specific adsorptions onto the sensor surface that must be carefully controlled.

DNA-Based Biosensors

Electrochemical DNA Biosensors

The majority of electrochemical DNA biosensors for plant pathogen determination are based on label-based and label-free voltammetric detection of DNA hybridization. Emerging approaches based on DNA translocation through nanopores, even though not reported yet for plant pathogen detection, show enormous potential in this field so they are also commented in the following sections.

Label-free DNA hybridization voltammetric detection

DNA hybridization can be monitored in label-free approaches based on amperometric, impedimetric and voltammetric detection including square-wave voltammetry (SWV), cyclic voltammetry (CV) and differential pulse voltammetry (DPV). [118-122]

An example of voltammetric approach has been recently reported by Malecka and co-workers for the label-free detection of picomolar concentrations of nucleic acid from *Plum pox virus* (PPV) glassy carbon electrodes (**Fig. 6A**).[123] Detection of the pathogen-related DNA, with the complementary target immobilized on the electrode was monitored by Osteryoung square wave voltammetry (OSWV). Voltammetric measurement of electron transfer changes due to the hybridization reaction allowed detecting 22-mer and 42-mer complementary target DNA sequences of PPV at 10–50 pg/ml concentration range. A good discrimination between infected

and healthy leaf samples is reported with a detection limit of 12.8 pg/ml but selectivity of this technique was not characterized by other phytopathogens.

Well-known approaches based on the use of methylene blue (MB) as hybridization indicator have also been recently reported for sugarcane white leaf disease (SWLD) detection. [124] Voltammetric determination of the plant phytoplasma (causal agent of SWLD) was carried out at glassy carbon electrode modified with chitosan. Electrostatic attraction of negatively charged DNA probe to glassy carbon electrode coated with cationic chitosan film for more efficient DNA immobilization, as alternative to covalent immobilization, were used in most of the previously mentioned approaches. Electrochemical detection of hybridization between ssDNA probe and target was performed by cyclic voltammetry (CV) and differential pulse voltammetry (DPV), using MB as a redox indicator, which is covalently attached to guanine bases. The electrochemical reduction of MB decreased after DNA hybridization due to unavailable guanine bases in dsDNA as a complete form, as expected. Following this strategy, a detection limit of 4.7 ng/µl of SWLD DNA was obtained, also distinguishing between target DNA from diseased sugarcane and non-target DNA from both healthy and infected sugarcane plants with other pathogens like *Sugarcane mosaic virus*. This biosensor showed good stability of DNA probe immobilization onto the chitosan with interest to develop an effective specific DNA biosensor.

Gold electrodes modified with nanocomposite membranes made of chitosan (CHIT) and zinc oxide nanoparticles (ZnO NPs) were also proposed as platforms for developing sensors for plant pathogen DNA voltammetric detection based on MB redox indicator. This kind of composite can improve the efficiency of the DNA probe immobilization thanks to its good biocompatibility and an enhanced electrochemical conductivity. Such is the case of the system recently proposed for *Trichoderma* (soil born fungi) determination. [125] Hybridization between DNA target of *Trichoderma* and its complementary probe immobilized on the nanocomposite modified electrode was investigated in this case by differential pulse voltammetry (DPV). The

fabricated DNA biosensor detected crude DNA taken from real samples (fungal mycelia) with high reproducibility, obtaining a detection limit of 10^{-19} mol/L. High selectivity for identification of *Trichoderma harzianum* against other *Tricoderma* species, probably mainly due to the high specificity of the designed probe DNA used as bioreceptor, has also been reported.

As final remark we can state that, although label-free DNA hybridization using voltammetric systems (and hybridization indicators) have great advantages in terms of low cost of analysis, not necessity of labeling step and possibility of analysis of small volumes, their poor sensitivity in complex real samples should be carefully considered before their application for plant pathogen analysis.

Nanochannels as emerging tools for electrochemical DNA analysis

Nanopore/nanochannel-based technologies are currently one of the most promising ones for rapid and efficient DNA analysis [126]. Even though no examples of application for plant pathogen determination using this technology are found yet in the bibliography, we preview that its enormous potential will make it possible in a short time and thus consider of great relevance to include some remarks in this review.

Nanopore/nanochannel biosensing systems are inspired by the microparticle counter device patented by Wallace Coulter more than 60 years ago. [127] It consists in simply measuring changes in the electrical conductance (electric current or voltage pulse) between two chambers separated by a microchannel when a micro-sized analyte passes through it, giving information about mobility, surface charge, and concentration of the analyte. This sensing principle has been extended in the last decades for nano-sized analytes evaluation using in this case nanometric channels, being the ssDNA analysis extensively reported. The typical approach consists in the monitoring of ssDNA molecules translocation (electrophoretically driven) through a single nanopore (biological or synthetic) which separates two chambers filled with an electrolyte solution.[128- 130] Such translocation produces changes in the constant current measured between

the chambers, being the current pulse length characteristic of each of the 4 DNA bases (A, T, C, G). (**Fig. 6B**). This ability has opened exciting perspectives for DNA sequencing as alternative to conventional real-time PCR. Not only single nanochannels, but also nanochannel arrays have been proposed for the electrical detection of DNA hybridization at the point-of-care. [131]

In addition to DNA, other molecules such as proteins or toxins have been detected using the single-nanochannel technology. [132] We would like also to highlight here very recent approaches reported on filamentous virus translocation monitoring through silicon nitride membranes (**Fig. 6C**).[134] The size and shape of this kind of virus is ideal for the analysis using these systems, since their stiffness avoid hernias formation making them able to pass through the channels in elongated forms, and generating well resolved signatures (easy distinguishable of the ones coming from virus collisions with the membrane), opening the way to reliable future label-free virus detection systems. Such systems could be applied for filamentous virus affecting plants from different genus like closterovirus (CTV) and potyvirus (PVX).

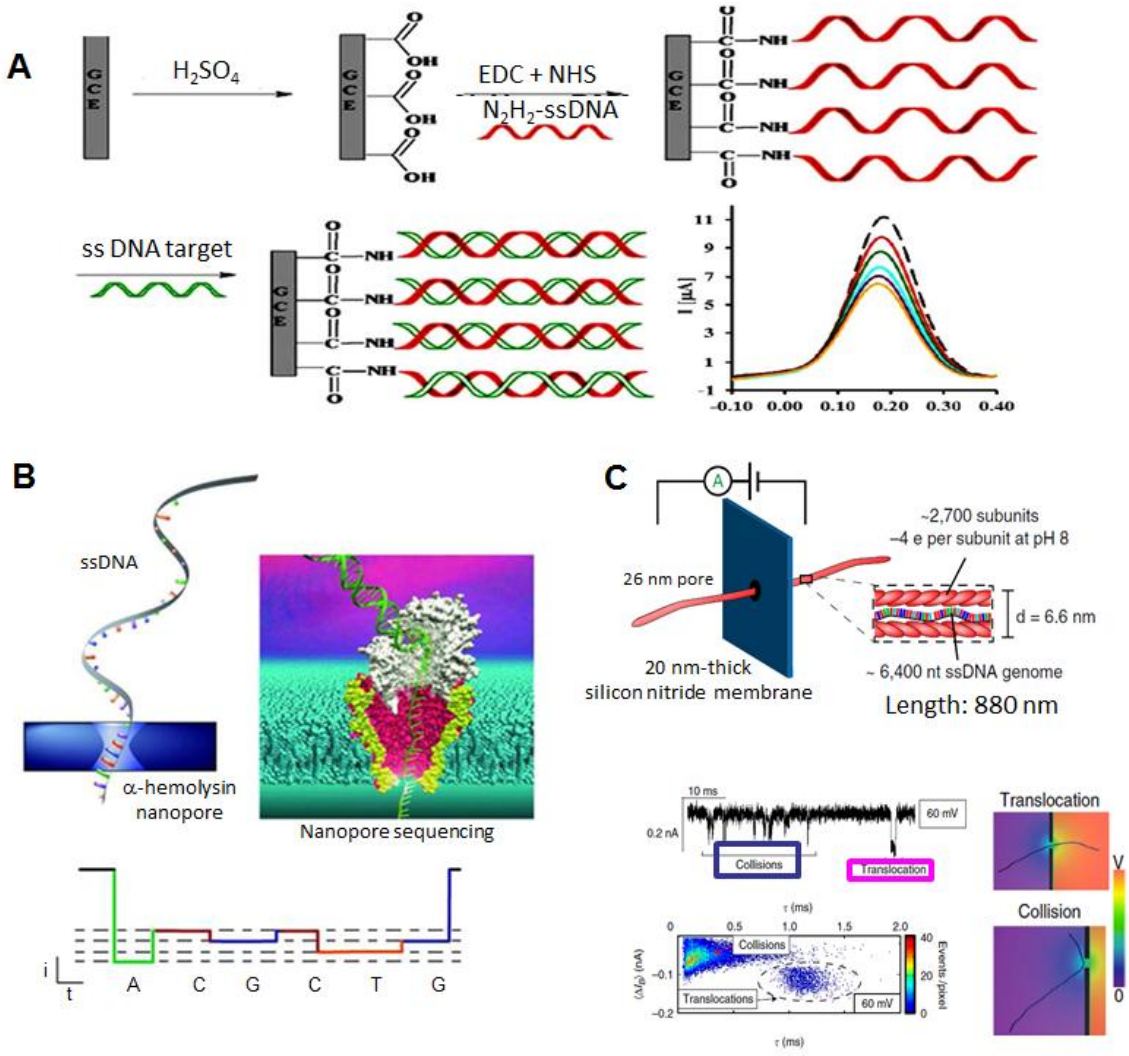

Fig. 6 (A) Example of label-free DNA hybridization approach based on voltammetric analysis applied for *Plum pox virus* (PPV) detection. Voltammetric signals correspond to 1-8 pM. Adapted with permission from [123]. (B) Scheme of the ssDNA translocation through a single α-hemolysin pore and the associated electrical signatures as potential tool for pathogen DNA sequencing: each of the four bases produces characteristic time series recordings. Adapted from [124] with permission. (C) Illustration of a filamentous virus translocation through a single nanopore drilled on silicon nitride membranes (up) and its signatures discriminated from collisions (down) Adapted from [133] with permission.

Optical DNA Sensors

Colorimetric detections of gold nanoparticles (AuNPs) in both lateral flow assays and in aggregation tests, together with the use of fluorescent and colorimetric based microarrays and electrochemiluninescence analysis are the most representative examples of optical approaches for plant pathogen DNA detection. The great potential of nanochannel arrays for this purpose is also highlighted in this section.

Lateral flow assays based on AuNPs

DNA detection on lateral flow (LF) test strips have been developed for the analysis of different plant diseases, in most cases using gold nanoparticle (AuNP) - labeled DNA probes. As example, a competitive DNA hybridization format was presented by Zhao and co-workers for *Acidovorax avenae subsp. Citrulli* (AAC) bacterial disease of melons.[134] The developed strip allowed reaching a low detection limit of 0.48nM. The selectivity of the strip was tested against five other plant bacterial pathogens *Xanthomonas campestris*, *Acidovorax avenae*, *Clavibacter michiganensis*, *Pesudomonas. syringae* and *Erwinia carotovora* and no cross reactivity was observed.

Another application of DNA hybridization on lateral flow using AuNPs-DNA probe was introduced by Wei and co-workers for early detection of *Banana bunchy top virus* (BBTV).[135] In this case, a direct sandwich assay consisting in AuNPs-DNA as detection probe and biotinylated-DNA as capture probe was developed. (**Fig.7**). Qualitative and quantitative measurements of test line color were monitored and a linear calibration plot was found between peak area of test line and different concentrations of target DNA, achieving a detection limit of 0.13 nM. BBTV-DNA lateral flow biosensor achieved higher sensitivity by ten times in comparison to that of electrophoresis. Selectivity of the strip was evaluated, using plant samples infected with other viruses such as *Banana streak virus* (BSV) and *Cucumber mosaic virus* (CMV).

AuNPs aggregation-based DNA analysis and related approaches

AuNPs aggregation-based tests have been extensively used for biomolecules detection and also recently proposed for the detection of plant pathogen DNA. These simple approaches are gaining a great attention for diagnostic applications due to visual detection possibility and low cost of analysis. . This is the case of the approach recently reported by Vaseghi and co-workers who applied this principle for *Pseudomonas syringae* detection (**Fig. 8A**). [136] The system was tested using other plant pathogenic bacteria such as *Pseudomonas viridiflava*, *Pectobacterium cartovortum sub cartovorum*, *Pseudomonas fluoresce*, *Xanthomonas alfalfae subsp. citrumelonis*, *Xanthomonas axonopodis pv. citr* and *Pseudomonas argenus*. The results of this assay showed high specificity and sensitivity in detecting as low as 15 ng/ml of target DNA of *P.syringae* .

Besides gold aggregation mechanism, bridging flocculation is very well-known approach in colloid chemistry since its introduction in 1950s. [137] This kind of approach based on reversible adsorption to differentiate between long and short DNA polymers and has been reported recently for rapid detection significant plant pathogens. [138] This method has been applied for the visual detection of *Pseudomonas syringae* as plant bacterial pathogen and two other devastating pathogenic plant fungi, *Fusarium oxysporum* and *Botrytis cinerea (***Fig. 8B).** Key advantage of flocculation is the reliable detection of the presence of pathogens in plants within very early disease stage nevertheless the plants are symptomless. Qualitative analysis enabled detecting of isothermal DNA amplicons as little as 0.5 ng/µl.

In spite of the great perspectives of these systems, important parameters like the interparticle gap during DNA duplex formation should be carefully considered in the design of the assay so as to avoid losses in sensitivity.

Fluorescent and colorimetric approaches in microfluidics and microarrays systems

Over the last decade, microfluidic chips have been developed as revolution in on-site microbial detection of viruses and bacteria that infect animals and humans.[139-142] First example of the application of a microfluidic system was described for phytopathology detection.[143] Later a similar approach using microfluidic based on silver nanoparticle that serves as detection agent (label) enables visual detection of fungal pathogens of *phytophthora* species.[144] Besides colorimetric approaches, turbidity-based microfluidic system was developed for determination of viral pathogens infecting orchids such as *Cymbidium mosaic virus* (CymMV) and *Capsicum chlorosis viru*s (CaCV).[145,146]

DNA microarray technology for large scale investigation of gene expression variations has been developed whereas it is difficult to be suited to automation due to the need of several manual manipulation steps. In 2000s, applications of DNA microarray were reported on identification of pathogens causing plant diseases.[147- 157] Recently Wang and Li designed microarray based on DNA sequences labeled with fluorescent tags for visual determination of three fungal plant pathogens (*Botrytis cinerea*, *Didymella bryoniae*, and *Botrytis squamosa*).[158] Glass chip and poldimethylsiloxane (PDMS) have been utilized as substrates for the developed microfluidic microarray. Fluorescence signals to the concentrations of target DNA were measured, detecting as low as 1 fM of DNA. Despite limited application of microarray on plant disease detection, microarray allowed flexible DNA probe formation, rapid DNA hybridization using small sample volume. A complete review addressing microarray application in detecting plant viruses was reported (**Fig. 9A**). [159]

Electrochemiluminscence-based DNA detection

The first report of DNA biosensor using $Ru(bpy)_3^{+2}$ electrochemiluminescence (ECL) detection protocol appeared in 1991, in which an excited state emitting light was formed as a result of generation of electron transfer reaction between two charged species such as Ru and TPA on electrode surface.[160,161] ECL has various analytical applications in medical diagnosis and environmental analysis.[162] In spite of the excellent sensitivity of these systems an important limitation appears within solution-based formats that require continuous supply of luminescence reagent. In the recent years, the application of ECL for detection of PCR products is described to quantify plant virus nucleic acid. Tang and co-workers introduced for the first time an improved ECL-PCR detection as a diagnostic assay in plant virology, taking advantage of magnetic beads as a separation tool for the hybridization product exploiting the high affinity of biotin-streptavidin. [163] Three plant viruses such as B*anana streak virus*, *Banana bunchy top virus*, and *Papaya leaf curl virus* were amplified by PCR, then hybridized with a tris(bipyridine) ruthenium (TBR)-labeled detector probe and a capture probe labeled with biotin. The hybridization products were captured onto streptavidin coated magnetic beads and the ECL signal of Ru $(bpy)_3^{2+}$ (TBR label) was generated by using tripropylamine (TPrA) as the co-reactant. This improved ECL-PCR method held a low detection limit down to 50 fM of PCR products through stable ECL signals. Not evaluated is the selectivity of ECL assay but the results showed many advantages over other detection assays including high sensitivity and stability for plant virus detection.

Nanochannel arrays as emerging platforms for DNA analysis

In addition to their properties for electrochemical analysis, nanoporous membranes are also excellent platforms for the development of optical biosensors for DNA analysis. Some nanoporous materials (i.e. nanoporous alumina and nanoporous silicon) possess optical properties that are altered by the presence of analytes captured in the inner walls of the nanochannels without the need of any label. Furthermore, fluorescent tags have also been used for DNA monitoring in nanochannels. [126] As in the case of the electrochemical ones, these optical approaches have not yet been applied for plant pathogen detection but we consider of great interest to show here their outstanding potential. The work by Meller's group for the optical single-molecule DNA sequencing can be selected as illustrative example.[164] A multicolor readout is used after conversion of the target DNA into a binary code, consisting in the biochemical conversion of the nucleotides to known oligonucleotides. Hybridization with molecular beacons, using two different fluorophores was finally detected by translocating the DNA/beacon complex through the nanochannel. Taking advantage of the nanochannels array, the specific location of each channel in the visual field of the optical detector, allowed the simultaneous readout of the array (**Fig. 9B**), which open the way to further applications for multidetection of DNA related to plant pathogens.

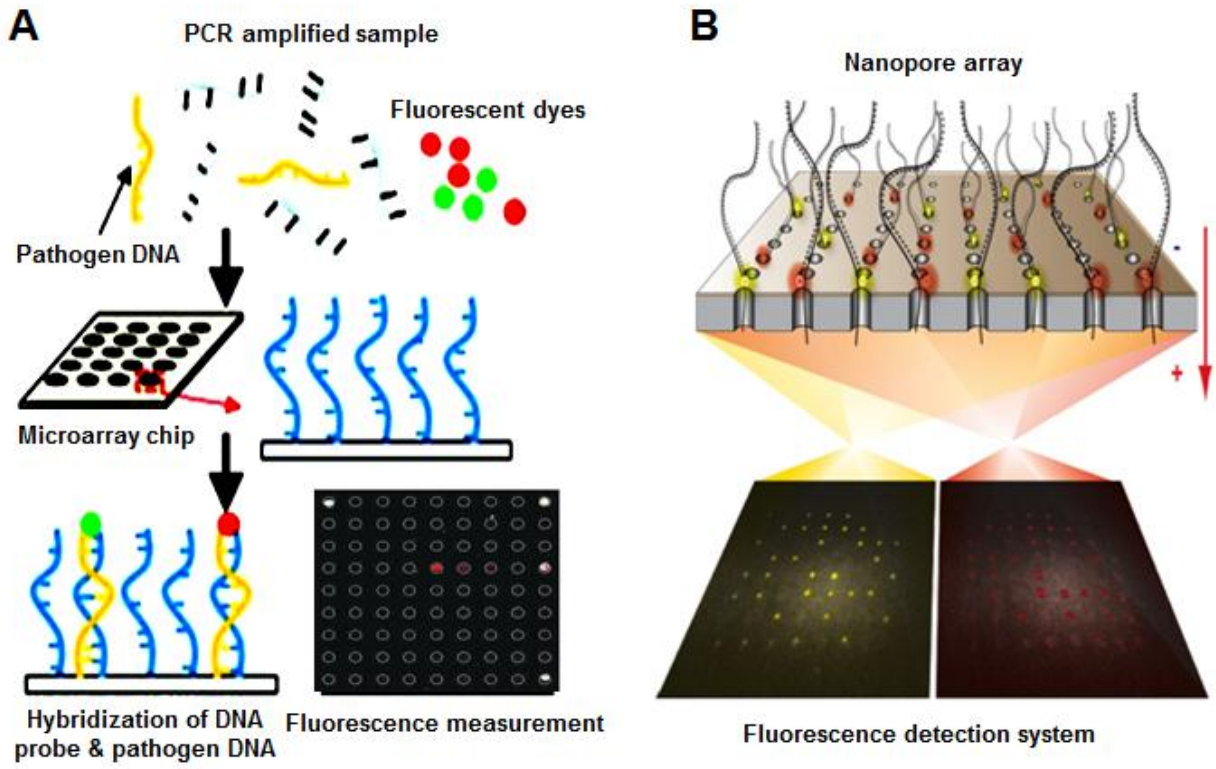

Fig.9 (A) Scheme of DNA microarray technique based on DNA hybridization for pathogen characterization applied for *Broad bean wilt virus* analysis. Red fluorescent pattern indicates to the presence of virus RNA. Adapted with permission from [20, 159]. (B) Illustration of the promising optical platforms based on nanochannel arrays for optical detection of DNA. Adapted with permission from [164].

Commercial Available Devices

Commercial availability of biological recognition elements (i.e. antibody, DNA probe, aptamer) is a key feature required for successful plant disease diagnosis. To date, most commercialized devices for plant pathogen detection based on immunoassays include lateral flow devices, tissue-print ELISA and plate-ELISA kit (**Fig. 10A-D)**. A variety of commercial kits based on immunoassay have been reported in literature such as pocket kit for orchid virus detection, Agritest lateral flow to detect *Erwinia amylovora* bacterial causal agent of pome trees moreover Foresite diagnostic commercial kit for *xanthomonas* wilt of banana plant.[165, 166] Polyclonal and monoclonal antisera are available on the market for diagnosis of viral, bacterial and fungal disease in plants for commercial use. Additionally, DNA& RNA extraction kits have

been designed to isolate total nucleic acid from a variety of plant materials, including leaves, bark and fruits. Examples of well tested kits are DNeasy and RNeasy Plant System from Qiagen, ISOLATE plant DNA kit from Bioline and GenElute plant genomic DNA from Sigma company. Emerging mobile applications are helpful tools for farmers in remote areas to detect and identify plant diseases. As example, Gene- Z is a promising plant disease mobile application based on microfluidic technology; it has applied on quantification of cancer markers. Lately, Gene- Z is ready to be brought to the market for analyzing plant pathogen in the field and it can be an interesting solution for an effective monitoring / control of plant disease spread. (**Fig. 10E)**.

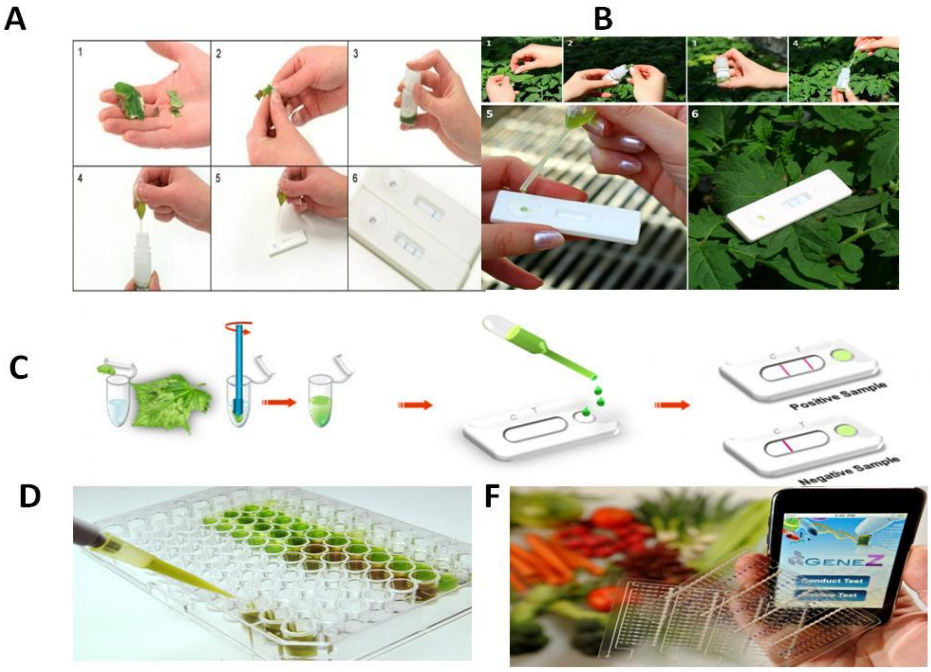

Fig. 10 Commercial devices for the detection of several plant diseases. (A-C) Lateral flow systems commercialized for *phytophthora* species, *Erwinia amylovora* and *Potato virus Y* detection. Adapted with permission from (A) Ref. www.lachandra.com. (B) Ref. www.pocketdiagnostic.com. (C) Ref . www.loewe-info.com. (D) ELISA kit for the detection of *Citrus tristeza virus*, *Acidovorax avenae ssp. citrulli* and *Botrytis cinerea*. Adapted with permission from Ref. www.loewe-info.com. (E) Hybrid smart phone application and microfluidic to identify plant pathogen in minutes as promising device not yet applied on plant disease detection. Adapted with permission from Ref. [167].

Conclusions

In this review we show that early detection of old, new and emerging infectious plant disease plays critical role in plant disease management and also could reduce the damage caused by plant diseases worldwide. Conventional diagnostic techniques could be time consuming, are related to special equipment and require still user/professionals with certain experience. To overcome these difficulties, recent advances in micro and nanotechnologies have enabled for developing biosensors for determination of pathogen infections in plants using antibody and DNA as biosensing receptors. This work intensively reviewed the developed antibody-based and nucleic acid-based biosensors in laboratories worldwide for plant disease detection. Most DNA biosensors techniques are based on determination of DNA hybridization events including electroluminescence, fluorescent and colorimetric approaches in addition to label-free voltammetric etc. In spite of advantages of DNA biosensors in terms of sensitivity, selectivity due to great recognition properties, their in-field application is still suffering from sample treatment requisites (eg. DNA extraction). On the other hand, antibody-based scenarios have been developed using QCM, SPR, fluorescent, voltammetric and label-free impedance detection techniques. Although one would take advantage of high affinity between antibody and specific antigen (related to plant disease) uncontrolled antibody immobilization could obstruct reaching efficient biosensing signal while developing the right detection tool. Although most of reported biosensors for plant disease detection are still for use at lab level, it is expected that more portable devices will emerge in the future being a strong support for an efficient diagnostic. Given the spread of plant disease there is a strong need to develop new biosensors that can be used directly in the field by farmers themselves. Selection of diagnostic route for plant disease detection relies on the event to be analyzed mainly involving i) phytosanitary analysis & plant quarantine ii) routine large scale surveys & disease risk assessment. Sanitary status testing requires the most sensitive method to avoid false positives and discard any pathogen to have pathogen-free mother plants for certification programs. In case of quarantine pathogen

monitoring while import/export of plant materials, experts recommend using more than one diagnostic method to reduce the risk of obtaining false (positives or negatives), therefore nucleic acid-based biosensing approaches are being suitable for fast, sensitive testing of small number of samples and for ensuring the quality of disease-free plant materials. However, antibody/antigen interactions methods can be appropriate for testing large number of suspicious plants for surveillance of plant disease spread. Moreover, selecting diagnostic method for large-scale plant disease screening to evaluate disease incidence requires proper attention to several aspects such as cost of each single test, availability of on-site evaluation and pre- and post-test probability of disease risk. In addition to the innovative field-based devices, novel approaches are needed to limit the possible introduction and spread of foreign plant diseases across national and international borders. Over the long term, we believe the use of nanotechnology with additional efforts will be helping to significantly develop high sensitive and selective biosensors for real-time monitoring of plant pathogens in the field conditions.

REFERENCES

(1) Pimentel, D., Zuniga, R., Morrison, D. *Ecol. Econ.* **2005**, *52*, 273–288.

(2) Oerke, E. *J. Agric. Sci.* **2006**, *144*, 31–43.

(3) Roberts, M.J., Schimmelpfennig, D.E., Ashley, E., Livingston, M.J., Ash, M.S., Vasavada, U., The Value of Plant Disease Early-Warning Systems: A Case Study of USDA‟s Soybean Rust Coordinated Framework; United States Department of Agriculture, Economic Research Service: Washington, DC, USA, 2006.

(4) Savary, S., Ficke, A., Aubertot, J., Hollier, C. *Food Secur.* **2012**, *4*, 519–537.

(5) Martinez, A. Georgia Plant Disease Loss Estimates, 2006.

(6) Martinez, A. Georgia Plant Disease Loss Estimates, 2013.

(7) Dean, R., Van Kan, J.A., Pretorius, Z.A., Hammond, Kosack, K.E., Di Pietro, A., Spanu, P.D., Rudd, J.J., Dickman, M., Kahmann, R., Ellis, J., Foster, G.D. *Mol. Plant Pathol.* **2012**, *13*, 414-430.

(8) Mansfield, J., Genin, S., Magori, S., Citovsky, V., Sriariyanum, M., Ronald, P., Dow, M.A.X., Verdier, V., Beer, S.V., Machado, M.A., Toth, I.A.N. *Mol. Plant Pathol.* **2012**, *13*, 614-629.

(9) Scholthof, K.B.G., Adkins, S., Czosnek, H., Palukaitis, P., Jacquot, E., Hohn, T., Hohn, B., Saunders, K., Candresse, T., Ahlquist, P., Hemenway, C. *Mol. Plant Pathol*. **2011**, *12*, 938-954.

(10) Rybicki, E. P. *Arch. Virol*. **2015**, *160*, 17-20.

(11) López, M.M., Bertolini, E., Olmos, A., Caruso, P., Gorris, M.T., Llop, P., Penyalver, R., Cambra, M. *Int. Microbiol.* **2003**, *6*, 233–243.

(12) Al-Hiary, H., Bani-Ahmad, S., Reyalat, M., Braik, M., ALRahamneh, Z. *Int. J. Comput. Appl.* **2011**, *17*, 31-38.

(13) Anderson, P.K., Cunningham, A.A., Patel, N.G., Morales, F.J., Epstein, P.R. ,Daszak, P. *Trends Ecol. Evol*. **2004**, *19*, 535–44.

(14) Strange, R.N, Scott, P.R. *Annu. Rev. Phytopathol*. **2005**, *43*, 83–116.

(15) Brassier, C.M. *Plant Pathol.* **2008**, *57*, 792–808.

(16) Vincelli, P., Tisserat, N. *Plant Dis*. **2008**, *82*, 660–69.

(17) Miller, S.A., Beed, F.D., Harmon, C.L. *Annu. Rev.Phytopathol.* **2009**, *47*, 15–38.

(18) Scala, A., Allmann, S., Mirabella, R., Haring, M.A., Schuurink, R.C. *Int. J. Mol. Sci*. **2013**, *14*, 17781-17811.

(19) Sankaran, S., Mishra, A., Ehsani, R., Davis, C. *Comput. Electron*. *Agric*. **2010**, *72*, 1-13.

(20) Nezhad, A.S. *Lab on a Chip* **2014**, *14*, 2887-2904.

(21) Fang, Y., Ramasamy, R.P. Biosens. **2015**, *5*, 537-561.

(22) Martinelli, F., Scalenghe, R., Davino, S., Panno, S., Scuderi, G., Ruisi, P., Villa, P., Stroppiana, D., Boschetti, M., Goulart, L.R., Davis, C.E. *Agron. Sustain.e Dev.* **2015**, *35*, 1-25.

(23) Lin, N.S., Hsu, Y.H., Hsu, H.T. *Phytopathol.* **1990**, *80*, 824-828.

(24) Minsavage, G.V., Thompson, C.M., Hopkins, D.L., Leite, R.M.V.B.C., Stall, R.E. *Phytopathol.* **1994**, *84*, 456–461.

(25) Anwar Haq, M., Collin, H.A., Tomsett, A.B., Jones, M.G. *Physiol. Mol.* **2003**, *62*, 185–189.

(26) Das, A.K. *Curr. Sci.* **2004**, 87, 1183–1185.

(27) Teixeira, D.C., Danet, J.L., Eveillard, S., Martins, E.C., Junior, W.C.J., Yamamoto, P.T., Lopes, S.A., Bassanezi, R.B., Ayres, A.J., Saillard, C., Bové, J.M. *Mol. Cell. Probes* **2005**, *19*, 173–179.

(28) Li, W., Hartung, J.S., Levy, L. *J. Microbiol.Methods* **2006**, *66*, 104–115.

(29) Lacava, P.T., Li, W.B., Araújo, W.L., Azevedo, J.L., Hartung, J.S. *J. Microbiol.Methods* **2006**, *65*, 535–541.

(30) Saponari, M., Manjunath, K., Yokomi, R.K. *J Virol. Methods* **2008**, *147*, 43–53.

(31) Urasaki, N., Kawano, S., Mukai, H., Uemori, T., Takeda, O., Sano, T. *J. Gen. Plant Pathol*. **2008**, *74*, 151–155.

(32) Fang, Y., Xu, L.H., Tian, W.X., Huai, Y., Yu, S.H., Lou, M.M., Xie, G.L. *Rice Sci.* **2009**, *16*, 157–160.

(33) Li, W., Abad, J.A., French-Monar, R.D., Rascoe, J., Wen, A., Gudmestad, N.C., Secor, G.A., Lee, I.M., Duan, Y., Levy, L. *J. Microbiol.Methods* **2009**, *78*, 59–65.

(34) Ruiz-Ruiz, S., Ambrós, S., Carmen Vives, M., Navarro, L., Moreno, P., Guerri, J. *J. Virol. Methods* **2009**, *160*, 57–62.

(35) Gutiérrez-Aguirre, I., Mehle, N., Deli´ c, D., Gruden, K., Mumford, R., Ravnikar, M. *J. Virol. Methods* **2009**, *162* , 46–55.

(36) Yvon, M., Thébaud, G., Alary, R., Labonne, G. *Mol. Cell Probes* **2009**, *23*, 227–234.

(37) Avrameas, S. *Immunochem*. **1969**, *6*, 43-52.

(38) Van Weemen, B.K., Schuurs, A.H.W.M. *FEBS letters* **1971**, *15*, 232-236.

(39) Garnsey, S.M., Permar, T.A., Cambra, M., Henderson, C.T. In Proc. 12th Conf. IOCV (39-50). IOCV Riverside, CA, 1993.

(40) Cambra, M., Gorris, M.T., Román, M.P., Terrada, E., Garnsey, S.M., Camarasa, E., Olmos, A., Colomer, M., 2000. In 14th Conference of the International Organization of Citrus Virologist. da GRAÇA, JV (34-41).

(41) Nolasco, G., Sequeira, Z., Soares, C., Mansinho, A., Bailey, A.M., Niblett, C.L. *Eur. J. Plant Pathol.* **2002**, *108*, 293-298.

(42) Holzloehner, P., Schliebs, E., Maier, N., Funer, J., Micheel, B., Heilmann, K. *J. Immunol.* **2013**, *190*(Meeting Abstracts 1), 135-14.

(43) Escoffier, L., Ganau, M., Wong, J. Commercializing nanomedicine: industrial applications, patents, and ethics, 2016.

(44) Louws, F.J., Rademaker, J.L.W., De Bruijn, F.*J. Annu. Rev. Phytopathol.* **1999**, *37*, 81-125.

(45) Schaad, N.W., Frederick, R.D. *Can. J. Plant Pathol.* **2002**, *24*, 250-258.

(46) Eggins, B.R. Chem. Sensors Biosens., New York, 2008.

(47) Sadanandom, A., Napier, R.M. *Curr. Opin. Plant Biol*. **2010**, *13*, 736–743.

(48) Singh, A., Poshtiban, S., Evoy, S. *Sens*. **2013**, *13*, 1763-1786.

(49) Skottrup, P.D., Nicolaisen, M., Justesen, A.F. *Biosens. Bioelectron*. **2008**, *24*, 339-348.

(50) Hushiarian, R., Yusof, N.A., Abdullah, A.H., Ahmad, S.A.A., Dutse, S.W. *Anal. Chem. Res*. **2015**, *6*, 17-25.

(51) http://www.crec.ifas.ufl.edu/extension/greening/symptoms.shtml. Viewed on Sunday, 22, May, 2016.

(52) Schofield, D.A., Bull, C.T., Rubio, I., Wechter, W.P., Westwater, C., Molineux, I.J. *Bioengineered* **2013**, *4*, 50-54.

(53) Engvall, E., Perlmann, P. *Immunochem.* **1971**, *8*, 871-874.

(54) Rossier, J.S., Girault, H.H. *Lab on a Chip* **2001**, *1*, 153-157.

(55) Sarkar, P., Pal, P.S., Ghosh, D., Setford, S.J.,Tothill, I.E. *Int. J. Pharm*. **2002**, *238*, 1-9.

(56) Paternolli, C., Antonini, M., Ghisellini, P., Nicolini, C., 2004. Langmuir 20(26), 11706-11712.

(57) Zhang, Y., Jiao, K., Liu, C., Yang, Z.X. *Electroanal*. **1995a**, *7*,283-286.

(58) Zhang, Y., Jiao, K., Liu, C., Yang, Z.X. *Electroanal*. **1995b**, *7*, 283-286.

(60) Lee, H.Y., Jung, H.S., Fujikawa, K., Park, J.W., Kim, J.M., Yukimasa, T., Sugihara, H., Kawai, T. *Biosens. Bioelectron.* **2005**, *21*, 833-838.

(61) Thompson, R.Q., Barone, G.C., Halsall, H.B., Heineman, W.R. *Anal. Biochem*. **1991**, *192*, 90-95.

(62) Jiang, T., Halsall, H.B., Heineman, W.R., Giersch, T.,Hock, B. *J. Agric.Food Chem*. **1995**, *43*, 1098-1104.

(63) Jiao, K., Sun, W., Zhang, S.S. *Fresenius' J. Anal. Chem*. **2000**, *367*, 667-671.

(64) Zhao, Y., Liu, L., Kong, D., Kuang, H., Wang, L., Xu, C. *ACS App. Mater. Interfaces* **2014,** *6*, 21178-21183.

(65) Jarocka, U., Radecka, H., Malinowski, T., Michalczuk, L.,Radecki, *J. Electroanal.* **2013**, *25*, 433-438.

(66) Newman, A. L., Hunter, K. W., Stanbro, W. D. In Proc. 2nd Int. Meet. Chem. Sens. France, 1986, 596-598.

(67) Bataillard, P., Gardies, F., Jaffrezic-Renault, N., Martelet, C., Colin, B., Mandrand, B. *Anal. Chem.* **1988**, *60*, 2374-2379.

(68) Katz, E., Willner, I. *Electroanal*. **2003**, *15*, 913-947.

(69) K'Owino, I.O., Sadik, O.A. *Electroanal.* **2005**, *17*, 2101-2113.

(70) Prodromidis, M.I. Pak. *J. Anal. Environ. Chem*. **2007**, *2*, 69-71.

(71) Daniels, J.S., Pourmand, N. *Electroanal*. **2007**, *19*, 1239-1257.

(72) Kausaite-Minkstimiene, A., Ramanaviciene, A., Kirlyte, J., Ramanavicius, A. *Anal. Chem.* **2010**, *82*, 6401-6408.

(73) Porter, M.D., Bright, T.B., Allara, D.L., Chidsey, C.E. *J Am. Chem. Soc.* **1987**, *109*, 3559-3568.

(74) Love, J.C., Estroff, L.A., Kriebel, J.K., Nuzzo, R.G., Whitesides, G.M. *Chem. Rev.* **2005**, *105*,1103-1169.

(75) Jarocka, U., Wąsowicz, M., Radecka, H., Malinowski, T., Michalczuk, L.,Radecki, *J. Electroanal.* **2011**, *23*, 2197-2204.

(76) Kanazawa, K.K., Gordon, J.G. *Anal.Chem.* **1985**, 57, 1770-1771.

(77) O'sullivan, C.K., Guilbault, G.G. *Biosens. Bioelectron.* **1999**, *14*, 663-670.

(78) Si, S.H., Li, X., Fung, Y.S., Zhu, D.R. *Microchem. J.* **2001**, *68*, 21-27.

(79) Pohanka, M., Skládal, P., Pavliš, O. *J. Immunoass. Immunochem.* **2007**, 29, 70-79.

(80) Liu, F., Li, Y., Su, X.L., Slavik, M.F., Ying, Y., Wang, J. *Sens. Instrum. Food Qual. Saf.* **2007**, *1*, 161-168.

(81) Bragazzi, N.L., Amicizia, D., Panatto, D., Tramalloni, D., Valle, I., Gasparini, R. *Adv. Protein Chem. Struct. Biol.* **2015**, *101*, 149-211.

(82) Eun, A.J.C., Huang, L., Chew, F.T., Li, S.F.Y., Wong, S.M. *J. Virol. Methods* **2002**, 99, 71-79.

(83) Papadakis, G., Skandalis, N., Dimopoulou, A., Glynos, P., Gizeli, E. *PloS one* **2015**, *10*, e0132773.

(84) Huang, X., Xu, J., Ji, H.F., Li, G., Chen, H. *Anal. Methods* **2014**, *6*, 4530-4536.

(85) Parolo, C., Merkoçi, A. *Chem. Soc. Reviews* **2013**, *42*, 450-457.

(86) Quesada-González, D., Merkoçi, A. *Biosens. Bioelectron.* **2015**, 73, 47-63.

(87) Parolo, C., de la Escosura-Muñiz, A., Merkoçi, A. *Biosens. Bioelectron.* **2013a**, *40*, 412-416.

(88) Parolo, C., Medina-Sánchez, M., de la Escosura-Muñiz, A., Merkoçi, A. *Lab on a Chip* **2013b** , *13*, 386-390.

(89) Rivas, L., de la Escosura-Muñiz, A., Serrano, L., Altet, L., Francino, O., Sánchez, A., Merkoçi, A. *Nano Res*. **2015**, 8, 3704-3714.

(90) Rivas, L., Medina-Sánchez, M., de la Escosura-Muñiz, A., Merkoçi, A. *Lab on a Chip* **2014**, *14*, 4406-4414.

(91) Morales-Narváez, E., Naghdi, T., Zor, E., Merkoçi, A. *Anal.Chem.* **2015**, *87*, 8573-8577.

(92) Nunes Pauli,G.E.,de la Escosura-Muñiz, A., Parolo, C., Bechtold, I.H., Merkoçi, A. *Lab on a Chip* **2015**, *15*, 399-405.

(93) Tsuda, S., Kameya-Iwaki, M., Hanada, K., Kouda, Y., Hikata, M., Tomaru, K. *Plant Dis*. **1992**, *76*, 466-469.

(94) Danks, C., Barker, I. *EPPO Bulletin* **2000**, 30, 421-426.

(95) Salomone, A., Mongelli, M., Roggero, P.,Boscia, D. *J. Plant Pathol*. **2004**, 43-48.

(96) Drygin, Y.F., Blintsov, A.N., Grigorenko, V.G., Andreeva, I.P., Osipov, A.P., Varitzev, Y.A., Uskov, A.I., Kravchenko, D.V.,Atabekov, J.G. *Appl. Microbiol. Biotech.* **2012**, *93*, 179-189.

(97) Feng, M., Kong, D., Wang, W., Liu, L., Song, S., Xu, C. *Sensors* **2015**, *15*, 4291-4301.

(98) Zhang, F., Zou, M., Chen, Y., Li, J., Wang, Y., Qi, X., Xue, Q. *Biosens. Bioelectron*. **2014**, *51*, 29-35.

(99) Charlermroj, R., Himananto, O., Seepiban, C., Kumpoosiri, M., Warin, N., Oplatowska, M., Gajanandana, O., Grant, I.R., Karoonuthaisiri, N., Elliott, C.T. *PloS one* **2013**, *8*, e62344.

(100) Bergervoet, J.H., Peters, J., van Beckhoven, J.R., van den Bovenkamp, G.W., Jacobson, J.W., van der Wolf, J.M. *J. Virol. Methods* **2008**, *149*, 63-68.

(101) Kim, J.S., Taitt, C.R., Ligler, F.S., Anderson, G.P. *Sens. Instrum. Food Qual. Saf.* **2010**, *4*, 73-81.

(102) Mushaben, E.M., Brandt, E.B., Hershey, G.K.K., Le Cras, T.D. *PloS one* **2013**, *8*, e54426.

(103) Van Regenmortel, M.H., Pellequer, J.L. *Pept. Res*. **1993**, *7*, 224-228.

(104) Deisingh, A.K., Thompson, M. Can. *J. Microbiol.* **2004**, *50*, 69-77.

(105) Bergwerff, A.A., Van Knapen, F. *J. AOAC Intern.* **2006**, *89*, 826-831.

(106) Mazumdar, S.D., Barlen, B., Kramer, T., Keusgen, M. *J. Microbiol. Methods* **2008**, *75*, 545-550.

(107) Dudak, F.C., Boyacı, İ.H. *Biotech. J.* **2009**, *4*, 1003-1011.

(108) Altschuh, D., Dubs, M.C., Weiss, E., Zeder-Lutz, G., Van Regenmortel, M.H.

Biochem. **1992**, *31*, 6298–6304.

(109) Boltovets, P.M., Boyko, V.R., Kostikov, I.Y., Dyachenko, N.S., Snopok, B.A., Shirshov, Y.M. *J. Virol. Methods* **2002**, *105*, 141-146.

(110) Zezza, F., Pascale, M., Mulè, G., Visconti, A. *J. Microbial. Methods* **2006**, *66*, 529-537.

(111) Torrance, L., Ziegler, A., Pittman, H., Paterson, M., Toth, R., Eggleston, I. *J. Virol. Methods* **2006**, *134*, 164-170.

(112) Skottrup, P., Hearty, S., Frøkiær, H., Leonard, P., Hejgaard, J., O'Kennedy, R., Nicolaisen, M., Justesen, A.F. *Biosens. Bioelectron.* **2007a**, *22*, 2724-2729.

(113) Skottrup, P., Nicolaisen, M., Justesen, A.F. *J. Microbiol. Methods* **2007b**, *68*, 507-515.

(114) Wang, R., Minunni, M., Tombelli, S., Mascini, M. *Biosens. Bioelectron*. **2004**, *20*, 598-605.

(115) Candresse, T., Lot, H., German-Retana, S., Krause-Sakate, R., Thomas, J., Souche, S., Delaunay, T., Lanneau, M.,Le Gall, O. *J. Gen. Virol.* **2007**, *88*, 2605-2610.

(116) Lautner, G., Balogh, Z., Bardóczy, V., Mészáros, T., Gyurcsányi, R.E. *Analyst* **2010**, *135*, 918-926.

(117) Lin, H.Y., Huang, C.H., Lu, S.H., Kuo, I.T., Chau, L.K. *Biosens. Bioelectron.* **2014**, *51*, 371-378.

(118) Liu, X. J., Tan, W. H. *Anal. Chem.* **1999**, *71*, 5054.

(119) Azek, F.,Grossiord, C., Joannes, M., Limoges, B., Brossier, P. *Anal. Biochem.* **2000**, *284*, 107.

(120) Wang, J., Li, J. H., Baca, A. J., Hu, J. B., Zhou, F. M., Yan, W.,Pang, D. W. *Anal. Chem*. **2003**, *75*, 3941.

(121) Gao, Z., Rafea, S., Lim, L. H. *Adv. Mater.* **2007**, *19*, 602.

(122) Lillis, B., Manning, M., Hurley, E., Berney, H., Duane, R., Mathewson, A., Sheehan, M. M. *Biosens. Bioelectron.* **2007**, *22*, 1289.

(123) Malecka, K., Michalczuk, L., Radecka, H.,Radecki, J. *Sensors* **2014**, *14*, 18611-18624.

(124) Wongkaew, P., Poosittisak, S. *Am. J. Plant Sci*. **2014**, *5*, 2256

(125) Siddiquee, S., Rovina, K., Yusof, N.A., Rodrigues, K.F., Suryani, S. *Sens. Biosens. Res.* **2014**, *2*, 16–22.

(126) De la Escosura-Muñiz, A., Merkoçi, A. *ACS Nano* **2012**, *6* , 7556–7583.

(127) Coulter, W.H. U.S. Patent 2656508 A, 1953.

(128) Kasianowicz, J., Brandin, E., Branton, D., Deamer, D. Proc. Natl. Acad. Sci. 1996, USA, 93, 13770–13773.

(129) Bayley, H., Cremer, P.S. *Nature* **2001**, *413*, 226–230.

(130) Siwy, Z.S., Howorka, S. *Chem. Soc. Rev.* **2010**, *39*, 1115–1132.

(131) De la Escosura-Muñiz, A., Merkoçi, A. *Chem. Commun.* **2010**, *46*, 9007-9009.

(132) De la Escosura-Muñiz, A., Merkoçi, A. *TRAC* **2016**, *79* ,134–150.

(133) McMullen, A., de Haan, H.W., Tang, J.X., Stein, D. *Nat. Commun*. **2014**, *5*, 4171.

(134) Zhao, W., Lu, J., Ma, W., Xu, C., Kuang, H., Zhu, S. *Biosens. Bioelectron*. **2011**, *26*, 4241-4244.

(135) Wei, J., Liu, H., Liu, F., Zhu, M., Zhou, X., Xing, D. *ACS appl. Mater. interfaces* **2014**, *6*, 22577–22584.

(136) Vaseghi, A., Safaie, N., Bakhshinejad, B., Mohsenifar, A., Sadeghizadeh, M. *Sens. Actuators B- Chem.* **2013**, *181*, 644-651.

(137) Ruehrwein, R.A., Ward, D.W. *Soil Sci.* **1952**, *73*, 485-492.

(138) Wee, E.J.H., Lau, H.Y., Botella, J.R., Trau, M. *Chem. Commun*. **2015**, *51*, 5828-5831.

(139) Figeys, D., Pinto, D. *Anal. Chem.* **2000**, *72*, 330.

(140) Kricka, L. *J. Clin. Chim. Acta* **2001**, *307*, 219-223.

(141) Huang, C.H., Lai, G.H., Lee, M.S., Lin, W.H., Lien, Y.Y., Hsueh, S.C., Kao, J.Y., Chang, W.T., Lu, T.C., Lin, W.N., Chen, H.J. *J. App. Microbiol.* **2010**, *108*, 917-924.

(142) Wang, C.H., Lien, K.Y., Wu, J.J., Lee, G.B. *Lab on a Chip* **2011**, *11*, 1521-1531.

(143) Julich, S., Riedel, M., Kielpinski, M., Urban, M., Kretschmer, R., Wagner, S., Fritzsche, W., Henkel, T., Möller, R., Werres, S. *Biosens. Bioelectron.* **2011**, 26, 4070-4075.

(144) Schwenkbier, L., Pollok, S., König, S., Urban, M., Werres, S., Cialla-May, D., Weber, K., Popp, *J. Anal.Methods* **2015**, *7*, 211-217.

(145) Chang, W.H., Yang, S.Y., Lin, C.L., Wang, C.H., Li, P.C., Chen, T.Y., Jan, F.J., Lee, G.B. *Nanomed.: Nanotech. Biol. Med.* **2013**, *9*, 1274-1282.

(146) Lin, C.L., Chang, W.H., Wang, C.H., Lee, C.H., Chen, T.Y., Jan, F.J., Lee, G.B. *Biosens. Bioelectron.* **2015**, *63*, 572-579.

(147) Bonants, P., De Weerdt, M., Van Beckhoven, J., Hilhorst, R., Chan, A., Boender, P., Zijlstra, C., Schoen, C. In: Abstracts Agricultural Biomarkers for Array Technology, Management Committee Meeting, Wadenswil (Vol. 20), 2002.

(148) Bystricka, D., Lenz, O., Mraz, I., Dědic, P., Sip, M., 2002. Acta Virol. 47(1), 41-44.

(149) Nicolaisen, M. In: Abstracts Agricultural Biomarkers for Array Technology, Management Committee Meeting, Wadenswil (vol. 22), 2002.

(150) Perez-Ortin, J.E. In: Abstracts Agricultural Biomarkers for Array Technology, Management Committee Meeting, Wadenswil (vol. 13), 2002.

(151) Sip, M., 2002. In: Abstracts Agricultural Biomarkers for Array Technology, Management Committee Meeting, Wadenswil (vol.24).

(152) Schoen, C., De Weerdt, M., Hillhorst, R., Chan A., Boender, P., Zijlstra, C., Bonants, P.,In: Abstracts Agricultural Biomarkers for Array Technology, Management Committee Meeting, Wadenswil (vol. 11), 2002.

(153) Schoen, C., De Weerdt, M., Hillhorst, R., Boender, P., Szemes, M., Bonants, P. In: Abstracts of the 19th International Symposium on Virus and Virus-like Diseases of Temperate Fruit Crops, Valencia (vol. 108), 2003.

(154) Boonham, N., Walsh, K., Smith, P., Madagan, K., Graham, I., Barker, I. *J. Virol. Method*s **2003**, *108*, 181-187.

(156) Mumford, R.A., Jarvis, B., Harju, V., Boonham, N., Skelton, A. *Plant Pathol.* **2006** , *55*, 819-819.

(157) Zhang, Y., Yin, J., Jiang, D., Xin, Y., Ding, F., Deng, Z., Wang, G., Ma, X., Li, F., Li, G., Li, M. *PloS one* **2013**, *8*, e64474.

(158) Wang, L., Li, P.C. *J. Agri. Food Chem.* **2007**, *55*, 10509–10516.

(159) Boonham, N., Tomlinson, J., Mumford, R. *Annu. Rev. Phytopathol.* **2007**, *45*, 307-328.

(160) Blackburn, G.F., Shah, H.P., Kenten, J.H., Leland, J., Kamin, R.A., Link, J., Peterman, J., Powell, M.J., Shah, A.,Talley, D.B.*Clin. Chem.* **1991**, *37*, 1534-1539.

(161) Richter, M.M. *Chem. Reviews* **2004**, *104*, 3003-3036.

(162) Van Ingen, H.E., Chan, D.W., Hubl, W., Miyachi, H., Molina, R., Pitzel, L., Ruibal, A., Rymer, J.C., Domke, I. *Clin. Chem*. **1998**, *44*, 2530-2536.

(163) Tang, Y.B., Xing, D., Zhu, D.B., Liu, J.F. *Anal. Chim. Acta* **2007**, *582*, 275-280.

(164) McNally, B., Singer, A., Yu, Z., Sun, Y., Weng, Z., Meller, A. *Nano Lett.* **2010**, *10*, 2237–2244.

(165) Braun-Kiewnick, A., Altenbach, D., Oberhänsli, T., Bitterlin, W., Duffy, B. *J. Microbiol. Methods* **2011**, *87*, 1-9.

(166) Hodgetts, J., Karamura, G., Johnson, G., Hall, J., Perkins, K., Beed, F., Nakato, V., Grant, M., Studholme, D.J., Boonham, N.,Smith, *J. Plant Pathol.* **2015**, *64*, 559-567.

(167) < http://www.treehugger.com

Chapter II

Objectives

This thesis aims at developing sensitive, affordable and portable biosensors based on nanomaterials for the determination of nucleic acid related to plant pathogens. The work strives to contribute to the keeping up in the advancements of biosensing systems relevant to plant infection diagnostics which would be an essential solution in the future to the issues of plant disease monitoring and food security. Following **Chapter I**, state-of-the-art on the latest trends in the development of advantageous biosensors based on both antibody and DNA receptors for early plant disease detection, as well as the use of different nanomaterials such as nanochannels and metallic nanoparticles for the development of innovative and sensitive biosensing systems for the detection of pathogens (i.e. bacteria and viruses) at the point-of-care is given. The next sections of this dissertation will describe three diagnostic biosensing strategies for the detection of citrus tristeza virus (CTV) related nucleic acid using electrical and optical transducing techniques. The electrical sensing of CTV through DNA hybridization based approach and the *in situ* amplified nucleic acid method will be achieved on carbon sensing substrate modified with gold nanoparticles, while paper-based sensors will be operated in lateral flow format for the gold nanoparticle-based optical detection of CTV. Furthermore, all aspects of the developed biosensing systems, from the bioassay and biosensor design to their development and optimization are presented in which will be organized in the following manner:

Chapter III will present highly specific DNA hybridization sensor based on AuNP-modified SPCE employing label-free impedance for the detection of the CTV-related nucleic acid, together with dedicating emphasis to the study of electrodeposition time of AuNPs, whose precise particle size and shape will be required for the enhancement of DNA hybridization rate. A set of voltammetric studies of deposited AuNPs will be discussed. Particular attention will be paid for assembling the thiolated DNA probe as sensing layer for biosensor construction. The main sensor design aspects such as AuNPs size, probe DNA concentration and immobilization

time together with DNA hybridization time will be optimized, in order to precisely select the best working conditions for this diagnostic platform.

Chapter IV will cover the whole process undertaken for preparation of *in situ* nucleic acid amplification on gold nanoparticle-modified sensor for sensitive and quantitative detection of CTV. Plant disease (*Citrus tristeza* virus (CTV)) diagnostics was selected as relevant target for the demonstration of the proof-of-concept. This chapter will include two parts, the first one focuses on the design of RPA amplification assay, primers design, optimization of all essential bioassay aspects such as amplification temperature, volume and screening primers and finally the electrophoresis analysis for RPA products. The second part of this chapter will demonstrate label-free highly integrated *in situ* RPA amplification/detection approach at room temperature that takes advantage of the high sensitivity offered by gold nanoparticle-modified sensing substrates and electrochemical impedance spectroscopic (EIS) detection.

Chapter V focuses on the application of isothermal nucleic acid amplification technology in simple lateral flow platform. The preparation of AuNP-based LFA for the highly sensitive direct detection of RPA amplified nucleic acid, the assembling of lateral flow step, the conjugation of AuNPs to the antibodies used for colorimetric detection, as well as the optimization of all working conditions and finally the analytical performance of the bioassay in LF will be explored. Moreover, aiming at truly achieving the point of care requirements of simple and affordable diagnostic technologies, the work here will present the possibility of amplifying nucleic acid without heat source and visual color detection. This approach would be of great potential as point of care diagnostics.

Chapter III

Impedance Detection of Plant Virus

Electrochemical Detection of Plant Virus Using Gold Nanoparticle-Modified Electrodes

Plant diseases have great impact on global plant production threating world food security.[1, 2] Their causal agents include nonpathogenic factors such as environment, mechanical and chemical or pathogenic agents mainly viruses, fungi, bacteria and nematodes, etc. The most frequent methods for plant disease detection are based on nucleic acid and protein analysis. Over the past two decades, major advances in nanotechnology have allowed plant pathologists to integrate new technologies with molecular biology for plant disease diagnosis. In recent years, several reviews on developing biosensing systems for plant disease detection were reported.[3-6] Among major citrus viruses, *Citrus tristeza virus* (CTV) has caused high plant death rates around the world especially where citrus seedlings grafted onto sour orange rootstocks (the most susceptible to sever strains of tristeza) are cultivated.[7,8] Tristeza infects the phloem cells then systematically invades the tree causing variable symptoms that may include small fruit with low quality, general yellowing, step-pitting and quick decline. [9-11]The CTV-infected plants may display symptoms ranging from mild to severe depending mostly on the virus variant and susceptibility of plant variety. According to European and Mediterranean Plant Protection Organization (EPPO), CTV is a quarantine pathogen. Most reported serological assays to identify the coat protein of CTV are mainly ELISA, direct tissue print immunoassays (Bar-Joseph *et al*., 1978; Huang *et al*., 2004) and very recently lateral flow immunoassay and label-free electrochemical immunosensor were developed for CTV detection.[12,13] Since reverse transcription polymerase chain reaction (RT-PCR) and dot- blot hybridization based methods are the most commonly used in molecular diagnostics of CTV, a combination of reverse

transcription with loop-mediated isothermal amplification technology (RT-LAMP) has been recently developed.[14,15] However, these methodologies are time-consuming, requiring specialized personnel and also have limitations related to primer design.

Applications of electrochemical nucleic acid sensing in disease diagnostics are growing tremendously over the last decades. Electrical detection of DNA hybridization using sensors has offered great sensitivity, cost-effective and easy rapid DNA analysis avoiding the limits of classical DNA hybridization detection techniques such as membrane blots and gel electrophoresis.

To date, several studies have reviewed electrochemical nucleic acid biosensors based on different electrochemical approaches and have discussed the recent strategies for DNA immobilization and hybridization detection techniques.[19-24] Earlier publications addressed detection of nucleic acid of infectious agents using voltammetric, amperometric and impedance electrochemical approaches.[25-28] Notably, DNA hybridization biosensors based on electrochemical spectroscopy impedance (EIS) are being developed in both label-free formats and label-based approaches using mostly gold nanoparticle (AuNP) and cadmium sulfide quantum dot (CdS QD) as tags [29-37] also employing other nanomaterials.[30-32, 38-42]

Modification of electrode surface for immobilization of biorecognition receptor (i.e. DNA probes, antibody, aptamer, etc.) is the key to successful monitoring of DNA hybridization event. Most of such impedimetric DNA sensors have been designed forming self-assembled monolayers (SAM) on gold electrodes and films of conducting polymers (i.e. pyrrole) and nanomaterials, especially AuNPs, as electrode modifiers.[43-45] Introducing AuNPs into electrochemical DNA sensing electrodes offers several advantages over other metal nanoparticles and oxides. Unlike graphene and iron oxides, the strong stable gold (Au) –sulfur (S) bond together with their unique properties such as large surface and high conductivity, providing efficient immobilization of bio-receptor probes have made AuNPs as the most popular

nanomaterial, extensively exploited in the design of biosensors.[46-48] Label-free sensors using impedimetric detection and label-based voltammetric approaches using enzymes or methylene blue tags on gold and carbon electrodes have been extensively reported.[49-53]

Due to significant improvement in biosensor technology over the last two decades, applications of screen-printed electrodes (SPEs) in electrochemical DNA hybridization biosensors are in increase because of their simplicity, portability and the use of economical substrates. Moreover these SPEs offer the possibility of small-volume bioassays and can be combined with electrodeposited nanoparticles, especially AuNPs.[33, 54-56]

In this context, we propose for the first time to combine the advantages of AuNP-modified electrodes and EIS-based DNA hybridization detection for the development of a biosensor for CTV-related DNA determination. Such biosensor would be of high potential interest for in-field applications in the relevant field of plant pathogen detection. A scheme of the developed DNA biosensing platform is shown at Figure 1.

The presence of AuNPs in the as-modified electrode (200 seconds of electrodeposition) was also evaluated by CV in 0.5 M H_2SO_4 solution (Figure 3A). An anodic current peak at around +0.9 V and a cathodic counterpart at around +0.5 V were observed for the AuNP-modified electrodes (Figure 3A-solid line), which reflect the oxidation of AuNPs and the subsequent reduction of the gold oxide species back to metallic gold, respectively. In contrast, there was no appearance of any distinct faradaic current peak for bare SPCE (Figure 3A-dotted line).

The effect of the AuNPs on the electrode electron transfer was also evaluated by CV in 0.5 mM $K_3[Fe(CN)_6]/K_4[Fe(CN)_6]$ (Figure 3B). A pair of well-defined red-ox peaks corresponding to oxidation/reduction of the pair $Fe[(CN)_6]^{3-}$/ $Fe[(CN)_6]^{4-}$ at +0.36 V/+0.12 V were observed for both the bare (Figure 3B-dotted line) and AuNP-modified SPCE (Figure 3B-solid line). The increase in the electron transfer on the electrode thanks to the presence of the AuNPs is evident when comparing the peak current intensities, observing an increase of 28 % in the current for the modified SPCE.

Impedimetric investigation in 0.5 M $K_3[Fe(CN)_6]/K_4[Fe(CN)_6]$ solution also evidences the modification of SPCEs with AuNPs. A well-defined semicircle along Z‟ with diameter corresponding to Rct resistance was obtained for both bare (Figure 3C-dotted line) and AuNP-modified SPCE (Figure 3C-solid line). The lower impedance recorded for the modified electrode (185 % decrease in the Rct) evidences the improved electrical conductivity raised by the presence of AuNPs.

DNA Hybridization Biosensor Optimization

The main parameters affecting the performance of the DNA hybridization biosensor (performed following the experimental procedure described at *section 2.2*, fixing a target ssDNA concentration of 1 μM) were evaluated by EIS. Nyquist plots were recorded in 0.5 mM $K_3[Fe(CN)_6]/K_4[Fe(CN)_6]$ containing 0.1 M KCl solution and the signals were normalized by following the equation described at *section 2.3*.

Since deposition time tunes particle size and shape, the effect of the gold electrodeposition time and optimum particle size for high DNA hybridization rate was first evaluated (Figure 4A). Preceding this, we have studied the behavior of thiolated ssDNA probes on varying diameter of AuNPs. The immobilized thiolated ssDNA had the highest signal value onto AuNPs with average diameter of 25 nm (obtained over 25 s) and then the charge transfer resistance decreased with the increasing of particle size. In contrast, the hybridization with target ssDNA using 25 nm AuNPs had the lowest ΔRct signal value. This is probably because small AuNPs completely packed with the thiolated DNA probe, not allowing sufficient space for target DNA to hybridize (data not shown). Therefore, the optimum size of AuNPs corresponding to thiolated probe does not accurately reflect the needed thiolated probe density in DNA hybridization assays. Notably, while gold electrodeposition time increases (from 10 s - 200 s), ΔRct values of DNA hybridization increased reaching the highest for 200 s (average diameter of 50 nm). Longer deposition times (600 s - 800 s) showed a decrease in the ΔRct values and poor reproducibility, which is in line with what was observed by SEM analysis. From SEM images homogenous AuNPs with controlled shape and size were generated at 200 s while non-homogenous bigger gold particles were observed at 600 s (particles diameter data at *supplementary information)* and this may lead to irreproducibility of the DNA sensor. Overall, particles with an average diameter of 50 nm afforded the best DNA hybridization rate, thus 200 s was then selected as the optimum gold electrodeposition time.

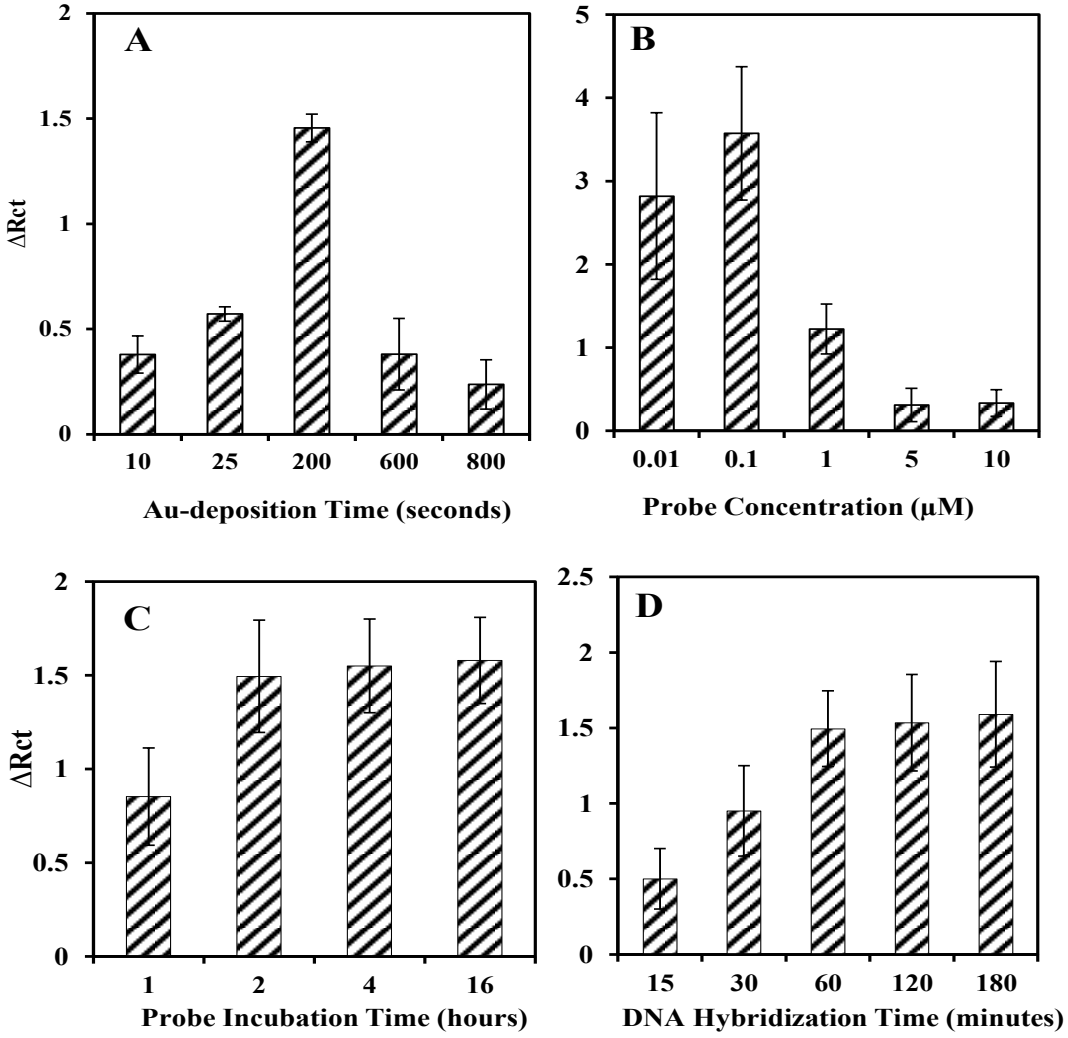

Figure 4. Optimization of DNA hybridization biosensor. Normalized values corresponding to $\Delta R_{ct}=(R-R_0)/R_0$ are represented. ΔR_{ct} values were recorded after DNA hybridization with CTV-related DNA and control DNA (1 μM) following **A)** AuNPs deposition times (ranging 10 s - 800 s) at potential of -0.4 V; thiolated ssDNA probe (1 μM) incubated for 2 h; DNA hybridization time: 1 h **B)** Different probe ssDNA concentrations (0.01, 0.1, 1, 5, and 10) μM on AuNP-modified SPCE (200 s); probe incubation time: 2h; DNA hybridization time: 1 h **C)** Probe incubation times (1, 2, 4 and 16 h) of thiolated ssDNA probe (0.1 μM) using AuNP- modified SPCE (200 s); DNA hybridization time: 1 h. **D)** DNA hybridization times (15, 30, 60 , 120 and 180 min) on AuNP- modified SPCE (200 s) incubated with 0.1 μM of thiolated ssDNA probe for 2 h.

Thiolated ssDNA probe concentration and immobilization time were also investigated. AuNP-modified electrodes were incubated with a wide range of thiolated probe ssDNA concentrations (0.01, 0.1, 1, 5 and 10 μM). A gradual increase in the values of ΔRct was observed for the smaller concentrations, observing a decrease for values higher than 0.1 μM (Figure 4B). This suggests that high probe ssDNA concentrations saturate the surface of AuNPs, hindering the signal discrimination after hybridization. In view of these results, a ssDNA probe concentration of 0.1 μM was selected for further studies.

Other parameter affecting the formation of the immobilized ssDNA probe sensing layer is the DNA probe incubation time, which was found to influence the DNA hybridization kinetics. The AuNP-modified SPCE electrodes were exposed to a 0.1 μM of thiolated ssDNA probe for various times (1, 2, 4 and 16 h) and EIS measurements after DNA hybridization were recorded (Figure 4C). The ΔRct steadily increased for short times. After 2 h of probe ssDNA incubation and later hybridization with target ssDNA enlarged the diameter of semicircle to evidence the presence of sufficient attached ssDNA probe to recognize the target DNA and produce high analytical signal after hybridization. The ΔRct values increased with the increasing in DNA probe incubation time under water-saturated atmosphere at 4°C, demonstrating data saturation up to 16 h. The electrochemical data indicated that the incubation period of 2 h was optimum for our biosensing system.

Finally, the effect of DNA hybridization time on the analytical signal was studied (Figure 4D). While membrane blot techniques require up to 16 hours or longer for base pairing interaction, DNA hybridization on small electrode surface modified with adequate probe ssDNA concentration using micro volume of solutions typically require 1-2 h for hybridization to occur. The AuNP- modified SPCE electrodes coated with thiolated ssDNA probe were incubated with target ssDNA for various times (15, 30, 60, 120 and 180 min) to lead to duplex DNA formation. A steady increase in the ΔRct was observed over DNA hybridization times up to 60 min,

noticing saturation in the signal for longer times. DNA hybridization time of 1 h was consequently chosen for the next investigation.

Citrus tristeza-Related Nucleic Acid Detection

Citrus tristeza virus has many characterized strains causing different symptomology. A 14-mer target ssDNA with sequence 5‟-TTACACATCGATCC-3‟ was selected as characteristic of the major coat protein (P25) of CTV (Niblett, 2000). The optimized DNA sensor was tested for different target ssDNA concentrations under the optimized conditions (AuNPs deposition time: 200 s, Probe concentration: 0.1 μM, probe incubation time: 2 h and DNA hybridization time: 1 h). In the EIS Nyquist plot, the diameter of semicircle enlarged when target ssDNA concentration increased as shown at Figure 5A. Control assays performed with a non-specific target strand characteristic of Psorosis, another citrus virus genome (5‟-TTACACAAGGATCT-3‟) (Figure 5A-a) demonstrated our sensing system ability to differentiate between CTV-related and non-CTV-related DNA.

The normalized R_{ct} values vs the CTV-related DNA concentrations were plotted (Figure 5B), finding a logarithmic relationship in the range of 0.1 to 10 μM, adjusted to the following equation:

$$\Delta Rct\ (\Omega) = 1.4199 \ln[CTV(\mu M)] + 5.83\ (r=0.99) \quad (\Delta R_{ct}= (R-R_0)/R_{0.})$$

A limit of detection (LOD) of 100 nM was estimated, as the target concentration giving a signal equal to the blank signal plus three times its standard deviation.

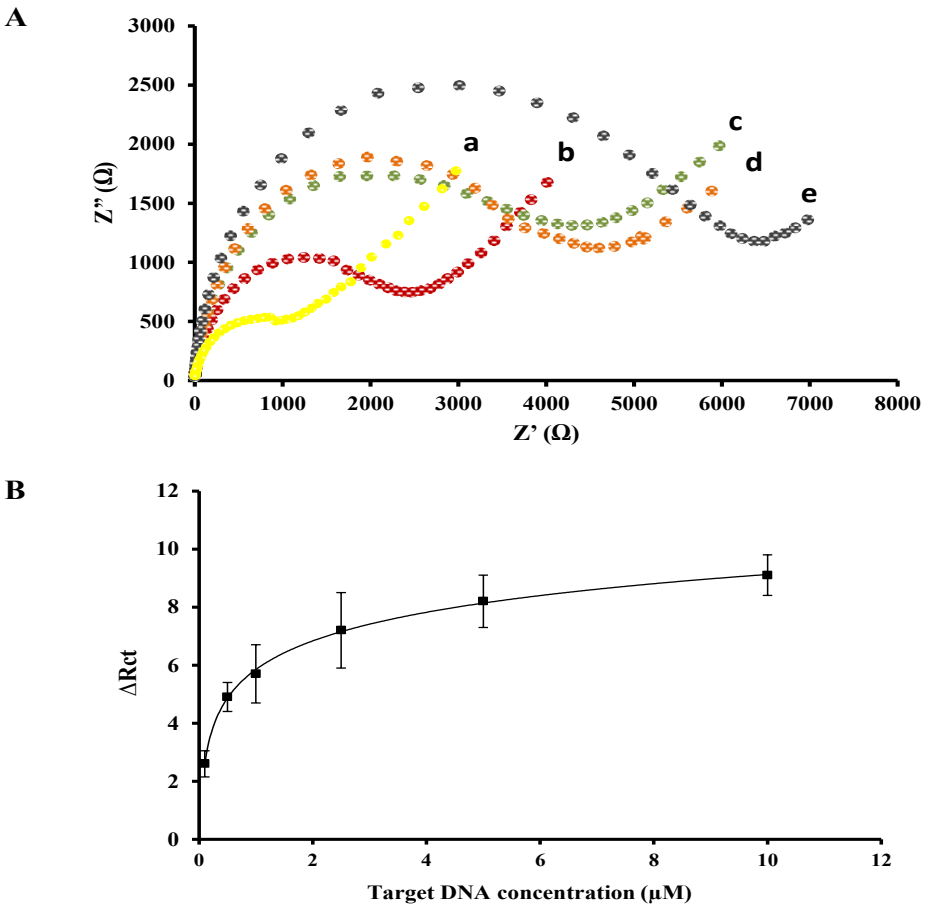

12

Figure 5. A) Nyquist plots recorded for control DNA **a)** and CTV-related ssDNA concentrations of 0.1 µM **b)**, 0.5 µM **c)**, 1 µM **d)** and 10 µM **e)**. Electrolyte: 0.5 mM $K_3[Fe(CN)_6]/K_4[Fe(CN)_6]$ containing 0.1 M KCl; Potential: 0.2 V; Amplitude: 5 mV; Frequency range: 10 KHz to 0.5 Hz. **B)** Calibration curve obtained by plotting the normalized R_{ct} values vs the logarithm of different CTV-related DNA concentrations in the range of 0.1 to 10 µM. Other experimental conditions as described in the text.

Additionally, interference studies were performed to examine the selectivity of our developed DNA sensor. Under optimized experiment conditions, the thiolated ssDNA-AuNP modified electrodes were covered with solutions of target DNA mixed with interferents (partially and fully non-complementary DNAs) at 1:0; 1:1; 1:5 and 1:10 ratios. Notably, the impedance results were significantly affected when the concentration of partially non-complementary DNA was 10 times the target DNA concentration (data not shown). To improve the sensor selectivity,

probe DNA with spacer of poly (AT) was served to form the recognition layer. Additionally, mercaptohexanol (MCH) was used as backfiller to minimize and effectively inhibit any non-specific adsorption of nucleobases, as reported in previous studies.

Gold nanoparticle surfaces were treated with poly (AT)-thiolated ssDNA probe in the presence of MCH (with DNA: MCH = 1: 0.1) for initial DNA immobilization process. Impedance measurements performed in target DNA solutions containing interfering of non-complementary DNA sequences, suggesting better selective DNA interaction as no significant interferences were observed (Figure 6A).

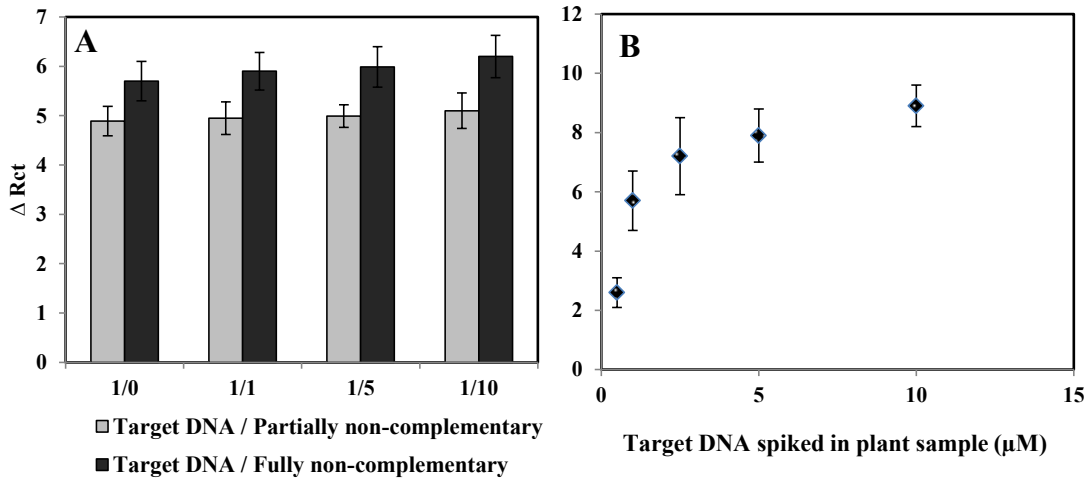

Figure 6. A) Interference study on the MCH/poly (AT) thiolated ssDNA-AuNPs modified electrodes towards a) target DNA/fully non-complementary and b) target DNA/ partially non-complementary at different rations (n=3) **B)** Effect of the concentration of CTV-related DNA (from of 0.5 to 10 µM) spiked in real plant samples on thenormalized R_{ct} values .

The same system reported above was tested in leaf extracts from healthy citrus plants to assess its ability to quantify CTV nucleic acid in real biological samples. Leaf extracts were prepared in hybridization buffer and diluted 5 times and then spiked with five different target DNA concentrations (0.5, 1, 2.5, 5 and 10 µM). ΔRct were recorded and the results proved

enough sensor sensitivity to detect the target DNA concentration as low as 500 nM (Figure 6B). Moreover, the biosensor ability to recover different target DNA concentrations from plant sample matrix was studied and the results demonstrated the satisfactory recovery within the range of 90-97% (Table 1).

Spiked CTV (μM)	ΔRct in hybridization buffer	ΔRct in plant sample	Recovery %
0.5	2.6	1.65	95
1	5.7	5	97
2.5	7.1	6.16	94
5	7.9	7	90
10	8.9	7.98	92

Table 1. Recovery study of the developed DNA biosensor in spiked plant samples with (0.5, 1, 2.5, 5 and 10 μM) of synthetic CTV-DNA.

The reproducibility of responses for a 1 μM of target ssDNA on the thiolated ssDNA-AuNP surfaces was also studied, obtaining a relative standard deviation (RSD) of 17% which demonstrated the good performance of this proof-of-concept approach. For further improvements so as to get better repeatability between the different electrodes, intra- and inter-day assays variability were performed on MCH/poly (AT) thiolated ssDNA-AuNPs sensing layer (Table 2). The intra-day assays were conducted on the same single day while the inter-day assays required one assay/day for 5 sequential days. The mean value, standard deviation and coefficient of variation were calculated using five different target DNA concentrations (10, 20, 30, 40 and 50 μM). For these target DNA concentration , the mean coefficient of variation values of intra- and inter- day precision assays were 6.78 % and 7.72 % , both of which are less than 10% of RSD. These results indicate the good reproducibility performance of the proposed DNA sensor.

Table 2. Intra- and inter-day reproducibility assays of the CTV-DNA sensor.

Target Concentration (μM)	Intra-assay (n=4)			Inter-assay (n=4)		
	ΔRct	S.D	Coefficient of variation %	ΔRct	S.D	Coefficient of variation %
10	9.12	0.3	3.28	8.90	0.43	4.83
20	10.33	0.5	4.84	10.56	0.59	5.58
30	11.89	1	8.4	11.07	0.89	8.03
40	12.57	1.3	10.34	12.88	1.26	9.78
50	12.76	0.9	7.05	12.90	1.34	10.38

Conclusions

We have developed the first DNA hybridization sensor based on AuNP- modified SPCE employing label-free impedance for the detection of CTV-related nucleic acid. AuNPs were electrochemically deposited on the working carbon electrode for its easy preparation and strong affinity with bio-recognition receptors with reactive groups (e.i. thiols). Covalent attachment of thiolated ssDNA probe was obtained to form the sensing layer that recognizes target ssDNA. A simple rapid label-free impedance detection of CTV was developed on AuNP-modified electrodes and faradic impedance was used to investigate the electrochemical performance. Impedance was selected as the best parameter to monitor the interfacial charge transfer changes of the electrode surface resulting from duplex DNA formation. To evaluate the sensor performance corresponding to selectivity and reproducibility, interference studies along with intra- and inter-day assays were conducted. The use of MCH and poly AT thiolated DNA probe has enhanced the sensor selectivity when it was tested against partially and fully non-complementary DNA sequences. The results demonstrated that 2 h is needed to form the recognition layer (MCH/poly (AT) thiolated ssDNA probe) followed by detecting the target DNA through base pairing time no longer than 1 h and finally within 5 min a detectable stable electrochemical signal is generated and collected. Our DNA sensor showed a logarithm relation in the range of 0.1-10 μM of CTV-related DNA with LOD of 100 nM with a total assay time of 65 min (60 min DNA hybridization and 5 min readout). Moreover, the results demonstrated the

good reproducibility of the biosensors with RSD less than 10%. The developed DNA sensor exhibits great advantages over previously reported dot-blot hybridization approaches for CTV-nucleic acid based detection in terms of simplicity, time of analysis and ability to do quantitative analysis. The proposed biosensor is of high potential interest for in-field applications in the relevant field of plant pathogen detection, which would overcome the limitations of classical methods such as dot-blot hybridization.

References

(1) Roberts, M.J., Schimmelpfennig, D.E., Ashley, E., Livingston, M.J., Ash, M.S., Vasavada, U., The Value of Plant Disease Early-Warning Systems: A Case Study of USDA‟s Soybean Rust Coordinated Framework; United States Department of Agriculture, Economic Research Service: Washington, DC, USA, 2006.

(2) Savary, S., Ficke, A., Aubertot, J., Hollier, C. *Food Secur*. **2012**, *4*, 519–537.

(3) Fang, Y. and Ramasamy, R.P. *Biosens*. **2015**, *5*, 537-561.

(4) Khater, M., de la Escosura-Muñiz, A., Merkoçi, A. *Biosens. Bioelectron.* **2017**, *93*, 72-86.

(5) Martinelli, F., Scalenghe, R., Davino, S., Panno, S., Scuderi, G., Ruisi, P., Villa, P., Stroppiana, D., Boschetti, M., Goulart, L.R., Davis, C.E. *Agron. Sustaine. Dev.* **2015**, *35*, 1-25.

(6) Nezhad, A.S. *Lab Chip* **2014**, *14*, 2887-2904.

(70) Harper, S. J., & Cowell, S. J. *J. Citrus Pathol*. **2016**, *3*(1).

(8) Moreno, P., Ambrós, S., Albiach-Martí, MR., Guerr,i J., Peña, L. *Mol. Plant Pathol.* **2008**, *9*, 251–268.

(9) Bar-Joseph, M. *J. Citrus Pathol.* **2015** , *2*(1).

(10) Bar-Joseph, M., Marcus, R., Lee, RF. *Annu. Rev. Phytopathol.* **1989**, *27*, 291–316.

(11) Licciardello, G., Scuderi, G., Ferraro, R., Giampetruzzi, A., Russo, M., Lombardo, A., Catara, A. *Arch. Virol.* **2015**, *160*, 2583-2589.

(12) Bar-Joseph, M., Garnsey, S. M., Gonsalves, D., Moscovitz, M., Purcifull, D. E., Clark, M. F., Loebenstein, G. *Phytopathol*. **1979**, *69*, 190-194.

(13) Huang, Z., Rundell, P. A., Guan, X., Powell, C. A. *Plant Dis.* **2004**, *88*, 625-629.

(14) Haji-Hashemi, H., Norouzi, P., Safarnejad, M. R., Ganjali, M. R. *Sens. Actuator B-Chem.* **2017**, *244*, 211-216.

(15) Maheshwari, Y., Selvaraj, V., Hajeri, S., Ramadugu, C., Keremane, M. L., Yokomi, R. K. *Phytoparasit.* **2017**, *45*, 333-340.

(16) Korkmaz, S., Cevik, B., Onder, S., Koc, K., Bozan, O. *N. Z. J. Crop. Horticul. Scienc*. **2008**, *36*, 239-246.

(17) Yokomi, R. K., Saponari, M., Sieburth, P. *J. Phytopathol*. **2010**, *10*, 319-327.

(18) Warghane, A., Misra, P., Bhose, S., Biswas, K. K., Sharma, A. K., Reddy, M. K., Ghosh, D. K. *J. Virol. Methods* **2017**, *250*, 6-10.

(19) Castañeda, M. E., Alegret, S., Merkoci, A. *Electroanalysis* **2007**, *19*, 743-753.

(20) Merkoçi, A., Aldavert, M., Marın, S., Alegret, S. *Trends in Anal. Chem.* **2005**, *24*, 341-349.

(21) Wang, J. *Anal. Chim. Acta* **2002**, *469*, 63-71.

(22) Castañeda, M. T., Alegret, S., Merkoçi, A. Biosensors and Biodetection; Methods in Molecular Biology™, vol 504. Humana Press, 2009.

(23) Park, J. Y., Park, S. M. *Sens*. **2009**, 9, 9513-9532.

(24) Rashid, J. I. A., Yusof, N. A. Sens. Bio-Sens. Res 2017.

(25) Hassen, W. M., Chaix, C., Abdelghani, A., Bessueille, F., Leonard, D., Jaffrezic-Renault, N. *Sen. Actuators B: Chem.* **2008**, *134*, 755-760.

(26) Pournaghi-Azar, M. H., Alipour, E., Zununi, S., Froohandeh, H., Hejazi, M. S. *Biosens. Bioelectron.* **2008**, *24*, 524-530.

(27) Cash, K. J., Heeger, A. J., Plaxco, K. W., Xiao, Y. *Anal. Chem.* **2008**, *81*, 656-661.

(28) Benvidi, A., Firouzabadi, A. D., Tezerjani, M. D., Moshtaghiun, S. M., Mazloum-Ardakani, M., Ansarin, A. *J. Electron. Chem.* **2015**, *750*, 57-64.

(29) Wang, J., Liu, G., Polsky, R., Merkoçi, A. *Electrochem. Commun.* **2002**, *4*, 722-726.

(30) Wang, J., Liu, G., Merkoçi, A. *J. Am. Chem. Soc.* **2003a**, *125*, 3214-3215.

(31) Wang, J., Liu, G., Merkoçi, A. *Anal. Chim. Acta* **2003b** , *482*, 149-155.

(32) Wang, J., Polsky, R., Merkoci, A., Turner, K. L. *Langmuir* **2003c** , *19*, 989-991.

(33) Bonanni, A., Esplandiu, M. J., Del Valle, M. *Electrochim. Acta* **2008**, *53*, 4022-4029.

(34) Pumera, M., Castaneda, M. T., Pividori, M. I., Eritja, R., Merkoçi, A., Alegret, S. *Langmuir* **2005**, *21*, 9625-9629.

(35) Rasheed, P. A., Sandhyarani, N. *Microchim. Acta.* **2017**, *184*, 981-1000.

(36) Xu, Y., Cai, H., He, P. G., Fang, Y. Z. *Electroanal*. **2004**, *16*, 150-155.

(37) Ribovski, L., Zucolotto, V., Janegitz, B. C. *Microchem. J.* **2017**, *133*, 37-42.

(38) De la Escosura-Muñiz, A., Baptista Pires, L., Serrano, L., Altet, L., Francino, O., Sánchez, A., Merkoçi, A. *Small* **2016**, *12*, 205-213.

(39) De la Escosura-Muñiz, A., Mekoçi, A. *Chem. Comm*. **2010**, *46*, 9007-9009.

(40) De la Escosura-Muñiz, A., Merkoçi, A. Nucleic Acid Nanotechnology, Springer, Berlin, Heidelberg, 305-332, 2014.

(41) Mayorga-Martinez, C. C., Chamorro-García, A., Serrano, L., Rivas, L., Quesada-Gonzalez, D., Altet, L., Merkoçi, A. *J. Mater. Chem. B* **2015**, *3*, 5166-5171.

(42) Merkoçi, A. *Biosens. Bioelectron.* **2010**, *26*, 1164-1177.

(43) Travas-Sejdic, J., Peng, H., Kilmaitin, P. A., Cannell, M. B., Bowmaker, G. A., Cooney, R. P., Soeller, C. *Synth. Metals* **2005**, *152*, 37-40.

(44) Ito, T., Hosokawa, K., Maeda, M. *Biosens. Bioelectron.* **2007**, *22*, 1816-1819.

(45) Li, X., Shen, L., Zhang, D., Qi, H., Gao, Q., Ma, F., Zhang, C. *Biosens. Bioelectron*. **2008**, *23*, 1624-1630.

(46) Deng, C., Chen, J., Nie, Z., Wang, M., Chu, X., Chen, X., Yao, S. *Anal. Chem.* **2008**, *81*, 739-745.

(47) Mazloum-Ardakani, M., Rajabzadeh, N., Benvidi, A., Heidari, M. M. *Anal. Biochem.* **2013**, *443*, 132-138.

(48) Zhang, L., Li, Z., Zhou, X., Yang, G., Yang, J., Wang, H., Lu, Y. *J. Electroanal. Chem.* **2015**, *757*, 203-209.

(49) Cui, M., Wang, Y., Wang, H., Wu, Y., Luo, X. *Sens. Actuator B-Chem.* **2017**, *244*, 742-749.

(50) Lai, R. Y., Weiwei, Y. A. N. G., 2011. U.S. Patent Application No. 12/967,547.

(51) Liu, S. F., Li, Y. F., Li, J. R., Jiang, L. *Biosens, Bioelectron.* **2005**, *21*, 789-795.

(52) Peng, H. P., Hu, Y., Liu, P., Deng, Y. N., Wang, P., Chen, W., Lin, X. H. *Sen. Actuators B: Chem.* **2015**, *207*, 269-276.

Chapter IV

In situ Detection of Amplified Virus Nucleic Acid

In situ Plant Virus Nucleic Acid Isothermal Amplification Detection on Gold Nanoparticle-Modified Electrodes

Recombinase polymerase amplification (RPA) has received much attention in recent years due to its versatility and isothermal performance, which may offer effective replacement to Polymerase chain reaction (PCR) in molecular detection.[1-4] Unlike PCR, RPA technology is based on three main components (recombinase, single-stranded DNA-binding protein and polymerase) which allow amplification at constant temperature (ranging from 37°C - 40°C) and as a result the need for thermal cycling is omitted.[5,6] The required temperature for RPA is lower than for other emerged isothermal amplification methods such as nucleic acid sequence-based amplification (NASBA), loop-mediated isothermal amplification (LAMP), rolling circle amplification (RCA) and helicase dependent amplification (HDA).[7-11]In spite of the great advantages of RPA, DNA purification and detection after amplification involving hazardous, time-consuming and expensive equipment is still required for getting qualitative information. Alternative methodologies taking advantage of the use of labeled primers for detecting RPA amplified products in lateral flow [12-14], and electrochemical approaches have been proposed for such purpose. [15, 16] Some efforts have been also devoted to RPA integration into microfluidic devices with fluorescence detection.[17] However, these methods lack of integration of RPA amplification and detection in the same device, which would be strongly needed for in-field diagnostic applications.

Such highly integrated devices have been recently achieved with the so-called solid-phase RPA amplification, in which one of the primers is directly immobilized on the sensing

surface. Label-free optical approaches [18,19], and enzymatic label-based electrochemical ones with high degree of integration have been reported.[20] However, heat sources are needed for getting detectable signals, which represents an important practical limitation.

In this context, we propose a label-free highly integrated *in situ* RPA amplification/detection approach at room temperature, taking advantage of the high sensitivity achieved combining the use of gold nanoparticle (AuNP)-modified sensing substrates and electrochemical impedance spectroscopic (EIS) detection. A scheme of the developed nucleic acid amplification/detection system is shown at Figure 1.Plant disease (*Citrus tristeza* virus (CTV)) is selected as relevant target for the demonstration of the proof-of-concept.

Recent studies estimating that plant diseases may cause global economic losses exceeding billions of dollars annually put in value the relevance of such diseases. [21] Early detection of pathogens in pre-symptomatic plants is of key importance for avoiding the development and spread of the disease. Plant pathogen determination is currently performed through antibody-based enzyme-linked immunosorbent assays (ELISA) and lateral flow immunoassays (LFIA) [22-28] ,and nucleic acid-based analysis [29-31], as alternative to the traditional diagnostic methods including symptoms observation, regular in-field inspections, and laboratory analysis by experienced plant pathologists .[32] Over the last decade, it has been noticed that antibody and DNA based biosensing applications in the field of plant disease diagnostics have been increasing .[33-36]

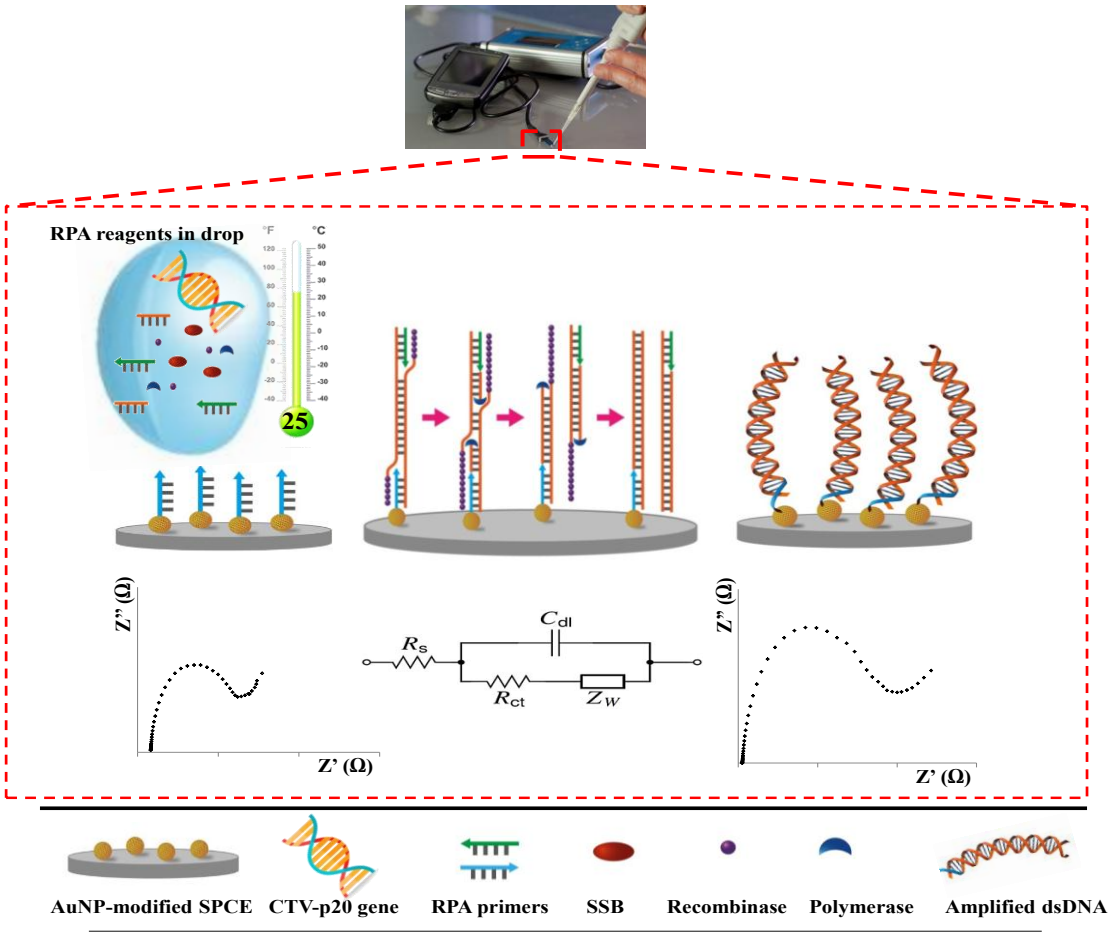

Figure 1. The stepwise of the developed label-free *in situ* isothermal RPA amplification/detection biosensor on primer-modified SPCE-AuNP electrodes employing impedance for the determination of CTV-related nucleic acid.

Design of RPA for CTV Detection Assay

After designing of RPA primers to specifically detect CTV, gel electrophoresis was carried out to screen the selected primer sets (Table S1, in the *supplementary information*). The best analytical band was produced by F1/R1 primer pair which was able to amplify the expected size amplicons of 278-bp, being then chosen for next experiments. The optimum conditions recommended by manufacturer , which included favorable temperature of 37ºC, total reaction volume 50 µL and interval mixing upon Mg salt addition were applied to perform RPA reaction

for 30 min, resulting in amplified 278-bp CTV-p20 gene fragments in the concentration range 0.1 pg μL^{-1} to 100 pg μL^{-1} that were visualized in gel (Figure 2A).

The ability of the RPA to work at room temperature (25 ±3°C) was then evaluated. RPA experiments for CTV-p20 gene target concentration ranging from 0.1 pg μL^{-1} to 100 pg μL^{-1} were performed within 30 min amplification at such temperature. Products obtained gave detectable bands in the gel only for the higher concentrations assayed (100 pg μL^{-1} and 10 pg μL^{-}) (Figure 2B), evidencing the DNA amplification under these conditions.

RPA conditions were modified in order to be more suitable to perform *in situ* amplification on primer-modified SPCE-AuNP electrodes. With the aim of simulating the conditions that will be found on the electrode surface, small reaction volumes of 15 µL were evaluated under amplification at 37°C and room temperature. The signals got from large reaction volumes of 50 µL incubated at 37°C were detectable for CTV-p20 gene target concentration as low as 0.1 pg μL^{-1} while small reaction volumes of 15 µL gave signals only detectable for target concentration as high as 10 pg μL^{-1}(Figure 2C). The 100 pg μL^{-1} CTV-p20 gene target concentration showed a detectable signal after amplification of the small volume at RT while no amplicons were generated from lower target concentrations (Figure 2D). The effect of Mg salt addition without mixing step was also evaluated, reaching the same sensitivity than with previous mixing (data not shown).

The good performance of the thiolated forward primer (SH-(AT_7)-F1) was evaluated by Nanodrop nucleic acid quantification (see the *supplementary information)*.

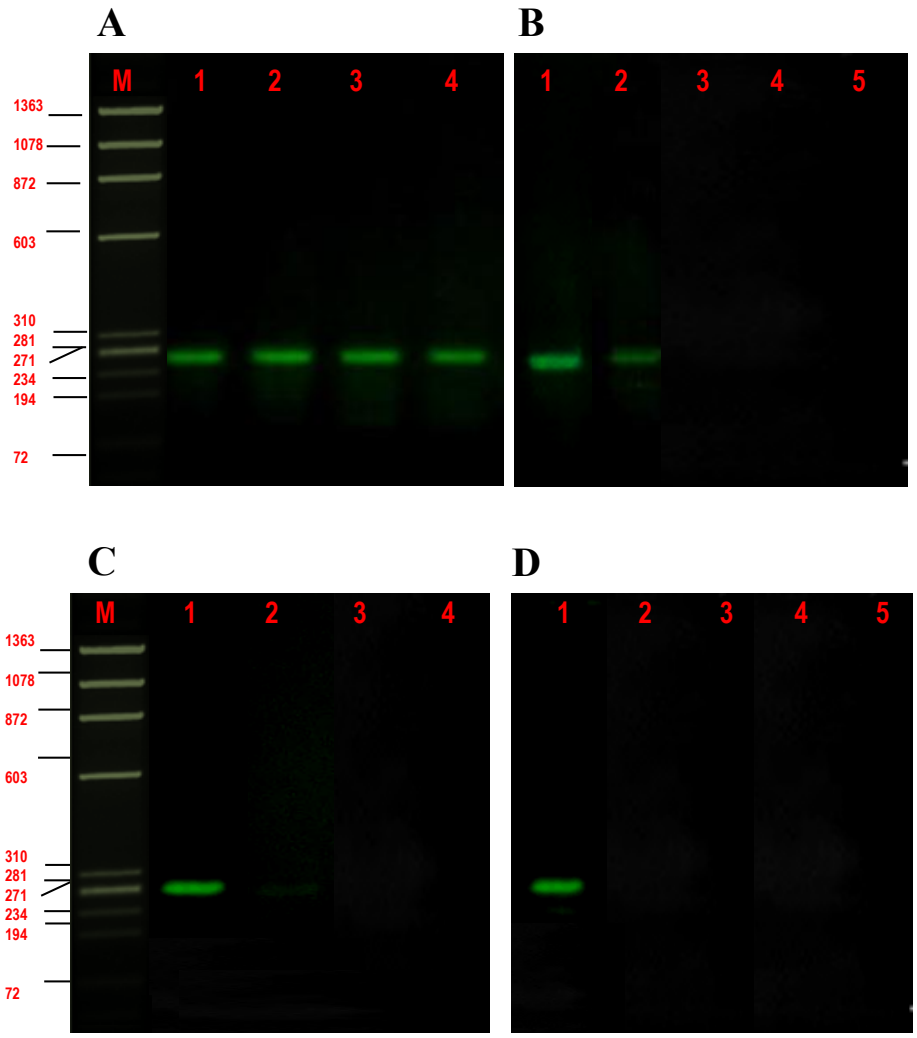

Figure 2

Figure 2. Gel electrophoresis analysis of RPA amplicons for CTV detection following **A.** Optimum isothermal RPA conditions: RPA amplification temperature: 37°C; total reaction volume: 50 µL **B.** Isothermal RPA reactions at room temperature with 50 µL total reaction volume. Isothermal RPA of small reaction volume (15 µL) incubated at different temperatures **C.** 37ºC and **D.** Room temperature. All isothermal RPA reaction times were 30 min. M = Phi-X 174/HaeIII Marker , 1 = 100 pg μL^{-1} , 2 = 10 pg μL^{-1} ,3 = 1 pg μL^{-1}, 4 = 0.1 pg μL^{-1} , 5 = NTC. Bands size: 278-bp for CTV-p20 gene.

Electrochemical Characterization and Optimization of The *In Situ* Isothermal RPA on Electrode Surface

The optimized RPA conditions were transferred to the SPCE-AuNP electrode surface. All the reagent solutions were added to the electrode, previously modified with the forward primer (SH-(AT_7)-F1). CTV-p20 gene was lastly added to the RPA mixture on the electrode to start the reaction (Figure 1).

The Nyquist plots recorded for the electrodes showed a high increase in the electrode resistance upon the RPA performed with a CTV-p20 target concentration of 1 ng μL^{-1} (Figure 3A), demonstrating the attachment of amplified DNA to the electrode.

However, when testing RPA solutions with negative control, unspecific EIS response was observed (data not shown). In order to prevent the interference from RPA chemical reagents and to reduce unspecific adsorption of enzymes, the three most commonly used washing buffers in chips and microfluidic domain for nucleic acid amplification methods were evaluated. After amplification, electrodes were carefully washed with three different washing buffers PBS 10mM, 2x SSC and PBST containing 0.05% (v/v) Tween 20. As a result of using PBST washing buffer, the unspecific EIS signal was highly decreased after amplifying with negative control showing the effective removal of the rest of RPA components that may remain on the electrode after amplification (Figure 3B). The supplement of Tween detergent in the washing buffer (PBST) resulted in greatly reduced non-specific binding of RPA reagents on electrode surfaces, suggesting their effective release. Moreover, it is important to note that the high viscosity of RPA solutions makes the post-amplification washing step essential for the EIS signal enhancement.

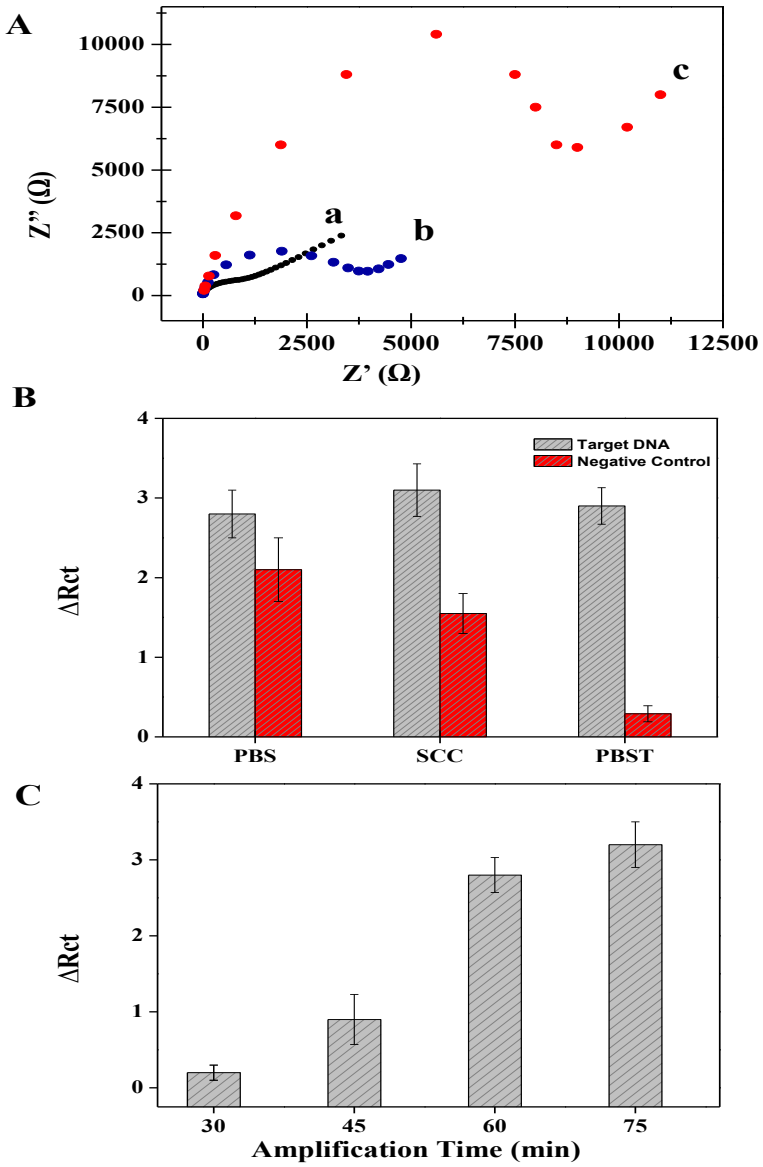

Figure 3: A. Nyquist plots recorded for SPCE-AuNP electrode a) upon SH-(AT_7)-F1primer immobilization b) and *in situ* isothermal RPA with CTV-p20 target concentration of 1 ng μL^{-1} c)**. B.** Effect of washing with different buffers after the *in situ* isothermal RPA performed for the CTV-p20 (target DNA) and for blank control (NTC) on the analytical signal. DNA concentration: 1 ng μL^{-1}. **C.** Effect of the *in situ* isothermal RPA amplification time (30, 45, 60 and 75 min) on the analytical signal for a CTV-p20 target concentration of 1 ng μL^{-1}.

Finally, the effect of the time of the *in situ* isothermal RPA reaction on the electrochemical signal was also studied. As shown in Figure 3C, no detectable signals were obtained for reaction times below 30 min. R_{ct} values increased then with the reaction time in the range 30 -60 min, when a signal saturation was noticed. It‟s worthy to note that such optimum amplification time in solid-phase is longer than the one typically used for the RPA in homogeneous phase (60 min), as expected. [20] Furthermore, the lower temperature used probably also contributes to such longer time required.

In situ Citrus tristeza-related Nucleic Acid DNA Amplification/Detection

The ability of our biosensor for the quantification of CTV-related DNA was evaluated. The *in situ* isothermal RPA amplification/detection biosensor on primer-modified SPCE-AuNP electrode was performed for different CTV-p20 target concentrations under the optimized conditions (Primer concentration: 0.1 μM, primer immobilization time: 2 h, RPA amplification time: 1 h at room temperature; washing in PBST buffer). According to the EIS Nyquist plot, as the target concentration increased, the diameter of semicircle enlarged as shown at Figure 4A.

The normalized R_{ct} values vs the CTV-p20 target concentrations were plotted (Figure 4B), finding a logarithmic relationship in the range of 1 to 500 pg μL^{-1}, adjusted to the following equation:

$$\Delta Rct\ (\Omega) = 0.2267\ \ln[CTV(pg\ \mu L^{-1})] + 3.36\ (r=0.993) \quad (\Delta R_{ct} = (R-R_0)/R_{0.})$$

The limit of detection (LOD) was found to reach 1 pg μL^{-1}(calculated as the target concentration producing a signal equivalent to the blank signal plus three folds its standard deviation).

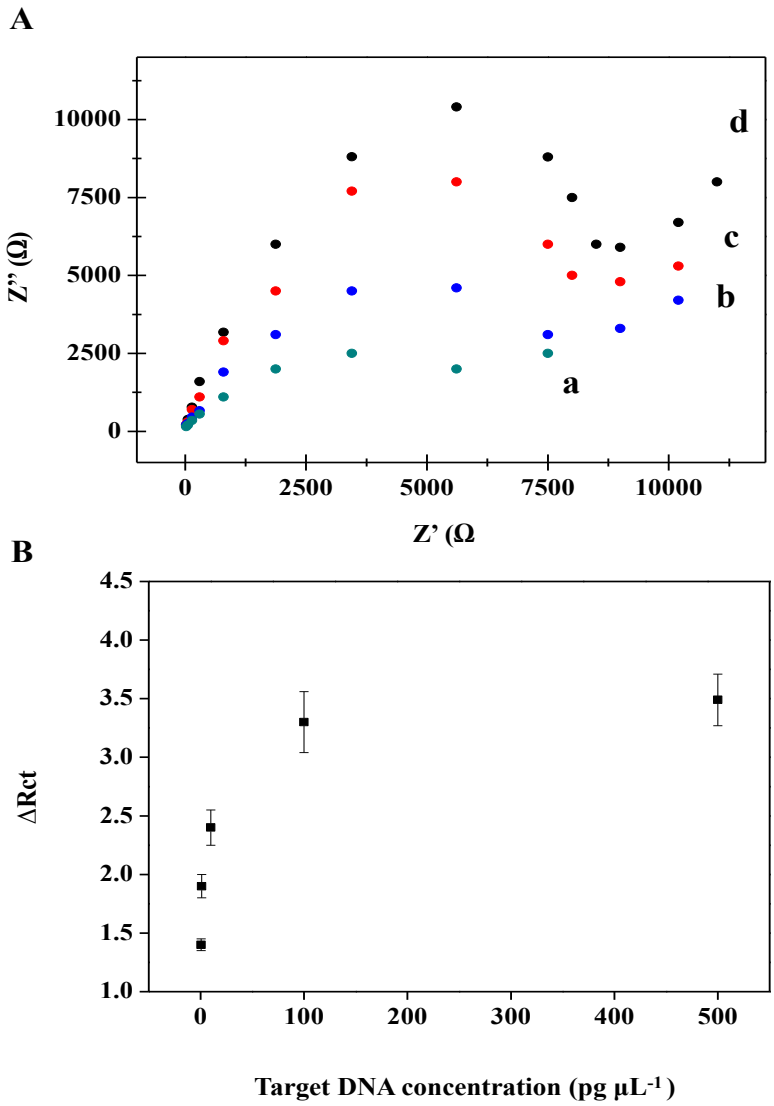

Figure 4. Normalized values corresponding to $\Delta R_{ct}=(R-R_0)/R_0$ are represented. **A.** Nyquist plots recorded for SPCE-AuNPs electrodes upon *in situ* RPA amplification performed for *Citrus psorosis virus* (CPsV) gene (negative control-NTC) a) and CTV-p20 target at b) 10, c) 100 and d) 1000 pgµL^{-1}**.** Electrolyte: 0.5 mM K_3 [Fe (CN) $_6$]/K_4 [Fe (CN) $_6$] containing 0.1 M KCl; Potential: 0.2 V; Amplitude: 5 mV; Frequency range: 10 KHz to 0.005 Hz. **B.** Calibration curve obtained by plotting the normalized R_{ct} values ($\Delta R_{ct}=(R-R_0)/R_0$) vs the logarithm of t CTV- p20 gene target concentration in the range of 1 pg µL^{-1}to 500 pg µL^{-1}. Other experimental conditions as described in the text.

The limit of detection achieved by the label-free *in situ* isothermal RPA on primer-modified SPCE-AuNP electrodes was 100 times lower than that of the modified RPA assay, showing that the integration of *in situ* isothermal RPA with impedance approach allowed a highly sensitive detection of nucleic acid.

Additionally, specificity studies were performed to examine the ability of our developed *in situ* RPA sensor to differentiate between CTV-related and non-CTV-related DNAs. These studies were performed with a non-specific gene sequences characteristic of *Citrus psorosis virus* (CPsV), as it is claimed to be the second important citrus virus, and also *Citrus caxicia viroid* (CCaV), which is likely to be present in complex infection with CTV in the infected citrus trees in nature. Under optimized experiment conditions, primer-modified SPCE-AuNP electrodes were coated with RPA solutions prepared with CTV-p20 gene target and controls. Impedance measurements shown in Figure 5A evidence a clear discrimination between the specific and non-specific DNA, demonstrating the specificity of our sensing system to CTV-related nucleic acid.

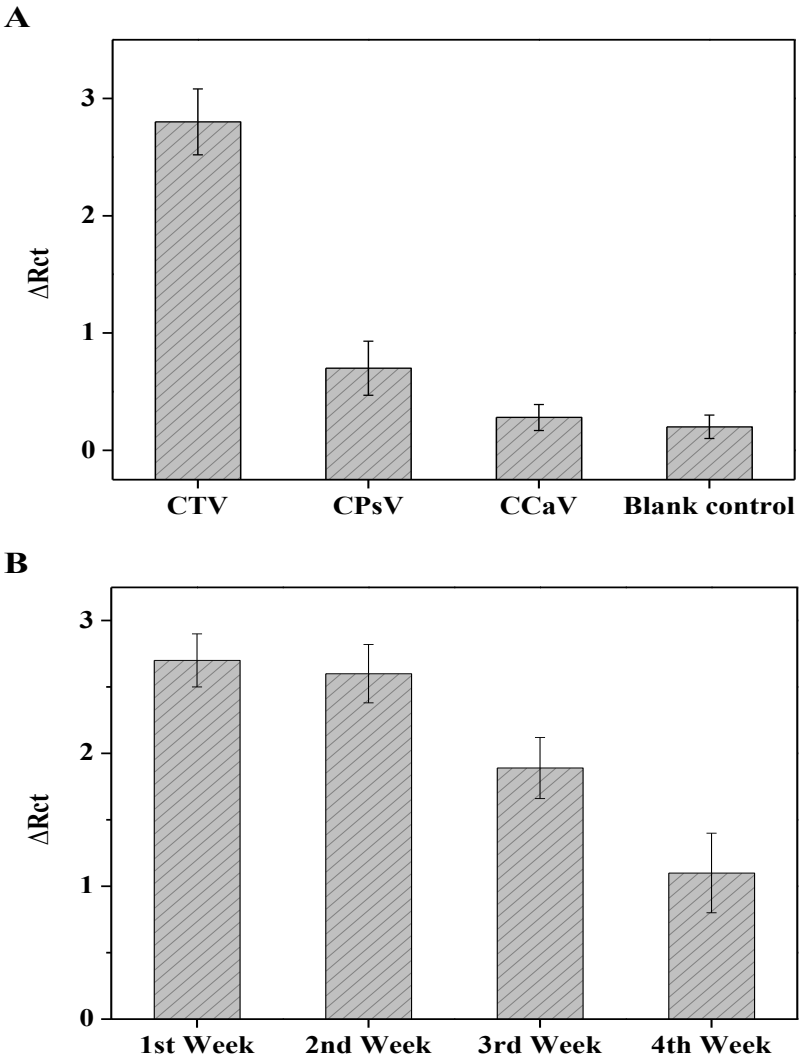

Figure 5. A. Normalized R_{ct} values ($\Delta R_{ct}=(R-R_0)/R_0$) obtained for *in situ* RPA performed with specific target CTV- p20 gene and non-specific CPsV and CCaV sequences, as well as for a blank control **B.** Effect of storage on the performance of SPCE-AuNP electrodes for *in situ* isothermal RPA within four weeks.

The storage stability of SPCE-AuNP electrodes was also investigated by monitoring the impedance response of *in situ* RPA each week up to 1 month. The sensor has showed an extended shelf-life of working for more than three weeks. Along with that, the repeatability of responses for a 100 pg $\mu L^{-1}$of CTV-p20 gene target on the thiolated primer-modified SPCE-AuNP surfaces was studied through intra- and inter-day assays, obtaining a relative standard

deviation (RSD) of 8 % which demonstrated the good performance of this proof-of-concept approach.

Conclusions

We have developed the first integrated label-free *in situ* isothermal RPA amplification/detection based on AuNP-modified SPCE employing impedance for the detection of CTV-related nucleic acid. Specific primers for p20 gene of CTV genome were designed and RPA amplified products were investigated by gel electrophoresis. Then, the effect of both reaction volume and amplification temperature was also evaluated by gel analysis. For *in situ* isothermal RPA, AuNP-modified electrodes were coated with thiolated forward primer (SH-(AT_7)-F1) to form the sensing layer that recognizes CTV-p20 target and start the direct synthesis of duplex DNA onto electrode surface. A simple electrochemical detection of CTV was performed using faradic impedance to characterize the electrochemical performance before and after *in situ* amplification. Charge transfer resistance parameter was selected to monitor the changes on the electrode surface which results from the immobilization of sensing layer and the amplified duplex DNA. Our *in situ* isothermal RPA amplification/detection sensor showed a logarithm relation in the range of 1 to 500 pg $\mu L^{-1}$of CTV-related nucleic acid with LOD of 1000 fg $\mu L^{-1}$with a total assay time of 80 min (60 min RPA amplification and 20 min readout). The sensor performance including specificity and storage life along with intra- and inter-day assays was also studied. Moreover, the results demonstrated the good reproducibility of the biosensors with RSD below 10%. Compared with other methods (i.e. PCR or RPA analyzed by the routine gel electrophoresis), this *in situ* RPA sensor exhibits great advantages in terms of simplicity (no heat source and no label required), sensitivity and portability together with allowing quantitative analysis of nucleic acid. The proposed biosensor is of high potential interest for in-field applications for plant pathogen early detection, which would overcome the limitations of classical molecular methods such as PCR.

References

(1) James, A.; Macdonald, J. *Expert Rev. Mol. Diagn*. **2015**, *15, 1475-1489*.

(2) Daher, R.K.; Stewart, G.; Boissinot, M.; Bergeron, M.G. *Clin. Chem*. **2016**, *62, 947–958*.

(3) Moore, M.D.; Jaykus, L.A. *Future Virol*. **2017**, *12, 421-429*.

(4) Lobato, I.M.; Sullivan, C.K. *TrAC, Trends Anal. Chem*. **2018**, *98, 19–35*.

(5) Chen, G.; Dong, J., Yuan, Y.; Li, N.; Huang, X.; Cui, X.;Tang, Z. *Sci. Rep.* **2016,** *6*, 34582.

(6) Wang, J.; Liu, L.; Wang, J.; Sun, X.; Yuan, W. *PloS one*, **2017**, *12, .e0166903*.

(7) Compton, J. *Nature* **1991**, *350*, 91-92.

(8) Notomi, T.; Okayama, H.; Masubuchi, H.; Yonekawa, T.; Watanabe, K.; Amino, N.; Hase, T. *Nucleic Acids Res.* **2000**, *28, e63*.

(9) Gusev, Y.; Sparkowski, J.; Raghunathan, A.; Ferguson Jr, H.; Montano, J.; Bogdan, N.; Schweitzer, B.; Wiltshire, S.; Kingsmore, S.F.; Maltzman, W.; Wheeler, V. *Am. J. Pathol*. **2001**,*159, 63–69*.

(10) Vincent, M.; Xu, Y.; Kong, H. *EMBO Rep*. **2004**, *5, 795–800*.

(11) Piepenburg, O.; Williams, C.H.; Stemple, D.L.; Armes, N.A. *PLoS Biol.* **2006**, *4, 1115–1121*.

(12) Rivas, L.; de la Escosura-Muñiz, A.; Serrano, L.; Altet, L.; Francino, O.; Sánchez, A.; Merkoçi, A. *Nano Res.* **2015**, *8, 3704-3714*.

(13) Sun, K.; Xing, W.; Yu, X.; Fu, W.; Wang, Y.; Zou, M.; Luo, Z.; Xu, D. *Parasites vectors* **2016**, *9, 476*.

(14) Wu, YA.D.; Xu, M.J.; Wang, Q.Q.; Zhou, C.X.; Wang, M.; Zhu, X.Q.; Zhou, D.H. *Vet. Parasitol*. **2017**, *243, 199-203*.

(15) De la Escosura-Muñiz, A.; Baptista Pires, L.; Serrano, L.; Altet, L.; Francino, O.; Sánchez, A.; Merkoçi, A. *Small* **2016**, *12, 205-213*.

(16) Tsaloglou, M. N.; Nemiroski, A.; Camci-Unal, G.; Christodouleas, D. C.; Murray, L. P.; Connelly, J. T.; Whitesides, G. M. *Anal. Biochem*. **2018**, *543, 116-121*.

(17) Li, Z.; Liu, Y.; Wei, Q.; Liu, Y.; Liu, W.; Zhang, X.; Yu, Y. *PLoS One* **2016**, *11, e0153359.*

(18) Shin, Y.; Perera, A. P.; Kee, J. S.; Song, J.; Fang, Q.; Lo, G. Q.; Park, M. K. *Sens. Actuators, B*. **2013a** , *177, 404-411*.

(19) Shin, Y.; Perera, A. P.; Kim, K. W.; Park, M. K. *Lab Chip* **2013b**, *13, 2106-2114*.

(20) Del Río, J. S.; Lobato, I. M.; Mayboroda, O.; Katakis, I.; O'Sullivan, C. K. *Anal. Bioanal. Chem.* **2017**, *409, 3261-3269*.

(21) Agrios, G. N. Environmental effects on the development of infectious plant disease. Plant pathol. 5th edn, Elsevier Academic Press, 2005.

(22) Punja, Z.K.; De Boer, S.H. Sanfaçon, H. Eds. Biotech and plant disease management; Cabi, 2007.

(23) Alvarez, A. M. *Annu. Rev. Phytopathol.* **2004**, *42, 339-366*.

(24) Narayanasamy, P. Detection of fungal pathogens in plants. In Microbial Plant Pathogens-Detection and Disease Diagnosis: Springer, Dordrecht 2011, 5-199.

(25) Macario, A.J.; De Macario, E.C. In; Monoclonal Antibodies Against Bacteria; New York State Department of Health, Albany, New York 1985, 213-247.

(26) Comstock, J.C.; Irey, M.S. *Plant Dis.* **1992,** *76, 1033*.

(27) Thornton, C.R. Production of monoclonal antibodies to plant pathogens. In Plant Pathology ; Humana Press, Totowa, NJ. 2009, 63-74.

(28) Tomlinson, J.A.; Dickinson, M.J.; Boonham, N. *Phytopath*. **2010**, *100, 143-149*.

(29) Ward, E.; Foster, S.J.; Fraaije, B.A.; Mccarteny, H.A. *Ann. of Appl. Biol*. **2004**, *145, 1-16.*

(30) Price, J.A.; Smith, J.; Simmons, A.; Fellers, J.; Rush, C.M. *J. of virol. Meth.* **2010**, *165, 198-201*.

(31) Dai, J.; Peng, H.; Chen, W.; Cheng, J.; Wu, Y *J. of App. Micro*. **2013**, *114, 502-508.*

(32) Horsfall J. G.; Cowling E. B., Ed. Plant Disease: An Advanced Treatise; New York, NY: Academic Press, 1977.

(33) Nezhad, A.S. *Lab Chip* **2014**, *14, 2887-2904*.

(34) Fang, Y.; Ramasamy, R.P. *Biosens*. **2015**, *5, 537-561*.

(35) Martinelli, F.; Scalenghe, R.; Davino, S.; Panno, S.; Scuderi, G.; Ruisi, P.; Villa, P.; Stroppiana, D.; Boschetti, M.; Goulart, L.R.; Davis, C.E. *Agron. Sustaine. Dev.* **2015**, *35, 1-25.*

(36) Khater, M.; de la Escosura-Muñiz, A.; Merkoçi, A. *Biosens. Bioelectron.* **2017**, *93, 72-86.*

(37) Khater, M.; de la Escosura-Muñiz, A.; Quesada-González, D.; Merkoçi, A. *Anal. Chem. Acta* **2019**, *1046, 123-131.*

Chapter V

Paper-based Virus Nucleic Acid Testing

Highly Sensitive Direct Detection of Plant Virus Nucleic Acid Amplification on Gold Nanoparticle-based Paper Sensor

Nucleic Acid Diagnostic Methods

Nucleic acid based testing is a fundamental diagnostic tool for pathogen detection. More recently, nanotechnology applications related to nucleic acid amplification and biosensing systems have become highly important in healthcare, environment, food and agriculture testing.[1] Thank to nucleic acid amplification technologies, pathogen infection can be detected within the early stage of a disease. Polymerase chain reaction (PCR), the conventional nucleic acid amplification method suffers from some limitations such as time-consuming analysis and the need for thermal-cycle equipment.[2-5] In the last decade, isothermal RPA is different approach has been extensively used as an alternative to PCR.[6-11] In this approach, a novel chemistry was implemented which allows the amplification at constant temperature in range between 37-42 °C.[12-14] Although being highly sensitive and rapid amplification method, the use of laboratory equipment for the analysis of RPA products and trained personnel are still required.

Nucleic Acid Lateral Flow Immunoassays

To overcome the aforementioned limitation, nucleic acid lateral flow immunoassay (NALFI) has combined isothermal RPA with lateral flow tests as they offer colorimetric detection of the results without equipment to perform and are relatively simple format to use outside laboratory setting.[15-17] A variety of commercial RPA kits compatible with universal test strips based on sandwich immunoassays have been reported for rapid detection of animal, plant, food and human pathogens.[18-24]These methodologies are based on the use of gold nanoparticles

as tags for colorimetric detection taking advantage of their facile synthesis and good biocompatibility with biomolecules such as antibodies. Many efforts have also been made to improve the LF performance based on gold nanoparticles by using different immunoreactions.[25-27] However, all of these systems have some practical limitations related to the post-amplification treatment and dilution as well as to the fact that heat source for reaching the favourable amplification temperature is a common practical limitation for isothermal amplified nucleic acid detection in lateral flow.

In this context, we present simple, rapid highly sensitive RPA test strip for CTV detection at room temperature, taking advantage of direct detection of undiluted amplified products in one-single tube achieved via RPA liquid chemistry. Our nucleic acid lateral flow dipstick in sandwich format using AuNPs tags was developed to recognize biotin/FITC amplicons without dilution and post-amplification clean process. A scheme of the isothermal nucleic acid detection in lateral flow immunosystem is shown at Figure 1.

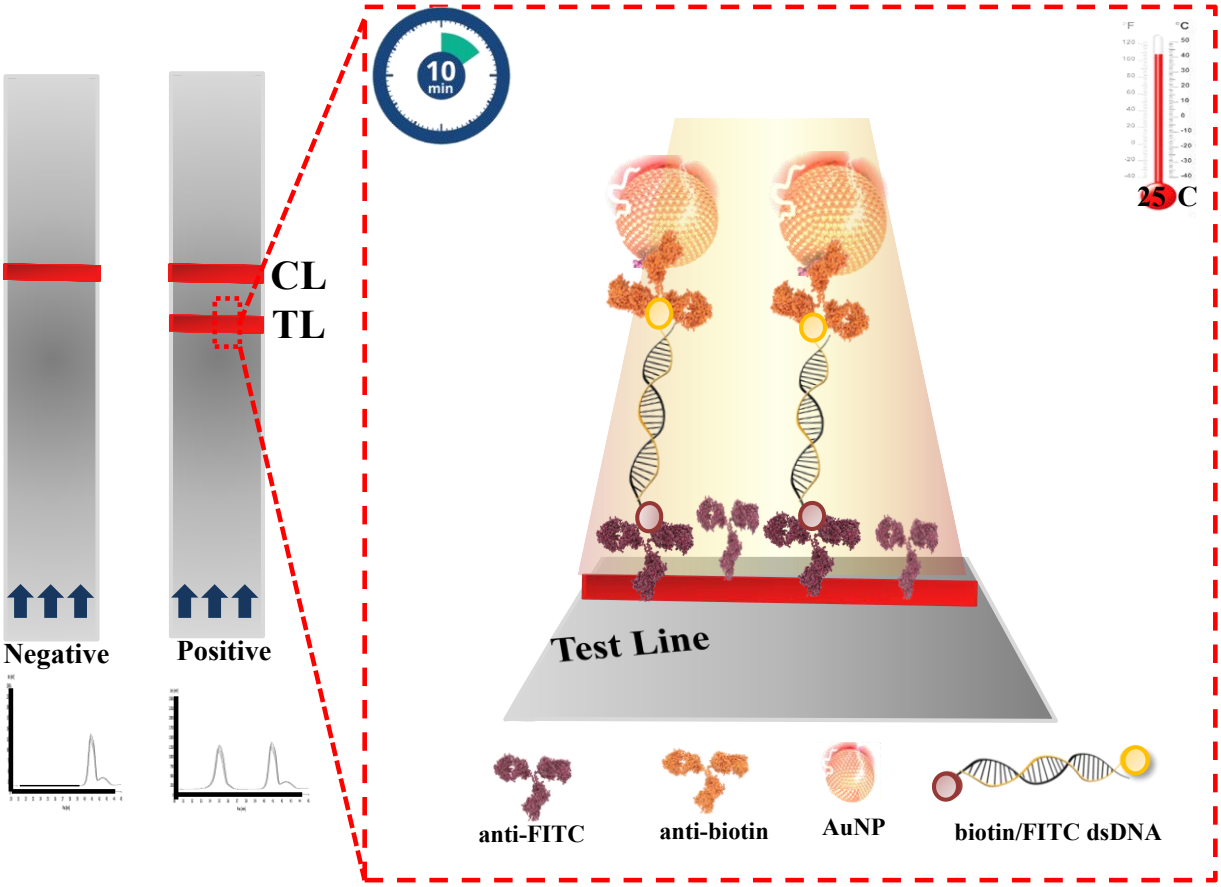

Figure 1. Schematic representation of the sandwich lateral flow based on gold nanoparticles for isothermal RPA detection of CTV-related nucleic acid.

Gold Nanoparticle-Bioconjugate for Isothermal RPA-LF Test

For the LF immunoassay, sandwich direct format based on double antibody-analyte immunoreaction was employed. Bioconjugates of AuNP-anti-biotin used to recognize the biotin/FITC amplified nucleic acid related to CTV-p20 gene forming the immunocomplex and hence be detected by capture anti-FITC antibody immobilized on the test line.

AuNPs of 20 nm were synthesized using seeded growth method [28] and the obtained nanoparticles were monitored using TEM and DLS. TEM micrographs showed typical morphology of AuNPs with mean diameter of 20 nm ± 5.6 (Figure S1, Supporting Information). Monodispersed AuNPs were synthesized and according to DLS measurement, NP hydrodynamic diameter is of 25 nm ± 8 (Figure S2, Supporting Information).

Isothermal RPA-LF Optimization

Fundamentally, RPA reaction relies on three key components (single strand binding protein, a recombinase and a strand displacing DNA polymerase) and magnesium salt to perform amplification assay. As isothermal technique, RPA mechanism works at single incubation temperature in the range between 37 to 42 °C as recommended by the manufacturer. With RPA assay, amplification time is relatively short as within 20 min of reaction time at 42 °C, a detectable level can be reached. Forward and reverse primers labeled with biotin and FITC, respectively, were designed and characterized for next experiments (Figure 2A). These primers are specific to CTV amplifying 278-bp fragment of p20 gene in the virus genome. To perform

RPA reaction using modified format of the existing RPA liquid assay, concentrations of labeled primers, enzymes, salt and DNTPs were followed as in the optimum conditions recommended by the manufacturer except total reaction volumes. With the aim of studying the ability of RPA to work in small reaction volumes, different total volumes 5, 10, 25 and 50 µL were evaluated under 37 °C amplification temperature for 30 min using the same target concentration. The assayed volumes (10, 25 and 50 µL) resulted in products with detectable signals by nanodrop quantification, evidencing the DNA amplification with volume as less as 10 µL, being then selected in LF analysis (Figure 2B).

For lateral flow detection of RPA products, LF test dipsticks were designed to recognize biotin/FITC RPA amplified products using anti-FITC as capture antibody to form the test line (TL) and anti-biotin labeled with AuNPs as reporter nanogold bioconjugate while biotin immobilized on control line (CL). After amplification of 10 µL of RPA reaction volumes for 30 min of incubation at 37 °C, a solution of undiluted biotin/FITS RPA amplified for CTV-p20 gene and the nanogold bioconjugate was prepared and then the test initiated when the as-prepared LF dipstick was directly immersed into the RPA/nanoglod bioconjugate solution. As the fluid migrated up the absorbent pad, test and control lines were appeared and can be seen by eye within 10 min, demonstrating the success of preliminary attempts in lateral flow.

The preliminary results demonstrated the success of testing undiluted RPA amplicon in lateral flow, however, in testing RPA solution were performed in the absence of the target gene as no template control (NTC), false positive signal was observed (data not shown).

In order to eliminate non-specific binding that led to false positive signals, most common running buffers used in lateral flow were evaluated. Upon amplification, RPA @ nanoglod bioconjugate solutions were prepared in three different running buffers PBS 10mM, PBST containing 0.05% (v/v) Tween 20 and 10% (v/v) of BSA and TBS 1x. Solutions prepared in PBST/BSA highly reduce the false positive results obtained from RPA performed with negative control (Figure 3A). This result suggests the effective role of the supplemented Tween/BSA in running buffer on LF performance by preventing the non-specific signals. Furthermore, the use of suitable running buffer is essential key for LF signal enhancement.

The use of heat source to reach the optimum amplification temperature is still considered as constrain for in-field pathogen detection. Toward achieving amplification without heat equipment, RPA reactions were then tested at different temperature between (20-42°C). RPA experiments performed at each temperature within 30 min amplification of CTV-p20 gene target concentration 100 pg μL^{-1} (Figure 3B). Notably, while products amplified under temperatures lower than the recommended range, color intensity was only detectable for amplification temperature as low as 25°C (room temperature), thus was chosen for next studies.

Ultimately, the effect of RPA reaction time on the lateral signal was also assessed. Product from 100 pg CTV-p20 gene amplification at room temperature within 10 min generated low intensity signal that can only be detected by colorimetric reader. As shown in Figure 4, greatly detectable color signals obtained from RPA reaction times in the range from 20 to 40 min while a color saturation was observed over 40 min.

Isothermal RPA-LF for CTV Detection

The amplification of CTV-related nucleic acid was performed in conventional PCR following previously reported method and in our optimized isothermal RPA assay. The visual detection of amplified DNA was then evaluated on our nucleic acid based paper sensor (Figure 4A).

The RPA reactions were performed for different CTV-p20 target concentrations under the optimized conditions (RPA volume: 10, RPA amplification time 20 min at room temperature) and then RPA @ nanoglod bioconjugate was prepared in TBST/BSA buffer for LF detection. According to optical density measurement, as the target concentration increased, the intensity of color of test line increased as shown in Figure 4A. When RPA results compared to those of PCR, the detection sensitivity achieved by RPA @ AuNP-LF assay was ten times higher than the PCR in lateral flow detection, showing an enhancement of LF signal resulted from coupling isothermal amplified DNA without dilution with gold nanoparticle colorimetric detection (Figure 4B and 4C).

.

Interference Studies

Citrus plant disease infections in the field may occur by mixture of pathogens including virus and viroid under natural conditions. In this sense, the pathogen interference studies were performed to evaluate the cross-reaction with a non-specific sequence characteristic of CCaV.

Therefore, under optimized experiment conditions, RPA @ AuNP-LF strips were tested in RPA solutions containing the target DNA and CCaV as interferant at 1:0, 1:1, 1:10 ratios. The optical measurements showed no significant change in the obtained signals thanks to BSA supplement in the running buffer which is mainly used as blocking agent to reduce effectively non-specific adsorption of interfering agents (Figure 5B).

Conclusions

In summary, we have developed nucleic acid lateral flow dipstick in sandwich format using AuNPs tags to recognize biotin/FITC amplicons. We demonstrated that nucleic acid amplified by isothermal RPA can be detected directly without dilution in a paper based dipstick immunoassay. Specific primers labeled with biotin and FITC were employed to generate the biotin/FITC amplicons. We found that RPA assayed in small volumes under room temperature (no heat source) is able to increase assay sensitivity as direct detection of RPA amplicon in the paper sensor was performed. Compared to the conventional PCR, it is important to note that RPA can enhance the sensitivity of LF assay and thus enable visual analysis of nucleic acid in a simple paper immunoassay format. Moreover, the results demonstrated the ability of our biosensor to discriminate between CTV-related nucleic acid and other non related pathogen sequences. These results can provide selective diagnosis of viral vs. viroid infections which is of high potential interest for in-filed plant disease diagnostics.

References

(1) Craighead, H., Leong, K. Applications: Biotechnology, medicine, and healthcare. En *Nanotechnology Research Directions: IWGN Workshop Report*. Springer, Dordrecht, 2000. p. 153-172.

(2) Zhao, Y., Chen, F., Li, Q., Wang, L., Fan, C. *Chemi. Reviews* **2015**, *115*, 12491-12545.

(3) Deng, H., Gao, Z. *Anal. Chim. Acta* **2015**, *853*, 30-45.

(4) Li, J., Macdonald, J. *Biosens. Bioelectron.* **2015**, *64*, 196-211.

(5) Notomi, T., Mori, Y., Tomita, N., Kanda, H. *J. Microbiol.* **2015**, *53*, 1-5.

(6) Zeng, R., Luo, J., Gao, S., Xu, L., Song, Z., Dai, F. *Mol. Cell. probes* **2019**, *43*, 84-85.

(7) Kim, N. Y., Oh, J., Lee, S. H., Kim, H., Moon, J. S., Jeong, R. D. *Plant Pathol J.* **2018**, *34*, 575.

(8) Ma, L., Cong, F., Zhu, Y., Wu, M., Xu, F., Huang, R., Moore, R., Guo, P. *Mol. Cell. probes* **2018**, *41*, 27-31.

(9) Geng, Y., Liu, S., Wang, J., Nan, H., Liu, L., Sun, X., Li, D., Liu, M., Wang, J., Tan, K. *Food Anal. Methods* **2018**, *11*, 2847-2856.

(10) Santiago-Felipe, S., Tortajada-Genaro, L. A., Morais, S., Puchades, R., Maquieira, Á. *Food Chem.* **2015**, *174*, 509-515.

(11) Kapoor, R., Srivastava, N., Kumar, S., Saritha, R. K., Sharma, S. K., Jain, R. K., Baranwal, V. K. *Arch. Virol.* **2017**, *162*, 2791-2796.

(12) Piepenburg, O., Williams, C. H., Stemple, D. L., Armes, N. A. *PLoS Boil.* **2006**, *4*, e204.

(13) Santiago-Felipe, S., Tortajada-Genaro, L. A., Puchades, R., Maquieira, A. *Anal. Chim. Acta* **2014**, *811*, 81-87.

(14) Lobato, I. M., O'Sullivan, C. K. *Trac Trends in Anal. Chem.* **2018**, *98*, 19-35.

(15) Yang, Y., Qin, X., Wang, G., Jin, J., Shang, Y., Zhang, Z. *Virol. J.* **2016**, *13*, 46.

(16) Lai, M. Y., Ooi, C. H., Lau, Y. L. *Am. J. Trop. Med. Hyg.* **2018**, *98*, 700-703.

(17) Powell, M. L., Bowler, F. R., Martinez, A. J., Greenwood, C. J., Armes, N., Piepenburg, O. *Anal. Biochem.* **2018**, *543*, 108-115.

(18) Liu, W. J., Yang, Y. T., Du, S. M., Yi, H. D., Xu, D. N., Cao, N., Jiang, D. L., Huang, Y. M., Tian, Y. B. *J. Virol. Methods* **2019**, *266*, 34-40.

(19) Zhao, G., Wang, H., Hou, P., He, C., He, H. *J. Vet. Sci.* **2018**, *19*, 242-250.

(20) Ghosh, D. K., Kokane, S. B., Kokane, A. D., Warghane, A. J., Motghare, M. R., Bhose, S.,Sharma, A.k., Reddy, M. K. *PloS one* **2018**, *13*, e0208530.

(21) Hu, J., Huang, R., Sun, Y., Wei, X., Wang, Y., Jiang, C., Geng, Y., Sun, X., Jing, J., Gao, H.,Wang, Z., Wang, Z., Dong, C. *J Microbiol. Methods* **2019**, *158*, 25-32.

(22) Du, X. J., Zang, Y. X., Liu, H. B., Li, P., Wang, S. *J. Food Sci.* **2018**, *83*, 1041-1047.

(23) Qi, Y., Shao, Y., Rao, J., Shen, W., Yin, Q., Li, X., Chen, H., Li, J., Zeng, W., Zheng, S., Liu, S., Li, Y. *PloS one* **2018**, *13*, e0207811.

(24) Hu, S., Zhong, H., Huang, W., Zhan, W., Yang, X., Tang, B., Chen, K., Wang, J., Hu, T., Zhang, C., Zhou, Z., Luo, M. *Diagn. Mmicrobiol. Infect. Dis.* **2019**, *93*, 9-13.

(25) Rivas, L., de La Escosura-Muñiz, A., Pons, J., Merkoçi, A. Lateral flow biosensors based on gold nanoparticles. In *Comprehensive analytical chemistry* (Vol. 66, pp. 569-605), Elsevier, 2014.

(26) Parolo, C., de la Escosura-Muñiz, A., Merkoçi, A. B*iosens. Bioelectron.* **2013**, *40*, 412-416.

(27) Rivas, L., de la Escosura-Muñiz, A., Serrano, L., Altet, L., Francino, O., Sánchez, A., Merkoçi, A. *Nano Research* **2015**, *8*, 3704-3714.

(28) Khater, M., de la Escosura-Muñiz, A., Altet, L., Merkoçi, A. *Anal. Chem.* **2019**, *91*, 4790-4796.

(29) Bastús, N. G., Comenge, J., Puntes, V. *Langmuir* **2011**, *27*, 11098-11105.

(30) Quesada-González, D., Jairo, G. A., Blake, R. C., Blake, D. A., Merkoçi, A. *Sci. Rep.* **2018**, *8*, 16157.

Annex I-Experimental Section

Chapter III-Electrochemical Detection of Plant Virus Using Gold Nanoparticle-modified Electrodes

Chemicals and equipment

Gold (III) chloride hydrate ($HAuCl_4$, 99.9%), potassium hexacyanoferrate (III), potassium hexacyanoferrate (II), tris (2-carboxyethyl) phosphine (TCEP), NaCl, $MgCl_2$, $CaCl_2$, 6-Mercaptohexanol (MCH) and phosphate buffered saline were obtained from Sigma Aldrich (Spain). CTV immunostrips were provided by Agdia inc. (USA). Oligonucleotides were purchased from Isogen (Spain). Sequences are the following: Thiolated ssDNA probe: 5,,-GGATCGATGTGTAA-3,,-$(CH_2)_6$–HS; Target ssDNA (fully complementary; characteristic of CTV): 5‟‟-TTACACATCGATCC -3‟‟; partially non complementary ssDNA (characteristic of Psorosis virus): 5‟‟-TTACACAAGGATCT-3‟‟; fully non complementary ssDNA 5,,-TAGGATTAGCCGCATTCAGG-3‟‟ as control sequences. Thiolated ssDNA probe was pre-treated as detailed at the *supplementary information*. All buffer solutions were prepared with ultrapure water of Milli-Q water purification system (with resistivity of 18.2 MΩ cm). The supporting electrolyte was 0.5 mM solution of $K_3[Fe(CN)_6]/K_4[Fe(CN)_6]$ in 0.1M KCl. DNA probe and target sequences were diluted in 34 mM Tris-HCl, pH 7.4 buffer. The washing solution was 0.01 M phosphate buffered saline (PBS; pH 7.4). Stock solutions of the oligonucleotides were prepared in TE (0.01 M Tris-HCl; pH 8.2 and 0.001 M EDTA) buffer solution and kept frozen at -20 ºC. Healthy citrus leaves were provided by Universitat Autònoma de Barcelona in Spain and for detailed preparation of leaf extracts and its screening for CTV, see the *supplementary information.* SEM images of the modified carbon working electrode with

electrodeposited gold nanoparticles were obtained using a FEI Quanta™ 650 field emission gun scanning electron microscope (FEI, USA). Images were analyzed using Image J software (National Institutes of Health, USA) for measuring particles size and density. All electrochemical measurements were recorded using Autolab potentiosat PGS00 supported by two different softwares: FRA for impedance spectra analysis and GPES for voltammetric analysis. Home-made screen-printed carbon electrodes (SPCEs) preparation is detailed at the *supplementary information*.

Methods

AuNPs electrodeposition

Two-step electrochemical pre-treatment was applied on SPCEs under a potential of +1.6 V for 120 s and of +1.8 V for 60 s in acidic solution (0.1 M acetate buffer; pH 4.7). Major advantages of this pretreatment included cleaned carbon surface from possible printing contaminants, higher hydrophilicity and better electron transfer at the working electrode surface (Pereira *et al*., 2011). Importantly, the working pH of 1-3 for gold solution to perform deposition was found to be significantly favorable for controlling particle size and distribution over carbon electrodes (Karoonian *et al*., 2012). The deposition process of AuNPs on SPCEs was performed by immersion into a gold solution of pH 1 (0.01% $HAuCl_4$, / 0.1 M NaCl in the presence of 1.5 wt% HCl). Reduction of chloride gold (III) complexes to gold (0) and further deposition were achieved by applying a constant negative potential of -0.4 V for a determined time (from 10 s to 1200 s). Then the modified SPCEs were carefully rinsed and dried with nitrogen gas. After deposition of AuNPs onto carbon working electrode, AuNP-SPCE was characterized using CV, EIS and SEM.

Probe ssDNA immobilization and hybridization with target ssDNA

The covalent attachment of thiolated ssDNA probes onto the deposited AuNPs of the pretreated electrodes was performed by incubation of 15 µL of thiolated ssDNA probes solution at room temperature for 2 h. After that, the electrodes were rinsed with PBS and Milli-Q water (3X). The concentration and incubation time of thiolated ssDNA probe were optimized as shown at *DNA hybridization biosensor optimization section*. Hybridization with complementary target ssDNA was performed by adding 15 µL and incubating during 60 min at room temperature. The same procedure was followed for the control assays with the non-complementary strand.

Electrochemical measurements

CV and EIS were used for the characterization of the AuNP-modified SPCEs, while the stepwise of the biosensor was characterized by EIS technique.

CVs were carried out in 0.5 M H_2SO_4 and 0.5 mM $K_3[Fe(CN)_6]/K_4[Fe(CN)_6]$ in 0.1 M KCl from +1.4 to -0.6 V at a scan rate of 50 mV/s. EIS measurements were performed in 0.5 mM $K_3[Fe(CN)_6]/K_4[Fe(CN)_6]$ in 0.1 M KCl within frequency ranging from 10 KHz to 0.5 Hz and alternating voltage amplitude of 5 mV. The results of impedance measurements were represented in the form of the Nyquist plot which visually shows the system dynamics.

The diameter of semicircle in the Nyquist plot is assigned to $Fe[(CN)_6]^{4-/3-}$ charge transfer resistance (Rct) at high frequency when a line portion yielded from mass transfer limitation process at low frequencies. The difference in charge transfer resistance before and after DNA hybridization and duplex DNA (dsDNA) formation (ΔR_{ct}) were obtained following equation $\Delta R_{ct}= (R-R_0)/R_0$. Here R and R_0 are charge transfer resistance of dsDNA and ssDNA, respectively. For analytical analysis, R_{ct} was measured by fitting data to equivalent circuits (Randless circuit) using the tools of the FRA software. Mean and standard deviation for all EIS reported results were calculated to represent obtained data. EIS and CV tests were conducted under ambient conditions.

Chapter IV-In Situ Plant Virus Nucleic Acid Isothermal Amplification Detection on Gold Nanoparticle-modified Electrodes

Chemicals and equipment

Gold (III) chloride hydrate ($HAuCl_4$, 99.9%), potassium hexacyanoferrate (III), potassium hexacyanoferrate (II), tris (2-carboxyethyl) phosphine (TCEP), NaCl, $MgCl_2$, $CaCl_2$, 6-Mercaptohexanol (MCH) and phosphate buffered saline were obtained from Sigma Aldrich (Spain). The target and control sequences together with six primers were synthesized by Integrated DNA Technologies (Coralville, USA) (Table S1, in the *supplementary information*). TwistAmp Basic Kit containing all enzymes and reagents necessary for the amplification of DNA (TwistDx Ltd, Cambridge, UK). For purification of post-amplification DNA products, DNA clean and concentrator kit was purchased from Ecogen (Spain). Thiolated primer was pre-treated as detailed at the *supplementary information*. All buffer solutions were prepared with ultrapure water of Milli-Q water purification system (with resistivity of 18.2 MΩ cm). The supporting electrolyte was 0.5 mM solution of $K_3[Fe(CN)_6]/K_4[Fe(CN)_6]$ in 0.1M KCl.Thiolated primer was diluted in 34 mM Tris-HCl, pH 7.4 buffer. The washing solutions were 0.01 M phosphate buffered saline (PBS; pH 7.4), PBST (PBS and 0.05% (v/v) Tween 20, pH 7.4) and 2 × SCC buffer (300 mM sodium chloride 30 mM sodium citrate), with pH adjusted to 7.2. Stock solutions of the oligonucleotides were prepared in TE (0.01 M Tris-HCl; pH 8.2 and 0.001 M EDTA) buffer solution and kept frozen at -20 ºC. Ultrapure agarose and 50X TAE buffer (Tris-acetate-EDTA) were purchased from Invitrogen for electrophoresis of amplified nucleic acid. The agarose gel was stained by the green fluorescent Midori DNA stain. Electrophoresis was

carried out using Mupid®-one and followed by gel-documentation under UV light at 300 nm. Nanodrop 1000 was used to quantify of DNA concentrations after RPA amplification with thiolated forward primer. Block heater was used for the incubation of RPA reactions. All electrochemical measurements were recorded using Autolab potentiosat PGS00 supported by FRA for impedance spectra analysis. Home-made screen-printed carbon electrodes (SPCEs) preparation is detailed at the *supplementary information*.

Methods

RPA assay of CTV related nucleic acid

The sequence of p20 gene (549nt) responsible for systemic infection was first selected in CTV genome. Such sequence is specific to CTV and does not relate to other closteridea viruses, major component of CTV and highly produced in infected trees. Three forward and two reverse primers were designed (between 25 and 35 bp) to amplify the p20 of 378-bp of CTV genomic nucleic acid, following the RPA manufacture‟s manual. Then the primer combinations were screened by gel electrophoresis in order to select the optimal primer pair which has great sensitivity and specificity for CTV.

For the RPA assays (50 µL reaction volume), a master mix composed of 2.4 µL of primers (10 µM), 29.5 µL of rehydration buffer and 13.8 µL of CTV-p20 gene and DNase-free water was first prepared. After dividing aliquots of the master mix into reaction tubes and mixing with TwistAmp basic Freeze-dried enzyme pellets, the RPA reactions were started immediately by adding magnesium acetate (280 mM). The reaction tubes were incubated at 37°C for 30 min. RPA reactions were performed without the target gene as no template control (NTC). Following post-amplification purification, amplicons were analysed in 2% agarose gel.

In situ isothermal RPA on gold nanoparticle modified electrodes

SPCEs modification with AuNPs and thiolated nucleic acid immobilization were performed following a previously optimized procedure.[37] Briefly, the electrodes were pre-treated by applying oxidative potentials of +1.6 V for 120 s and of +1.8 V for 60 s in acetate buffer, followed by rinsing with PBS and Milli-Q water (3X) and dried using nitrogen. Carbon working electrodes were then immersed into a gold solution (0.01% HAuCl4, / 0.1 M NaCl in the presence of 1.5 wt% HCl) and a constant negative potential of -0.4 V for 200 s was applied for achieving a homogenous formation of well distributed spherical AuNPs of 50 nm. The thiolated forward primer (SH-(AT_7)-F1) was pre-reduced using TCEP as detailed at the *supplementary information*. AuNP-modified SPCEs were then incubated with 15 µL of 0.1µM SH-(AT_7)-F1 prepared with 1 mM MCH solution at ratio (1:0.1) for 2 h at room temperature. After that, the electrodes were thoroughly rinsed using PBS and dried with nitrogen gas.

RPA solutions were then prepared for the surface amplification and detection of the target sequence of (P_{20} gene) on the AuNP-modified SPCEs. For master mix of RPA reaction preparation, 29.5 µL of rehydration buffer, 2.4 µL of reverse primer (10 µM) and 13.2 µL of DNase-free water were mixed and added to the freeze-dried enzyme pellet. Then, this mixture was mixed well with 2.5 µL of magnesium acetate at concentration of 280 mM. After that, the 50 µL reaction volume was divided into 10 µL aliquots and added to AuNP-modified SPCEs. Finally, 5 µL of the P20 gene from the target plant virus genome that ranges in concentrations from 1 pg μL^{-1} to 1 ng μL^{-1} was added to the previously prepared 10 µL RPA solution. The solid phase isothermal amplification assays were performed at room temperature (25 ±3°C) for 60 min. Additionally, the AuNP-modified SPCEs with RPA solutions containing water or other unrelated DNAs as negative controls were evaluated.

Electrochemical measurements

The *in situ* isothermal RPA was characterized by electrochemical impedance spectroscopy (EIS). Impedance measurements were performed in 0.5 mM $K_3[Fe(CN)_6]/K_4[Fe(CN)_6]$ in 0.1 M KCl within frequency ranging from 10 KHz to 0.005 Hz and alternating voltage amplitude of 5 mV. The Nyquist plots of impedance which represent the system dynamics were employed to detect the isothermal amplified DNA (278- bp) on the AuNP-modified SPCEs.

The change in the semicircle diameter of the impedance represents the charge transfer resistance (R_{ct}) of Fe $[(CN)_6]^{4-/3-}$ at the modified electrode surface. The difference in charge transfer resistance before and after DNA amplification forming duplex DNA (dsDNA), (ΔR_{ct}) was obtained following the equation: $\Delta R_{ct}= (R-R_0)/R_0$, where R and R_0 are charge transfer resistance of amplified dsDNA and primer ssDNA, respectively. For accurate analytical analysis, the recorded R_{ct} was fitted to the equivalent circuits (Randless circuit) using FRA. All EIS reported results were analyzed by calculating means and standard deviation to represent obtained data. All impedance experiments were conducted under ambient conditions.

Chapter V- Highly Sensitive Direct Detection of Plant Virus Nucleic Acid Amplification on Gold Nanoparticle-based Paper Sensor

Chemicals and equipment

Gold (III) chloride hydrate ($HAuCl_4$, 99.9%), bovine serum albumin (BSA), anti-FITC antibody, trisodium citrate, Tween 20, phosphate buffer saline (PBS) tablets and the reagents to prepare phosphate buffer non-saline (PB; sodium phosphate basic and dibasic) and borate buffer (BB; sodium tetraborate and boric acid) were purchased from Sigma Aldrich. Anti-biotin antibody was purchased from Bionova and biotin was obtained from Invitrogen.

The target CTV nucleic acid P_{20} gene of 378-bp sequence: 5′TACTAGTATAACGTATTAAACACTTTAGTGAGGAGTTTTGTTTGAATCAAACAATATGCGAGCTTACTTTAGTGT TAACGATTACATAAGCCTTTTGGCTAAGGTTGGTTCAGTTGTGGAACGTTTGTGCGATCCCAGCGTAACTCTCACG GAAGTGATGGACGAAATTAATGATTTTAACTCGTTTCTCGCTTTGGTGCACTCTATGAAGTCGGACATGAACGGCG ATCATCAGGATGGTCACCATGAGATGGGTGAACATAAATCTCGGTTGTTGTGCAATATAGAGGCGAAACTGCGAG TGCTTCTCGACATCATAAGACGTCGGTTTACTCGCGAAAAACTGCTCTGTACCAGTGCTACAGATGTTGTGGGCTT 3′ and control sequence of *Citrus Cachexia viroid* (CCaV 100-bp) sequence: 5‟‟CTGGGGAATTCTCGAGTTGCCGCATAAGGCAAGCAAAGAAAAAACAAGGCAGGGAGGAGACTTACCTGAGAA AGGAGCCCCGGGGCAACTCTTCTCAGAA3‟‟ together with labeled forward primer with biotin (5-biotin F20) 5‟‟- ACAATATGCGAGCTTACTTTA-3‟‟ and reverse primer with FITC label (5-FITC R20) 5'- CCGACGTCTTATGATGTCGAG -3' were synthesized by Integrated DNA Technologies (Coralville, USA).[28] TwistAmp Liquid Basic Kit containing all enzymes and reagents necessary for the amplification of DNA (TwistDx Ltd, Cambridge, UK). PCR kit containing GoTaq DNA polymerase, $Mgcl_2$ and DNTPs was purchased from Invitrogen (Spain). All buffer solutions were prepared with ultrapure water of Milli-Q water purification system (with resistivity of 18.2 MΩ

cm). The running solutions were 0.01 M phosphate buffered saline (PBS; pH 7.4), PBST (PBS and 0.05% (v/v) Tween 20, pH 7.4) and 2× SCC buffer (300 mM sodium chloride 30 mM sodium citrate), with pH adjusted to 7.2. Stock solutions of the oligonucleotides were prepared in TE (0.01 M Tris-HCl; pH 8.2 and 0.001 M EDTA) buffer solution and kept frozen at -20 ºC. Cellulose membrane (CFSP001700), nitrocellulose membrane (HF180) and adhesive laminated cards (HF000MC100) were purchased from Millipore. DNA upon RPA amplification with labeled primers was quantified by Nanodrop 1000. Block heater was used for the incubation of RPA reactions. All glassware was cleaned with agua regia, rinsed with deionized water before use.

An Isoflow dispenser from Imagene Technology, Allegra 64 R Centrifuge, Biosan TS-100 Thermoshaker, strip reader from COZART-SpinReact, Tecnai G2 F20 TEM (FEI), SpectraMax iD3 Multi-Mode Microplate Reader. Malvern Zetasizer Nano 26.

Methods

Lateral Flow Dipstick Preparation

Cellulose membrane was used as sample and absorbent pads when detection pad was prepared from nitrocellulose membrane. Both biotin (1 mg/mL) and anti-FITC polyclonal antibody (1 mg/mL) solutions were dispensed onto the detection pad as control line (CL) and test line, respectively. The detection pad was dried at 37 °C for 2 hours and stored at room temperature under dry conditions until use. All membranes were assembled onto an adhesive laminated card backing 5.5 cm width $_x$30 cm length. The detection pad was firstly assembled in the middle of the card, then sample was assembled 1mm overlapped the detection pad on one side while the absorbent pad was over the detection pad around 3 mm distant from the control line on the other side of the adhesive card . Finally, the strips were cut to a width of 3.5 mm using a guillotine and stored at room temperature under dry conditions.

Synthesis and Characterization of Gold Nanoparticles (AuNPs)

AuNPs of approximately ≈ 20 nm diameter were synthesized by following the growth seeded method.[29] A solution of 2.2 mM sodium citrate was prepared in final volume of 150 mL Milli-Q water in three-necked round-bottomed flask, a condenser attached to the middle neck is being used to prevent solvents from evaporation. This solution was heated to boiling point; 1 mL of $HAuCl_4$ (25 mM) was added under continuous vigorous stirring. The change of the solution color was observed from yellow to soft pink in 10 min resulting in Au seeds of ≈10nm. The reaction was then allowed to cool to 90 °C. Then, 1 mL of sodium citrate (60 mM) and 1 mL of a $HAuCl_4$ solution (25 mM) were chronologically injected (time delay ≈2 min). After 30 min, this process was repeated twice; up to ≈ 20 nm gold particles were grown. The AuNPs were characterized by transmission electron microscopy and DLS (see more details, supporting information).

Antibiotin-AuNP Bioconjugate

The conjugation of antibody to gold nanoparticle was performed using method previously developed by our group.[30] The pH of AuNP solutions were first adjusted by 0.01 mM borate buffer to reach pH 9. Solutions of anti-biotin antibody of 200 µg/mL were prepared in PB and aliquots of 100 µL were then added to 1.5 mL of AuNP solution and incubated for 20 minutes at room temperature. After the conjugation of antibodies on the surface of gold, a solution of BSA 1% (w/v, 100 µL) was utilized to block the rest gold particle surface and the mixture was allowed to by incubating the mixture for additional 20 minutes. To remove the excess of antibody, a centrifugation at 14000 rpm for 20 minutes at 4 °C was performed. The supernatant was discarded and the pellet was resuspended in 0.2 mL PBS buffer. Spectral analysis of the synthesised AuNPs and anti-biotin AuNP conjugates was in the 350 to 700 nm range, showing

shift in the absorbance peak after conjugation (see Supporting Information). Moreover, the conjugated anti-biotin AuNPs were measured by Z potential (see Supporting Information).

Conventional PCR

For the PCR assays (25 µl final reaction volume), a master mix of 5 µl target gene,1X GoTaq Flexi DNA polymerase buffer , 1,5 mM MgCl2, 0,2mM dNTPs, 0,2µM of each biotin-forward and FITC-reverse primers of the target CTV-p20 gene (ref) and 0,2µl of GoTaq Flexi DNA polymerase (5U/µl). For amplification, an initial denaturation at 95°C for 5 min, followed by 40 cycles of the main three step of amplification including dsDNA denaturation at 95°C for 30s, primers annealing at 56°C for 1 min and extension at 72°C for 1 min. PCR products were also incubated for additional 7 min at 72°C for final DNA extension, prior to be maintained at 4°C until LF analysis.

RPA Assay for CTV

According to Twist manufacturer instructions with some modification, RPA assays were performed. Briefly, for the RPA assays (10 µL reaction volume), a master mix composed of 10 µM primers , 1.8 mM dNTPs , 2X reaction buffer, 10X Basic E-Mix, CTV-p20 gene and DNase-free water was first prepared. The RPA reactions were commenced immediately by adding magnesium acetate (280 mM). The reaction tubes were incubated at room temperature for 20 min. RPA reactions were also performed without the target gene as no template control (NTC).

RPA-LF Assay Performance

Solutions of RPA amplicon and gold conjugates at volume ratio 1:2 were mixed with 100 µL of PBST containing 1% BSA of running buffer. These mixtures were then applied on the sample pad of the strips. After 5 minutes, TL and CL were formed on the detection pad. After 15-20 minutes, images of the strips were taken using a mobile phone camera and the color intensity of TL was measured by the strip reader.

Annex II-Supporting Information

Chapter III-Electrochemical detection of plant virus using gold nanoparticle-modified electrodes

Screen-printed carbon electrodes preparation

The electrochemical transducers were homemade screen-printed carbon electrodes (SPCEs) consisting of three electrodes in a single strip: working electrode (WE), reference electrode (RE) and counter electrode (CE). The full size of the sensor strip was 29mm x 6.7mm, and the WE diameter was 3mm. The fabrication of the SPCEs was carried out in three steps in the semi-automatic screen-printing machine DEK248 (DEK International, Switzerland), using a different stencil, with the corresponding patterns, for each layer. First, a graphite layer (Electrodag 423SS carbon ink for WE and CE) was printed onto the polyester sheet (Autostat HT5, McDermid Autotype, UK). After curing for 30 min at 95ºC, a second layer was printed with silver/silver chloride ink (Electrodag 6037SS for the RE). After another curing for 30 min at 95ºC, the insulating layer was printed using insulating ink (Minico 7000 Blue, Acheson Industries, The Netherlands) to protect the contacts and define the sample interaction area. Finally, the SPCEs were cured again at 95ºC for 20 min.

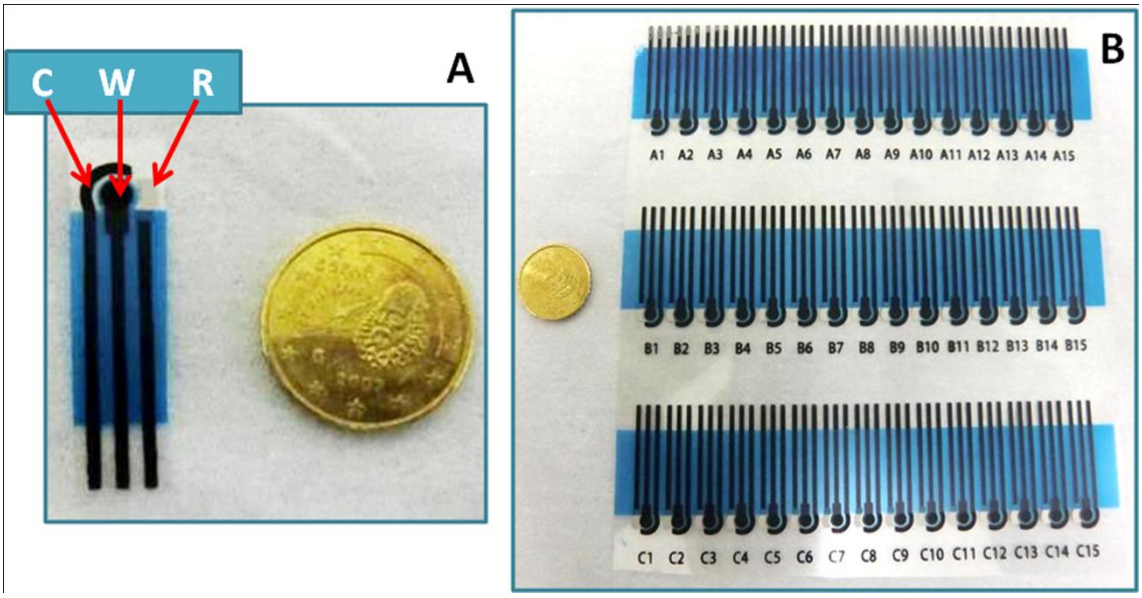

Figure SM-1: (A) Detail of one SPCE, containing the three electrodes in the working area; R- Ag/AgCl reference electrode, W- carbon working electrode and C- carbon counter electrode. (B) Images of the 45 SPCE sensors sheet obtained following the experimental procedure.

Thiolated ssDNA pre-treatment

Prior to DNA probe immobilization, thiolated ssDNA probe is reduced before use. According to the manufacturer‟s recommended protocol, first of all, the lyophilized probe was re-suspended by adding 200 µL of 10 mM TCEP then the solution was shaked for 60 min at room temperature. Second was precipitation step by adding 150 µL of 3 M NaAc and 750 µL of EtOH and incubating 20 min at –20 °C. At last, it was spinned for 5 min at 13 000 rpm, the supernatant was discarded and let the pellet to dry at room temperature.

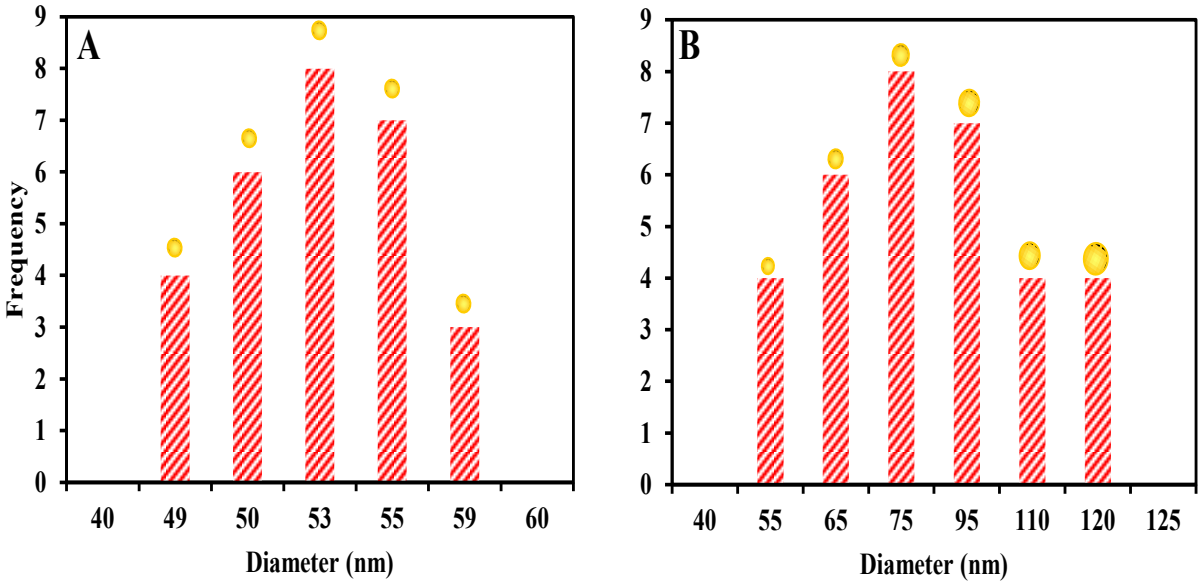

Figure SM-2: The diameter of AuNPs after electrodeposition times of (A) 200 s (average AuNPs size 53± nm) and (B) 600 s; AuNPs diameter (ranging 60-100 nm) at potential of – 0.4 V.

Citrus leaf extracts and its screening for CTV

Citrus leaves were collected and tested with CTV-immunostrips following the manufacture‟s protocol. Briefly, 0.15 g of citrus leaf was placed in mesh bag and ground in sample extract buffer. Immediately after grinding, the strip was placed into the leaf extract bags for CTV testing. The strip was remained in the extract for almost 30 min and only the control line appeared confirming the sample is negative for CTV and can be used for further experiments (e.i interference and recovery studies of our biosensor).

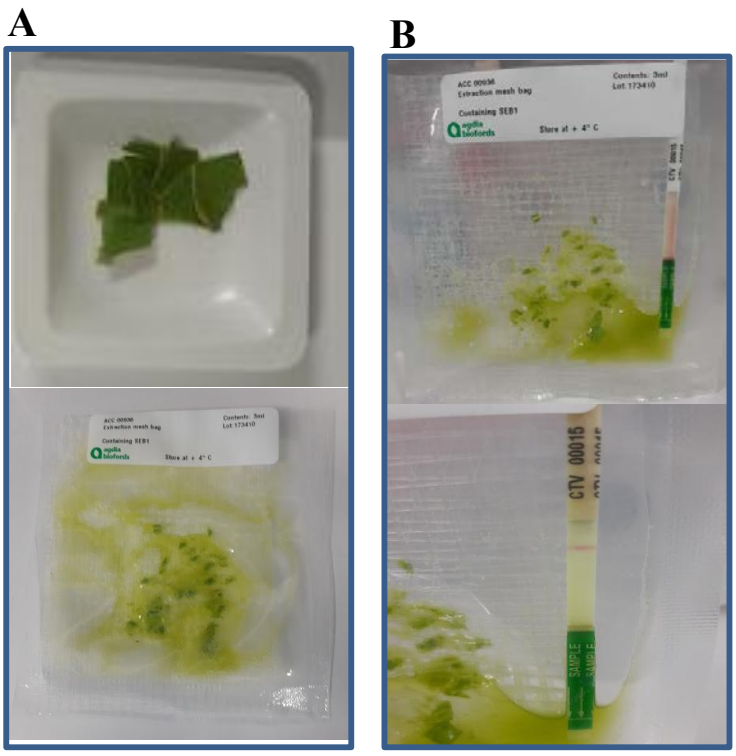

Figure SM-3: (A) citrus leaf extracts preparation (B) Lateral flow immunoassay for CTV testing.

Chapter IV-In situ plant virus nucleic acid isothermal amplification detection on gold nanoparticle-modified electrodes

Name	Sequence (5'→3')
CTV nucleic acid (P_{20} gene 378-bp)	TACTAGTATAACGTATTAAACACTTTAGTGAGGAGTTTTGTTTGAATC AAACAATATGCGAGCTTACTTTAGTGTTAACGATTACATAAGCCTTTT GGCTAAGGTTGGTTCAGTTGTGGAACGTTTGTGCGATCCCAGCGTAAC TCTCACGGAAGTGATGGACGAAATTAATGATTTTAACTCGTTTCTCGC TTTGGTGCACTCTATGAAGTCGGACATGAACGGCGATCATCAGGATGG TCACCATGAGATGGGTGAACATAAATCTCGGTTGTTGTGCAATATAGA GGCGAAACTGCGAGTGCTTCTCGACATCATAAGACGTCGGTTTACTCG CGAAAAACTGCTCTGTACCAGTGCTACAGATGTTGTGGGCTT

P20 specific primers

F1	ACA ATA TGC GAG CTT ACT TTA
F2	CTA GCG GAC AAA CTT TCG TTT CTG
F3	CCT TTC TGA CGA AAG CAA C
R1	CCG ACG TCT TAT GAT GTC GAG
R2	CGT GTT TTC TAC CAC AAT CCA CG
SH-(AT_7)-F1	ATATATATATATAT ACA ATA TGC GAG CTT ACT TTA
Control DNAs	
Citrus Cachexia viroid (CCaV 100-bp)	CTGGGGAATTCTCGAGTTGCCGCATAAGGCAAGCAAAGAAAAAACAA GGCAGGGAGGAGACTTACCTGAGAAAGGAGCCCCGGGGCAACTCTTC TCAGAA
Citrus Psorosis virus (CPsV 100-bp)	ACTCAAGCTATAAAATCCCTGAGGAAATTAGCTGATATAACAATAGG AACATTTTCTAATGCAAAAATTAATGATATCGAAGAAGCTGTCGTCTG CCCAA

Table S1: Sequences of target nucleic acid (a 378-bp highly conserved region of CTV p20 protein gene, Genbank accession number: KP268286). Controls are *Citrus Cachexia viroid* (CCaV 100-bp; GenBank: AF213502) and *Citrus Psorosis virus* (CPsV 100-bp; GenBank: AM268299). Forward primers: (F1, F2, F3 and SH-(AT_7)-F1). Reverse primers: (R1, R2).

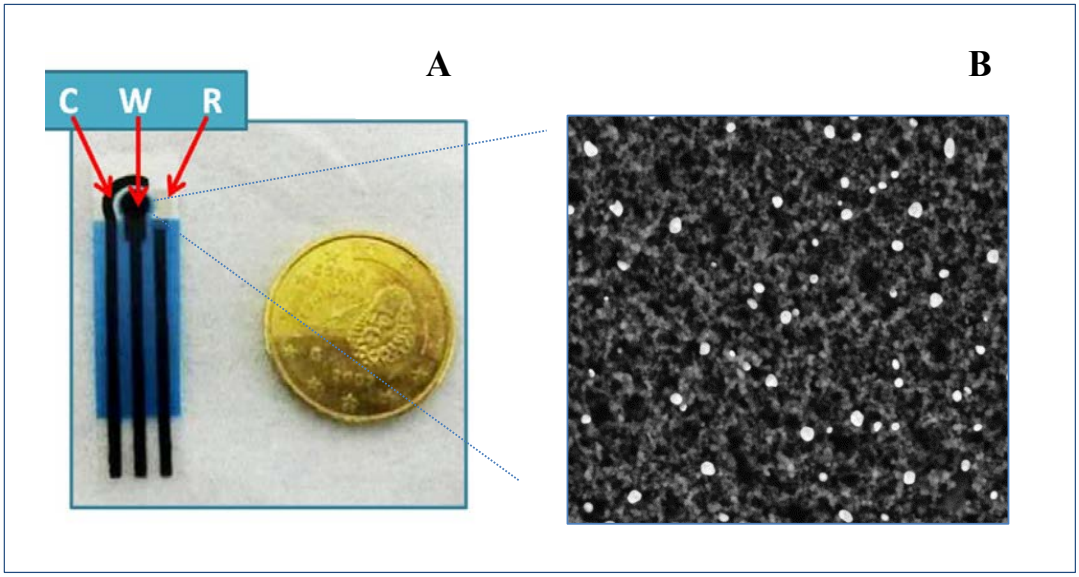
A
B
C
W
R

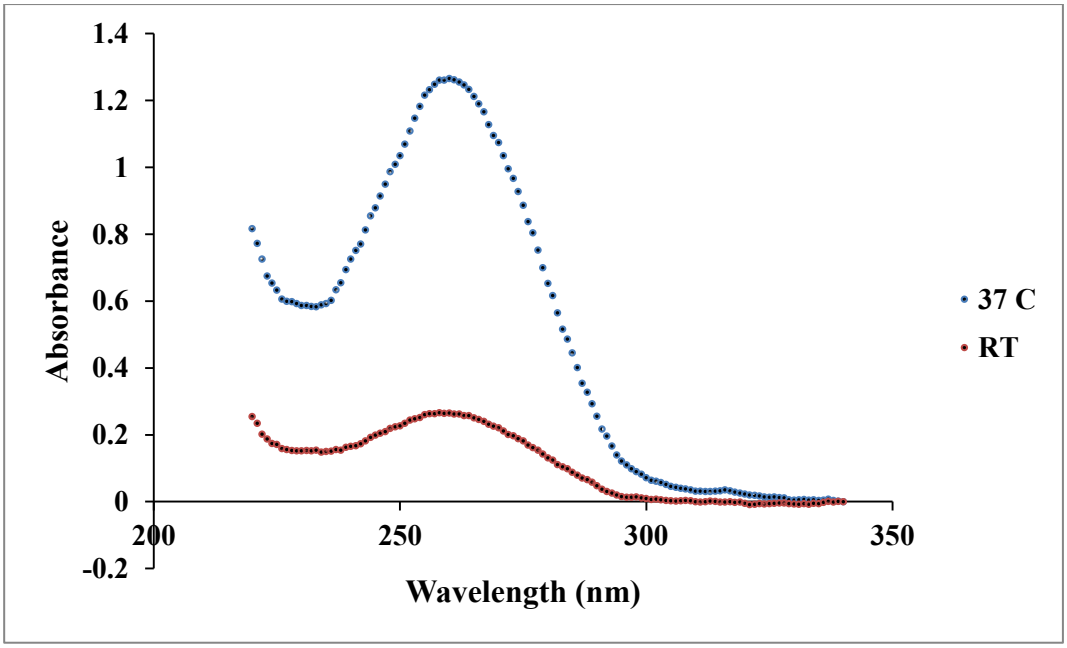

Figure S2: Nanodrop nucleic acid quantification of RPA amplicons in solutions using (SH-(AT_7)-F1) as forward primer; Amplification temperature: 37°C and RT; p20 concentration: 0.1 ng μL^{-1}; Amplification time: 30 min.

Chapter V- Highly Sensitive Direct Detection of Plant Virus Nucleic Acid Amplification on Gold Nanoparticle-based Paper Sensor

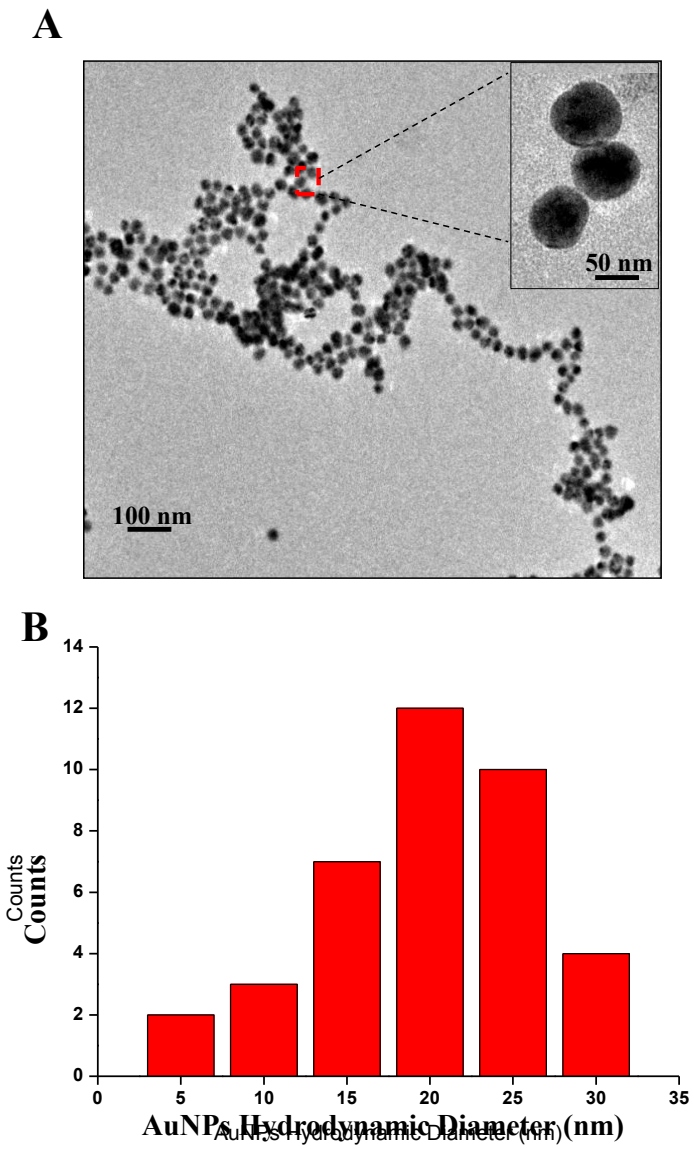

Figure S1: Synthesized AuNPs characterized by A) TEM and B) DLs

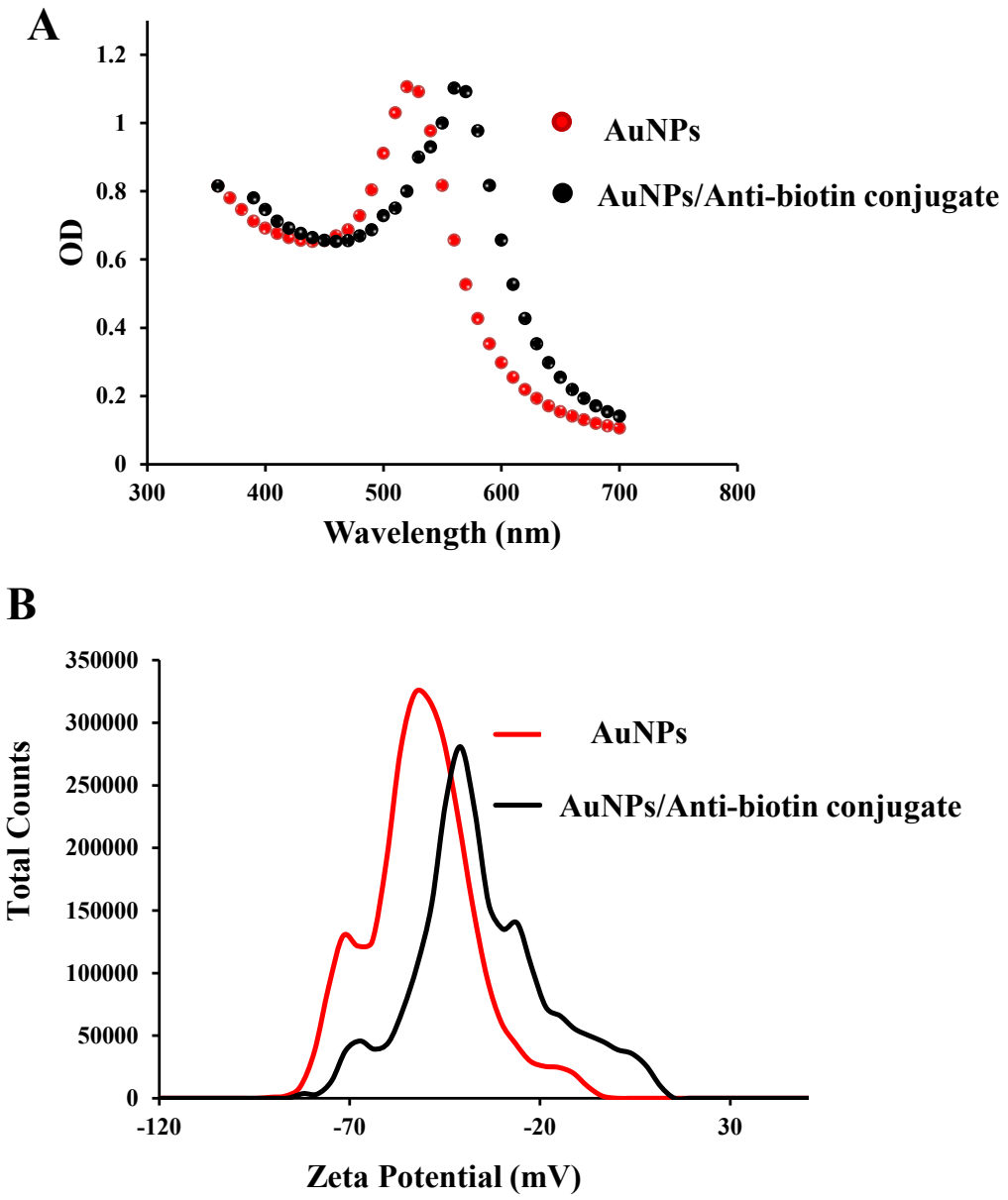

Figure S2: Characterization of gold nanoparticles before and after conjugation with antibody by A) UV-spectroscopy and B) Z potential**.**

Annex III-List of Abbreviations

Acronym	Definition
AuNPs	Gold Nanoparticles
BSA	Bovine Serum Albumin
CL	Control Line
CTV	Citrus tristeza virus
CCaV	Citrus cachexia viroid
DNA	Doxyribonucleci acid
DPV	Differntical Pluse Voltametry
EDTA	1-Ethyl-3-(3-dimethylaminopropyl) carbodiimide
EIS	Electrochemical Impedance Spectroscopy
ELISA	Enzyme-Linked Immunosorbent Assay
FITC	Fluorescein Amidite
LFA	Lateral Flow
LFA	Lateral Flow Assay
LFIA	Lateral Flow Immunoassay
LoD	Limit of Detection
LAMP	Loop-Mediated Isothermal Amplification
NALF	Nucleic Acid Lateral Flow
NALFI	Nucleic acid Lateral Flow Immunoassay
NC	Nitrocellulose
NPa	Nanoparticles
PBS	Phosphate Buffer Saline
PCR	Polymerase Chain Reaction
POC	Point-of-Care testing

Rct	Charge-transfer Resistance
RPA	Recombinase Polymerase Amplification
RSD	Relative Standard Deviation
SPCE	Screen-printed Carbon Electrode
ssDNA	single-strabded Deoxyribonucleic acid
TL	Test line
UV-Vis	Ultraviolet-visible

Annex IV-Scientific Publications

Biosensors and Bioelectronics 93 (2017) 72–86

Contents lists available at ScienceDirect

Biosensors and Bioelectronics

journal homepage: www.elsevier.com/locate/bios

Biosensors for plant pathogen detection

Mohga Khater[a,b], Alfredo de la Escosura-Muñiz[a], Arben Merkoçi[a,c,*]

[a] Catalan Institute of Nanoscience and Nanotechnology (ICN2), CSIC and Barcelona Institute of Science and Technology, Campus UAB, 08193 Barcelona, Spain
[b] On leave from Agricultural Research Center (ARC), Ministry of Agriculture and Land Reclamation, Giza, Egypt
[c] ICREA, Pg. Lluís Companys 23, 08010 Barcelona, Spain

ARTICLE INFO

Keywords:
Plant pathogen
Bacteria
Virus
Biosensor
Point-of-care
Nanomaterial
Antigen
DNA

ABSTRACT

Infectious plant diseases are caused by pathogenic microorganisms such as fungi, bacteria, viruses, viroids, phytoplasma and nematodes. Worldwide, plant pathogen infections are among main factors limiting crop productivity and increasing economic losses. Plant pathogen detection is important as first step to manage a plant disease in greenhouses, field conditions and at the country boarders. Current immunological techniques used to detect pathogens in plant include enzyme-linked immunosorbent assays (ELISA) and direct tissue blot immunoassays (DTBIA). DNA-based techniques such as polymerase chain reaction (PCR), real time PCR (RT-PCR) and dot blot hybridization have also been proposed for pathogen identification and detection. However these methodologies are time-consuming and require complex instruments, being not suitable for in-situ analysis. Consequently, there is strong interest for developing new biosensing systems for early detection of plant diseases with high sensitivity and specificity at the point-of-care. In this context, we revise here the recent advancement in the development of advantageous biosensing systems for plant pathogen detection based on both antibody and DNA receptors. The use of different nanomaterials such as nanochannels and metallic nanoparticles for the development of innovative and sensitive biosensing systems for the detection of pathogens (i.e. bacteria and viruses) at the point-of-care is also shown. Plastic and paper-based platforms have been used for this purpose, offering cheap and easy-to-use really integrated sensing systems for rapid on-site detection. Beside devices developed at research and development level a brief revision of commercially available kits is also included in this review.

1. Introduction

Plant pathogens are one of the causes for low agricultural productivity worldwide. Main reasons are new, old and emerging plant infectious diseases. Their rates of spread, incidence and severity have become a significant threat to the sustainability of world food supply (Pimentel et al., 2005; Oerke, 2006; Roberts et al., 2006; Savary et al., 2012). Despite the lack of sufficient information for the economic losses, it was reported from plant disease loss estimates in U.S state of Georgia that total losses caused by plant diseases and their control costs reached roughly 647.2 million dollars in 2006 and then continued up to 821.85 million dollars in 2013 (Martinez, 2006, 2013). Top ten list of economically and scientifically important plant pathogens includes fungi, bacteria and viruses (Dean et al., 2012; Mansfield et al., 2012; Scholthof et al., 2011; Rybicki, 2015) (Table 1).

Plants display different symptoms on leaves, stems and fruits due to plant disease infections (López et al., 2003; Al-Hiary et al., 2011) (Fig. 1). These symptoms are particularly useful for visual observation as a conventional first step for plant disease diagnosis but it fails in detecting the presence of pathogen in early infection stages when plant infections are symptomless..

Early detection of plant pathogens plays an important role in plant health monitoring. It allows to manage disease infections in greenhouse systems and in the field during different stages of plant disease development and also to minimize the risk of the spread of disease infections as well as to prevent introduction of new plant diseases, especially quarantine pathogens at country boarder (Anderson et al., 2004; Strange and Scott, 2005; Brassier, 2008; Vincelli and Tisserat, 2008; Miller et al., 2009). Many strategies have been widely used for diagnosing plant disease problems including DNA-based methods and immunoassays, for the detection of pathogen protein and nucleic acid extracted from infected plant materials, as direct laboratory based techniques in addition to visual inspection of plant symptoms in the field (López et al., 2003) (Fig. 2A).

On the other hand there are other indirect strategies based on analysis of volatile organic compounds (VOC) that plants release as

* Corresponding author.
E-mail address: arben.merkoci@icn2.cat (A. Merkoçi).

http://dx.doi.org/10.1016/j.bios.2016.09.091
Received 15 June 2016; Received in revised form 15 September 2016; Accepted 26 September 2016
Available online 28 September 2016
0956-5663/

Table 1
Top ten important plant pathogenic bacteria, fungi and viruses published by Molecular Plant pathology (Dean et al., 2012; Mansfield et al., 2012; Scholthof et al., 2011; Rybicki, 2015).

Plant pathogen	Fungi	Bacteria	Virus
1	Magnaporthe oryzae	Pseudomonas syringae	Tobacco mosaic virus
2	Botrytis cinerea	Ralstonia solanacearum	Tomato spotted wilt
3	Puccinia spp.	Agrobacterium tumefaciens	Tomato yellow leaf curl
4	Fusarium graminearum	Xanthomonas oryzae	Cucumber mosaic
5	Fusarium oxysporum	Xanthomonas campestris	Potato virus Y
6	Blumeria graminis	Xanthomonas axonopodis	Cauliflower mosaic
7	Mycosphaerella graminicola	Erwinia amylovora	African cassava mosaic
8	Colletotrichum spp	Xylella fastidiosa	Plum pox
9	Ustilago maydis	Dickeya (dadantii and solani)	Brome mosaic
10	Melampsora lini	Pectobacterium carotovorum	Potato virus X

defense mechanism against pathogen attack (Scala et al., 2013) (Fig. 2B). Some recent reviews have described in detail the strategies for monitoring of volatile compounds in plants for disease detection (Sankaran et al., 2010; Nezhad, 2014; Fang and Ramasamy, 2015; Martinelli et al., 2015).

Several previous studies addressed plant disease diagnosis and pathogen detection using nucleic acid -based methods, mainly consisting of polymerase chain reaction (PCR) followed by DNA hybridization detection, to determine the genetic content of pathogen (Lin et al., 1990; Minsavage et al., 1994; Anwar Haq et al., 2003; Das, 2004; Teixeira et al., 2005; Li et al., 2006; Lacava et al., 2006; Saponari et al., 2008; Urasaki et al., 2008; Fang et al., 2009; Li et al., 2009; Ruiz-Ruiz et al., 2009; Gutiérrez-Aguirre et al., 2009; Yvon et al.,2009). Alternatively, immunoassays, also known as serological assays, including enzyme-linked immunosorbent assay (ELISA), lateral flow devices (LF), tissue print ELISA or direct dot blot immunoassay (DTBIA) have been used to detect the pathogen antigens (Avrameas, 1969; Van Weemen and Schuurs, 1971; Garnsey et al., 1993; Cambra et al., 2000; Nolasco et al., 2002; Holzloehner et al., 2013; Escoffier et al., 2016). Immunoassay technology using monoclonal antibodies offers a high specificity for plant virus detection, being ideal for testing large scale plant samples and for the on-site detection of plant pathogens, as done with tissue print ELISA and LF devices. In contrast, nucleic acid based methods are more accurate and specific enough to detect single target pathogen within a mixture containing more than one analyte and highly effective for detection of multiple targets.

In spite of these advantages, molecular detection methods have some limitations in detecting pathogens at low titres in materials such as seeds and insect vectors or at early infection stages. Furthermore, false negative results can be produced from cross contamination with PCR reagents which completely block amplification of target DNA, while false positive results can be generated by cross-amplification of PCR-generated fragments of non-target DNA. Another limitation is related to the disability to apply PCR for plant pathogen detection in the field (Louws et al., 1999; Schaad and Frederick, 2002; López et al., 2003; Martinelli et al., 2015). To overcome such limitations, innovative and portable biosensors have emerged in the last years, being widely used as diagnostic tools in clinical, environmental and food analysis.

Pathogen biosensing strategies are based on biological recognition using different receptors such as antibodies, DNA probe, phage and others (Eggibs, 2002; Sadanandom and Napier, 2010; Singh et al., 2013) (Fig. 3).

Antibody-based biosensors can allow sensitive and rapid qualitative and quantitative analysis of pathogens offering also label-free possibilities. It is important to note that this general approach is limited by the quality of the antibody employed and its storage condition that could affect antibody stability. Also pathogen size can interfere in some measurements such as the ones based on surface plasmon resonance (SPR). DNA based biosensors show advantages over antibody based ones mostly related to their better sensitivity thanks to the use of nucleic acid amplification techniques, which allows to detect plant pathogen before appearance of disease symptoms. However, they have some limitations related to the selection and synthesis of specific DNA probes as well as to the fact that detecting short DNA sequence of long double stranded DNA is a common problem in applying biosensing systems for DNA detection (Skottrup et al., 2008; Fang and Ramasamy, 2015; Hushiarian et al., 2015). Recently, phage-based DNA biosensor for sensing and targeting bacterial plant pathogens has been reported

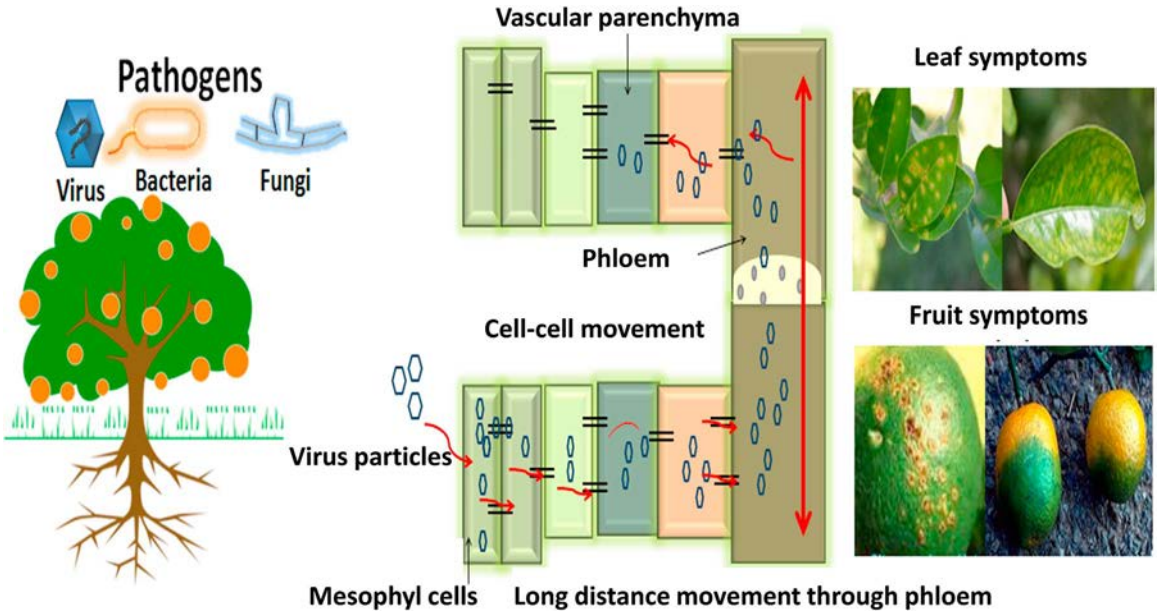

Fig. 1. Illustration of bacterial disease symptoms on citrus leaves and fruits. Adapted with permission from < http://www.crec.ifas.ufl.edu > (Viewed on Sunday, 22, May 2016).

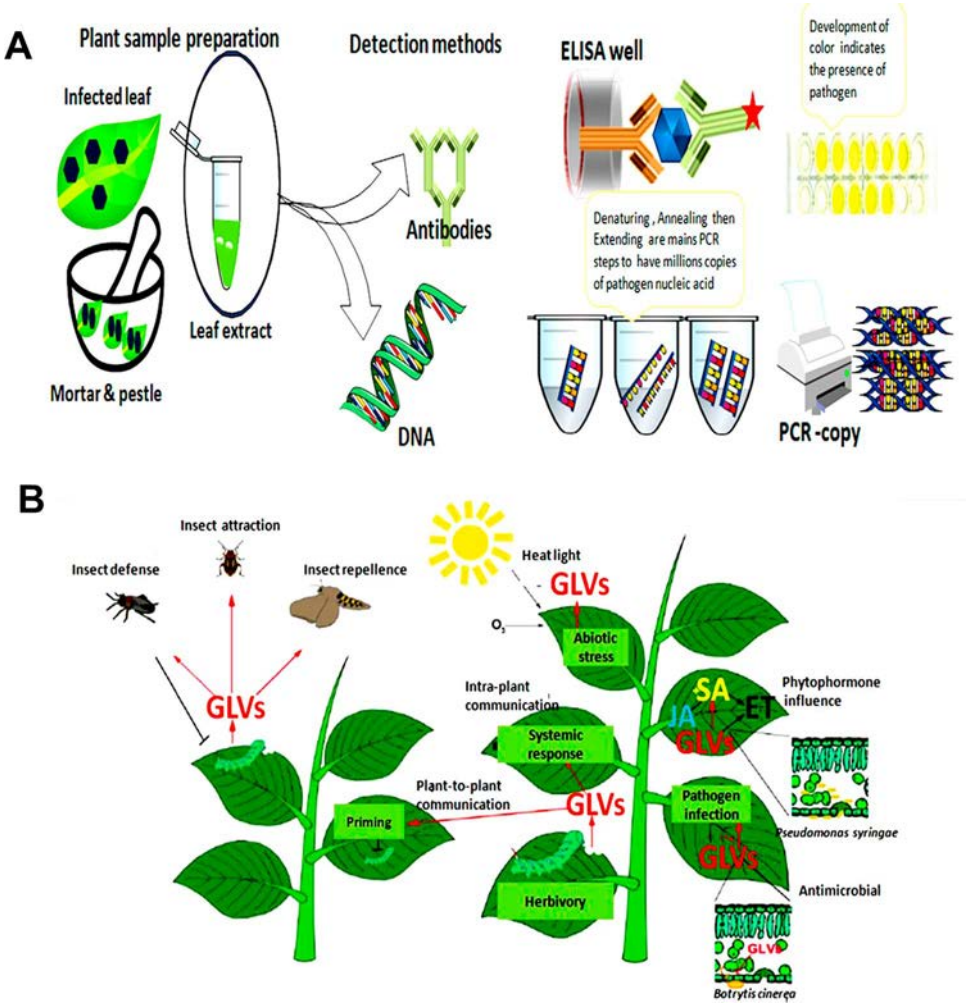

Fig. 2. (A) Schematic representation of the procedure for leaf extraction for pathogenic protein and DNA detection based on ELISA and PCR respectively. (B) Illustration of the green leaf volatiles (GLVs: jasmonic acid (JA), salicylic acid (SA) and ethylene (ET)) released during herbivory, pathogen infection and abiotic stress. Adapted with permission from Scala et al. (2013).

(Fang and Ramasamy, 2015). Bioluminescent-phage based technology was developed for determination the presence of *Pseudomonas cannabina* pv *alisalensis* that infects cruciferous vegetables (Schofield et al., 2013). The major advantage of this technology is that detecting nucleic acid of only viable bacterial cells, and as a result, no false positive was obtained. Nevertheless, the reporter phage expression can be inhibited by presence of some chemical compounds in the tested leaves such as thioethers glucosinolate and isothiocyanate.

Along the following sections, the most representative examples of antibody-based and DNA-based plant pathogen detection methods using optical and electrochemical techniques are summarized (see Table 2), also discussing advantages and limitations. An overview about the commercially available devices will also be shown together with concluding remarks.

2. Antibody-based biosensors

2.1. Electrochemical immunosensors

Most of the reported electrochemical immunosensors for plant pathogen detection are based on label-free technologies (impedimetric and quartz crystal microbalance-based ones) and enzymatic label-based voltammetric approaches on mercury, gold and carbon electrodes as detailed in the following sections.

2.1.1. Voltammetric detection based on the use of enzymes

In the last three decades, enzyme-linked immunosorbent assay (ELISA) has become the most widely used serological technique in diagnostics since the first publication on using ELISA to quantify rabbit IgG levels (Engvall and Perlmann, 1971). Enzyme immunoassay has been coupled with electrochemical detection methods to diagnose both clinical and plant pathogens with higher sensitivity and selectivity (Rossier and Girault, 2001; Sarkar et al., 2002; Paternolli et al., 2004). This electrochemical enzyme-linked immunoassay (ECEIA) has incorporated enzyme catalysis (enzyme label- substrate complex in presence of H_2O_2) followed by electrochemical reducing reaction through amperometric and voltammetric techniques (Zhang et al., 1995a, 1995b; Lee et al., 2005). Stable voltammetric peaks are achieved by controlling the pH of both enzymatic reaction and electrolyte solutions. Highly preferred is the use of Horseradish peroxidase (HRP) and alkaline phosphatase (AP) as enzyme labels since they have a variety of suitable substrates to reach the required sensitivity (Thompson et al., 1991; Jiang et al., 1995). Despite of high sensitivity of these sensing systems, the low availability of enzyme-conjugated antibodies represents an important limitation. Furthermore, enzymatic products can be highly affected by the pH of the electrolyte solution being another drawback in case of enzymatic reactions occurring in the same medium of the final electrochemical measurement.

Jiao et al. (2000) applied a voltammetric indirect ELISA based on horseradish peroxidase (HRP) detection system to detect the plant

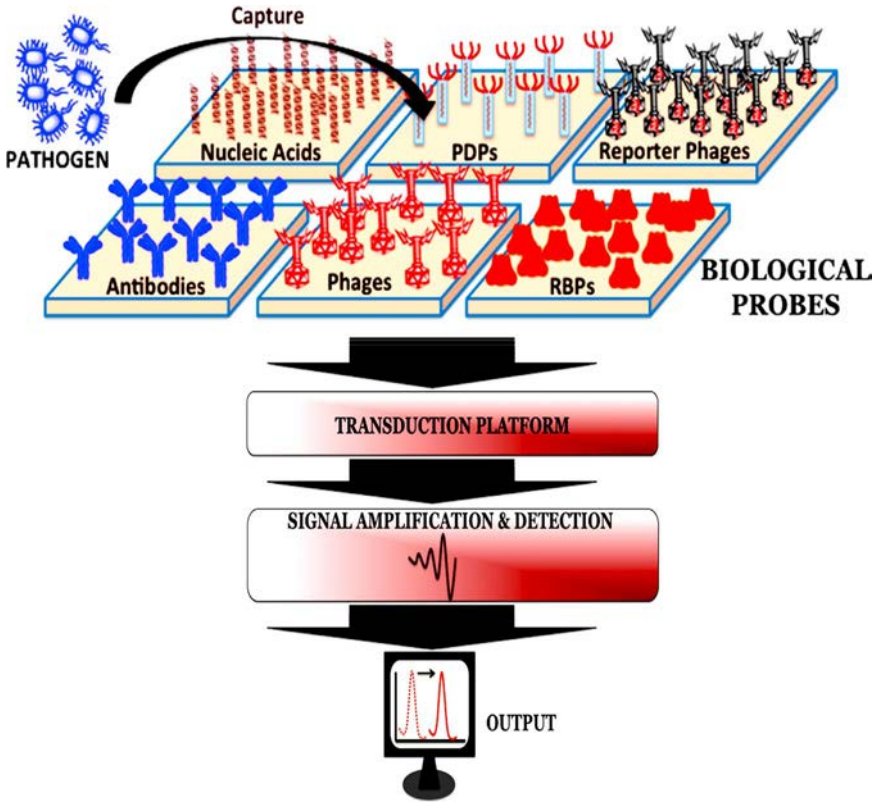

Fig. 3. Schematic of pathogen identification strategies using different biological recognition probes including antibodies, DNA probe, phage, PDPs (phage display peptides) and RBPs (phage receptor binding proteins). Adapted with permission from Singh et al. (2013).

virus called *Cucumber mosaic virus* (CMV) using two different HRP substrates: *o*-aminophenol (OAP) and *o*-phenylenediamine (OPD). Such indirect ELISA has three main steps: (i) immobilization of virus antigen which is either a purified CMV or leaf extract prepared by grinding infected nicotiana leaves with PBS buffer; (ii) incubation with specific antibody for CMV detection; (iii) immunoreaction with sec-

Table 2
Summary of various biosensing techniques used for plant pathogen detection.

Biosensors	Detection	Assay format	Sensing plant pathogen	Detection limit
Antibody-based	Electrochemical/Enzyme label Electrochemical/AuNPs tag	• Voltammetric Enzyme-based detection	• *Cucumber mosaic virus* • *Pantoea stewartii sbusp. stewartii*	• 0.5 ng/ml • 7.8×10^{3} cfu/ml
	Electrochemical/label-free	• Electrochemical impedance spectroscopy (EIS)-based detection • Quartz crystal microbalance-based approaches	• *Plum pox virus* • *Prunus necrotic ringspot virus* • *Maize chlorotic mottle virus*	• 10 pg/ml • Not reported • 250 ng/ml.
	Optical/AuNPs tag	• Lateral Flow immunoassays	• *Potato virus x* • *Pantoea stewartii sbusp. Stewartii*	• 2 ng/ml • 10^{5} cfu/ml
	Optical/ fluorescent tag	• Fluorescent approaches	• *Pantoea stewartii sbusp. Stewartii* • *Acidovorax avenae* subsp. *citrulli* • *Chilli vein-banding mottle virus* • *Watermelon silver mottle virus* • *Melon yellow spot virus*	• 10^{3} cfu/ml • 6×10^{5} cfu/ml • 1.0 ng/ml • 20.5 ng/ml • 35.3 ng/ml
	Optical/ label free	• Surface plasmon resonance (SPR) systems	• *Cymbidium mosaic virus* • *Odontoglossum ringspot virus*	• 48 pg/ml • 42 pg/ml
DNA-based	Electrochemical/label-free	• DNA hybridization voltammetric detection	• *Plum pox virus* • sugarcane white leaf disease • *Trichoderma harzianum*	• 12.8 pg/ml • 4.7 ng/μl • 10^{-19} mol/L
	Optical/AuNPs tags	• Lateral Flow immunoassays • AuNPs aggregation-based DNA analysis • bridging flocculation	• *Acidovorax avenae* subsp. *Citrulli* • *Banana bunchy top virus* • *Pseudomonas syringae*	• 0.48 nM • 0.13 nM • 15 ng/ml
	Optical/magnetic tag		• *Pseudomonas syringae*	• 0.5 ng/μl
	Optical/fluorescent tag	• Fluorescent approach in DNA microarrays	• *Botrytis cinerea*	• 1 fM
	Optical/ luminescent tag	• Electrochemiluminscence-based DNA detection	• *Banana streak virus* • *Banana bunchy top virus*	• 50 fM • 50 fM

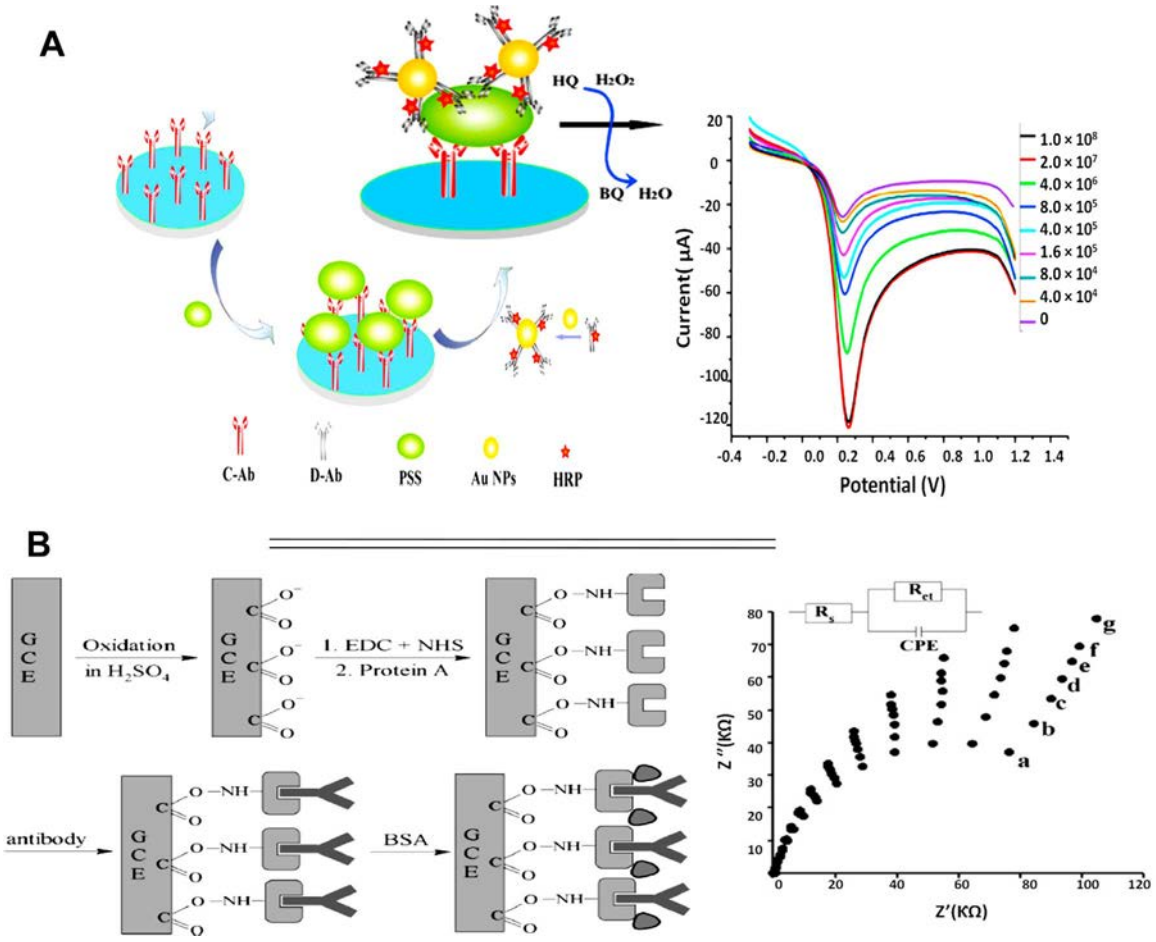

Fig. 4. Example of electrochemical enzyme-linked immunoassay (ECEIA) sensor using gold nanoparticles as carriers of enzyme-labeled antibodies for signal amplification, applied for *Pantoea stewartii sbusp. Stewartii* (PSS) plant bacterial pathogen detection, together with the voltammetric signals obtained for PSS concentrations in the range of 2.0×10^7–4.0×10^4 cfu/ml. Adapted with permission from Zhao et al. (2014). (B) Representative scheme of electrochemical spectroscopy impedance (EIS) immunosensor for *Prunus necrotic ringspot virus* (PNRV) DNA determination on glassy carbon electrodes together with the EIS spectra obtained for different dilutions of infected leaf extracts ranging: 100–0.01%. Adapted with permission from Jarocka et al. (2013).

ondary antibody labeled with HRP. The current derived from the reduction of the enzymatic product is measured by linear sweep voltammetry using a hanging mercury electrode. The sensitivity found for the ECEIA detection of CMV is almost four to ten times higher than that of the standard spectrophotometric ELISA, reaching detection limits as low as 0.5 ng/ml using OAD as substrate, also exhibiting high selectivity against four different pathogens: *Tobacco mosaic virus* (TMV), *Potato virus Y* (PVY), *Southern bean mosaic virus* (SBMV), *Tomato aspermy virus* (ToAV) and *Turnip mosaic virus* (TuMV).

Recently gold nanoparticles have been used as tags to amplify the analytical signal and significantly enhance the immunological assay's sensitivity. As an example, Zhao et al. (2014) presented for the first time an ECEIA using gold nanoparticle tags loaded by antibodies labeled with HRP to detect *Pantoea stewartii sbusp. stewartii* (PSS) plant bacterial pathogen (Fig. 4A).

Linear voltammetric measurements were done in PBS solution containing hydroquinone (HQ) as enzyme substrate and H_2O_2 as oxidant agent for monitoring the reduction of benzoquinone (BQ). In comparison to conventional ELISA assay, the ECEIA for PSS detection was 20 times more sensitive, reaching a detection limit of 7.8×10^3 cfu/ml. Besides sensitivity, this approach enabled sensitive and specific detection of the PSS antigen against other plant bacterial diseases such as panicle blight, leaf streak and *Cercospora* leaf spot on rice together with black spot of crucifer.

2.1.2. Label-free electrochemical impedance spectroscopy (EIS)-based detection

Over two decades ago, impedimetric based immunosensors were introduced by Newman and Martelet using techniques that involve electrochemical impedance spectroscopy (EIS) which studies the electrode-solution interface changes and detects that impedance changes produced by biomolecular interactions including DNA hybridization and protein immunocomplex formation (Newman et al., 1986; Bataillard et al., 1988; Katz and Willner, 2003; K'Owino and Sadik, 2005; Prodromidis, 2007; Daniels and Pourmand, 2007). Although impedance biosensing systems are sensitive and can effectively trace reactions occurring upon, their selectivity in real complex sample is a key problem limiting commercial applications. Most impedimetric biosensors are in label-free format and use self-assembled monolayers (SAMs) as immobilization method to obtain well-ordered monolayers on the surface of the electrode and achieve better antibody-antigen interaction efficiency (Kausaite-Minkstimiene et al., 2010).

Thiol SAMs formation on gold electrodes is the most reported substrate (Porter et al., 1987; Love et al., 2005) that has been used for impedimetric detection of plant pathogens. One of these approaches has been reported by Jarocka et al. (2011) for *Plum pox virus* (PPV) detection on gold electrodes, taking also advantage of AuNPs for stable antibody immobilization while retaining higher biological activity. Anti-PPV antibodies immobilized onto a 1,6-hexanedithiol/AuNPs modified gold electrode were used for the recognition of purified

PPV. Leaf extract from infected leaves of nicotiana was also prepared and used as plant virus antigen sources for analysis. The resulting impedimetric PVV immunosensor was more sensitive than conventional detection methods assayed, such as AgriStrip rapid immunochromatographic assay, being able to detect the presence of 0.01% of infected plant material in the diluted healthy samples with a detection limit of 10 pg/ml.

The same group later reported a similar approach for the detection of *Prunus necrotic ringspot virus* (PNRSV) using in this case glassy carbon electrodes as platforms and transducers (Jarocka et al., 2013). In this case, they took advantage of protein A, covalently connected to the electrode, for anti-PNRSV antibodies immobilization (Fig. 4B). The as-prepared immunosensor was incubated for 30 min with leaf extracts from healthy and PNRSV infected cucumber leaves. The stepwise preparation of the immunosensor was verified with electrochemical impedance spectroscopy (EIS) and cyclic voltammetry (CV) observing the expected increase in the electron-transfer resistance (R_{ct}), which was directly measured with EIS. The immunosensor displayed a very good sensitivity and selectivity against *Plum pox virus* (PPV) and was able to detect PNRSV in plant materials diluted up to ten thousand-fold.

2.1.3. Label-free quartz crystal microbalance-based approaches

Quartz crystal microbalance (QCM) biosensors are based on recording changes in oscillation frequency on the surface of the crystal that produce electrical field (Kanazawa and Gordon, 1985). QCM-based immunosensors are highly sensitive and allow label-free detection.. Many applications have been reported for detecting foodborne pathogens as well as on environmental and clinical analysis (O'sullivan and Guilbault, 1999; Si et al., 2001; Pohanka et al., 2007; Liu et al., 2007; Bragazzi et al., 2015). Since their use in identifying orchid viruses as a first application for plant disease detection (Eun et al., 2002), a number of piezoelectric label-free immunosensors based on the use of QCM for plant disease determination has been rightly reviewed by Skottrup et al. (2008), and continued in the last years presenting multiplexed detection of three significant plant pathogenic bacteria (Papadakis et al., 2015). We highlight here the recent approach reported by Huang et al. (2014) developing QCM immunosensor based on self-assembled monolayers (SAMs) for identification of *Maize chlorotic mottle virus* (MCMV). SAMs were formed on the gold surface of QCM crystal layer by layer using mercaptopropanoic and mercaptoundecanoic acids and antibodies specific to MCMV. Quantification measurements were obtained by observing the changes in the QCM crystal frequency. This biosensor showed a similar sensitivity as ELISA, recording limit of detection of 250 ng/ml. Moreover the developed immunosensor showed high selectivity against similar viruses, such as *Maize Dwarf Mosaic Virus* (MDMV) and *Wheat streak mosaic virus* (WSMV).

In spite of their high sensitivity, QCM-based measurements are highly affected by the environmental conditions, representing an important limitation that should be solved for point-of-care applications.

2.2. Optical immunosensors

Main optical immunosensors for plant pathogen detection are based on lateral flow devices (paper-based sensors), fluorescence approaches and surface plasmon resonance (SPR) systems as explained in the following sections.

2.2.1. Lateral flow immunoassays (LFIAs)

Paper-based sensors are well known advantageous devices for diagnostics applications (Parolo and Merkoçi, 2013). Lateral flow (LF) is a paper analytical device, also known as immunochromotographic strip, composed of four different pads: sample pad, made of cellulose, where the sample is dropped; conjugate pad made of glass fiber, impregnated with the bioconjugates solution (label particle and a receptor for the analyte), detection pad, made of nitrocellulose where test line (TL) and control line (CL) are printed and adsorption pad, also made of cellulose (Quesada-González and Merkoçi, 2015). Sandwich and competitive lateral flow immunoassays (LFIAs) are the main LF formats. In a typical sandwich assay, when the sample is added on the sample pad the liquid starts flowing to the conjugate pad where the analyte (if present) is linked to the label particles, previously conjugated with a specific bioreceptor. The conjugate flows by capillarity along the detection pad to the absorbent pad, passing through the TL, where it is captured only if the sample has the analyte (positive response), and to the CL, being here always captured, evidencing that the assay works.

In addition to antibodies, aptamers and DNA probes are employed as biological recognition elements which can be labeled with AuNPs, magnetic nanoparticles, fluorescent nanoparticles and enzymes among others so as to generate the color evolution at the test line. The advantages of LFIAs in terms of rapidity, stability and direct on-site analysis make them one of the most popular diagnostic tools in medical diagnostics, food safety, environmental analysis and plant disease detection. Workings with LFIAs have demonstrated very interesting opportunities for signal enhancements via use of nanomaterials (nanoparticles, graphene etc.) in addition to simple changes in platform architecture including vertical flow format. (Parolo et al., 2013a, 2013b; Rivas et al., 2014, 2015; Morales-Narváez et al., 2015; Nunes-Pauli et al., 2015). The first LFIA for plant pathogen detection was designed to detect *Tobacco mosaic virus* (TMV) (Tsuda et al., 1992). Since this first design, LFIAs have been proposed for the detection of several plant pathogens (Danks and Barker, 2000). Particularly, LFIAs in sandwich format using AuNPs tags have been utilized to plant viruses such as *Citrus tristeza virus* (CTV) and *Potato virus X* (PVX) and also plant pathogenic bacteria like *Erwinia amylovor*a, *Banana xanthomonas* and *Pantoea stewartii* as will be commented in the following paragraphs.

Salomone et al. (2004) developed a LFIA using standard antibody-based sandwich format and AuNPs as label to detect *Citrus tristeza virus* (CTV) from citrus leaves and fruits. Qualitative results showed sensitivity as high as ELISA test with good correlation. The specificity of the assay was also acceptable, obtaining a level of 5% of false positive results.

A similar approach was later developed for the identification of *Potato virus x* (Drygin et al., 2012). The reported sensitivity was found to reach 2 ng/ml while selectivity was tested against major potato seed viruses such as *Potato virus Y* (PVY), *Potato virus M* (PVM) and *Potato virus A* (PVA). Very recently, Feng et al. (2015) performed a rapid detection of *Pantoea stewartii sbusp. stewartii* (PSS) extracted from corn seed samples using a LFIA (Fig. 5A). The LFIA was performed in the presence of three other plant pathogenic bacteria (*Burkholderia glumae*, *Xanthomonas oryzae* and *Pseudomonas syringae*) and none were detected, evidencing an excellent selectivity. The assay displayed a detection limit of 10^5 cfu/ml of PSS..

In addition to the use of AuNPs for colorimetric detection, fluorescent tags have also been proposed in LFIAs for plant pathogen detection. This is the case of lanthanide chelate-loaded silica nanoparticles that were used for the determination of *Pantoea stewartii sbusp. stewartii* (PSS), the bacterial pathogen of Stewart's wilt in sweet corn (Zhang et al., 2014). Samples from healthy and infected corn seeds were analyzed following the standard sandwich assay format. The fluorescence strips allowed to detect a low concentration of PSS (10^3 cfu/ml) in less than 30 min with limit of detection hundredfold lower than ELISA and AuNPs labeled strips.

In spite of their great advantages, LFIAs suffer important limitations related to their low sensitivity and only qualitative/semiquantitative results. Although the sensitivity is highly improved using fluorescent tags as alternative to traditional colorimetric ones, the need of fluorescence reader (no visual detection possibilities) is an important limitation for rapid and in-field qualitative analysis. For this

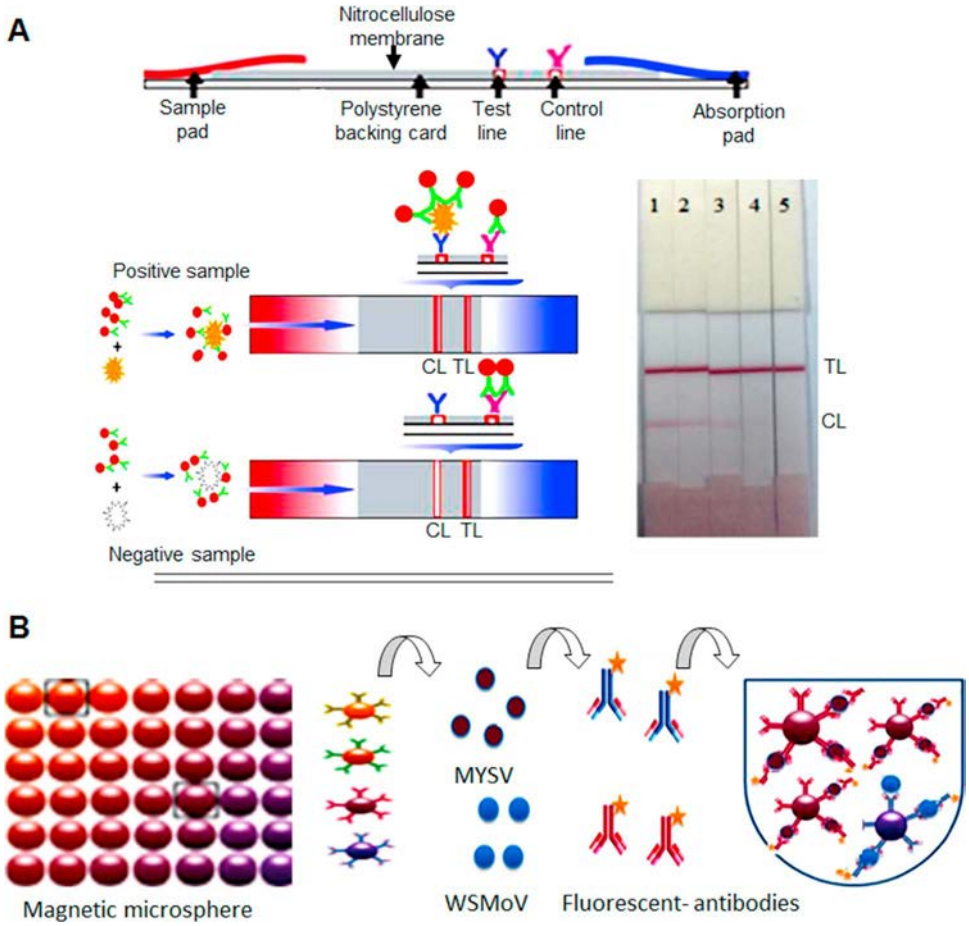

Fig. 5. (A) Scheme of a lateral flow immunoassay (LFIA) based on gold nanoparticles designed for detection of *Pantoea stewartii sbusp. Stewartii* (PSS) plant pathogenic bacteria and pictures of the strips for pathogen concentrations from 1×10^7 to 1×10^5 cfu/ml. Adapted with permission from Feng et al. (2015). (B) Scheme of magnetic microsphere immunoassay for multidetection of *Watermelon silver mottle virus* (WSMoV) and *Melon yellow spot virus* (MYSV) plant viruses. Adapted with permission from Charlermroj et al. (2013).

reason, colorimetric LFIAs, mainly based on AuNPs, are still the most commonly used for point-of-care analysis.

2.2.2. Fluorescent approaches

Microsphere sandwich immunoassay technology based on fluorescence-loaded magnetic microsphere and fluorophore- antibodies has been applied for detecting multiple analytes such as biomarkers, food and plant pathogens (Bergervoet et al., 2008; Kim et al., 2010; Mushaben et al., 2013). A recent study has taken a direct application in the use of microsphere immunoassay technology for multiplex plant pathogens simultaneously (Charlermroj et al., 2013). Specific antibodies to plant bacterial pathogen *Acidovorax avenae* subsp. *citrulli* (AAC) and three other plant viruses such as *Chilli vein-banding mottle virus* (CVbMV), *Watermelon silver mottle virus* (WSMoV) and *Melon yellow spot virus* (MYSV) were loaded onto a set of fluorescence-coded MagPlex microsphere (Fig. 5B). This technology based on measuring the fluorescence intensity of R-phycoerythrin tag enables to determine the antigen of the four plant pathogens. The limits of detection for AAC, CVbMV, WSMoV and MYSV are 6×10^5 cfu/ml, 1.0 ng/ml, 20.5 ng/ml and 35.3 ng/ml, respectively.

In spite of great advantages, mainly related to sensitivity and ability to detect multiple pathogens in a single assay, the main limitations of these systems are related to the complexity of the assay together with the need of fluorescent readers.

2.2.3. Surface plasmon resonance (SPR) systems

Surface Plasmon resonance (SPR) technology is based on monitoring changes of refractive index on the sensor surface after ligand-biomolecule interaction. SPR biosensors have been used in detecting pathogenic microorganism causing microbial contamination, food spoilage and plant infection (Vanregenmortel and Pellequer, 1993; Deisingh and Thompson, 2004; Bergwerff and Van Knapen, 2006; Mazumdar et al., 2008; Dudak and Boyacı, 2009). The most important advantages of this technique rely on the label-free possibilities together with their ability to effectively measure/follow the bioaffinity reactions.

Since more than two decades ago, the first SPR biosensor for *Tobacco mosaic virus* (TMV) was described (Altschuh et al., 1992).

SPR based biosensors have been object of a review (Skottrup et al., 2008) so we detail here some representative examples. For instance, label free biosensors based on SPR were developed to detect plant pathogens including *Cowpea mosaic virus, Tobacco mosaic virus* and *Lettuce mosaic virus* as plant viruses and *Fusarium culmorum, Phythothora infestans and Puccinia striiformis* as fungal plant pathogens (Boltovets et al., 2002; Zezza et al., 2006; Torrance et al., 2006; Skottrup et al., 2007a, 2007b). A number of different SPR biosenosrs using DNA probe, antibody and aptamer are reported in the literature for monitoring plant pathogens (Wang et al., 2004; Candresse et al., 2007; Lautner et al., 2010). In very recent years, Lin et al. (2014) developed a label free SPR immunosensor using gold nanorods (AuNRs) for investigation of two viruses of orchid *Cymbidium mosaic virus* (CymMV) or *Odontoglossum ringspot virus* (ORSV). Antibodies specific to orchid viruses were modified with AuNRs as sensing layers that offer a wide spectral region help in decreasing the color interference problem caused by sample matrix. This technology was exploited for achieving 48 and 42 pg/ml as detection limits for CymMV and ORSV, respectively. The stability of the established SPR biosensing system was not reported while the specificity was investigated using mixture of target and non-target viral antigen; perfor-

mances were compared by observing signal changes due to viral antigen- antibody binding on the surface of AuNRs.

In spite of the above mentioned advantages, a serious drawback in the use of this technology are the non-specific adsorptions onto the sensor surface that must be carefully controlled.

3. DNA-based biosensors

3.1. Electrochemical DNA biosensors

The majority of electrochemical DNA biosensors for plant pathogen determination are based on label-based and label-free voltammetric detection of DNA hybridization. Emerging approaches based on DNA translocation through nanopores, even though not reported yet for plant pathogen detection, show enormous potential in this field so they are also commented in the following sections.

3.1.1. Label-free DNA hybridization voltammetric detection

DNA hybridization can be monitored in label-free approaches based on amperometric, impedimetric and voltammetric detection including square-wave voltammetry (SWV), cyclic voltammetry (CV) and differential pulse voltammetry (DPV) (Liu and Tan, 1999; Azek et al., 2000; Wang et al., 2003; Gao et al., 2007; Lillis et al., 2007).

An example of voltammetric approach has been recently reported by Malecka et al. (2014) for the label-free detection of picomolar concentrations of nucleic acid from *Plum pox virus* (PPV) glassy carbon electrodes. (Fig. 6A). Detection of the pathogen-related DNA, with the complementary target immobilized on the electrode was monitored by Osteryoung square wave voltammetry (OSWV). Voltammetric measurement of electron transfer changes due to the hybridization reaction allowed detecting 22-mer and 42-mer complementary target DNA sequences of PPV at 10–50 pg/ml concentration range. A good discrimination between infected and healthy leaf samples is reported with a detection limit of 12.8 pg/ml but selectivity of this technique was not characterized by other phytopathogens..

Well-known approaches based on the use of methylene blue (MB) as hybridization indicator have also been recently reported for sugarcane white leaf disease (SWLD) detection (Wongkaew and Poosittisak, 2014). Voltammetric determination of the plant phytoplasma (causal agent of.SWLD) was carried out at glassy carbon electrode modified with chitosan. Electrostatic attraction of negatively charged DNA probe to glassy carbon electrode coated with cationic chitosan film for more efficient DNA immobilization, as alternative to covalent immobilization, were used in most of the previously mentioned approaches. Electrochemical detection of hybridization between ssDNA probe and target was performed by cyclic voltammetry (CV) and differential pulse voltammetry (DPV), using MB as a redox indicator, which is covalently attached to guanine bases. The electrochemical reduction of MB decreased after DNA hybridization due to unavailable guanine bases in dsDNA as a complete form, as expected. Following this strategy, a detection limit of 4.7 ng/μl of SWLD DNA was obtained, also distinguishing between target DNA from diseased sugarcane and non-target DNA from both healthy and infected sugarcane plants with other pathogens like *Sugarcane mosaic virus*. This biosensor showed good stability of DNA probe immobilization onto the chitosan with interest to develop an effective specific DNA biosensor.

Gold electrodes modified with nanocomposite membranes made of chitosan (CHIT) and zinc oxide nanoparticles (ZnO NPs) were also proposed as platforms for developing sensors for plant pathogen DNA voltammetric detection based on MB redox indicator. This kind of composite can improve the efficiency of the DNA probe immobilization thanks to its good biocompatibility and an enhanced electrochemical conductivity. Such is the case of the system recently proposed for *Trichoderma* (soil born fungi) determination (Siddiquee et al., 2014). Hybridization between DNA target of *Trichoderma* and its complementary probe immobilized on the nanocomposite modified electrode was investigated in this case by differential pulse voltammetry (DPV). The fabricated DNA biosensor detected crude DNA taken from real samples (fungal mycelia) with high reproducibility, obtaining a detection limit of 10^{-19} mol/L. High selectivity for identification of *Trichoderma harzianum* against other *Tricoderma* species, probably mainly due to the high specificity of the designed probe DNA used as bioreceptor, has also been reported.

As final remark we can state that, although label-free DNA hybridization using voltammetric systems (and hybridization indicators) have great advantages in terms of low cost of analysis, not necessity of labeling step and possibility of analysis of small volumes, their poor sensitivity in complex real samples should be carefully considered before their application for plant pathogen analysis.

3.1.2. Nanochannels as emerging tools for electrochemical DNA analysis

Nanopore/nanochannel-based technologies are currently one of the most promising ones for rapid and efficient DNA analysis (De la Escosura-Muñiz and Merkoçi, 2012). Even though no examples of application for plant pathogen determination using this technology are found yet in the bibliography, we preview that its enormous potential will make it possible in a short time and thus consider of great relevance to include some remarks in this review.

Nanopore/nanochannel biosensing systems are inspired by the microparticle counter device patented by Wallace Coulter more than 60 years ago (Coulter, 1953). It consists in simply measuring changes in the electrical conductance (electric current or voltage pulse) between two chambers separated by a microchannel when a micro-sized analyte passes through it, giving information about mobility, surface charge, and concentration of the analyte. This sensing principle has been extended in the last decades for nano-sized analytes evaluation using in this case nanometric channels, being the ssDNA analysis extensively reported. The typical approach consists in the monitoring of ssDNA molecules translocation (electrophoretically driven) through a single nanopore (biological or synthetic) which separates two chambers filled with an electrolyte solution (Kasianowicz et al., 1996; Bayley and Cremer, 2001; Siwy and Howorka, 2010). Such translocation produces changes in the constant current measured between the chambers, being the current pulse length characteristic of each of the 4 DNA bases (A, T, C, G). (Fig. 6B). This ability has opened exciting perspectives for DNA sequencing as alternative to conventional real-time PCR. Not only single nanochannels, but also nanochannel arrays have been proposed for the electrical detection of DNA hybridization at the point-of-care (De la Escosura-Muñiz and Merkoçi, 2010).

In addition to DNA, other molecules such as proteins or toxins have been detected using the single-nanochannel technology (De la Escosura-Muñiz and Merkoçi, 2016). We would like also to highlight here very recent approaches reported on filamentous virus translocation monitoring through silicon nitride membranes (McMullen et al., 2014) (Fig. 6C). The size and shape of this kind of virus is ideal for the analysis using these systems, since their stiffness avoid hernias formation making them able to pass through the channels in elongated forms, and generating well resolved signatures (easy distinguishable of the ones coming from virus collisions with the membrane), opening the way to reliable future label-free virus detection systems. Such systems could be applied for filamentous virus affecting plants from different genus like closterovirus (CTV) and potyvirus (PVX).

3.2. Optical DNA sensors

Colorimetric detections of gold nanoparticles (AuNPs) in both lateral flow assays and in aggregation tests, together with the use of fluorescent and colorimetric based microarrays and electrochemiluninescence analysis are the most representative examples of optical approaches for plant pathogen DNA detection. The great potential of nanochannel arrays for this purpose is also highlighted in this section.

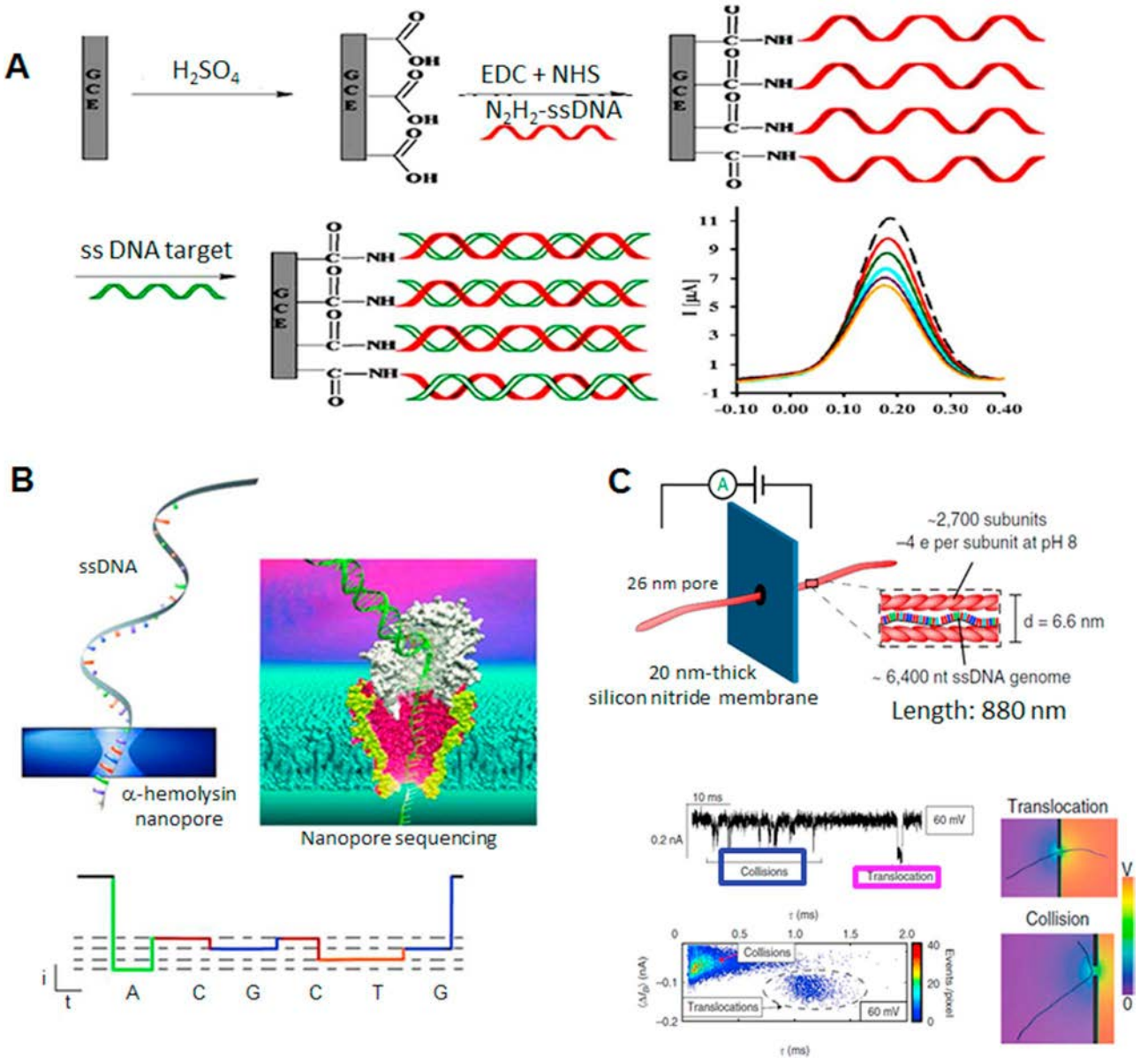

Fig. 6. (A) Example of label-free DNA hybridization approach based on voltammetric analysis applied for *Plum pox virus* (PPV) detection. Voltammetric signals correspond to 1–8 pM. Adapted with permission from Malecka et al. (2014). (B) Scheme of the ssDNA translocation through a single α-hemolysin pore and the associated electrical signatures as potential tool for pathogen DNA sequencing: each of the four bases produces characteristic time series recordings. Adapted from Kasianowicz et al. (1996) with permission. (C) Illustration of a filamentous virus translocation through a single nanopore drilled on silicon nitride membranes (up) and its signatures discriminated from collisions (down) Adapted from McMullen et al. (2014) with permission.

3.2.1. Lateral flow assays based on AuNPs

DNA detection on lateral flow (LF) test strips have been developed for the analysis of different plant diseases, in most cases using gold nanoparticle (AuNP)- labeled DNA probes. As example, a competitive DNA hybridization format was presented by Zhao et al. (2011) for *Acidovorax avenae subsp. Citrulli* (AAC) bacterial disease of melons.. The developed strip allowed reaching a low detection limit of 0.48 nM. The selectivity of the strip was tested against five other plant bacterial pathogens *Xanthomonas campestris*, *Acidovorax avenae*, *Clavibacter michiganensis*, *Pesudomonas. syringae* and *Erwinia carotovora* and no cross reactivity was observed.

Another application of DNA hybridization on lateral flow using AuNPs-DNA probe was introduced by Wei et al. (2014) for early detection of *Banana bunchy top virus* (BBTV). In this case, a direct sandwich assay consisting in AuNPs-DNA as detection probe and biotinylated-DNA as capture probe was developed. (Fig. 7). Qualitative and quantitative measurements of test line color were monitored and a linear calibration plot was found between peak area of test line and different concentrations of target DNA, achieving a detection limit of 0.13 nM. BBTV-DNA lateral flow biosensor achieved higher sensitivity by ten times in comparison to that of electrophoresis. Selectivity of the strip was evaluated, using plant samples infected with other viruses such as *Banana streak virus* (BSV) and *Cucumber mosaic virus* (CMV).

3.2.2. AuNPs aggregation-based DNA analysis and related approaches

AuNPs aggregation-based tests have been extensively used for biomolecules detection and also recently proposed for the detection of plant pathogen DNA. These simple approaches are gaining a great attention for diagnostic applications due to visual detection possibility and low cost of analysis.. This is the case of the approach recently reported by Vaseghi and co-workers (Vaseghi et al., 2013) who applied this principle for *Pseudomonas syringae* detection (Fig. 8A). The

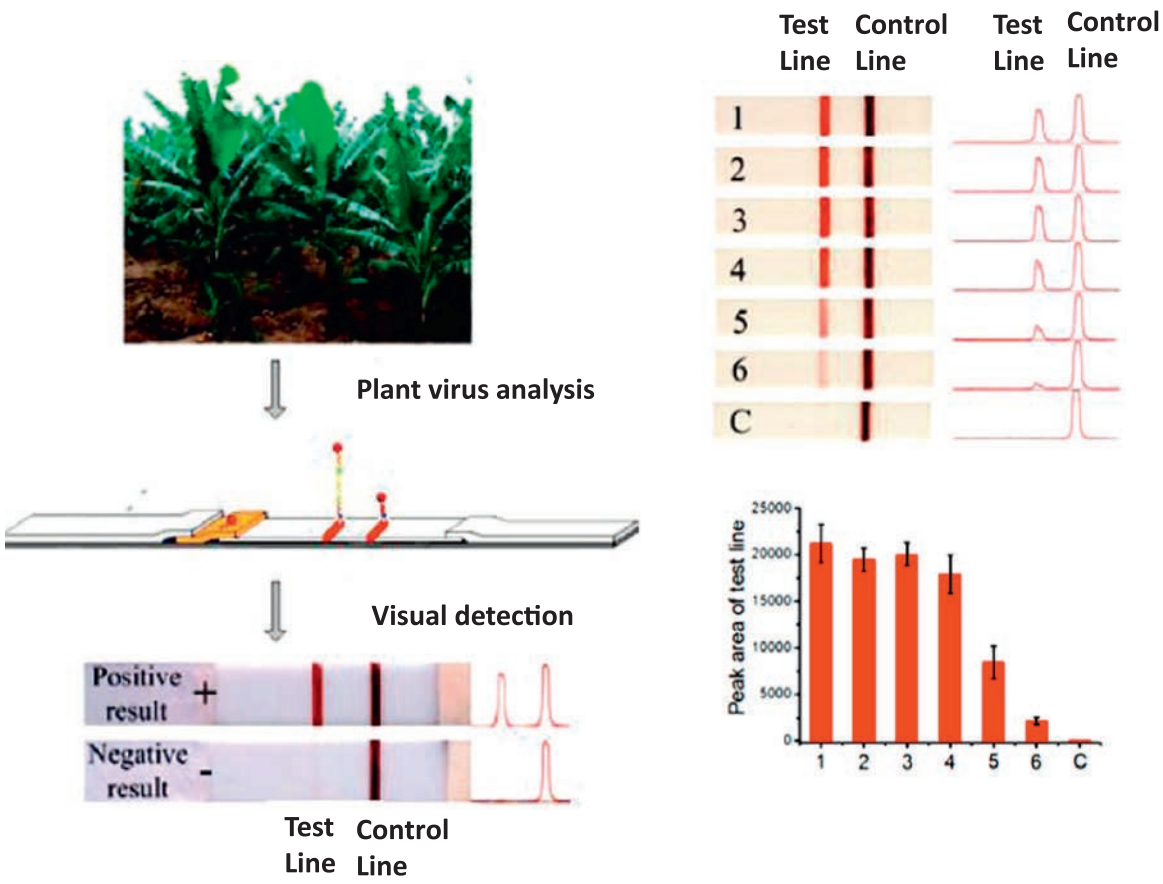

Fig. 7. Lateral flow based on DNA hybridization using DNA probe labeled with AuNPs for *Banana bunchy top virus* (BBTV) detection, qualitative and semi quantitative measurements using different concentrations of BBTV (from 8×10^6 to 8×10 copy/μl) nucleic acid (right up) and a bar chart demonstrating its corresponding peak areas of the test line (right down). Adapted with permission from Wei et al. (2015).

system was tested using other plant pathogenic bacteria such as *Pseudomonas viridiflava*, *Pectobacterium cartovortum sub cartovorum*, *Pseudomonas fluoresce*, *Xanthomonas alfalfae subsp. citrumelonis*, *Xanthomonas axonopodis pv. citr* and *Pseudomonas argenus*. The results of this assay showed high specificity and sensitivity in detecting as low as 15 ng/ml of target DNA of *P.syringae*.

Besides gold aggregation mechanism, bridging flocculation is very well-known approach in colloid chemistry since its introduction in 1950s (Ruehrwein and Ward, 1952). This kind of approach based on reversible adsorption to differentiate between long and short DNA polymers and has been reported recently for rapid detection significant plant pathogens (Wee et al., 2015). This method has been applied for the visual detection of *Pseudomonas syringae* as plant bacterial pathogen and two other devastating pathogenic plant fungi, *Fusarium oxysporum* and *Botrytis cinerea* (Fig. 8B). Key advantage of flocculation is the reliable detection of the presence of pathogens in plants within very early disease stage nevertheless the plants are symptomless. Qualitative analysis enabled detecting of isothermal DNA amplicons as little as 0.5 ng/μl.

In spite of the great perspectives of these systems, important parameters like the interparticle gap during DNA duplex formation should be carefully considered in the design of the assay so as to avoid losses in sensitivity.

3.2.3. Fluorescent and colorimetric approaches in microfluidics and microarrays systems

Over the last decade, microfluidic chips have been developed as revolution in on-site microbial detection of viruses and bacteria that infect animals and humans (Figeys and Pinto, 2000; Kricka, 2001; Huang et al., 2010; Wang et al., 2011). First example of the application of a microfluidic system was described for phytopathology detection (Julich et al., 2011). Later a similar approach using microfluidic based on silver nanoparticle that serves as detection agent (label) enables visual detection of fungal pathogens of *phytophthora* species (Schwenkbier et al., 2015). Besides colorimetric approaches, turbidity-based microfluidic system was developed for determination of viral pathogens infecting orchids such as *Cymbidium mosaic virus* (CymMV) and *Capsicum chlorosis virus* (CaCV) (Chang et al., 2013; Lin et al., 2015).

DNA microarray technology for large scale investigation of gene expression variations has been developed (Schena et al., 1995) whereas it is difficult to be suited to automation due to the need of several manual manipulation steps. In 2000s, applications of DNA microarray were reported on identification of pathogens causing plant diseases (Bonants et al., 2002; Bystricka et al., 2002; Nicolaisen, 2002; Perez-Ortin, 2002; Sip, 2002; Schoen et al., 2002, 2003; Boonham et al., 2003; Mumford et al., 2006; Zhang et al., 2013). Recently Wang and Li (2007) designed microarray based on DNA sequences labeled with fluorescent tags for visual determination of three fungal plant pathogens (*Botrytis cinerea*, *Didymella bryoniae*, and *Botrytis squamosa*). Glass chip and poldimethylsiloxane (PDMS) have been utilized as substrates for the developed microfluidic microarray. Fluorescence signals to the concentrations of target DNA were measured, detecting as low as 1 fM of DNA. Despite limited application of microarray on plant disease detection, microarray allowed flexible DNA probe formation, rapid DNA hybridization using small sample volume. A complete review addressing microarray application in detecting plant viruses was reported (Boonham et al., 2007; Fig. 9A).

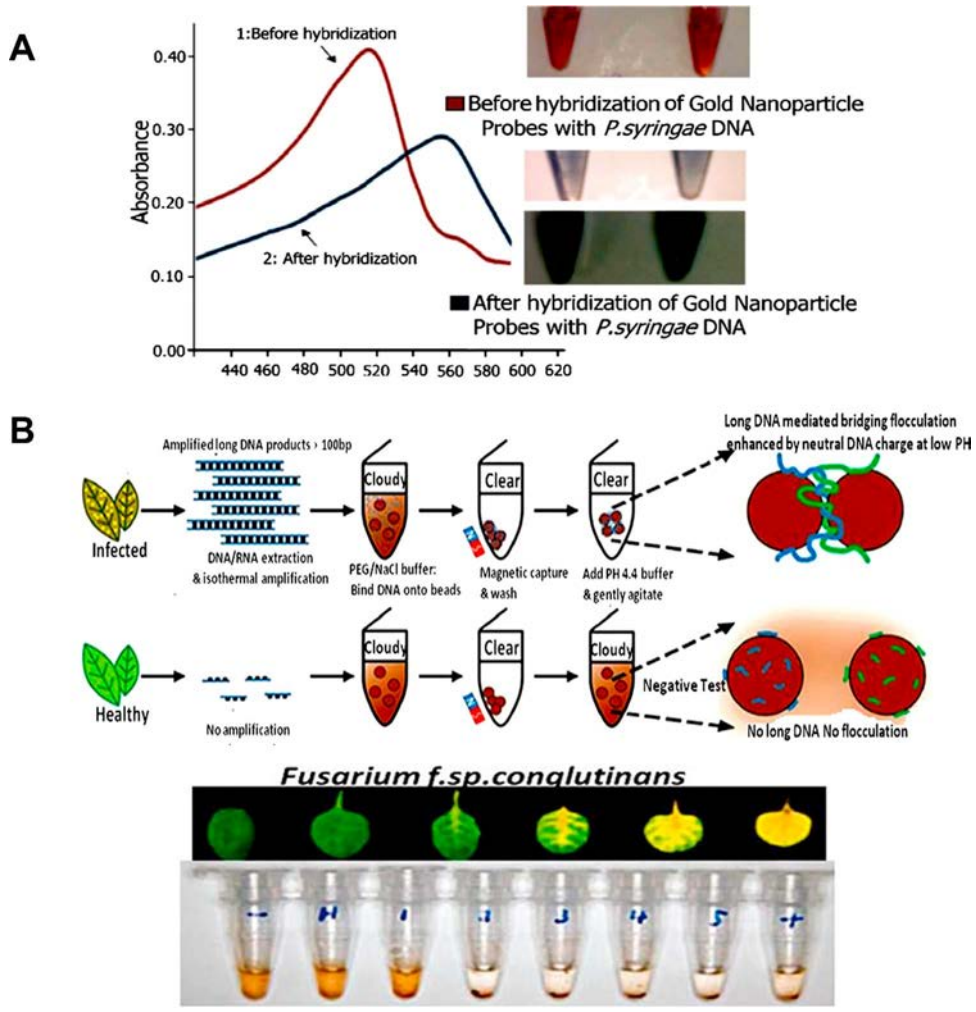

Fig. 8. (A) AuNPs aggregation for detection of DNA of *Pesudomonas syringae*, an important plant pathogenic bacterium with wide host plant range. Adapted with permission from Vaseghi et al. (2013). (B) Scheme of a qualitative assay based on bridging flocculation of isothermally DNA amplicons (up) and its application in detecting phytopathogenic fungi *Fusarium* f.sp.*conglutinans* at different infection stages (down). Adapted with permission from Wee et al. (2015).

3.2.4. Electrochemiluminscence-based DNA detection

The first report of DNA biosensor using $Ru(bpy)_3^{+2}$ electrochemiluminescence (ECL) detection protocol appeared in 1991, in which an excited state emitting light was formed as a result of generation of electron transfer reaction between two charged species such as Ru and TPA on electrode surface (Blackburn et al., 1991; Richter, 2004). ECL has various analytical applications in medical diagnosis and environmental analysis (Van Ingen et al., 1998). In spite of the excellent sensitivity of these systems an important limitation appears within solution-based formats that require continuous supply of luminescence reagent. In the recent years, the application of ECL for detection of PCR products is described to quantify plant virus nucleic acid. Tang et al. (2007) introduced for the first time an improved ECL-PCR detection as a diagnostic assay in plant virology, taking advantage of magnetic beads as a separation tool for the hybridization product exploiting the high affinity of biotin-streptavidin. Three plant viruses such as B*anana streak virus*, *Banana bunchy top virus*, and *Papaya leaf curl virus* were amplified by PCR, then hybridized with a tris(bipyridine) ruthenium (TBR)-labeled detector probe and a capture probe labeled with biotin. The hybridization products were captured onto streptavidin coated magnetic beads and the ECL signal of Ru $(bpy)_3^{2+}$ (TBR label) was generated by using tripropylamine (TPrA) as the co-reactant. This improved ECL-PCR method held a low detection limit down to 50 fM of PCR products through stable ECL signals. Not evaluated is the selectivity of ECL assay but the results showed many advantages over other detection assays including high sensitivity and stability for plant virus detection.

3.2.5. Nanochannel arrays as emerging platforms for DNA analysis

In addition to their properties for electrochemical analysis, nanoporous membranes are also excellent platforms for the development of optical biosensors for DNA analysis. Some nanoporous materials (i.e. nanoporous alumina and nanoporous silicon) possess optical properties that are altered by the presence of analytes captured in the inner walls of the nanochannels without the need of any label. Furthermore, fluorescent tags have also been used for DNA monitoring in nanochannels (De la Escosura-Muñiz and Merkoçi, 2012). As in the case of the electrochemical ones, these optical approaches have not yet been applied for plant pathogen detection but we consider of great interest to show here their outstanding potential. The work by Meller's group (McNally et al., 2010) for the optical single-molecule DNA sequencing can be selected as illustrative example. A multicolor readout is used after conversion of the target DNA into a binary code, consisting in the biochemical conversion of the nucleotides to known oligonucleotides. Hybridization with molecular beacons, using two different fluorophores was finally detected by translocating the DNA/beacon complex through the nanochannel. Taking advantage of the nanochannels array, the specific location of each channel in the visual field of the optical

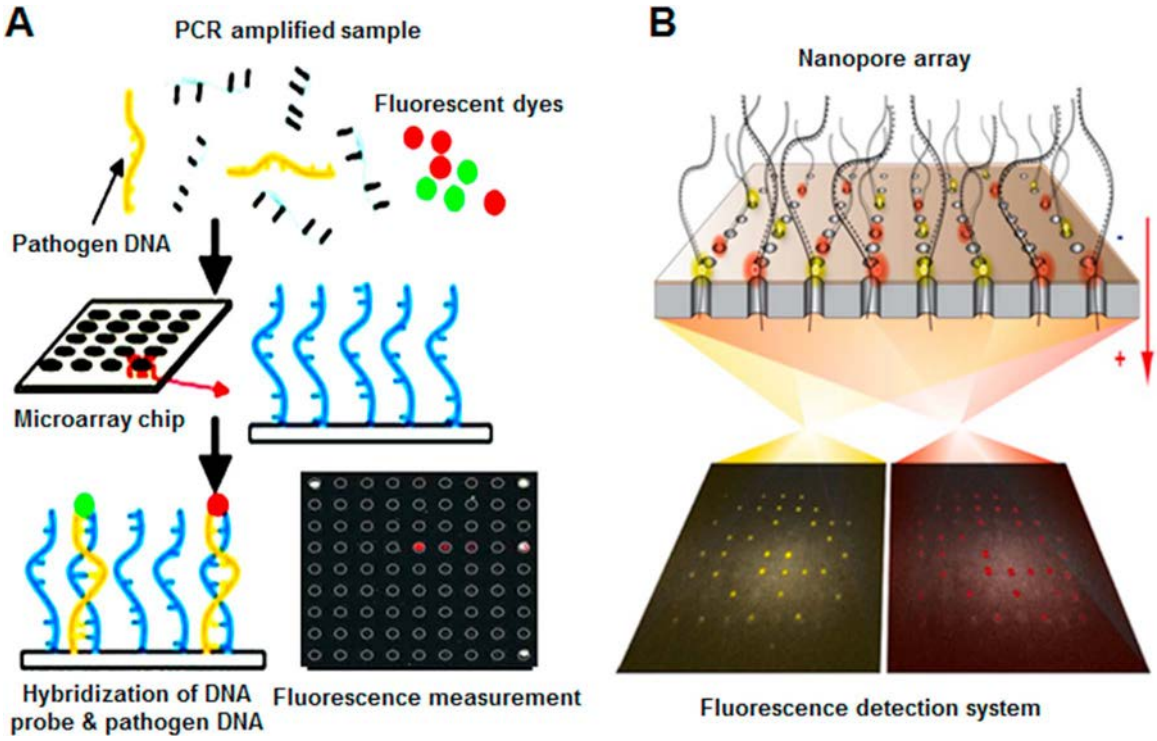

Fig. 9. (A) Scheme of DNA microarray technique based on DNA hybridization for pathogen characterization applied for *Broad bean wilt virus* analysis. Red fluorescent pattern indicates to the presence of virus RNA. Adapted with permission from Boonham et al. (2007), Nezhad (2014). (B) Illustration of the promising optical platforms based on nanochannel arrays for optical detection of DNA. Adapted with permission from McNally et al. (2010).

detector, allowed the simultaneous readout of the array (Fig. 9B), which open the way to further applications for multidetection of DNA related to plant pathogens.

4. Commercial available devices

Commercial availability of biological recognition elements (i.e. antibody, DNA probe, aptamer) is a key feature required for successful plant disease diagnosis. To date, most commercialized devices for plant pathogen detection based on immunoassays include lateral flow devices, tissue-print ELISA and plate-ELISA kit (Fig. 10A–D). A variety of commercial kits based on immunoassay have been reported in literature such as pocket kit for orchid virus detection, Agritest lateral flow to detect *Erwinia amylovora* bacterial causal agent of pome trees moreover Foresite diagnostic commercial kit for *xanthomonas* wilt of banana plant (Braun-Kiewnick et al., 2011; Hodgetts et al., 2015). Polyclonal and monoclonal antisera are available on the market for diagnosis of viral, bacterial and fungal disease in plants for commercial use. Additionally, DNA & RNA extraction kits have been designed to isolate total nucleic acid from a variety of plant materials, including leaves, bark and fruits. Examples of well tested kits are DNeasy and RNeasy Plant System from Qiagen, ISOLATE plant DNA kit from Bioline and GenElute plant genomic DNA from Sigma company. Emerging mobile applications are helpful tools for farmers in remote areas to detect and identify plant diseases. As example, Gene- Z is a promising plant disease mobile application based on microfluidic technology; it has applied on quantification of cancer markers. Lately, Gene- Z is ready to be brought to the market for analyzing plant pathogen in the field and it can be an interesting solution for an effective monitoring / control of plant disease spread. (Fig. 10E).

5. Conclusion

In this review we show that early detection of old, new and emerging infectious plant disease plays critical role in plant disease management and also could reduce the damage caused by plant diseases worldwide. Conventional diagnostic techniques could be time consuming, are related to special equipment and require still user/professionals with certain experience. To overcome these difficulties, recent advances in micro and nanotechnologies have enabled for developing biosensors for determination of pathogen infections in plants using antibody and DNA as biosensing receptors. This work intensively reviewed the developed antibody-based and nucleic acid-based biosensors in laboratories worldwide for plant disease detection. Most DNA biosensors techniques are based on determination of DNA hybridization events including electroluminescence, fluorescent and colorimetric approaches in addition to label-free voltammetric etc. In spite of advantages of DNA biosensors in terms of sensitivity, selectivity due to great recognition properties, their in-field application is still suffering from sample treatment requisites (eg. DNA extraction). On the other hand, antibody-based scenarios have been developed using QCM, SPR, fluorescent, voltammetric and label-free impedance detection techniques. Although one would take advantage of high affinity between antibody and specific antigen (related to plant disease) uncontrolled antibody immobilization could obstruct reaching efficient biosensing signal while developing the right detection tool. Although most of reported biosensors for plant disease detection are still for use at lab level, it is expected that more portable devices will emerge in the future being a strong support for an efficient diagnostic. Given the spread of plant disease there is a strong need to develop new biosensors that can be used directly in the field by farmers themselves. Selection of diagnostic route for plant disease detection relies on the event to be analyzed mainly involving (i) phytosanitary analysis and plant quarantine (ii) routine large scale surveys and disease risk assessment. Sanitary status testing requires the most sensitive method to avoid false positives and discard any pathogen to have pathogen-free mother plants for certification programs. In case of quarantine pathogen monitoring while import/export of plant materials, experts recommend using more than one diagnostic method to reduce the risk of obtaining false (positives or negatives), therefore nucleic acid-based biosensing

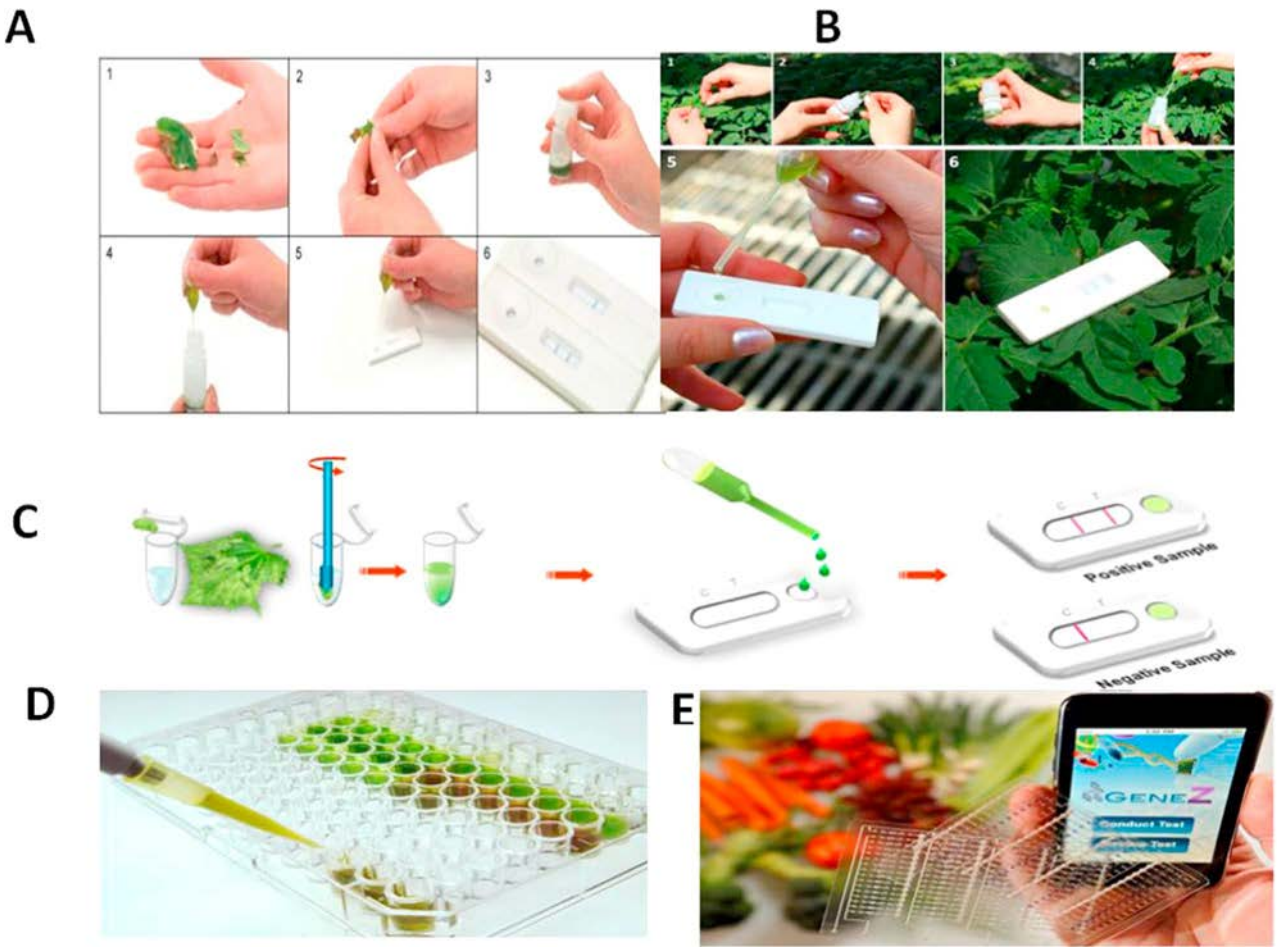

Fig. 10. Commercial devices for the detection of several plant diseases. (A–C) Lateral flow systems commercialized for *phytophthora* species, *Erwinia amylovora* and Potato virus Y detection. Adapted with permission from: (A) LaChandra bioscience pvt. Ltd. All rights reserved. (B) Abingdon Health Ltd., owner of the trademark Pocket Diagnostic®. All rights reserved. (C) Loewe® Biochemica GmbH. All rights reserved. (D) ELISA kit for the detection of *Citrus tristeza* virus, *Acidovorax avenae ssp. citrulli* and *Botrytis cinerea*. Adapted with permission from Loewe® Biochemica GmbH. All rights reserved. (E) Hybrid smart phone application and microfluidic to identify plant pathogen in minutes as promising device not yet applied on plant disease detection. Adapted with permission from < http://www.treehugger.com > (Viewed on Sunday, 22, May 2016)

approaches are being suitable for fast, sensitive testing of small number of samples and for ensuring the quality of disease-free plant materials. However, antibody/antigen interactions methods can be appropriate for testing large number of suspicious plants for surveillance of plant disease spread. Moreover, selecting diagnostic method for large-scale plant disease screening to evaluate disease incidence requires proper attention to several aspects such as cost of each single test, availability of on-site evaluation and pre- and post-test probability of disease risk. In addition to the innovative field-based devices, novel approaches are needed to limit the possible introduction and spread of foreign plant diseases across national and international borders. Over the long term, we believe the use of nanotechnology with additional efforts will be helping to significantly develop high sensitive and selective biosensors for real-time monitoring of plant pathogens in the field conditions.

Acknowledgments

We acknowledge support from the Spanish MINECO under Project MAT2014-52485-P and through the Severo Ochoa Centers of Excellence Program under Grant SEV-2013-0295. The support from Secretaria d'Universitats i Recerca del Departament d'Economia i Coneixement de la Generalitat de Catalunya (Grant 2014 SGR 260) is also acknowledged.

References

Al-Hiary, H., Bani-Ahmad, S., Reyalat, M., Braik, M., ALRahamneh, Z., 2011. Mach. Learn. 14, 5.
Altschuh, D., Dubs, M.C., Weiss, E., Zeder-Lutz, G., Van Regenmortel, M.H., 1992. Biochem. 31 (27), 6298–6304.
Anderson, P.K., Cunningham, A.A., Patel, N.G., Morales, F.J., Epstein, P.R., Daszak, P., 2004. Trends Ecol. Evol. 19, 535–544.
Anwar Haq, M., Collin, H.A., Tomsett, A.B., Jones, M.G., 2003. Physiol. Mol. 62 (3), 185–189.
Avrameas, S., 1969. Immunochem 6 (1), 43–52.
Azek, F., Grossiord, C., Joannes, M., Limoges, B., Brossier, P., 2000. Anal. Biochem. 284, 107.
Bataillard, P., Gardies, F., Jaffrezic-Renault, N., Martelet, C., Colin, B., Mandrand, B., 1988. Anal. Chem. 60 (21), 2374–2379.
Bayley, H., Cremer, P.S., 2001. Nature 413, 226–230.
Bergervoet, J.H., Peters, J., van Beckhoven, J.R., van den Bovenkamp, G.W., Jacobson, J.W., van der Wolf, J.M., 2008. J. Virol. Methods 149 (1), 63–68.
Bergwerff, A.A., Van Knapen, F., 2006. J. AOAC Int. 89 (3), 826–831.
Boltovets, P.M., Boyko, V.R., Kostikov, I.Y., Dyachenko, N.S., Snopok, B.A., Shirshov, Y.M., 2002b. J. Virol. Methods 105 (1), 141–146.
Bonants, P.De Weerdt, M.Van Beckhoven, J.Hilhorst, R.Chan, A.Boender, P.Zijlstra, C. Schoen, C., 2002. In: Abstracts Agricultural Biomarkers for Array Technology, Management Committee Meeting, Wadenswil (Vol. 20).
Boonham, N., Tomlinson, J., Mumford, R., 2007. Annu. Rev. Phytopathol. 45, 307–328.
Boonham, N., Walsh, K., Smith, P., Madagan, K., Graham, I., Barker, I., 2003. J. Virol. Methods 108 (2), 181–187.
Bragazzi, N.L., Amicizia, D., Panatto, D., Tramalloni, D., Valle, I., Gasparini, R., 2015. Adv. Protein Chem. Struct. Biol. 101, 149–211.
Brassier, C.M., 2008. Plant Pathol. 57, 792–808.
Braun-Kiewnick, A., Altenbach, D., Oberhänsli, T., Bitterlin, W., Duffy, B., 2011. J.

Microbiol. Methods 87 (1), 1–9.
Bystricka, D., Lenz, O., Mraz, I., Dědic, P., Sip, M., 2002. Acta Virol. 47 (1), 41–44.
Cambra, M.Gorris, M.T.Román, M.P.Terrada, E.Garnsey, S.M.Camarasa, E.Olmos, A. Colomer, M., 2000. In: Proceedings of the 14th Conference of the International Organization of Citrus Virologist. da GRAÇA, JV (34-41).
Candresse, T., Lot, H., German-Retana, S., Krause-Sakate, R., Thomas, J., Souche, S., Delaunay, T., Lanneau, M., Le Gall, O., 2007. J. Gen. Virol. 88 (9), 2605–2610.
Chang, W.H., Yang, S.Y., Lin, C.L., Wang, C.H., Li, P.C., Chen, T.Y., Jan, F.J., Lee, G.B., 2013. Nanomed.: Nanotech. Biol. Med. 9 (8), 1274–1282.
Charlermroj, R., Himananto, O., Seepiban, C., Kumpoosiri, M., Warin, N., Oplatowska, M., Gajanandana, O., Grant, I.R., Karoonuthaisiri, N., Elliott, C.T., 2013. PloS One 8 (4), e62344.
Coulter, W.H., 1953. U.S. Patent 2656508A.
Daniels, J.S., Pourmand, N., 2007. Electroanal 19 (12), 1239–1257.
Danks, C., Barker, I., 2000. EPPO Bull. 30 (3–4), 421–426.
Das, A.K., 2004. Curr. Sci. 87 (9), 1183–1185.
De la Escosura-Muñiz, A., Merkoçi, A., 2010. Chem. Commun. 46, 9007–9009.
De la Escosura-Muñiz, A., Merkoçi, A., 2012. ACS Nano 6 (9), 7556–7583.
De la Escosura-Muñiz, A., Merkoçi, A., 2016. TRAC 79 (2016), 134–150.
Dean, R., Van Kan, J.A., Pretorius, Z.A., Hammond, Kosack, K.E., Di Pietro, A., Spanu, P.D., Rudd, J.J., Dickman, M., Kahmann, R., Ellis, J., Foster, G.D., 2012. Mol. Plant Pathol. 13 (4), 414–430.
Deisingh, A.K., Thompson, M., 2004. Can. J. Microbiol. 50 (2), 69–77.
Drygin, Y.F., Blintsov, A.N., Grigorenko, V.G., Andreeva, I.P., Osipov, A.P., Varitzev, Y.A., Uskov, A.I., Kravchenko, D.V., Atabekov, J.G., 2012. Appl. Microbiol. Biotech. 93 (1), 179–189.
Dudak, F.C., Boyacı, İ.H., 2009. Biotech. J. 4 (7), 1003–1011.
Eggibs, B., 2002. Chem. Sens. Biosens..
Engvall, E., Perlmann, P., 1971. Immunochemistry 8 (9), 871–874.
Escoffier, L., Ganau, M., Wong, J., 2016. Commer. Nanomed.: Ind. Appl. Pat. Ethics.
Eun, A.J.C., Huang, L., Chew, F.T., Li, S.F.Y., Wong, S.M., 2002. J. Virol. Methods 99 (1), 71–79.
Fang, Y., Ramasamy, R.P., 2015. Biosensors 5 (3), 537–561.
Fang, Y., Xu, L.H., Tian, W.X., Huai, Y., Yu, S.H., Lou, M.M., Xie, G.L., 2009. Rice Sci. 16 (2), 157–160.
Feng, M., Kong, D., Wang, W., Liu, L., Song, S., Xu, C., 2015. Sensors 15 (2), 4291–4301.
Figeys, D., Pinto, D., 2000. Anal. Chem. 72 (9), 330.
Gao, Z., Rafea, S., Lim, L.H., 2007. Adv. Mater. 19, 602.
Garnsey, S.M.Permar, T.A.Cambra, M.Henderson, C.T., 1993. In: Proceedings of the 12th Conference. IOCV (39-50). IOCV Riverside, CA.
Gutiérrez-Aguirre, I., Mehle, N., Deli´ c, D., Gruden, K., Mumford, R., Ravnikar, M., 2009. J. Virol. Methods 162 (1–2), 46–55.
Hodgetts, J., Karamura, G., Johnson, G., Hall, J., Perkins, K., Beed, F., Nakato, V., Grant, M., Studholme, D.J., Boonham, N., Smith, J., 2015. Plant Pathol. 64 (3), 559–567.
Holzloehner, P., Schliebs, E., Maier, N., Funer, J., Micheel, B., Heilmann, K., 2013. J. Immunol. 190(Meet. Abstr. 1, (135-14).
Huang, C.H., Lai, G.H., Lee, M.S., Lin, W.H., Lien, Y.Y., Hsueh, S.C., Kao, J.Y., Chang, W.T., Lu, T.C., Lin, W.N., Chen, H.J., 2010. J. Appl. Microbiol. 108 (3), 917–924.
Huang, X., Xu, J., Ji, H.F., Li, G., Chen, H., 2014. Anal. Methods 6 (13), 4530–4536.
Hushiarian, R., Yusof, N.A., Abdullah, A.H., Ahmad, S.A.A., Dutse, S.W., 2015. Anal. Chem. Res 6, 17–25.
Jarocka, U., Radecka, H., Malinowski, T., Michalczuk, L., Radecki, J., 2013. Electroanalytical 25 (2), 433–438.
Jarocka, U., Wąsowicz, M., Radecka, H., Malinowski, T., Michalczuk, L., Radecki, J., 2011. Electroanalytical 23 (9), 2197–2204.
Jiang, T., Halsall, H.B., Heineman, W.R., Giersch, T., Hock, B., 1995. J. Agric. Food Chem. 43 (4), 1098–1104.
Jiao, K., Sun, W., Zhang, S.S., 2000. Fresenius' J. Anal. Chem. 367 (7), 667–671.
Julich, S., Riedel, M., Kielpinski, M., Urban, M., Kretschmer, R., Wagner, S., Fritzsche, W., Henkel, T., Möller, R., Werres, S., 2011. Biosens. Bioelectron. 26 (10), 4070–4075.
Kanazawa, K.K., Gordon, J.G., 1985. Anal. Chem. 57 (8), 1770–1771.
Kasianowicz, J.Brandin, E.Branton, D.Deamer, D., 1996. Proceedings. Natl. Acad. Sci. USA, 93, 13770–13773.
Katz, E., Willner, I., 2003. Electroanalytical 15 (11), 913–947.
Kausaite-Minkstimiene, A., Ramanaviciene, A., Kirlyte, J., Ramanavicius, A., 2010. Anal. Chem. 82 (15), 6401–6408.
Kim, J.S., Taitt, C.R., Ligler, F.S., Anderson, G.P., 2010. Sens. Instrum. Food Qual. Saf. 4 (2), 73–81.
K'Owino, I.O., Sadik, O.A., 2005. Electroanalytical 17 (23), 2101–2113.
Kricka, L.J., 2001. Clin. Chim. Acta 307 (1), 219–223.
Lacava, P.T., Li, W.B., Araújo, W.L., Azevedo, J.L., Hartung, J.S., 2006. J. Microbiol. Methods 65, 535–541.
Lautner, G., Balogh, Z., Bardóczy, V., Mészáros, T., Gyurcsányi, R.E., 2010. Analyst 135 (5), 918–926.
Lee, H.Y., Jung, H.S., Fujikawa, K., Park, J.W., Kim, J.M., Yukimasa, T., Sugihara, H., Kawai, T., 2005. Biosens. Bioelectron. 21 (5), 833–838.
Li, W., Abad, J.A., French-Monar, R.D., Rascoe, J., Wen, A., Gudmestad, N.C., Secor, G.A., Lee, I.M., Duan, Y., Levy, L., 2009. J. Microbiol. Methods 78 (1), 59–65.
Li, W., Hartung, J.S., Levy, L., 2006. J. Microbiol. Methods 66 (1), 104–115.
Lillis, B., Manning, M., Hurley, E., Berney, H., Duane, R., Mathewson, A., Sheehan, M.M., 2007. Biosens. Bioelectron. 22, 1289.
Lin, C.L., Chang, W.H., Wang, C.H., Lee, C.H., Chen, T.Y., Jan, F.J., Lee, G.B., 2015. Biosens. Bioelectron. 63, 572–579.
Lin, H.Y., Huang, C.H., Lu, S.H., Kuo, I.T., Chau, L.K., 2014. Biosens. Bioelectron. 51, 371–378.
Lin, N.S., Hsu, Y.H., Hsu, H.T., 1990. Phytopathology 80 (9), 824–828.
Liu, F., Li, Y., Su, X.L., Slavik, M.F., Ying, Y., Wang, J., 2007. Sens. Instrum. Food Qual. Saf. 1 (4), 161–168.
Liu, X.J., Tan, W.H., 1999. Anal. Chem. 71, 5054.
López, M.M., Bertolini, E., Olmos, A., Caruso, P., Gorris, M.T., Llop, P., Penyalver, R., Cambra, M., 2003. Int. Microbiol. 6, 233–243.
Louws, F.J., Rademaker, J.L.W., De Bruijn, F.J., 1999. Annu. Rev. Phytopathol. 37 (1), 81–125.
Love, J.C., Estroff, L.A., Kriebel, J.K., Nuzzo, R.G., Whitesides, G.M., 2005. Chem. Rev. 105, 1103–1169.
Malecka, K., Michalczuk, L., Radecka, H., Radecki, J., 2014. Sensors 14 (10), 18611–18624.
Mansfield, J., Genin, S., Magori, S., Citovsky, V., Sriariyanum, M., Ronald, P., Dow, M.A.X., Verdier, V., Beer, S.V., Machado, M.A., Toth, I.A.N., 2012. Mol. Plant Pathol. 6, 614–629.
Martinelli, F., Scalenghe, R., Davino, S., Panno, S., Scuderi, G., Ruisi, P., Villa, P., Stroppiana, D., Boschetti, M., Goulart, L.R., Davis, C.E., 2015. Agron. Sustain. Dev. 35 (1), 1–25.
Martinez, A., 2006. 2006 Georgia Plant Disease Loss Estimates
Martinez, A., 2013. 2013 Georgia Plant Disease Loss Estimates
Mazumdar, S.D., Barlen, B., Kramer, T., Keusgen, M., 2008. J. Microbiol. Methods 75 (3), 545–550.
McMullen, A., de Haan, H.W., Tang, J.X., Stein, D., 2014. Nat. Commun. 5, 4171.
McNally, B., Singer, A., Yu, Z., Sun, Y., Weng, Z., Meller, A., 2010. Nano Lett. 10, 2237–2244.
Miller, S.A., Beed, F.D., Harmon, C.L., 2009. Annu. Rev. Phytopathol. 47, 15–38.
Minsavage, G.V., Thompson, C.M., Hopkins, D.L., Leite, R.M.V.B.C., Stall, R.E., 1994. Phytopathology 84, 456–461.
Morales-Narváez, E., Naghdi, T., Zor, E., Merkoçi, A., 2015. Anal. Chem. 87 (16), 8573–8577.
Mumford, R.A., Jarvis, B., Harju, V., Boonham, N., Skelton, A., 2006. Plant Pathol. 55 (6), (819-819).
Mushaben, E.M., Brandt, E.B., Hershey, G.K.K., Le Cras, T.D., 2013. PloS One 8 (1), e54426.
Newman, A.L.Hunter, K.W.Stanbro, W.D.1986. In: Proceedings of the 2nd Int. Meet. Chem. Sens. 596–598.
Nezhad, A.S., 2014. Lab Chip 14 (16), 2887–2904.
Nicolaisen, M., 2002. In: Abstracts Agricultural Biomarkers for Array Technology, Management Committee Meeting, Wadenswil (vol. 22).
Nolasco, G., Sequeira, Z., Soares, C., Mansinho, A., Bailey, A.M., Niblett, C.L., 2002. Eur. J. Plant Pathol. 108 (4), 293–298.
Nunes Pauli, G.E., de la Escosura-Muñiz, A., Parolo, C., Bechtold, I.H., Merkoçi, A., 2015. Lab Chip 15 (2), 399–405.
O'sullivan, C.K., Guilbault, G.G., 1999. Biosens. Bioelectron. 14 (8), 663–670.
Oerke, E.-C., 2006. J. Agric. Sci. 144, 31–43.
Papadakis, G., Skandalis, N., Dimopoulou, A., Glynos, P., Gizeli, E., 2015. PloS One 10 (7), e0132773.
Parolo, C., Merkoçi, A., 2013. Chem. Soc. Rev. 42 (2), 450–457.
Parolo, C., de la Escosura-Muñiz, A., Merkoçi, A., 2013a. Biosens. Bioelectron. 40 (1), 412–416.
Parolo, C., Medina-Sánchez, M., de la Escosura-Muñiz, A., Merkoçi, A., 2013b. Lab Chip 13 (3), 386–390.
Paternolli, C., Antonini, M., Ghisellini, P., Nicolini, C., 2004. Langmuir 20 (26), 11706–11712.
Perez-Ortin, J.E., 2002. In: Abstracts Agricultural Biomarkers for Array Technology, Management Committee Meeting, Wadenswil (vol. 13).
Pimentel, D., Zuniga, R., Morrison, D., 2005. Ecol. Econ. 52, 273–288.
Pohanka, M., Skládal, P., Pavliš, O., 2007. J. Immunoassay Immunochem. 29 (1), 70–79.
Porter, M.D., Bright, T.B., Allara, D.L., Chidsey, C.E., 1987. J. Am. Chem. Soc. 109 (12), 3559–3568.
Prodromidis, M.I., 2007. Pak. J. Anal. Environ. Chem. 2, 69–71.
Quesada-González, D., Merkoçi, A., 2015. Biosens. Bioelectron. 73, 47–63.
Richter, M.M., 2004. Chem. Rev. 104 (6), 3003–3036.
Rivas, L., de la Escosura-Muñiz, A., Serrano, L., Altet, L., Francino, O., Sánchez, A., Merkoçi, A., 2015. Nano Res. 8 (11), 3704–3714.
Rivas, L., Medina-Sánchez, M., de la Escosura-Muñiz, A., Merkoçi, A., 2014. Lab Chip 14 (22), 4406–4414.
Roberts, M.J., Schimmelpfennig, D.E., Ashley, E., Livingston, M.J., Ash, M.S., Vasavada, U., 2006. The Value of Plant Disease Early-Warning Systems: A Case Study of USDA's Soybean Rust Coordinated Framework;. United States Department of Agriculture, Economic Research Service, Washington, DC, USA.
Rossier, J.S., Girault, H.H., 2001. Lab Chip 1 (2), 153–157.
Ruehrwein, R.A., Ward, D.W., 1952. Soil Sci. 73 (6), 485–492.
Ruiz-Ruiz, S., Ambrós, S., Carmen Vives, M., Navarro, L., Moreno, P., Guerri, J., 2009. J. Virol. Methods 160 (1–2), 57–62.
Rybicki, E.P., 2015. Arch. Virol. 160 (1), 17–20.
Sadanandom, A., Napier, R.M., 2010. Curr. Opin. Plant Biol. 13, 736–743.
Salomone, A., Mongelli, M., Roggero, P., Boscia, D., 2004. J. Plant Pathol., 43–48.
Sankaran, S., Mishra, A., Ehsani, R., Davis, C., 2010. Comput. Electron. Agric. 72 (1), 1–13.
Saponari, M., Manjunath, K., Yokomi, R.K., 2008. J. Virol. Methods 147 (1), 43–53.
Sarkar, P., Pal, P.S., Ghosh, D., Setford, S.J., Tothill, I.E., 2002. Int. J. Pharm. 238 (1), 1–9.
Savary, S., Ficke, A., Aubertot, J., Hollier, C., 2012. Food Secur. 4, 519–537.
Scala, A., Allmann, S., Mirabella, R., Haring, M.A., Schuurink, R.C., 2013. Int. J. Mol. Sci. 14 (9), 17781–17811.

Schaad, N.W., Frederick, R.D., 2002. Can. J. Plant Pathol. 24 (3), 250–258.
Schoen, C.De Weerdt, M.Hillhorst, R.Boender, P.Szemes, M.Bonants, P., 2003. In: Proceedings of the Abstracts of the 19th International Symposium on Virus and Virus-like Diseases of Temperate Fruit Crops, Valencia (vol. 108).
Schoen, C.De Weerdt, M.Hillhorst, R.Chan A.Boender, P.Zijlstra, C.Bonants, P., 2002. In: Proceedings of the Abstracts Agricultural Biomarkers for Array Technology, Management Committee Meeting, Wadenswil (vol. 11).
Schofield, D.A., Bull, C.T., Rubio, I., Wechter, W.P., Westwater, C., Molineux, I.J., 2013. Bioengineered 4 (1), 50–54.
Siddiquee, S., Rovina, K., Yusof, N.A., Rodrigues, K.F., Suryani, S., 2014. Sens. Biosens. Res. 2, 16–22.
Scholthof, K.B.G., Adkins, S., Czosnek, H., Palukaitis, P., Jacquot, E., Hohn, T., Hohn, B., Saunders, K., Candresse, T., Ahlquist, P., Hemenway, C., 2011. Mol. Plant Pathol. 12 (9), 938–954.
Schwenkbier, L., Pollok, S., König, S., Urban, M., Werres, S., Cialla-May, D., Weber, K., Popp, J., 2015. Anal. Methods 7 (1), 211–217.
Si, S.H., Li, X., Fung, Y.S., Zhu, D.R., 2001. Microchem. J. 68 (1), 21–27.
Singh, A., Poshtiban, S., Evoy, S., 2013. Sensors 13 (2), 1763–1786.
Sip, M., 2002. In: Abstracts Agricultural Biomarkers for Array Technology, Management Committee Meeting, Wadenswil (vol.24).
Siwy, Z.S., Howorka, S., 2010. Chem. Soc. Rev. 39, 1115–1132.
Skottrup, P., Hearty, S., Frøkiær, H., Leonard, P., Hejgaard, J., O'Kennedy, R., Nicolaisen, M., Justesen, A.F., 2007a. Biosens. Bioelectron. 22 (11), 2724–2729.
Skottrup, P., Nicolaisen, M., Justesen, A.F., 2007b. J. Microbiol. Methods 68 (3), 507–515.
Skottrup, P.D., Nicolaisen, M., Justesen, A.F., 2008. Biosens. Bioelectron. 24 (3), 339–348.
Strange, R.N., Scott, P.R., 2005. Annu. Rev. Phytopathol. 43, 83–116.
Tang, Y.B., Xing, D., Zhu, D.B., Liu, J.F., 2007. Anal. Chim. Acta 582 (2), 275–280.
Teixeira, D.C., Danet, J.L., Eveillard, S., Martins, E.C., Junior, W.C.J., Yamamoto, P.T., Lopes, S.A., Bassanezi, R.B., Ayres, A.J., Saillard, C., Bové, J.M., 2005. Mol. Cell. Probes 19, 173–179.
Thompson, R.Q., Barone, G.C., Halsall, H.B., Heineman, W.R., 1991. Anal. Biochem. 192 (1), 90–95.
Torrance, L., Ziegler, A., Pittman, H., Paterson, M., Toth, R., Eggleston, I., 2006. J. Virol. Methods 134 (1), 164–170.
Tsuda, S., Kameya-Iwaki, M., Hanada, K., Kouda, Y., Hikata, M., Tomaru, K., 1992. Plant Dis. 76 (5), 466–469.
Urasaki, N., Kawano, S., Mukai, H., Uemori, T., Takeda, O., Sano, T., 2008. J. Gen. Plant Pathol. 74, 151–155.
Van Ingen, H.E., Chan, D.W., Hubl, W., Miyachi, H., Molina, R., Pitzel, L., Ruibal, A., Rymer, J.C., Domke, I., 1998. Clin. Chem. 44 (12), 2530–2536.
Van Regenmortel, M.H., Pellequer, J.L., 1993. Pept. Res. 7 (4), 224–228.
Van Weemen, B.K., Schuurs, A.H.W.M., 1971. FEBS Lett. 15 (3), 232–236.
Vaseghi, A., Safaie, N., Bakhshinejad, B., Mohsenifar, A., Sadeghizadeh, M., 2013. Sens. Actuators B- Chem. 181, 644–651.
Vincelli, P., Tisserat, N., 2008. Plant Dis. 82, 660–669.
Wang, C.H., Lien, K.Y., Wu, J.J., Lee, G.B., 2011. Lab Chip 11 (8), 1521–1531.
Wang, J., Li, J.H., Baca, A.J., Hu, J.B., Zhou, F.M., Yan, W., Pang, D.W., 2003. Anal. Chem. 75, 3941.
Wang, L., Li, P.C., 2007. J. Agri. Food Chem. 55 (26), 10509–10516.
Wang, R., Minunni, M., Tombelli, S., Mascini, M., 2004. Biosens. Bioelectron. 20 (3), 598–605.
Wee, E.J.H., Lau, H.Y., Botella, J.R., Trau, M., 2015. Chem. Commun. 51 (27), 5828–5831.
Wei, J., Liu, H., Liu, F., Zhu, M., Zhou, X., Xing, D., 2014. ACS appl. Mater. Interfaces 6 (24), 22577–22584.
Wongkaew, P., Poosittisak, S., 2014. Am. J. Plant Sci., 2014.
Yvon, M., Thébaud, G., Alary, R., Labonne, G., 2009. Mol. Cell Probes 23 (5), 227–234.
Zezza, F., Pascale, M., Mulè, G., Visconti, A., 2006. J. Microb. Methods 66 (3), 529–537.
Zhang, F., Zou, M., Chen, Y., Li, J., Wang, Y., Qi, X., Xue, Q., 2014. Biosens. Bioelectron. 51, 29–35.
Zhang, Y., Jiao, K., Liu, C., Yang, Z.X., 1995a. Electroanalytical 7 (3), 283–286.
Zhang, Y., Jiao, K., Liu, C., Yang, Z.X., 1995b. Electroanalytical 7 (3), 283–286.
Zhang, Y., Yin, J., Jiang, D., Xin, Y., Ding, F., Deng, Z., Wang, G., Ma, X., Li, F., Li, G., Li, M., 2013. PloS One 8 (5), e64474.
Zhao, W., Lu, J., Ma, W., Xu, C., Kuang, H., Zhu, S., 2011. Biosens. Bioelectron. 26 (10), 4241–4244.
Zhao, Y., Liu, L., Kong, D., Kuang, H., Wang, L., Xu, C., 2014. ACS App. Mater. Interfaces 6 (23), 21178–21183.

Analytica Chimica Acta 1046 (2019) 123–131

Contents lists available at ScienceDirect

Analytica Chimica Acta

journal homepage: www.elsevier.com/locate/aca

Electrochemical detection of plant virus using gold nanoparticle-modified electrodes

Mohga Khater [a, b], Alfredo de la Escosura-Muñiz [a], Daniel Quesada-González [a], Arben Merkoçi [a, c, *]

[a] Catalan Institute of Nanoscience and Nanotechnology (ICN2), CSIC and Barcelona Institute of Science and Technology, Campus UAB, 08193, Barcelona, Spain
[b] On Leave from Agricultural Research Center (ARC), Ministry of Agriculture and Land Reclamation, Giza, Egypt
[c] ICREA—Institucio Catalana de Recerca i Estudis Avançats, Pg. Lluís Companys 23, 08010, Barcelona, Spain

HIGHLIGHTS

- A rapid label-free impedimetric method for quantitative detection of *Citrus tristeza virus*.
- Thiolated DNA probe immobilized and optimized for DNA hybridization detection of *Citrus tristeza virus*.
- Optimized modifications on AuNPs modified screen-printed electrodes for stable and reproducible virus detection.

GRAPHICAL ABSTRACT

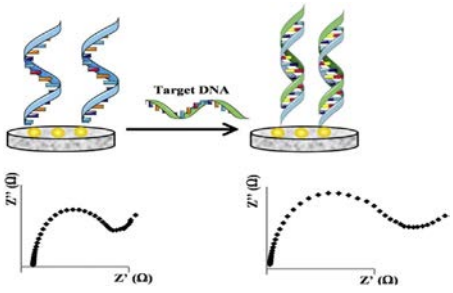

ARTICLE INFO

Article history:
Received 25 May 2018
Received in revised form
15 August 2018
Accepted 13 September 2018
Available online 15 September 2018

Keywords:
Electrochemical impedance spectroscopy
DNA
Gold-nanoparticles
Virus
Plant pathogen
Citrus tristeza virus

ABSTRACT

Tristeza is one of the destructive diseases of citrus causing by *citrus tristeza virus* (CTV). Historically, CTV has been associated with serious outbreaks of quick decline of citrus, therefore CTV monitoring is important aspect for avoiding such re-emerging epidemics, which would threat citrus production through the world. In this context, we have designed for the first time a label-free impedimetric biosensor for the detection of nucleic acid of CTV. The sensing platform based on a screen-printed carbon electrode (SPCE) was modified by electrodeposited gold nanoparticles (AuNPs), which allowed to efficiently immobilizing thiolated ssDNA probes as well to enhance the electrode conductivity. The growth of AuNPs was optimized and characterized using scanning electron microscopy (SEM), cyclic voltammetry (CV) and electrochemical impedance spectroscopy (EIS). We investigated the behavior of thiolated ssDNA probe layer and its hybridization with target DNA onto AuNP surfaces by EIS measurements in $Fe(CN_6)^{4-}/Fe(CN_6)^{3-}$ red-ox system. The main sensor design aspects such as AuNPs size, probe DNA concentration and immobilization time together with DNA hybridization time were optimized so as to achieve the best performance. Impedance values of DNA hybridization increased with Citrus tristeza-related synthetic DNA concentration, showing a logarithmic relation in the range of 0.1−10 μM. The results also indicate that the biosensor was able to selectively detect CTV nucleic acids in the presence of other non-specific DNAs. Moreover, we have demonstrated the good performance of the system in a real plant sample matrix. In addition, the sensor reproducibility enhanced after the hybridization onto MCH/poly (AT) thiolated DNA probes which was confirmed by intra- and inter-day variability assays.

* Corresponding author. Catalan Institute of Nanoscience and Nanotechnology (ICN2), CSIC and Barcelona Institute of Science and Technology, Campus UAB, 08193, Barcelona, Spain.
E-mail address: arben.merkoci@icn2.cat (A. Merkoçi).

https://doi.org/10.1016/j.aca.2018.09.031
0003-2670/

1. Introduction

Plant diseases have great impact on global plant production threating world food security [1,2]. Their causal agents include nonpathogenic factors such as environment, mechanical and chemical or pathogenic agents mainly viruses, fungi, bacteria and nematodes, etc. The most frequent methods for plant disease detection are based on nucleic acid and protein analysis. Over the past two decades, major advances in nanotechnology have allowed plant pathologists to integrate new technologies with molecular biology for plant disease diagnosis. In recent years, several reviews on developing biosensing systems for plant disease detection were reported [3–6]. Among major citrus viruses, *Citrus tristeza virus* (CTV) has caused high plant death rates around the world especially where citrus seedlings grafted onto sour orange rootstocks (the most susceptible to sever strains of tristeza) are cultivated [7,8]. Tristeza infects the phloem cells then systematically invades the tree causing variable symptoms that may include small fruit with low quality, general yellowing, step-pitting and quick decline [9–11]. The CTV-infected plants may display symptoms ranging from mild to severe depending mostly on the virus variant and susceptibility of plant variety. According to European and Mediterranean Plant Protection Organization (EPPO), CTV is a quarantine pathogen. Most reported serological assays to identify the coat protein of CTV are mainly ELISA, direct tissue print immunoassays [12,13], and very recently lateral flow immunoassay and label-free electrochemical immunosensor were developed for CTV detection [14,15]. Since reverse transcription polymerase chain reaction (RT-PCR) and dot-blot hybridization based methods are the most commonly used in molecular diagnostics of CTV, a combination of reverse transcription with loop-mediated isothermal amplification technology (RT-LAMP) has been recently developed [16–18]. However, these methodologies are time-consuming, requiring specialized personnel and also have limitations related to primer design. Applications of electrochemical nucleic acid sensing in disease diagnostics are growing tremendously over the last decades. Electrical detection of DNA hybridization using sensors has offered great sensitivity, cost-effective and easy rapid DNA analysis avoiding the limits of classical DNA hybridization detection techniques such as membrane blots and gel electrophoresis. To date, several studies have reviewed electrochemical nucleic acid biosensors based on different electrochemical approaches and have discussed the recent strategies for DNA immobilization and hybridization detection techniques [19–21] and [22–24]. Earlier publications addressed detection of nucleic acid of infectious agents using voltammetric, amperometric and impedance electrochemical approaches [25–28]. Notably, DNA hybridization biosensors based on electrochemical spectroscopy impedance (EIS) are being developed in both label-free formats and label-based approaches using mostly gold nanoparticle (AuNP) and cadmium sulfide quantum dot (CdS QD) as tags [29] and [30–37] also employing other nanomaterials [30–32,38–42]. Modification of electrode surface for immobilization of biorecognition receptor (i.e. DNA probes, antibody, aptamer, etc.) is the key to successful monitoring of DNA hybridization event. Most of such impedimetric DNA sensors have been designed forming self-assembled monolayers (SAM) on gold electrodes and films of conducting polymers (i.e. pyrrole) and nanomaterials, especially AuNPs, as electrode modifiers [43–45]. Introducing AuNPs into electrochemical DNA sensing electrodes offers several advantages over other metal nanoparticles and oxides. Unlike graphene and iron oxides, the strong stable gold (Au) −sulfur (S) bond together with their unique properties such as large surface and high conductivity, providing efficient immobilization of bio-receptor probes have made AuNPs as the most popular nanomaterial, extensively exploited in the design of biosensors [46–48]. Label-free sensors using impedimetric detection and label-based voltammetric approaches using enzymes or methylene blue tags on gold and carbon electrodes have been extensively reported [49–53].

Due to significant improvement in biosensor technology over the last two decades, applications of screen-printed electrodes (SPEs) in electrochemical DNA hybridization biosensors are in increase because of their simplicity, portability and the use of economical substrates. Moreover these SPEs offer the possibility of small-volume bioassays and can be combined with electrodeposited nanoparticles, especially AuNPs [33,54–56].

In this context, we propose for the first time to combine the advantages of AuNP-modified electrodes and EIS-based DNA hybridization detection for the development of a biosensor for CTV-related DNA determination. Such biosensor would be of high potential interest for in-field applications in the relevant field of plant pathogen detection.

2. Experimental section

2.1. Chemicals and equipment

Gold (III) chloride hydrate ($HAuCl_4$, 99.9%), potassium hexacyanoferrate (III), potassium hexacyanoferrate (II), tris (2-carboxyethyl) phosphine (TCEP), NaCl, $MgCl_2$, $CaCl_2$, 6-Mercaptohexanol (MCH) and phosphate buffered saline were obtained from Sigma Aldrich (Spain). CTV immunostrips were provided by Agdia inc. (USA). Oligonucleotides were purchased from Isogen (Spain). Sequences are the following: Thiolated ssDNA probe: 5'-GGATCGATGTGTAA-3'-$(CH_2)_6$–HS; Target ssDNA (fully complementary; characteristic of CTV): 5'-TTACACATCGATCC -3'; partially non complementary ssDNA (characteristic of Psorosis virus): 5′-TTACACAAGGATCT-3'; fully non complementary ssDNA 5'-TAGGATTAGCCGCATTCAGG-3' as control sequences. Thiolated ssDNA probe was pre-treated as detailed at the *supplementary information*. All buffer solutions were prepared with ultrapure water of Milli-Q water purification system (with resistivity of 18.2 MΩ cm). The supporting electrolyte was 0.5 mM solution of $K_3[Fe(CN)_6]/K_4[Fe(CN)_6]$ in 0.1 M KCl. DNA probe and target sequences were diluted in 34 mM Tris-HCl, pH 7.4 buffer. The washing solution was 0.01 M phosphate buffered saline (PBS; pH 7.4). Stock solutions of the oligonucleotides were prepared in TE (0.01 M Tris-HCl; pH 8.2 and 0.001 M EDTA) buffer solution and kept frozen at −20 °C. Healthy citrus leaves were provided by Universitat Autònoma de Barcelona in Spain and for detailed preparation of leaf extracts and its screening for CTV, see the *supplementary information.* SEM images of the modified carbon working electrode with electrodeposited gold nanoparticles were obtained using a FEI Quanta™ 650 field emission gun scanning electron microscope (FEI, USA). Images were analyzed using Image J software (National Institutes of Health, USA) for measuring particles size and density. All electrochemical measurements were recorded using Autolab potentiosat PGS00 supported by two different softwares: FRA for impedance spectra analysis and GPES for voltammetric analysis. Home-made screen-printed carbon electrodes (SPCEs) preparation is detailed at the *supplementary information*.

2.2. Methods

2.2.1. AuNPs electrodeposition

Two-step electrochemical pre-treatment was applied on SPCEs under a potential of +1.6 V for 120 s and of +1.8 V for 60 s in acidic solution (0.1 M acetate buffer; pH 4.7). Major advantages of this pretreatment included cleaned carbon surface from possible printing contaminants, higher hydrophilicity and better electron

transfer at the working electrode surface [57]. Importantly, the working pH of 1–3 for gold solution to perform deposition was found to be significantly favorable for controlling particle size and distribution over carbon electrodes [58]. The deposition process of AuNPs on SPCEs was performed by immersion into a gold solution of pH 1 (0.01% $HAuCl_4$,/0.1 M NaCl in the presence of 1.5 wt% HCl). Reduction of chloride gold (III) complexes to gold (0) and further deposition were achieved by applying a constant negative potential of −0.4 V for a determined time (from 10 s to 1200 s). Then the modified SPCEs were carefully rinsed and dried with nitrogen gas. After deposition of AuNPs onto carbon working electrode, AuNP-SPCE was characterized using CV, EIS and SEM.

2.2.2. Probe ssDNA immobilization and hybridization with target ssDNA

The covalent attachment of thiolated ssDNA probes onto the deposited AuNPs of the pretreated electrodes was performed by incubation of 15 μL of thiolated ssDNA probes solution at room temperature for 2 h. After that, the electrodes were rinsed with PBS and Milli-Q water (3X). The concentration and incubation time of thiolated ssDNA probe were optimized as shown at section 3.2.

Hybridization with complementary target ssDNA was performed by adding 15 μL and incubating during 60 min at room temperature. The same procedure was followed for the control assays with the non-complementary strand. A scheme of the developed DNA biosensing platform is shown at Fig. 1.

2.2.3. Electrochemical measurements

CV and EIS were used for the characterization of the AuNP-modified SPCEs, while the stepwise of the biosensor was characterized by EIS technique.

CVs were carried out in 0.5 M H_2SO_4 and 0.5 mM $K_3[Fe(CN)_6]$/$K_4[Fe(CN)_6]$ in 0.1 M KCl from +1.4 to −0.6 V at a scan rate of 50 mV/s. EIS measurements were performed in 0.5 mM $K_3[Fe(CN)_6]$/$K_4[Fe(CN)_6]$ in 0.1 M KCl within frequency ranging from 10 KHz to 0.5 Hz and alternating voltage amplitude of 5 mV. The results of impedance measurements were represented in the form of the Nyquist plot which visually shows the system dynamics.

The diameter of semicircle in the Nyquist plot is assigned to Fe $[(CN)_6]^{4-/3-}$charge transfer resistance (Rct) at high frequency when a line portion yielded from mass transfer limitation process at low frequencies. The difference in charge transfer resistance before and after DNA hybridization and duplex DNA (dsDNA) formation (ΔR_{ct}) were obtained following equation ΔR_{ct}= (R-R_0)/R_0. Here R and R_0 are charge transfer resistance of dsDNA and ssDNA, respectively. For analytical analysis, R_{ct} was measured by fitting data to equivalent circuits (Randless circuit) using the tools of the FRA software. Mean and standard deviation for all EIS reported results were calculated to represent obtained data. EIS and CV tests were conducted under ambient conditions.

3. Results and discussion

3.1. Characterization of AuNP-modified SPCEs

Gold deposition time was evaluated so as to obtain the optimum size and distribution of the AuNPs on the carbon working electrode for improving the analytical performance of our DNA hybridization biosensor. A constant negative potential of −0.4 V was applied for different deposition times (ranging from 10 s to 1600 s) and the obtained surface was monitored using SEM and EIS. As shown in Fig. 2, SEM images of the carbon working area of the SPCEs before and after gold electrodeposition at different times allow to verify AuNPs formation and to evaluate the particle size, morphology and density. A low amount (approx. 20 particles/μm^2) of small AuNPs (approx. 25 nm) with sharp tips was observed for short electrodeposition times in the range from 10 to 25 s. AuNPs nucleation increases then with the time, reaching saturation (approx. 50 particles/μm^2) for 200 s. An increase in the AuNPs size was observed for longer times, being larger than 85 nm for 1200 s. AuNPs aggregation was observed for electrodeposition times longer than 1200 s (data not shown). In view of these results, a compromise between AuNPs size, density, dispersity and experimental time is estimated for 200 s of electrodeposition, being such conditions selected as optimum for the further development of the DNA biosensor (as was also corroborated by the EIS characterization – see section 3.2).

The presence of AuNPs in the as-modified electrode (200 s of electrodeposition) was also evaluated by CV in 0.5 M H_2SO_4 solution (Fig. 3A). An anodic current peak at around +0.9 V and a

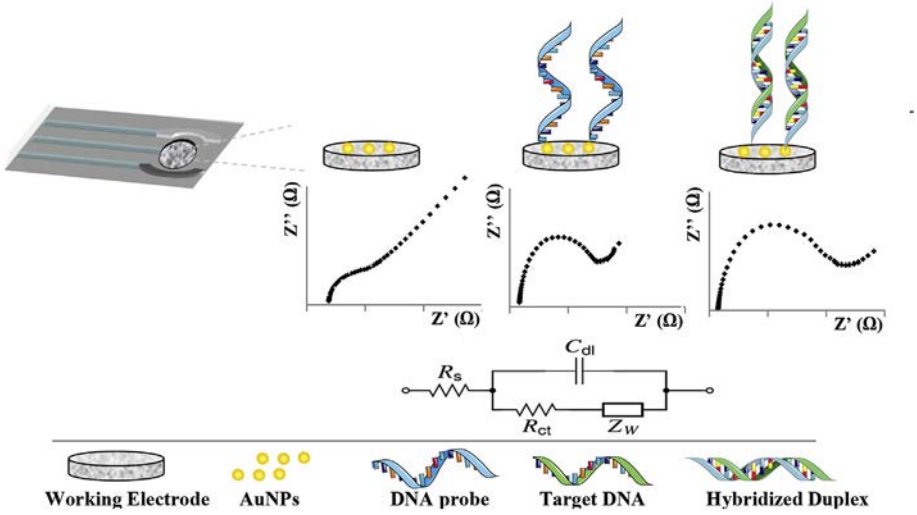

Fig. 1. Scheme of the developed DNA hybridization sensor based on AuNP- modified SPCE employing label-free impedance for the detection of CTV-related nucleic acid. Graphs illustrate the trend of the Nyquist plots for the stepwise of the biosensor. The equivalent circuit consists of four main parameters: solution resistance (Rs), Warburg impedance (Zw), double layer capacity (Cdl) and R_{ct} for charge transfer resistance between the modified electrode and red-ox system. All EIS measurements were based on R_{ct} values. (For interpretation of the references to colour in this figure legend, the reader is referred to the Web version of this article.)

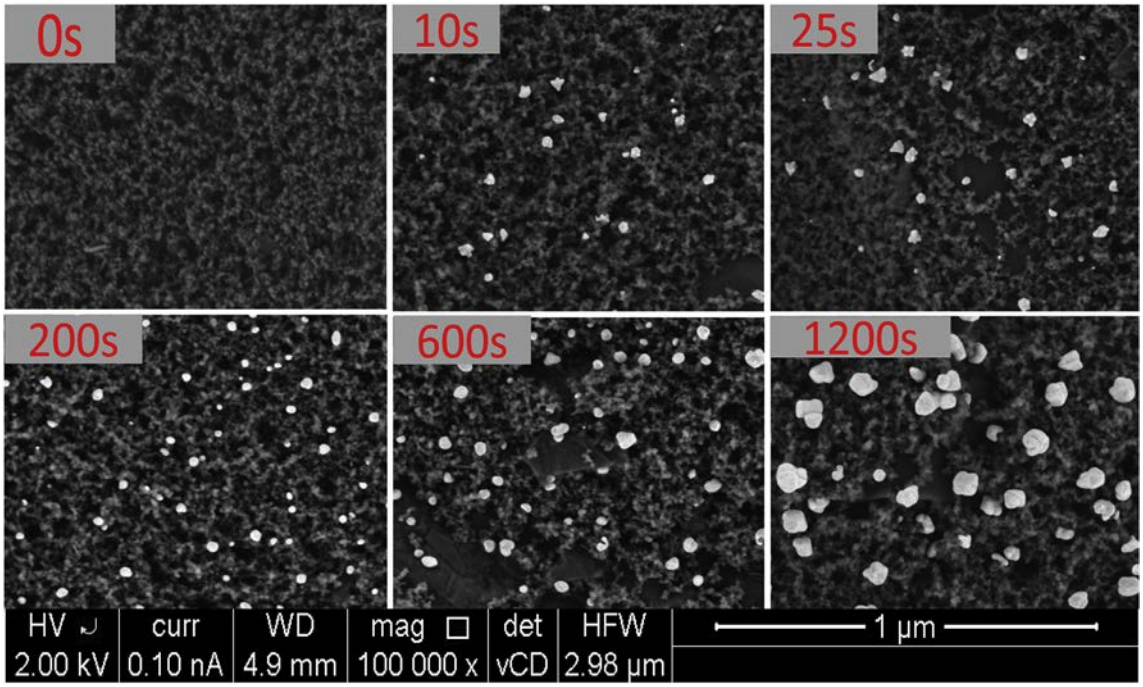

Fig. 2. SEM images of the carbon working area of SPCEs after different gold electrodeposition times (from 0 to 1200 s). Precursor: 0.01% $HAuCl_4$ solution. Deposition potential: 0.4 V. (For interpretation of the references to colour in this figure legend, the reader is referred to the Web version of this article.)

cathodic counterpart at around +0.5 V were observed for the AuNP-modified electrodes (Fig. 3A-solid line), which reflect the oxidation of AuNPs and the subsequent reduction of the gold oxide species back to metallic gold, respectively. In contrast, there was no appearance of any distinct faradaic current peak for bare SPCE (Fig. 3A-dotted line).

The effect of the AuNPs on the electrode electron transfer was also evaluated by CV in 0.5 mM $K_3[Fe(CN)_6]/K_4[Fe(CN)_6]$ (Fig. 3B). A pair of well-defined red-ox peaks corresponding to oxidation/reduction of the pair $Fe[(CN)_6]^{3-}/Fe[(CN)_6]^{4-}$ at +0.36 V/+0.12 V were observed for both the bare (Fig. 3B-dotted line) and AuNP-modified SPCE (Fig. 3B-solid line). The increase in the electron transfer on the electrode thanks to the presence of the AuNPs is evident when comparing the peak current intensities, observing an increase of 28% in the current for the modified SPCE.

Impedimetric investigation in 0.5 M $K_3[Fe(CN)_6]/K_4[Fe(CN)_6]$ solution also evidences the modification of SPCEs with AuNPs. A well-defined semicircle along Z' with diameter corresponding to Rct resistance was obtained for both bare (Fig. 3C-dotted line) and AuNP-modified SPCE (Fig. 3C-solid line). The lower impedance recorded for the modified electrode (185% decrease in the Rct) evidences the improved electrical conductivity raised by the presence of AuNPs.

3.2. DNA hybridization biosensor optimization

The main parameters affecting the performance of the DNA hybridization biosensor (performed following the experimental procedure described at section 2.2, fixing a target ssDNA concentration of 1 µM) were evaluated by EIS. Nyquist plots were recorded in 0.5 mM $K_3[Fe(CN)_6]/K_4[Fe(CN)_6]$ containing 0.1 M KCl solution and the signals were normalized by following the equation described at section 3.3.

Since deposition time tunes particle size and shape, the effect of the gold electrodeposition time and optimum particle size for high

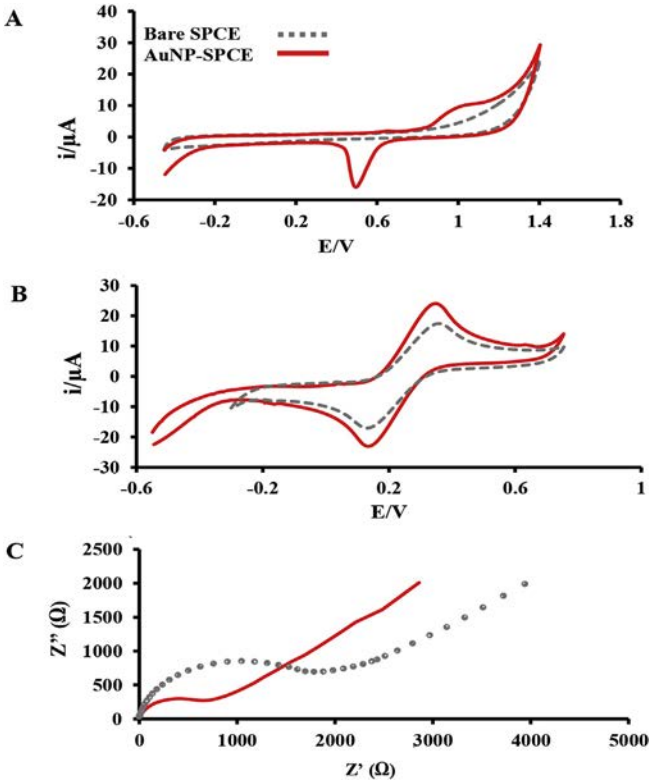

Fig. 3. Cyclic voltammograms (CVs) and Nyquist plots recorded for bare SPCEs (dotted lines) and AuNP-modified SPCEs after 200s of gold deposition (solid lines). **A.** CVs in 0.5 M H_2SO_4; **B.** CVs in 0.5 mM $K_3[Fe(CN)_6]/K_4[Fe(CN)_6]$ containing 0.1 M KCl. **C.** Nyquist plot obtained in 0.5 mM $K_3[Fe(CN)_6]/K_4[Fe(CN)_6]$ containing 0.1 M KCl. CVs are recorded from +1.4 to −0.6 V at scan rate of 50 mV/s. Nyquist plots recorded by applying potential of +0.2 V under amplitude of 5 mV in a frequency range of 10 KHz to 0.5 Hz. (For interpretation of the references to colour in this figure legend, the reader is referred to the Web version of this article.)

DNA hybridization rate was first evaluated (Fig. 4A). Preceding this, we have studied the behavior of thiolated ssDNA probes on varying diameter of AuNPs. The immobilized thiolated ssDNA had the highest signal value onto AuNPs with average diameter of 25 nm (obtained over 25 s) and then the charge transfer resistance decreased with the increasing of particle size. In contrast, the hybridization with target ssDNA using 25 nm AuNPs had the lowest ΔRct signal value. This is probably because small AuNPs completely packed with the thiolated DNA probe, not allowing sufficient space for target DNA to hybridize (data not shown). Therefore, the optimum size of AuNPs corresponding to thiolated probe does not accurately reflect the needed thiolated probe density in DNA hybridization assays. Notably, while gold electrodeposition time increases (from 10 s to 200 s), ΔRct values of DNA hybridization increased reaching the highest for 200 s (average diameter of 50 nm). Longer deposition times (600 s - 800 s) showed a decrease in the ΔRct values and poor reproducibility, which is in line with what was observed by SEM analysis. From SEM images homogenous AuNPs with controlled shape and size were generated at 200 s while non-homogenous bigger gold particles were observed at 600 s (particles diameter data at *supplementary information*) and this may lead to irreproducibility of the DNA sensor. Overall, particles with an average diameter of 50 nm afforded the best DNA hybridization rate, thus 200 s was then selected as the optimum gold electrodeposition time.

Thiolated ssDNA probe concentration and immobilization time were also investigated. AuNP-modified electrodes were incubated with a wide range of thiolated probe ssDNA concentrations (0.01, 0.1, 1, 5 and 10 μM). A gradual increase in the values of ΔRct was observed for the smaller concentrations, observing a decrease for values higher than 0.1 μM (Fig. 4B). This suggests that high probe ssDNA concentrations saturate the surface of AuNPs, hindering the signal discrimination after hybridization. In view of these results, a ssDNA probe concentration of 0.1 μM was selected for further studies.

Other parameter affecting the formation of the immobilized ssDNA probe sensing layer is the DNA probe incubation time, which was found to influence the DNA hybridization kinetics. The AuNP-modified SPCE electrodes were exposed to a 0.1 μM of thiolated ssDNA probe for various times (1, 2, 4 and 16 h) and EIS measurements after DNA hybridization were recorded (Fig. 4C). The ΔRct steadily increased for short times. After 2 h of probe ssDNA incubation and later hybridization with target ssDNA enlarged the diameter of semicircle to evidence the presence of sufficient attached ssDNA probe to recognize the target DNA and produce high analytical signal after hybridization. The ΔRct values increased

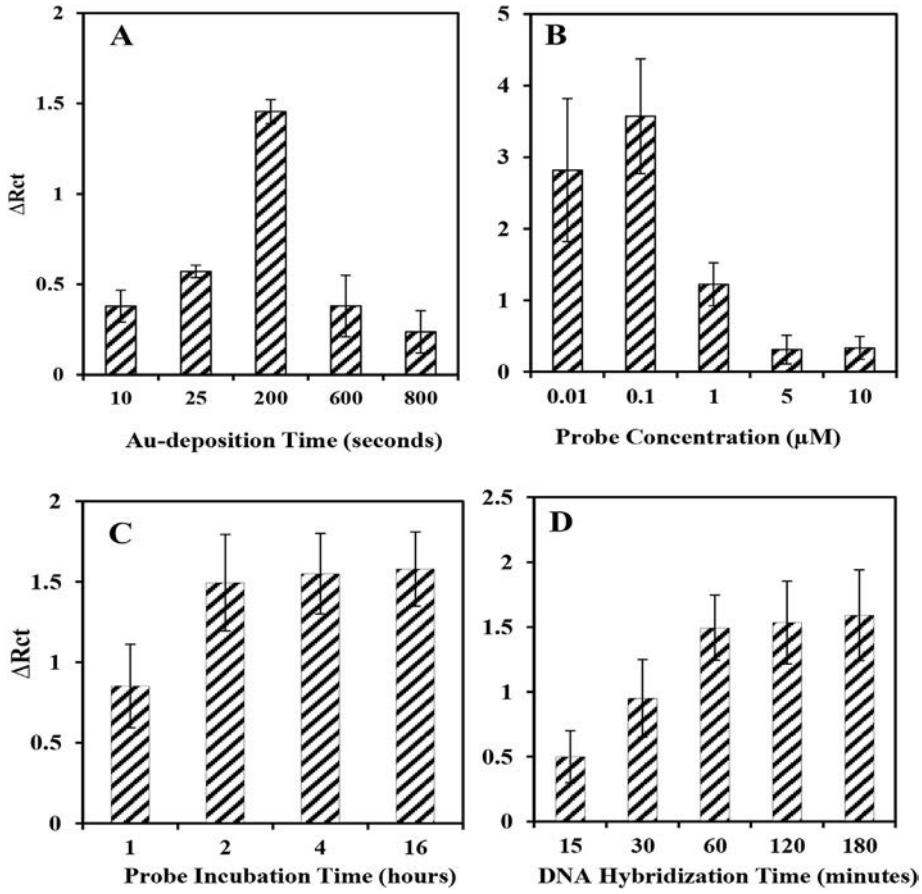

Fig. 4. Optimization of DNA hybridization biosensor. Normalized values corresponding to $\Delta R_{ct}=(R-R_0)/R_0$ are represented. ΔR_{ct} values were recorded after DNA hybridization with CTV-related DNA and control DNA (1 μM) following **A)** AuNPs deposition times (ranging 10 s - 800 s) at potential of −0.4 V; thiolated ssDNA probe (1 μM) incubated for 2 h; DNA hybridization time: 1 h. **B)** Different probe ssDNA concentrations (0.01, 0.1, 1, 5, and 10) μM on AuNP- modified SPCE (200 s); probe incubation time: 2 h; DNA hybridization time: 1 h. **C)** Probe incubation times (1, 2, 4 and 16 h) of thiolated ssDNA probe (0.1 μM) using AuNP- modified SPCE (200 s); DNA hybridization time: 1 h. **D)** DNA hybridization times (15, 30, 60, 120 and 180 min) on AuNP- modified SPCE (200 s) incubated with 0.1 μM of thiolated ssDNA probe for 2 h.

with the increasing in DNA probe incubation time under water-saturated atmosphere at 4 °C, demonstrating data saturation up to 16 h. The electrochemical data indicated that the incubation period of 2 h was optimum for our biosensing system.

Finally, the effect of DNA hybridization time on the analytical signal was studied (Fig. 4D). While membrane blot techniques require up to 16 h or longer for base pairing interaction, DNA hybridization on small electrode surface modified with adequate probe ssDNA concentration using micro volume of solutions typically require 1–2 h for hybridization to occur. The AuNP- modified SPCE electrodes coated with thiolated ssDNA probe were incubated with target ssDNA for various times (15, 30, 60, 120 and 180 min) to lead to duplex DNA formation. A steady increase in the ΔRct was observed over DNA hybridization times up to 60 min, noticing saturation in the signal for longer times. DNA hybridization time of 1 h was consequently chosen for the next investigation.

3.3. *Citrus tristeza*-related nucleic acid detection

Citrus tristeza virus has many characterized strains causing different symptomology. A 14-mer target ssDNA with sequence 5′-TTACACATCGATCC-3′ was selected as characteristic of the major coat protein (P25) of CTV [59]. The optimized DNA sensor was tested for different target ssDNA concentrations under the optimized conditions (AuNPs deposition time: 200 s, Probe concentration: 0.1 μM, probe incubation time: 2 h and DNA hybridization time: 1 h). In the EIS Nyquist plot, the diameter of semicircle enlarged when target ssDNA concentration increased as shown at Fig. 5A. Control assays performed with a non-specific target strand characteristic of Psorosis, another citrus virus genome (5′-TTACACAAGGATCT-3′) (Fig. 5A–a) demonstrated our sensing system ability to differentiate between CTV-related and non-CTV-related DNA.

The normalized R_{ct} values vs the CTV-related DNA concentrations were plotted (Fig. 5B), finding a logarithmic relationship in the range of 0.1–10 μM, adjusted to the following equation:

$$\Delta Rct\ (\Omega) = 1.4199 \ln[CTV(\mu M)] + 5.83\ (r = 0.99)\ (\Delta R_{ct} = (R\text{-}R_0)/R_0.)$$

A limit of detection (LOD) of 100 nM was estimated, as the target concentration giving a signal equal to the blank signal plus three times its standard deviation.

Additionally, interference studies were performed to examine the selectivity of our developed DNA sensor. Under optimized experiment conditions, the thiolated ssDNA-AuNP modified electrodes were covered with solutions of target DNA mixed with

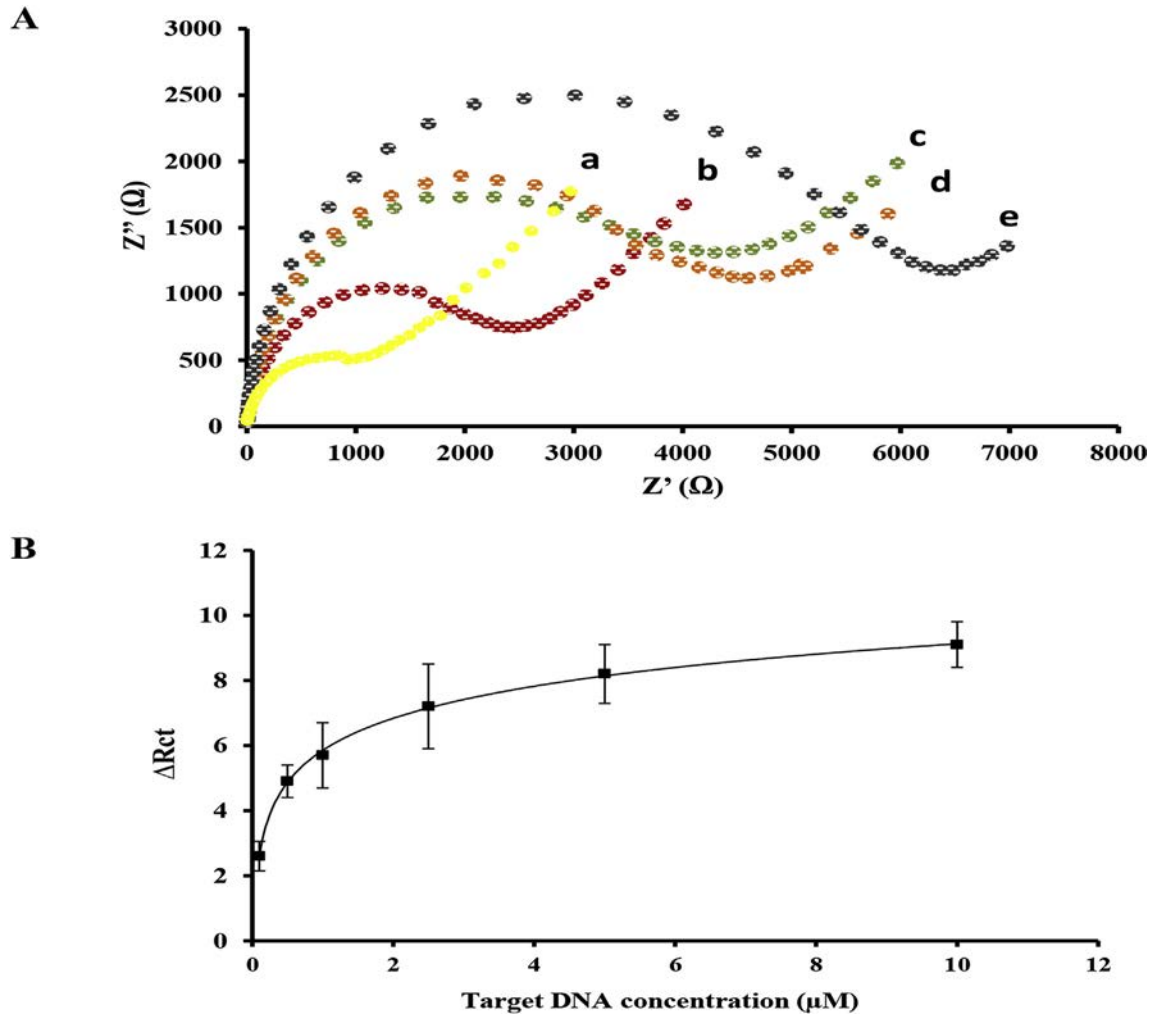

Fig. 5. A) Nyquist plots recorded for control DNA **a)** and CTV-related ssDNA concentrations of 0.1 μM **b)**, 0.5 μM **c)**, 1 μM **d)** and 10 μM **e)**. Electrolyte: 0.5 mM $K_3[Fe(CN)_6]/K_4[Fe(CN)_6]$ containing 0.1 M KCl; Potential: 0.2 V; Amplitude: 5 mV; Frequency range: 10 KHz to 0.5 Hz. **B)** Calibration curve obtained by plotting the normalized R_{ct} values vs the logarithm of different CTV-related DNA concentrations in the range of 0.1–10 μM. Other experimental conditions as described in the text.

interferents (partially and fully non-complementary DNAs) at 1:0; 1:1; 1:5 and 1:10 ratios. Notably, the impedance results were significantly affected when the concentration of partially non-complementary DNA was 10 times the target DNA concentration (data not shown). To improve the sensor selectivity, probe DNA with spacer of poly (AT) was served to form the recognition layer. Additionally, mercaptohexanol (MCH) was used as backfiller to minimize and effectively inhibit any non-specific adsorption of nucleobases, as reported in previous studies.

Gold nanoparticle surfaces were treated with poly (AT)-thiolated ssDNA probe in the presence of MCH (with DNA: MCH = 1: 0.1) for initial DNA immobilization process. Impedance measurements performed in target DNA solutions containing interfering of non-complementary DNA sequences, suggesting better selective DNA interaction as no significant interferences were observed (Fig. 6A).

The same system reported above was tested in leaf extracts from healthy citrus plants to assess its ability to quantify CTV nucleic acid in real biological samples. Leaf extracts were prepared in hybridization buffer and diluted 5 times and then spiked with five different target DNA concentrations (0.5, 1, 2.5, 5 and 10 μM). ΔRct were recorded and the results proved enough sensor sensitivity to detect the target DNA concentration as low as 500 nM (Fig. 6B). Moreover, the biosensor ability to recover different target DNA concentrations from plant sample matrix was studied and the results demonstrated the satisfactory recovery within the range of 90–97% (Table 1).

The reproducibility of responses for a 1 μM of target ssDNA on the thiolated ssDNA-AuNP surfaces was also studied, obtaining a relative standard deviation (RSD) of 17% which demonstrated the good performance of this proof-of-concept approach. For further improvements so as to get better repeatability between the different electrodes, intra- and inter-day assays variability were performed on MCH/poly (AT) thiolated ssDNA-AuNPs sensing layer (Table 2). The intra-day assays were conducted on the same single day while the inter-day assays required one assay/day for 5 sequential days. The mean value, standard deviation and coefficient of variation were calculated using five different target DNA concentrations (10, 20, 30, 40 and 50 μM). For these target DNA concentration, the mean coefficient of variation values of intra- and inter-day precision assays were 6.78% and 7.72%, both of which are less than 10% of RSD. These results indicate the good reproducibility performance of the proposed DNA sensor.

4. Conclusion

We have developed the first DNA hybridization sensor based on AuNP- modified SPCE employing label-free impedance for the detection of CTV-related nucleic acid. AuNPs were electrochemically deposited on the working carbon electrode for its easy preparation and strong affinity with bio-recognition receptors with reactive groups (e.i. thiols). Covalent attachment of thiolated ssDNA probe was obtained to form the sensing layer that recognizes target ssDNA. A simple rapid label-free impedance detection of CTV was developed on AuNP-modified electrodes and faradic impedance was used to investigate the electrochemical performance. Impedance was selected as the best parameter to monitor the interfacial charge transfer changes of the electrode surface resulting from duplex DNA formation. To evaluate the sensor performance corresponding to selectivity and reproducibility, interference studies

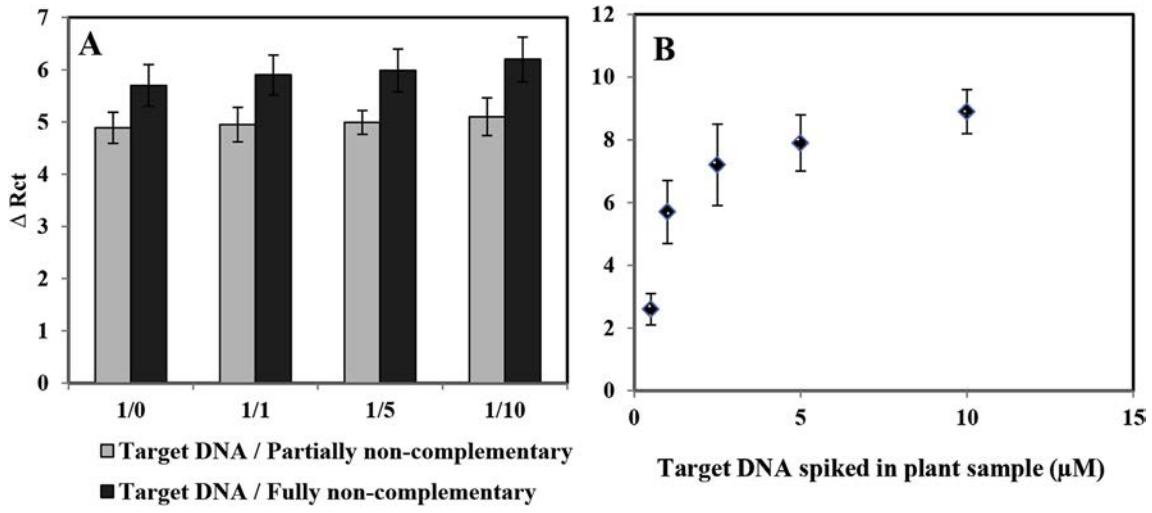

Fig. 6. A) Interference study on the MCH/poly (AT) thiolated ssDNA-AuNPs modified electrodes towards target DNA/fully non-complementary (black bar) and target DNA/partially non-complementary (gray bar) at different rations (n = 3) **B)** Effect of the concentration of CTV-related DNA (from of 0.5–10 μM) spiked in real plant samples on thenormalized R_{ct} values.

Table 1
Recovery study of the developed DNA biosensor in spiked plant samples with (0.5, 1, 2.5, 5 and 10 μM) of synthetic CTV-DNA.

Spiked CTV (μM)	ΔRct in hybridization buffer	ΔRct in plant sample	Recovery %
0.5	2.6	1.65	95
1	5.7	5	97
2.5	7.1	6.16	94
5	7.9	7	90
10	8.9	7.98	92

Table 2
Intra- and inter-day reproducibility assays of the CTV-DNA sensor.

Target Concentration (μM)	Intra-assay (n = 4)			Inter-assay (n = 4)		
	ΔRct	S.D	Coefficient of variation %	ΔRct	S.D	Coefficient of variation %
10	9.12	0.3	3.28	8.90	0.43	4.83
20	10.33	0.5	4.84	10.56	0.59	5.58
30	11.89	1	8.4	11.07	0.89	8.03
40	12.57	1.3	10.34	12.88	1.26	9.78
50	12.76	0.9	7.05	12.90	1.34	10.38

along with intra- and inter-day assays were conducted. The use of MCH and poly AT thiolated DNA probe has enhanced the sensor selectivity when it was tested against partially and fully non-complementary DNA sequences. The results demonstrated that 2 h is needed to form the recognition layer (MCH/poly (AT) thiolated ssDNA probe) followed by detecting the target DNA through base pairing time no longer than 1 h and finally within 5 min a detectable stable electrochemical signal is generated and collected. Our DNA sensor showed a logarithm relation in the range of 0.1–10 μM of CTV-related DNA with LOD of 100 nM with a total assay time of 65 min (60 min DNA hybridization and 5 min readout). Moreover, the results demonstrated the good reproducibility of the biosensors with RSD less than 10%. The developed DNA sensor exhibits great advantages over previously reported dot-blot hybridization approaches for CTV-nucleic acid based detection in terms of simplicity, time of analysis and ability to do quantitative analysis. The proposed biosensor is of high potential interest for in-field applications in the relevant field of plant pathogen detection, which would overcome the limitations of classical methods such as dot-blot hybridization.

Acknowledgments

The ICN2 is funded by the CERCA programme/Generalitat de Catalunya. The ICN2 is supported by the Severo Ochoa programme of the Spanish Ministry of Economy, Industry and Competitiveness (MINECO, grant no. SEV-2013-0295). Mohga Khater thanks Autonomous University of Barcelona for the opportunity of performing this work inside the framework of Biotechnology PhD Programme.

Appendix A. Supplementary data

Supplementary data to this article can be found online at https://doi.org/10.1016/j.aca.2018.09.031.

References

[1] M.J. Roberts, D.E. Schimmelpfennig, E. Ashley, M.J. Livingston, M.S. Ash, U. Vasavada, The Value of Plant Disease Early-warning Systems: a Case Study of USDA's Soybean Rust Coordinated Framework, United States Department of Agriculture, Economic Research Service, Washington, DC, USA, 2006.
[2] S. Savary, A. Ficke, J. Aubertot, C. Hollier, Food Secur. 4 (2012) 519–537.
[3] Y. Fang, R.P. Ramasamy, Biosensors 5 (3) (2015) 537–561.
[4] M. Khater, A. de la Escosura-Muñiz, A. Merkoçi, Biosens. Bioelectron. 93 (2017) 72–86.
[5] F. Martinelli, R. Scalenghe, S. Davino, S. Panno, G. Scuderi, P. Ruisi, P. Villa, D. Stroppiana, M. Boschetti, L.R. Goulart, C.E. Davis, Agron. Sustain. Dev. 35 (1) (2015) 1–25.
[6] A.S. Nezhad, Lab a Chip 14 (16) (2014) 2887–2904.
[7] S.J. Harper, S.J. Cowell, J. Citrus Pathol. 3 (1) (2016).
[8] P. Moreno, S. Ambrós, M.R. Albiach-Martí, i J. Guerr, L. Peña, Mol. Plant Pathol. 9 (2008) 251–268.
[9] M. Bar-Joseph, J. Citrus Pathol. 2 (1) (2015).
[10] M. Bar-Joseph, R. Marcus, R.F. Lee, Annu. Rev. Phytopathol. 27 (1989) 291–316.
[11] G. Licciardello, G. Scuderi, R. Ferraro, A. Giampetruzzi, M. Russo, A. Lombardo, A. Catara, Arch. Virol. 160 (2015) 2583–2589.
[12] M. Bar-Joseph, S.M. Garnsey, D. Gonsalves, M. Moscovitz, D.E. Purcifull, M.F. Clark, G. Loebenstein, Phytopathology 69 (1979) 190–194.
[13] Z. Huang, P.A. Rundell, X. Guan, C.A. Powell, Plant Dis. 88 (2004) 625–629.
[14] H. Haji-Hashemi, P. Norouzi, M.R. Safarnejad, M.R. Ganjali, Sensor. Actuator. B Chem. 244 (2017) 211–216.
[15] Y. Maheshwari, V. Selvaraj, S. Hajeri, C. Ramadugu, M.L. Keremane, R.K. Yokomi, Phytoparasitica 45 (2017) 333–340.
[16] S. Korkmaz, B. Cevik, S. Onder, K. Koc, O. Bozan, N. Z. J. Crop Hortic. Sci. 36 (2008) 239–246.
[17] R.K. Yokomi, M. Saponari, P.J. Sieburth, Phytopathology 10 (2010) 319–327.
[18] A. Warghane, P. Misra, S. Bhose, K.K. Biswas, A.K. Sharma, M.K. Reddy, D.K. Ghosh, J. Virol Meth. 250 (2017) 6–10.
[19] M.E. Castañeda, S. Alegret, A. Merkoci, Electroanalysis 19 (2007) 743–753.
[20] A. Merkoçi, M. Aldavert, S. Marín, S. Alegret, Trends Anal. Chem. 24 (2005) 341–349.
[21] J. Wang, Anal. Chim. Acta 469 (2002) 63–71.
[22] M.T. Castañeda, S. Alegret, A. Merkoçi, Biosensors and biodetection, Meth. Mol. Biol. 504 (2009) (Humana Press).
[23] J.Y. Park, S.M. Park, Sensors 9 (2009) 9513–9532.
[24] J.I.A. Rashid, N.A. Yusof, Sens. Bio-Sens. Res. (2017).
[25] W.M. Hassen, C. Chaix, A. Abdelghani, F. Bessueille, D. Leonard, N. Jaffrezic-Renault, Sensor. Actuator. B Chem. 134 (2008) 755–760.
[26] M.H. Pournaghi-Azar, E. Alipour, S. Zununi, H. Froohandeh, M.S. Hejazi, Biosens. Bioelectron. 24 (2008) 524–530.
[27] K.J. Cash, A.J. Heeger, K.W. Plaxco, Y. Xiao, Anal. Chem. 81 (2008) 656–661.
[28] A. Benvidi, A.D. Firouzabadi, M.D. Tezerjani, S.M. Moshtaghiun, M. Mazloum-Ardakani, A. Ansarin, J. Electron. Chem. 750 (2015) 57–64.
[29] J. Wang, G. Liu, R. Polsky, A. Merkoçi, Electrochem. Commun. 4 (2002) 722–726.
[30] J. Wang, G. Liu, A. Merkoçi, J. Am. Chem. Soc. 125 (2003a) 3214–3215.
[31] J. Wang, G. Liu, A. Merkoçi, Anal. Chim. Acta 482 (2003b) 149–155.
[32] J. Wang, R. Polsky, A. Merkoci, K.L. Turner, Langmuir 19 (2003c) 989–991.
[33] A. Bonanni, M.J. Esplandiu, M. Del Valle, Electrochim. Acta 53 (2008) 4022–4029.
[34] M. Pumera, M.T. Castaneda, M.I. Pividori, R. Eritja, A. Merkoçi, S. Alegret, Langmuir 21 (2005) 9625–9629.
[35] P.A. Rasheed, N. Sandhyarani, Microchim. Acta. 184 (2017) 981–1000.
[36] Y. Xu, H. Cai, P.G. He, Y.Z. Fang, Electroanalysis 16 (2004) 150–155.
[37] L. Ribovski, V. Zucolotto, B.C. Janegitz, Microchem. J. 133 (2017) 37–42.
[38] A. De la Escosura-Muñiz, L. Baptista Pires, L. Serrano, L. Altet, O. Francino, A. Sánchez, A. Merkoçi, Small 12 (2016) 205–213.
[39] A. De la Escosura-Muñiz, A. Mekoçi, Chem. Commun. (J. Chem. Soc. Sect. D) 46 (2010) 9007–9009.
[40] A. De la Escosura-Muñiz, A. Merkoçi, Nucleic Acid Nanotechnology, Springer, Berlin, Heidelberg, 2014, pp. 305–332.
[41] C.C. Mayorga-Martinez, A. Chamorro-García, L. Serrano, L. Rivas, D. Quesada-Gonzalez, L. Altet, A. Merkoçi, J. Mater. Chem. B 3 (2015) 5166–5171.
[42] A. Merkoçi, Biosens. Bioelectron. 26 (2010) 1164–1177.
[43] J. Travas-Sejdic, H. Peng, P.A. Kilmaitin, M.B. Cannell, G.A. Bowmaker, R.P. Cooney, C. Soeller, Synth. Met. 152 (2005) 37–40.
[44] T. Ito, K. Hosokawa, M. Maeda, Biosens. Bioelectron. 22 (2007) 1816–1819.
[45] X. Li, L. Shen, D. Zhang, H. Qi, Q. Gao, F. Ma, C. Zhang, Biosens. Bioelectron. 23 (2008) 1624–1630.
[46] C. Deng, J. Chen, Z. Nie, M. Wang, X. Chu, X. Chen, S. Yao, Anal. Chem. 81 (2008) 739–745.
[47] M. Mazloum-Ardakani, N. Rajabzadeh, A. Benvidi, M.M. Heidari, Anal. Biochem. 443 (2013) 132–138.
[48] L. Zhang, Z. Li, X. Zhou, G. Yang, J. Yang, H. Wang, Y. Lu, J. Electroanal. Chem. 757 (2015) 203–209.
[49] M. Cui, Y. Wang, H. Wang, Y. Wu, X. Luo, Sensor. Actuator. B Chem. 244 (2017) 742–749.
[50] Lai, R. Y., Weiwei, Y. A. N. G., 2011. U.S. Patent Application No. 12/967,547.
[51] S.F. Liu, Y.F. Li, J.R. Li, L. Jiang, Biosens. Bioelectron. 21 (2005) 789–795.
[52] H.P. Peng, Y. Hu, P. Liu, Y.N. Deng, P. Wang, W. Chen, X.H. Lin, Sensor. Actuator. B Chem. 207 (2015) 269–276.

[53] K. Zhang, H. Ma, L. Zhang, Y. Zhang, Electroanalysis 20 (2008) 2127–2133.
[54] F. Arduini, L. Micheli, D. Moscone, G. Palleschi, S. Piermarini, F. Ricci, G. Volpe, Trends Anal. Chem. 79 (2016) 114–126.
[55] D. Voccia, F. Bettazzi, E. Fratini, D. Berti, I. Palchetti, Anal. Bioanal. Chem. 408 (2016) 7271–7281.
[56] H. Wu, Y. Zuo, C. Cui, W. Yang, H. Ma, X. Wang, Sensors 13 (7) (2013) 8551–8563.
[57] S.V. Pereira, F.A. Bertolino, M.A. Fernández-Baldo, G.A. Messina, E. Salinas, M.I. Sanz, J. Raba, Analyst 136 (2011) 4745–4751.
[58] F.S. Karoonian, M. Etesami, N. Mohamed, Chemija 23 (4) (2012).
[59] Niblett, C. 2000. U.S. Patent No. 6,140,046. Washington, DC: U.S. Patent and Trademark Office.

analytical chemistry

Article

Cite This: Anal. Chem. 2019, 91, 4790−4796

pubs.acs.org/ac

In Situ Plant Virus Nucleic Acid Isothermal Amplification Detection on Gold Nanoparticle-Modified Electrodes

Mohga Khater,[†,‡] Alfredo de la Escosura-Muñiz,[†] Laura Altet,[§] and Arben Merkoçi*[,†,∥]

[†]Catalan Institute of Nanoscience and Nanotechnology (ICN2), CSIC and Barcelona Institute of Science and Technology, Campus UAB, 08193 Barcelona, Spain

[‡]On leave from Agricultural Research Center (ARC), Ministry of Agriculture and Land Reclamation, Giza, Egypt

[§]Vetgenomics, Edifici Eureka, Parc de Recerca UAB, 08193 Bellaterra, Barcelona, Spain

[∥]ICREA-Institucio Catalana de Recerca i Estudis Avançats, Pg. Lluís Companys 23, 08010 Barcelona, Spain

Supporting Information

ABSTRACT: Solid-phase isothermal recombinase polymerase amplification (RPA) offers many benefits over the standard RPA in homogeneous phase in terms of sensitivity, portability, and versatility. However, RPA devices reported to date are limited by the need for heating sources to reach sensitive detection. With the aim of overcoming such limitation, we propose here a label-free highly integrated in situ RPA amplification/detection approach at room temperature that takes advantage of the high sensitivity offered by gold nanoparticle (AuNP)-modified sensing substrates and electrochemical impedance spectroscopic (EIS) detection. Plant disease (*Citrus tristeza* virus (CTV)) diagnostics was selected as a relevant target for demonstration of the proof-of-concept. RPA assay for amplification of the P20 gene (387-bp) characteristic of CTV was first designed/optimized and tested by standard gel electrophoresis analysis. The optimized RPA conditions were then transferred to the AuNP-modified electrode surface, previously modified with a thiolated forward primer. The in situ-amplified CTV target was investigated by EIS in a $Fe(CN_6)^{4-}/Fe(CN_6)^{3-}$ red−ox system, being able to quantitatively detect 1000 fg μL^{-1} of nucleic acid. High selectivity against nonspecific gene sequences characteristic of potential interfering species such as *Citrus psorosis* virus (CPsV) and *Citrus caxicia* viroid (CCaV) was demonstrated. Good reproducibility (RSD of 8%) and long-term stability (up to 3 weeks) of the system were also obtained. Overall, with regard to sensitivity, cost, and portability, our approach exhibits better performance than RPA in homogeneous phase, also without the need of heating sources required in other solid-phase approaches.

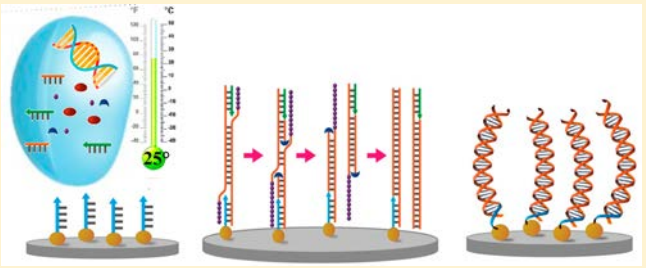

INTRODUCTION

Recombinase polymerase amplification (RPA) has received much attention in recent years due to its versatility and isothermal performance, which may offer effective replacement to polymerase chain reaction (PCR) in molecular detection.[1−4] Unlike PCR, RPA technology is based on three main components (recombinase, single-stranded DNA-binding protein, and polymerase) which allow amplification at constant temperature (ranging from 37 to 40 °C), and as a result the need for thermal cycling is omitted.[5,6] The required temperature for RPA is lower than that for other emerged isothermal amplification methods such as nucleic acid sequence-based amplification (NASBA), loop-mediated isothermal amplification (LAMP), rolling circle amplification (RCA), and helicase-dependent amplification (HDA).[7−11] In spite of the great advantages of RPA, DNA purification and detection after amplification involving hazardous, time-consuming, and expensive equipment is still required for getting qualitative information. Alternative methodologies taking advantage of the use of labeled primers for detecting RPA-amplified products in lateral flow[12−14] and electrochemical approaches have been proposed for such purpose.[15,16] Some efforts have been also devoted to RPA integration into microfluidic devices with fluorescence detection.[17] However, these methods lack integration of RPA amplification and detection in the same device, which would be strongly needed for in-field diagnostic applications.

Such highly integrated devices have been recently achieved with the so-called solid-phase RPA amplification, in which one of the primers is directly immobilized on the sensing surface. Label-free optical approaches[18,19] and enzymatic label-based electrochemical ones with high degree of integration have been reported.[20] However, heat sources are needed for getting detectable signals, which represents an important practical limitation.

Received: January 19, 2019
Accepted: March 7, 2019
Published: March 7, 2019

DOI: 10.1021/acs.analchem.9b00340
Anal. Chem. 2019, 91, 4790−4796

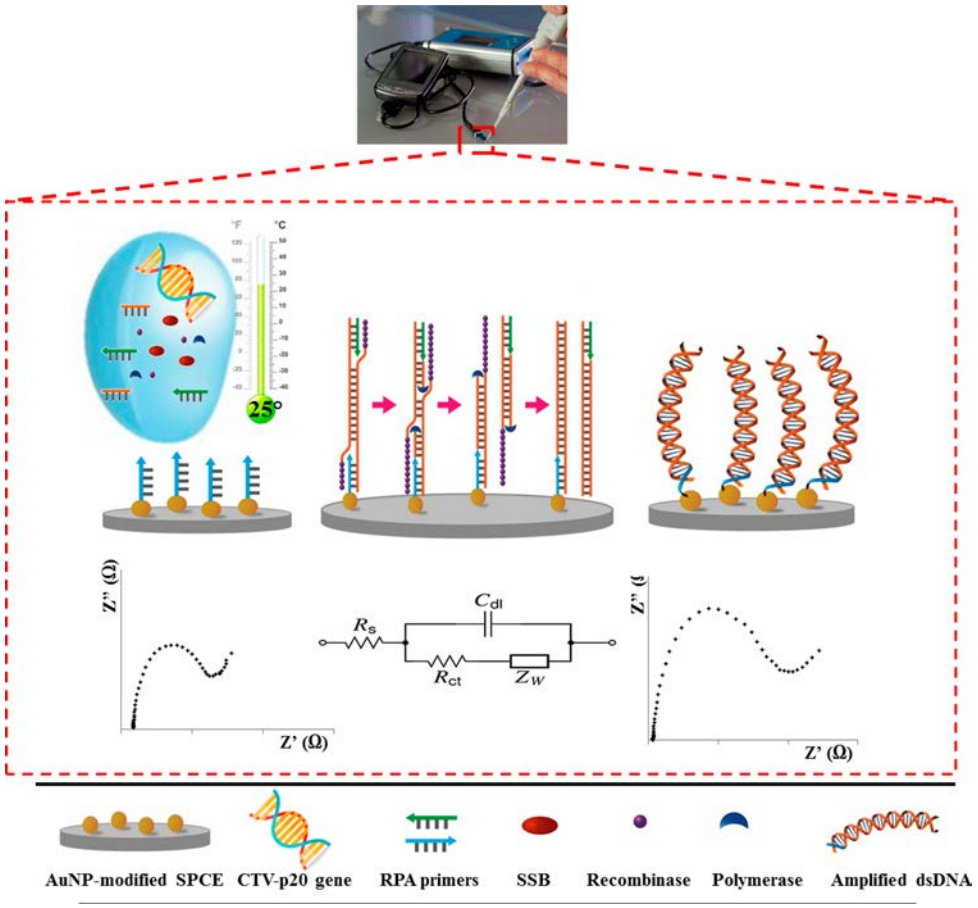

Figure 1. Steps of the developed label-free in situ isothermal RPA amplification/detection biosensor on primer-modified SPCE-AuNP electrodes employing impedance for the determination of CTV-related nucleic acid.

In this context, we propose a label-free highly integrated in situ RPA amplification/detection approach at room temperature taking advantage of the high sensitivity achieved combining the use of gold nanoparticle (AuNP)-modified sensing substrates and electrochemical impedance spectroscopic (EIS) detection. Plant disease (*Citrus tristeza* virus (CTV)) is selected as a relevant target for demonstration of the proof-of-concept. Recent studies estimating that plant diseases may cause global economic losses exceeding billions of dollars annually put in value the relevance of such diseases.[21] Early detection of pathogens in presymptomatic plants is of key importance for avoiding the development and spread of the disease. Plant pathogen determination is currently performed through antibody-based enzyme-linked immunosorbent assays (ELISA) and lateral flow immunoassays (LFIA)[22−28] and nucleic acid−based analysis[29−31] as alternative to the traditional diagnostic methods including symptoms observation, regular in-field inspections, and laboratory analysis by experienced plant pathologists.[32] Over the past decade it has been noticed that antibody- and DNA-based biosensing applications in the field of plant disease diagnostics have been increasing.[33−36] However, highly integrated approaches for in-field detection in presymptomatic plants, like the one we are proposing in this work, are still missing.

EXPERIMENTAL SECTION

Chemicals and Equipment. Gold(III) chloride hydrate ($HAuCl_4$, 99.9%), potassium hexacyanoferrate(III), potassium hexacyanoferrate(II), tris(2-carboxyethyl) phosphine (TCEP), NaCl, $MgCl_2$, $CaCl_2$, 6-mercaptohexanol (MCH), and phosphate-buffered saline were obtained from Sigma-Aldrich (Spain). The target and control sequences together with six primers were synthesized by Integrated DNA Technologies (Coralville, USA) (Table S1, in the Supporting Information). TwistAmp Basic Kit contains all enzymes and reagents necessary for amplification of DNA (TwistDx Ltd., Cambridge, UK). For purification of postamplification DNA products, a DNA clean and concentrator kit was purchased from Ecogen (Spain). Thiolated primer was pretreated as detailed at the Supporting Information. All buffer solutions were prepared with ultrapure water of a Milli-Q water purification system (with resistivity of 18.2 MΩ cm). The supporting electrolyte was a 0.5 mM solution of $K_3[Fe(CN)_6]/K_4[Fe(CN)_6]$ in 0.1 M KCl. Thiolated primer was diluted in 34 mM Tris-HCl, pH 7.4 buffer. The washing solutions were 0.01 M phosphate-buffered saline (PBS; pH 7.4), PBST (PBS and 0.05% (v/v) Tween 20, pH 7.4), and 2× SCC buffer (300 mM sodium chloride 30 mM sodium citrate) with pH adjusted to 7.2. Stock solutions of the oligonucleotides were prepared in TE (0.01 M Tris-HCl; pH 8.2 and 0.001 M EDTA) buffer solution and kept frozen at −20 °C. Ultrapure agarose and 50X TAE buffer (Tris-acetate-EDTA) were purchased from Invitrogen for electrophoresis of amplified nucleic acid. The agarose gel was stained by the green fluorescent Midori DNA stain. Electrophoresis was carried out using Mupid-one followed by gel documentation under UV light at 300 nm. Nanodrop 1000 was used to quantify DNA concentrations after RPA

DOI: 10.1021/acs.analchem.9b00340
Anal. Chem. 2019, 91, 4790−4796

amplification with thiolated forward primer. A block heater was used for incubation of RPA reactions. All electrochemical measurements were recorded using an Autolab potentiosat PGS00 supported by FRA for impedance spectra analysis. Home-made screen-printed carbon electrodes (SPCEs) preparation is detailed in the Supporting Information.

Methods. *RPA Assay of CTV-Related Nucleic Acid.* The sequence of p20 gene (549nt) responsible for systemic infection was first selected in CTV genome. Such sequence is specific to CTV and does not relate to other closteridea viruses, major component of CTV, and highly produced in infected trees. Three forward and two reverse primers were designed (between 25 and 35 bp) to amplify the p20 of 378-bp of CTV genomic nucleic acid, following the RPA manufacture's manual. Then the primer combinations were screened by gel electrophoresis in order to select the optimal primer pair which has great sensitivity and specificity for CTV.

For the RPA assays (50 μL reaction volume), a master mix composed of 2.4 μL of primers (10 μM), 29.5 μL of rehydration buffer, and 13.8 μL of CTV-p20 gene and DNase-free water was first prepared. After dividing aliquots of the master mix into reaction tubes and mixing with TwistAmp basic freeze-dried enzyme pellets, the RPA reactions were started immediately by adding magnesium acetate (280 mM). The reaction tubes were incubated at 37 °C for 30 min. RPA reactions were performed without the target gene as no template control (NTC). Following postamplification purification, amplicons were analyzed in 2% agarose gel.

In Situ Isothermal RPA on Gold Nanoparticle-Modified Electrodes. SPCEs modification with AuNPs and thiolated nucleic acid immobilization were performed following a previously optimized procedure.[37] Briefly, the electrodes were pretreated by applying oxidative potentials of +1.6 V for 120 s and +1.8 V for 60 s in acetate buffer, followed by rinsing with PBS and Milli-Q water (3×) and dried using nitrogen. Carbon working electrodes were then immersed into a gold solution (0.01% HAuCl4,/0.1 M NaCl in the presence of 1.5 wt % HCl), and a constant negative potential of −0.4 V for 200 s was applied for achieving a homogeneous formation of well-distributed spherical AuNPs of 50 nm. The thiolated forward primer (SH-(AT_7)-F1) was prereduced using TCEP as detailed at the Supporting Information. AuNP-modified SPCEs were then incubated with 15 μL of 0.1 μM SH-(AT_7)-F1 prepared with a 1 mM MCH solution at a ratio of 1:0.1 for 2 h at room temperature. After that the electrodes were thoroughly rinsed using PBS and dried with nitrogen gas.

RPA solutions were then prepared for thesurface amplification and detection of the target sequence of P_{20} gene on the AuNP-modified SPCEs. For the master mix of RPA reaction preparation, 29.5 μL of rehydration buffer, 2.4 μL of reverse primer (10 μM), and 13.2 μL of DNase-free water were mixed and added to the freeze-dried enzyme pellet. Then this mixture was mixed well with 2.5 μL of magnesium acetate at a concentration of 280 mM. After that the 50 μL reaction volume was divided into 10 μL aliquots and added to AuNP-modified SPCEs. Finally, 5 μL of the P20 gene from the target plant virus genome that ranges in concentration from 1 pg μL^{-1} to 1 ng μL^{-1} was added to the previously prepared 10 μL RPA solution. The solid-phase isothermal amplification assays were performed at room temperature (25 ± 3 °C) for 60 min. Additionally, the AuNP-modified SPCEs with RPA solutions containing water or other unrelated DNAs as negative controls were evaluated. A scheme of the developed nucleic acid amplification/detection system is shown in Figure 1.

Electrochemical Measurements. The in situ isothermal RPA was characterized by electrochemical impedance spectroscopy (EIS). Impedance measurements were performed in 0.5 mM $K_3[Fe(CN)_6]/K_4[Fe(CN)_6]$ in 0.1 M KCl within frequency ranging from 10 kHz to 0.005 Hz and an alternating voltage amplitude of 5 mV. The Nyquist plots of impedance which represent the system dynamics were employed to detect the isothermal amplified DNA (278-bp) on the AuNP-modified SPCEs.

The change in the semicircle diameter of the impedance represents the charge transfer resistance (R_{ct}) of Fe-$[(CN)_6]^{4-/3-}$ at the modified electrode surface. The difference in charge transfer resistance before and after DNA amplification forming duplex DNA (dsDNA) (ΔR_{ct}) was obtained following the equation $\Delta R_{ct} = (R - R_0)/R_0$, where R and R_0 are the charge transfer resistance of amplified dsDNA and primer ssDNA, respectively. For accurate analytical analysis, the recorded R_{ct} was fitted to the equivalent circuits (Randless circuit) using FRA. All EIS reported results were analyzed by calculating means and standard deviation to represent obtained data. All impedance experiments were conducted under ambient conditions.

RESULTS AND DISCUSSION

Design of RPA for CTV Detection Assay. After designing RPA primers to specifically detect CTV, gel electrophoresis was carried out to screen the selected primer sets (Table S1, in the Supporting Information). The best analytical band was produced by the F1/R1 primer pair which was able to amplify the expected size amplicons of 278-bp, being chosen for the next experiments. The optimum conditions recommended by the manufacturer, which included a favorable temperature of 37 °C, total reaction volume 50 μL, and interval mixing upon Mg salt addition, were applied to perform RPA reaction for 30 min, resulting in amplified 278-bp CTV-p20 gene fragments in the concentration range from 0.1 to 100 pg μL^{-1} that were visualized in the gel (Figure 2A).

The ability of the RPA to work at room temperature (25 ± 3 °C) was then evaluated. RPA experiments for CTV-p20 gene target concentration ranging from 0.1 to 100 pg μL^{-1} were performed within 30 min amplification at such temperature. Products obtained gave detectable bands in the gel only for the higher concentrations assayed (100 and 10 pg μL^{-1}) (Figure 2B), evidencing the DNA amplification under these conditions.

RPA conditions were modified in order to be more suitable to perform in situ amplification on primer-modified SPCE-AuNP electrodes. With the aim of simulating the conditions that will be found on the electrode surface, small reaction volumes of 15 μL were evaluated under amplification at 37 °C and room temperature. The signals obtained from large reaction volumes of 50 μL incubated at 37 °C were detectable for CTV-p20 gene target concentration as low as 0.1 pg μL^{-1}, while small reaction volumes of 15 μL gave signals only detectable for target concentration as high as 10 pg μL^{-1} (Figure 2C). The 100 pg μL^{-1} CTV-p20 gene target concentration showed a detectable signal after amplification of the small volume at RT, while no amplicons were generated from lower target concentrations (Figure 2D). The effect of Mg salt addition without a mixing step was also evaluated, reaching the same sensitivity as with previous mixing (data not shown).

DOI: 10.1021/acs.analchem.9b00340
Anal. Chem. 2019, 91, 4790−4796

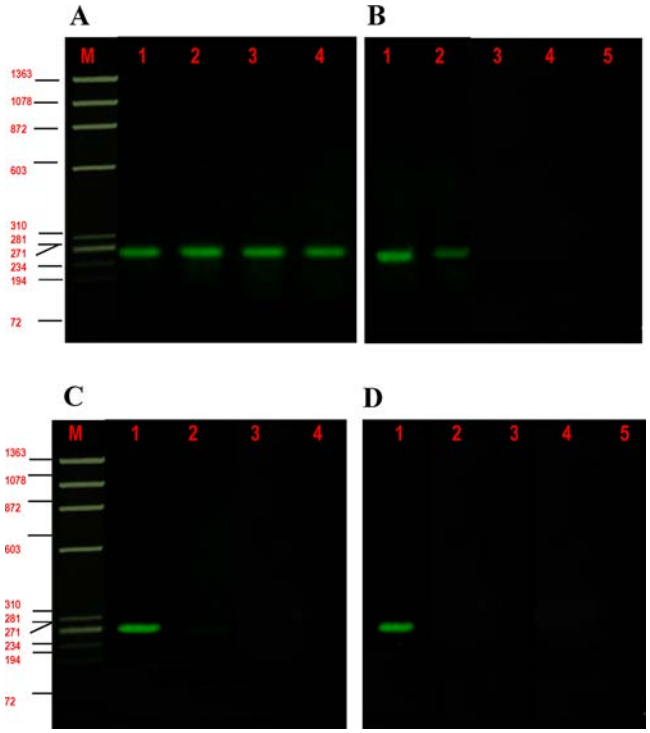

Figure 2. Gel electrophoresis analysis of RPA amplicons for CTV detection following. (A) Optimum isothermal RPA conditions: RPA amplification temperature, 37 °C; total reaction volume, 50 μL. (B) Isothermal RPA reactions at room temperature with a 50 μL total reaction volume. Isothermal RPA of small reaction volume (15 μL) incubated at different temperatures: (C) 37 °C and (D) room temperature. All isothermal RPA reaction times were 30 min. M = Phi-X 174/*Hae*III Marker, 1 = 100 pg μL^{-1}, 2 = 10 pg μL^{-1}, 3 = 1 pg μL^{-1}, 4 = 0.1 pg μL^{-1}, 5 = NTC. Band size: 278-bp for CTV-p20 gene.

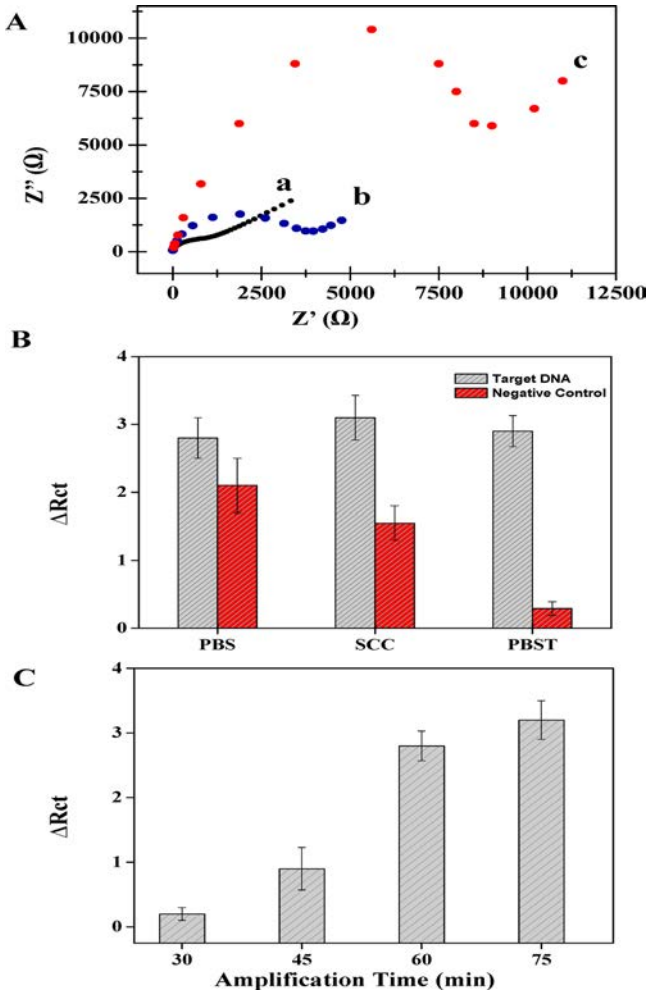

Figure 3. (A) Nyquist plots recorded for SPCE-AuNP electrode (a), upon SH-(AT_7)-F1primer immobilization (b), and in situ isothermal RPA with CTV-p20 target concentration of 1 ng μL^{-1} (c). (B) Effect of washing with different buffers after the in situ isothermal RPA performed for the CTV-p20 (target DNA) and for blank control (NTC) on the analytical signal. DNA concentration: 1 ng μL^{-1}. (C) Effect of the in situ isothermal RPA amplification time (30, 45, 60, and 75 min) on the analytical signal for a CTV-p20 target concentration of 1 ng μL^{-1}.

The good performance of the thiolated forward primer (SH-(AT_7)-F1) was evaluated by Nanodrop nucleic acid quantification (see the Supporting Information).

Electrochemical Characterization and Optimization of the in Situ Isothermal RPA on the Electrode Surface. The optimized RPA conditions were transferred to the SPCE-AuNP electrode surface. All reagent solutions were added to the electrode, previously modified with the forward primer (SH-(AT_7)-F1). The CTV-p20 gene was last added to the RPA mixture on the electrode to start the reaction (Figure 1).

The Nyquist plots recorded for the electrodes showed a high increase in the electrode resistance upon the RPA performed with a CTV-p20 target concentration of 1 ng μL^{-1} (Figure 3A), demonstrating the attachment of amplified DNA to the electrode.

However, when testing RPA solutions with negative control, unspecific EIS response was observed (data not shown). In order to prevent the interference from RPA chemical reagents and to reduce unspecific adsorption of enzymes, the three most commonly used washing buffers in chips and microfluidic domain for nucleic acid amplification methods were evaluated. After amplification, electrodes were carefully washed with three different washing buffers PBS 10 mM, 2× SSC, and PBST containing 0.05% (v/v) Tween 20. As a result of using PBST washing buffer, the unspecific EIS signal was highly decreased after amplifying with negative control showing effective removal of the rest of the RPA components that may remain on the electrode after amplification (Figure 3B). The supplement of Tween detergent in the washing buffer (PBST) resulted in greatly reduced nonspecific binding of RPA reagents on electrode surfaces, suggesting their effective release. Moreover, it is important to note that the high viscosity of RPA solutions makes the postamplification washing step essential for the EIS signal enhancement.

Finally, the effect of the time of the in situ isothermal RPA reaction on the electrochemical signal was also studied. As shown in Figure 3C, no detectable signals were obtained for reaction times below 30 min. R_{ct} values increased with the reaction time in the range 30−60 min, when a signal saturation was noticed. It is worthy to note that such optimum amplification time in the solid phase is longer than that typically used for the RPA in homogeneous phase (60 min) as expected.[20] Furthermore, the lower temperature used probably also contributes to such longer time required.

In Situ *C. tristeza*-Related Nucleic Acid DNA Amplification/Detection. The ability of our biosensor for quantification of CTV-related DNA was evaluated. The in situ isothermal

DOI: 10.1021/acs.analchem.9b00340
Anal. Chem. 2019, 91, 4790−4796

RPA amplification/detection biosensor on primer-modified SPCE-AuNP electrode was performed for different CTV-p20 target concentrations under the optimized conditions (primer concentration, 0.1 μM; primer immobilization time, 2 h; RPA amplification time, 1 h at room temperature; washing in PBST buffer). According to the EIS Nyquist plot, as the target concentration increased, the diameter of the semicircle enlarged as shown at Figure 4A.

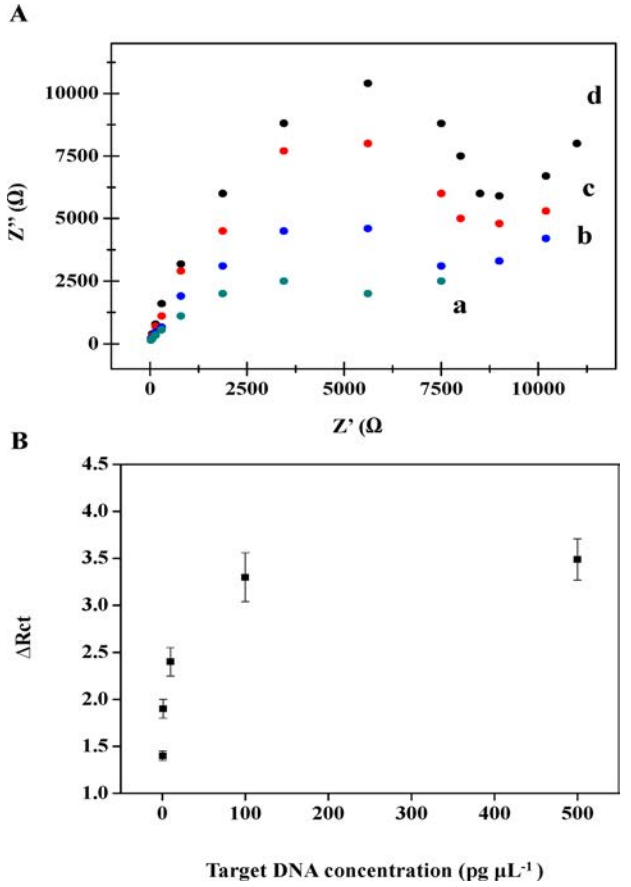

Figure 4. Normalized values corresponding to $\Delta R_{ct} = (R - R_0)/R_0$ are represented. (A) Nyquist plots recorded for SPCE-AuNPs electrodes upon in situ RPA amplification performed for *C. psorosis* virus (CPsV) gene (negative control-NTC) (a) and CTV-p20 target at (b) 10, (c) 100, and (d) 1000 pg μL^{-1}. Electrolyte: 0.5 mM $K_3[Fe(CN)_6]$/$K_4[Fe(CN)_6]$ containing 0.1 M KCl. Potential: 0.2 V. Amplitude: 5 mV. Frequency range: 10 kHz to 0.005 Hz. (B) Calibration curve obtained by plotting the normalized R_{ct} values ($\Delta R_{ct} = (R - R_0)/R_0$) vs the logarithm of *t* CTV-p20 gene target concentration in the range from 1 to 500 pg μL^{-1}. Other experimental conditions as described in the text.

The normalized R_{ct} values vs the CTV-p20 target concentrations were plotted (Figure 4B), finding a logarithmic relationship in the range from 1 to 500 pg μL^{-1}, adjusted to the following equation

$$\Delta R_{ct}(\Omega) = 0.2267 \ln[\mathrm{CTV(pg\ \mu L^{-1})}] + 3.36 (r = 0.993)$$
$$(\Delta R_{ct} = (R - R_0)/R_0)$$

The limit of detection (LOD) was found to reach 1 pg μL^{-1} (calculated as the target concentration producing a signal equivalent to the blank signal plus three-fold its standard deviation).

The limit of detection achieved by the label-free in situ isothermal RPA on primer-modified SPCE-AuNP electrodes was 100 times lower than that of the modified RPA assay, showing that integration of in situ isothermal RPA with the impedance approach allowed a highly sensitive detection of nucleic acid.

Additionally, specificity studies were performed to examine the ability of our developed in situ RPA sensor to differentiate between CTV-related and non-CTV-related DNAs. These studies were performed with a nonspecific gene sequence characteristic of *C. psorosis* virus (CPsV), as it is claimed to be the second important citrus virus, and also *Citrus caxicia* viroid (CCaV), which is likely to be present in complex infection with CTV in the infected citrus trees in nature. Under optimized experiment conditions, primer-modified SPCE-AuNP electrodes were coated with RPA solutions prepared with CTV-p20 gene target and controls. Impedance measurements shown in Figure 5A evidence a clear discrimination between the specific and the nonspecific DNA, demonstrating the specificity of our sensing system to CTV-related nucleic acid.

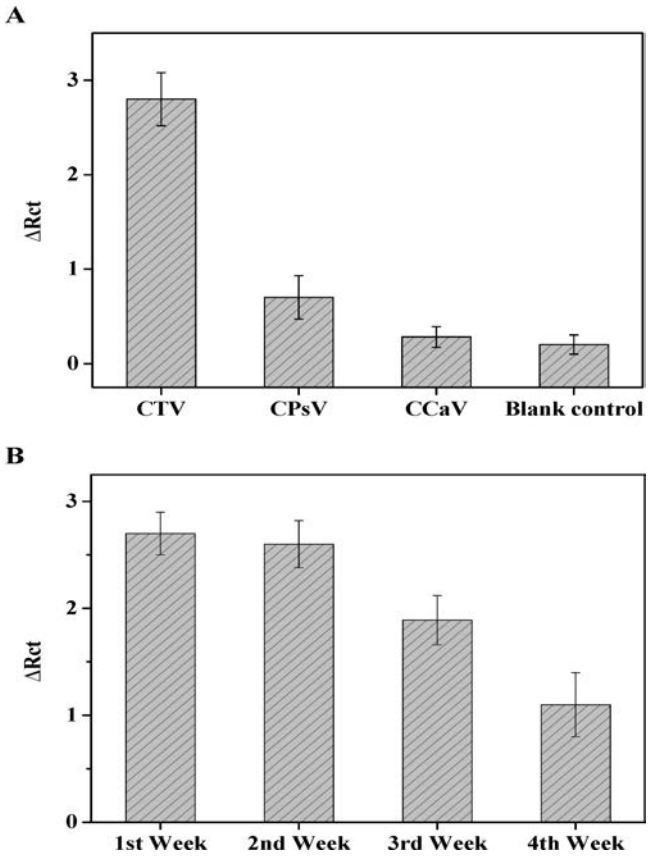

Figure 5. (A) Normalized R_{ct} values ($\Delta R_{ct} = (R - R_0)/R_0$) obtained for in situ RPA performed with specific target CTV-p20 gene and nonspecific CPsV and CCaV sequences as well as for a blank control. (B) Effect of storage on the performance of SPCE-AuNP electrodes for in situ isothermal RPA within 4 weeks.

The storage stability of SPCE-AuNP electrodes was also investigated by monitoring the impedance response of in situ RPA each week up to 1 month. The sensor showed an extended shelf life of working for more than 3 weeks. Along with that the repeatability of responses for a 100 pg μL^{-1} of CTV-p20 gene target on the thiolated primer-modified SPCE-AuNP surfaces

DOI: 10.1021/acs.analchem.9b00340
Anal. Chem. 2019, 91, 4790−4796

was studied through intra- and interday assays, obtaining a relative standard deviation (RSD) of 8%, which demonstrated the good performance of this proof-of-concept approach.

CONCLUSION

We developed the first integrated label-free in situ isothermal RPA amplification/detection based on AuNP-modified SPCE employing impedance for detection of CTV-related nucleic acid. Specific primers for the p20 gene of the CTV genome were designed, and RPA-amplified products were investigated by gel electrophoresis. Then the effect of both reaction volume and amplification temperature was also evaluated by gel analysis. For in situ isothermal RPA, AuNP-modified electrodes were coated with thiolated forward primer (SH-(AT_7)-F1) to form the sensing layer that recognizes CTV-p20 target and start the direct synthesis of duplex DNA onto the electrode surface. A simple electrochemical detection of CTV was performed using faradic impedance to characterize the electrochemical performance before and after in situ amplification. The charge transfer resistance parameter was selected to monitor the changes on the electrode surface, which results from immobilization of the sensing layer and the amplified duplex DNA. Our in situ isothermal RPA amplification/detection sensor showed a logarithm relation in the range from 1 to 500 pg μL^{-1} of CTV-related nucleic acid with LOD of 1000 fg μL^{-1} with a total assay time of 80 min (60 min RPA amplification and 20 min readout). The sensor performance including specificity and storage life along with intra- and interday assays was also studied. Moreover, the results demonstrated the good reproducibility of the biosensors with RSD below 10%. Compared with other methods (i.e., PCR or RPA analyzed by the routine gel electrophoresis), this in situ RPA sensor exhibits great advantages in terms of simplicity (no heat source and no label required), sensitivity, and portability together with allowing quantitative analysis of nucleic acid. The proposed biosensor is of high potential interest for in-field applications for plant pathogen early detection, which would overcome the limitations of classical molecular methods such as PCR.

ASSOCIATED CONTENT

Supporting Information

The Supporting Information is available free of charge on the ACS Publications website at DOI: 10.1021/acs.analchem.9b00340.

Sequences of target nucleic acid, controls and primers for RPA assay; details of fabrication and modification of carbon electrodes; pretreatment of thiolated primer ssDNA and Nanaodrop nucleic acid quantification of RPA amplicons in solution (DOC)

AUTHOR INFORMATION

Corresponding Author

*E-mail: arben.merkoci@icn2.cat.

ORCID

Alfredo de la Escosura-Muñiz: 0000-0002-9600-0253

Arben Merkoçi: 0000-0003-2486-8085

Notes

The authors declare no competing financial interest.

ACKNOWLEDGMENTS

The ICN2 is funded by the CERCA programme/Generalitat de Catalunya. ICN2 acknowledges the support of the Spanish MINECO for the Project MAT2017-87202-P and the Severo Ochoa Centers of Excellence Program under Grant SEV2201320295. M.K. thanks Autonomous University of Barcelona for the opportunity of performing this work inside the framework of Biotechnology PhD Programme.

REFERENCES

(1) James, A.; Macdonald, J. *Expert Rev. Mol. Diagn.* **2015**, *15*, 1475−1489.

(2) Daher, R. K.; Stewart, G.; Boissinot, M.; Bergeron, M. G. *Clin. Chem.* **2016**, *62*, 947−958.

(3) Moore, M. D.; Jaykus, L. A. *Future Virol.* **2017**, *12*, 421−429.

(4) Lobato, I. M.; O'Sullivan, C. K. *TrAC, Trends Anal. Chem.* **2018**, *98*, 19−35.

(5) Chen, G.; Dong, J.; Yuan, Y.; Li, N.; Huang, X.; Cui, X.; Tang, Z. *Sci. Rep.* **2016**, *6*, 34582.

(6) Wang, J.; Liu, L.; Wang, J.; Sun, X.; Yuan, W. *PLoS One* **2017**, *12*, No. e0166903.

(7) Compton, J. *Nature* **1991**, *350*, 91−92.

(8) Notomi, T.; Okayama, H.; Masubuchi, H.; Yonekawa, T.; Watanabe, K.; Amino, N.; Hase, T. *Nucleic Acids Res.* **2000**, *28*, No. e63.

(9) Gusev, Y.; Sparkowski, J.; Raghunathan, A.; Ferguson, H., Jr; Montano, J.; Bogdan, N.; Schweitzer, B.; Wiltshire, S.; Kingsmore, S. F.; Maltzman, W.; Wheeler, V. *Am. J. Pathol.* **2001**, *159*, 63−69.

(10) Vincent, M.; Xu, Y.; Kong, H. *EMBO Rep.* **2004**, *5*, 795−800.

(11) Piepenburg, O.; Williams, C. H.; Stemple, D. L.; Armes, N. A. *PLoS Biol.* **2006**, *4*, e204.

(12) Rivas, L.; de la Escosura-Muñiz, A.; Serrano, L.; Altet, L.; Francino, O.; Sánchez, A.; Merkoçi, A. *Nano Res.* **2015**, *8*, 3704−3714.

(13) Sun, K.; Xing, W.; Yu, X.; Fu, W.; Wang, Y.; Zou, M.; Luo, Z.; Xu, D. *Parasites Vectors* **2016**, *9*, 476.

(14) Wu, Y. A. D.; Xu, M. J.; Wang, Q. Q.; Zhou, C. X.; Wang, M.; Zhu, X. Q.; Zhou, D. H. *Vet. Parasitol.* **2017**, *243*, 199−203.

(15) De la Escosura-Muñiz, A.; Baptista Pires, L.; Serrano, L.; Altet, L.; Francino, O.; Sánchez, A.; Merkoçi, A. *Small* **2016**, *12*, 205−213.

(16) Tsaloglou, M. N.; Nemiroski, A.; Camci-Unal, G.; Christodouleas, D. C.; Murray, L. P.; Connelly, J. T.; Whitesides, G. M. *Anal. Biochem.* **2018**, *543*, 116−121.

(17) Li, Z.; Liu, Y.; Wei, Q.; Liu, Y.; Liu, W.; Zhang, X.; Yu, Y. *PLoS One* **2016**, *11*, No. e0153359.

(18) Shin, Y.; Perera, A. P.; Kee, J. S.; Song, J.; Fang, Q.; Lo, G. Q.; Park, M. K. *Sens. Actuators, B* **2013**, *177*, 404−411.

(19) Shin, Y.; Perera, A. P.; Kim, K. W.; Park, M. K. *Lab Chip* **2013**, *13*, 2106−2114.

(20) Del Río, J. S.; Lobato, I. M.; Mayboroda, O.; Katakis, I.; O'Sullivan, C. K. *Anal. Bioanal. Chem.* **2017**, *409*, 3261−3269.

(21) Agrios, G. N. *Environmental effects on the development of infectious plant disease. Plant pathol*, 5th ed.; Elsevier Academic Press, 2005.

(22) In *Biotech and plant disease management*; Punja, Z. K., De Boer, S. H., Sanfaçon, H., Eds.; Cabi, 2007.

(23) Alvarez, A. M. *Annu. Rev. Phytopathol.* **2004**, *42*, 339−366.

(24) Narayanasamy, P. Detection of fungal pathogens in plants. *Microbial Plant Pathogens-Detection and Disease Diagnosis*; Springer: Dordrecht, 2011; pp 5−199.

(25) Macario, A. J.; De Macario, E. C. *Monoclonal Antibodies Against Bacteria*; New York State Department of Health: Albany, NY, 1985; pp 213−247.

(26) Comstock, J. C.; Irey, M. S. *Plant Dis.* **1992**, *76*, 1033.

(27) Thornton, C. R. Production of monoclonal antibodies to plant pathogens. *Plant Pathology* ; Humana Press: Totowa, NJ, 2009; pp 63−74.

(28) Tomlinson, J. A.; Dickinson, M. J.; Boonham, N. *Phytopathology* **2010**, *100*, 143−149.

(29) Ward, E.; Foster, S. J.; Fraaije, B. A.; McCartney, H. A. *Ann. Appl. Biol.* **2004**, *145*, 1−16.

DOI: 10.1021/acs.analchem.9b00340
Anal. Chem. 2019, 91, 4790−4796

(30) Price, J. A.; Smith, J.; Simmons, A.; Fellers, J.; Rush, C. M. *J. Virol. Methods* **2010**, *165*, 198−201.
(31) Dai, J.; Peng, H.; Chen, W.; Cheng, J.; Wu, Y. *J. Appl. Microbiol.* **2013**, *114*, 502−508.
(32) In *Plant Disease: An Advanced Treatise*; Horsfall, J. G., Cowling, E. B., Eds.; Academic Press: New York, 1977.
(33) Nezhad, A. S. *Lab Chip* **2014**, *14*, 2887−2904.
(34) Fang, Y.; Ramasamy, R. P. *Biosensors* **2015**, *5*, 537−561.
(35) Martinelli, F.; Scalenghe, R.; Davino, S.; Panno, S.; Scuderi, G.; Ruisi, P.; Villa, P.; Stroppiana, D.; Boschetti, M.; Goulart, L. R.; Davis, C. E. *Agron. Sustainable Dev.* **2015**, *35*, 1−25.
(36) Khater, M.; de la Escosura-Muñiz, A.; Merkoçi, A. *Biosens. Bioelectron.* **2017**, *93*, 72−86.
(37) Khater, M.; de la Escosura-Muñiz, A.; Quesada-González, D.; Merkoçi, A. *Anal. Chim. Acta* **2019**, *1046*, 123−131.

DOI: 10.1021/acs.analchem.9b00340
Anal. Chem. 2019, 91, 4790−4796